

University of Trás-os-Montes and Alto Douro

**Mammary carcinogenesis in female rats: contribution to
monitoring and treatment**

PhD thesis in Veterinary Sciences - Clinic

ANA ISABEL ROCHA FAUSTINO

Supervisor: Professor Doutor Mário Manuel Dinis Ginja

Co-supervisor: Professora Doutora Rita Maria Pinho Ferreira

Co-supervisor: Professora Doutora Adelina Maria Gaspar Gama Quaresma



Vila Real, 2017

University of Trás-os-Montes and Alto Douro

**Mammary carcinogenesis in female rats: contribution to
monitoring and treatment**

PhD thesis in Veterinary Sciences - Clinic

Ana Isabel Rocha Faustino

Supervisor: Professor Doutor Mário Manuel Dinis Ginja

Co-supervisor: Professora Doutora Rita Maria Pinho Ferreira

Co-supervisor: Professora Doutora Adelina Maria Gaspar Gama Quaresma

Composition of the jury:

Vila Real, 2017

Original thesis presented by Ana Isabel Rocha Faustino at the University of Trás-os-Montes and Alto Douro, to obtain the Doctor's degree in
Veterinary Sciences - Clinic.

This work was supported by *Fundação para a Ciência e Tecnologia, Ministério da
Ciência, Tecnologia e Ensino Superior* (Portugal).

- SFRH/BD/102099/2014 -

FCT

Fundação para a Ciência e a Tecnologia
MINISTÉRIO DA CIÊNCIA, TECNOLOGIA E ENSINO SUPERIOR

To my Parents.

“Para mí no hay emoción o satisfacción comparable a la que produce la actividad creadora, tanto en ciencia como en el arte, literatura u otras ocupaciones del intelecto humano. Mi mensaje, dirigido sobre todo a la juventud, es que si sienten inclinación por la ciencia, la sigan, pues no dejará de proporcionarles satisfacciones inigualables. Ciertamente abundan los momentos de desaliento y frustración, pero estos se olvidan pronto, mientras que las satisfacciones no se olvidan jamás.”

Severo Ochoa

ACKNOWLEDGMENTS

Desejo expressar a mais sincera gratidão:

À Universidade de Trás-os-Montes e Alto Douro (UTAD), na pessoa do seu Magnífico Reitor Professor Doutor António Fontainhas Fernandes.

Ao orientador desta tese, o Professor Doutor Mário Ginja, Professor Auxiliar com Agregação da UTAD, pela transmissão de conhecimento, pela confiança e disponibilidade.

À Professora Doutora Rita Ferreira, Professora Auxiliar da Universidade de Aveiro, coorientadora destes trabalhos, pelo rigor científico demonstrado no decurso dos mesmos.

À Professora Doutora Adelina Quaresma, Professora Auxiliar da UTAD, coorientadora desta tese, pela ajuda prestada na componente histopatológica da mesma.

À Professora Doutora Paula A. Oliveira, um agradecimento muito especial, pois embora não seja coorientadora destes trabalhos teve um papel fundamental na sua concretização.

À Professora Doutora Maria João Neuparth, pela análise bioquímica das amostras.

À Professora Doutora Ana Margarida Calado, pela análise das neoplasias mamárias por microscopia eletrónica.

Ao Professor Doutor Bruno Colaço e à Professora Doutora Maria João Pires, por terem estado sempre presentes e disponíveis para ajudar no decurso dos trabalhos.

À Professora Doutora Aura Antunes Colaço pela simpatia e amabilidade.

Ao Professor Doutor Jorge Colaço pela ajuda no tratamento estatístico dos dados.

Ao Laboratório de Histologia e Anatomia Patológica da UTAD, na pessoa da Professora Doutora Maria dos Anjos Pires, pelo processamento das amostras e cedência do espaço para a realização da técnica de imunohistoquímica.

Ao Professor Doutor Joaquim Gabriel, ao Dr.º António Ramos e ao Doutor Rui Gil da Costa da Faculdade de Engenharia da Universidade do Porto, pela oportunidade de realizar o estudo termográfico das lesões da mama.

Ao Professor Doutor Jimmy Saunders e à Professora Doutora Katrien Vanderperren por me terem recebido na Faculdade de Medicina Veterinária da Universidade de Ghent, Bélgica.

À Sr.ª Ana Maria Machado, técnica do Laboratório de Análises Clínicas do Hospital Veterinário da UTAD, pela simpatia e ajuda em todos os momentos.

Às minhas colegas, pelo companheirismo e apoio.

À minha família. De modo muito especial aos meus Pais, sempre presentes e a quem jamais serei capaz de conseguir agradecer por tudo.

RESUMO

O cancro é um importante problema de saúde pública a nível mundial. De acordo com a Organização Mundial de Saúde, no ano de 2012, esta doença afetou 14 milhões de pessoas em todo o mundo. O cancro da mama é o mais frequente na mulher, tendo sido responsável por mais de meio milhão de mortes no ano de 2012. Este tipo de cancro é também o mais frequente nas cadelas não castradas e o terceiro mais frequente na gata. O desenvolvimento de cancro da mama encontra-se associado a diversos fatores de risco, como a idade, o sexo, a raça, fatores reprodutivos, a exposição aos estrogénios, a massa corporal, mutações genéticas e o estilo de vida.

Existem diversas opções médicas para o tratamento do cancro da mama, como a cirurgia, a radioterapia, a quimioterapia, a terapia hormonal e a imunoterapia. Contudo, a possível ineficácia, a imprevisibilidade da resposta do cancro à terapia instituída e os efeitos secundários associados à terapia constituem uma permanente preocupação no tratamento do cancro. Desta forma, é essencial investir na pesquisa de novas abordagens terapêuticas que possam melhorar o prognóstico e a qualidade de vida dos doentes oncológicos.

O modelo de cancro da mama quimicamente induzido no rato pela administração do agente carcinogénico *N*-metil-*N*-nitrosureia (MNU) é internacionalmente reconhecido para o estudo da carcinogénese mamária. Este modelo permite estudar diversos aspetos da carcinogénese mamária, como a patogenia, e as alterações genéticas e moleculares, bem como avaliar novas abordagens preventivas e terapêuticas.

Com esta tese pretendemos contribuir para a monitorização e tratamento do cancro da mama utilizando este modelo animal. Neste sentido, o crescimento e a vascularização das neoplasias foram monitorizados de forma não invasiva, recorrendo a métodos de diagnóstico por imagem, e foram avaliadas duas abordagens terapêuticas: o efeito do estilo de vida (prática de exercício físico) e a ação do fármaco anti-histamínico H1 de segunda geração e estabilizador dos mastócitos - cetotifeno.

Neste trabalho foram realizados dois protocolos experimentais, um para avaliar o efeito da prática de exercício físico moderado durante 35 semanas e outro para avaliar o efeito do cetotifeno na progressão e vascularização do cancro da mama. No primeiro protocolo, 50 ratos do sexo feminino da estirpe Sprague-Dawley foram aleatoriamente divididos em quatro grupos experimentais: MNU sedentário (n=15), MNU exercitado

(n=15), controlo sedentário (n=10) e controlo exercitado (n=10). Aos 50 dias de idade, os animais dos grupos MNU receberam uma injeção intraperitoneal do agente carcinogénico MNU. Após a administração, os animais foram exercitados num tapete rolante a uma velocidade de 20 m/min, 60 min/dia, 5 dias/semana, durante 35 semanas. No segundo protocolo experimental, 34 ratos do sexo feminino da estirpe Sprague-Dawley foram aleatoriamente divididos em cinco grupos experimentais: MNU (n=10), MNU + cetotifeno-1 (n=10), MNU + cetotifeno-2 (n=10), cetotifeno (n=2) e controlo (n=2). O desenvolvimento de cancro da mama foi induzido nos animais dos grupos MNU através da administração do agente carcinogénico MNU de acordo com as condições descritas no primeiro protocolo experimental. Os animais do grupo MNU + cetotifeno-1 receberam o fármaco anti-histamínico e inibidor da desgranulação dos mastócitos cetotifeno por via oral após a administração da MNU, durante 18 semanas. Os animais do grupo MNU + cetotifeno-2 apenas receberam o cetotifeno após o desenvolvimento da primeira neoplasia mamária. Os restantes grupos foram utilizados como controlos. Em ambos os protocolos experimentais, o crescimento das neoplasias e a vascularização foram monitorizados recorrendo a métodos não invasivos (utilização do paquímetro, ultrassonografia e termografia). No final dos ensaios, os animais sobreviventes foram sacrificados e foi realizada uma necrópsia completa.

De acordo com os nossos resultados, as neoplasias da mama induzidas pela MNU em ratos do sexo feminino crescem como uma superfície circular com pouca profundidade, assemelhando-se à forma de um esferoide oblato. A ultrassonografia é o método recomendado para a determinação do volume das neoplasias *in vivo*, enquanto o deslocamento de água e a determinação do volume com base na massa das neoplasias constituem as metodologias mais adequadas para determinar o volume após o sacrifício dos animais ou a excisão cirúrgica das neoplasias. A ultrassonografia e a termografia são métodos de imagem recomendados para a avaliação da vascularização das neoplasias. A análise das neoplasias por microscopia eletrónica revelou semelhanças entre as neoplasias induzidas pela MNU no rato e o cancro da mama da mulher.

A prática de exercício físico moderado durante 35 semanas inibiu a carcinogénese mamária, reduzindo a inflamação, o número total de neoplasias, o número de neoplasias por animal e a sua malignidade, e aumentou o período de latência. Adicionalmente, as neoplasias mamárias dos animais exercitados exibiram maior imunoexpressão dos recetores de estrogénios α , sugerindo uma maior diferenciação destas neoplasias e melhor resposta à terapia hormonal. Apesar de apresentarem menor malignidade, as neoplasias

dos animais exercitados exibiram maior vascularização quando comparadas com as neoplasias dos animais sedentários. Foi também observado que o cancro e a prática de exercício físico induzem algumas alterações ao nível do músculo esquelético. Nos animais com neoplasias (grupos MNU) foi observada uma menor ecogenicidade do músculo gastrocnémio sugestiva de uma menor infiltração de tecido adiposo, e níveis séricos de miostatina mais elevados provavelmente devido ao efeito catabólico do processo neoplásico no tecido muscular. O músculo gastrocnémio dos animais exercitados (MNU e controlo) exibiu menor ecogenicidade quando comparada com a ecogenicidade do músculo dos animais dos respetivos grupos sedentários devido à diminuição da infiltração de tecido adiposo nos grupos exercitados.

A administração do cetotifeno inibiu a desgranulação dos mastócitos. O principal efeito positivo desta inibição na carcinogénese mamária foi a redução da proliferação das neoplasias quando a desgranulação dos mastócitos foi inibida antes do desenvolvimento das mesmas.

De acordo com os nossos resultados, a prática de exercício físico moderado durante um longo período de tempo e a administração do cetotifeno são recomendadas para a prevenção e tratamento do cancro da mama.

Palavras-chave: cancro da mama, carcinogénese química, cetotifeno, exercício físico, mastócitos, *N*-metil-*N*-nitrosureia, rato, termografia, ultrassonografia, vascularização

ABSTRACT

Cancer is a major public health problem around the globe. According to the World Health Organization, 14 million of people were affected by this disease in the year 2012. Breast cancer is the most frequent cancer among women, being responsible for more than a half a million of deaths in 2012. It is also the most frequent cancer in intact female dogs and the third most frequent in female cats. Breast cancer development is intimately associated with several risk factors, namely age, sex, race, reproductive factors, estrogens exposure, body weight, genetic mutations and lifestyle.

Several medical options are available for breast cancer treatment, such as surgery, radiotherapy, chemotherapy, hormone therapy and immunotherapy. However, the possible ineffectiveness, the distinct response of cancer to the therapies and the devastating effects of some of these therapies for patients are the major concerns in cancer treatment. So, it is crucial to search for new or at least adjuvant therapies that may improve the lifespan and quality of life of oncologic patients.

The rat model of chemically-induced mammary cancer by the administration of the carcinogen *N*-methyl-*N*-nitrosourea (MNU) is internationally recognized for the study of mammary carcinogenesis. It allows to better understand several aspects of mammary carcinogenesis, namely pathogenesis, genetic and molecular basis, as well as to evaluate new preventive and therapeutic approaches.

With this thesis, we intend to contribute to the monitoring and treatment of mammary cancer using this animal model. For this purpose, mammary tumor growth and vascularization were non-invasively evaluated by imaging modalities, and two distinct therapeutic approaches were tested: we evaluated the role of lifestyle (practice of physical exercise) and the effects of the second-generation H1-antihistamine and mast cell stabilizer drug - ketotifen.

Two distinct experimental protocols were performed: one to evaluate the effects of long-term moderate exercise training and another to evaluate the effects of ketotifen in the progression and vascularization of mammary cancer. In the first experiment, 50 female Sprague-Dawley rats were randomly divided into four experimental groups: MNU sedentary (n=15), MNU exercised (n=15), control sedentary (n=10) and control exercised (n=10). At 50 days of age, animals from MNU groups received a single intraperitoneal injection of the carcinogen agent MNU. Then, animals were exercised on a treadmill

running at a velocity of 20 m/min, 60 min/day, five days a week, for 35 weeks. In the second experiment, 34 female Sprague-Dawley rats were randomly divided into five experimental groups: MNU (n=10), MNU + ketotifen-1 (n=10), MNU + ketotifen-2 (n=10), ketotifen (n=2) and control (n=2). Mammary tumor development was induced in animals from MNU groups by the administration of MNU according to the conditions described above. Animals from MNU + ketotifen-1 group were orally administered with ketotifen immediately after MNU administration for 18 weeks, while each animal from MNU + ketotifen-2 group only received ketotifen after the development of the first mammary tumor. The remaining groups were used as controls. Mammary tumor growth and vascularization were non-invasively monitored throughout both experiments, using caliper, ultrasound and thermography. At the end of the experiments, all survived animals were humanely sacrificed and submitted to a complete necropsy.

According to our results, MNU-induced mammary tumors in female rats grow as a circular surface with small depth, resembling the shape of an oblate spheroid. Ultrasonography is the recommended way to determine tumor volume *in vivo*, while water displacement or tumor weight are the best ways to assess tumor volume after animal sacrifice or tumor excision. Ultrasound and thermographic techniques are applicable to provide information on tumor vascularization. Electron microscopy analysis revealed similar features between MNU-induced mammary tumors in rats and women mammary tumors.

Lifelong moderate exercise training inhibited the carcinogenic response, by reducing inflammation, multiplicity, burden and malignancy, and increasing the cancer latency. Additionally, mammary tumors from exercised animals exhibited higher immunoexpression of estrogen receptors α , which is an indicator of tumor differentiation and better response to hormone therapy. Surprisingly, despite low malignancy, mammary tumors from exercised animals were more vascularized when compared with mammary tumors from sedentary animals. It was also observed that cancer and the practice of exercise training promoted some changes in the skeletal muscle. A lower echogenicity of *gastrocnemius* muscle suggestive of lower fat infiltration and higher myostatin serum levels were observed in animals with cancer (MNU-exposed groups) probably due to cancer-associated catabolic effects on body tissues. Exercised groups (MNU and control) also exhibited lower echogenicity when compared with respective sedentary groups due to the reduction of muscular fat.

Ketotifen inhibited mast cell degranulation. The main positive effect of this inhibition on mammary carcinogenesis was the reduction of mammary tumor proliferation when the mast cell degranulation was inhibited before tumor development.

According to our results, the practice of moderate exercise training for a long period of time and the administration of ketotifen are recommended for mammary cancer prevention and treatment.

Keywords: chemical carcinogenesis, exercise training, ketotifen, mammary cancer, mast cells, *N*-methyl-*N*-nitrosourea, rat, thermography, ultrasound, vascularization

LIST OF PUBLICATIONS RELATED WITH THIS WORK

The results of the present thesis were published in several formats: eleven full papers in SCI indexed journals, twelve abstracts in SCI indexed journals, one short communication and two abstracts in journals with referee, six oral communications in international conferences, five oral communications in national conferences, nine poster presentations in international conferences and four poster presentations in national conferences. Only the full papers and abstracts published or submitted for publication in SCI indexed journals are listed below. The remaining publications will be listed in the respective chapters.

1. Full papers published in SCI indexed journals

- **Faustino-Rocha AI**, Gama A, Neuparth MJ, Oliveira PA, Ferreira R, Ginja M. 2017. Mast cells on mammary carcinogenesis: host or tumor supporters? *Anticancer Research* 37 (3): 1013-1021. (Times cited: 1)
- **Faustino-Rocha AI**, Gama A, Oliveira PA, Vanderperren K, Saunders JH, Pires MJ, Ferreira R, Ginja M. 2017. A contrast-enhanced ultrasonographic study about the impact of long-term exercise training on mammary tumors vascularization. *Journal of Ultrasound in Medicine*. (Accepted for publication)
- **Faustino-Rocha AI**, Gama A, Oliveira PA, Vanderperren K, Saunders JH, Pires MJ, Ferreira R, Ginja M. 2017. Modulation of mammary tumors vascularization by mast cells: ultrasonographic and histopathological approaches. *Life Sciences* 176 (2017): 35-41.
- **Faustino-Rocha AI**, Gama A, Oliveira PA, Ferreira R, Ginja M. 2017. Antihistamines as promising drugs in cancer therapy. *Life Sciences* 172 (2017): 27-41. *Review*.

- **Faustino-Rocha AI**, Calado AM, Gama A, Ferreira R, Ginja M, Oliveira PA. 2016. Electron microscopy findings in MNU-induced mammary tumors. *Microscopy and Microanalysis* 22 (5): 1056-1061. DOI: 10.1017/S1431927616011661.

- **Faustino-Rocha AI**, Silva A, Gabriel J, Gil da Costa RM, Moutinho M, Oliveira PA, Gama A, Ferreira R, Ginja M. 2016. Long-term exercise training as a modulator of mammary cancer vascularization. *Biomedicine & Pharmacotherapy* 81 (2016): 273-280. DOI: 10.1016/j.biopha.2016.04.030. (Times cited: 6)

- **Faustino-Rocha AI**, Gama A, Oliveira PA, Alvarado A, Neuparth MJ, Ferreira R, Ginja M. 2016. Effects of lifelong exercise training on mammary tumorigenesis induced by MNU in female Sprague-Dawley rats. *Clinical and Experimental Medicine*. 17 (2): 151-160. DOI: 10.1007/s10238-016-0419-0. (Times cited: 8)

- **Faustino-Rocha AI**, Gama A, Oliveira PA, Alvarado A, Fidalgo-Gonçalves L, Ferreira R, Ginja M. 2016. Ultrasonography as the gold standard for *in vivo* volumetric determination of chemically-induced mammary tumors. *In vivo* 30: 465-472. (Times cited: 1)

- **Faustino-Rocha AI**, Ferreira R, Oliveira PA, Gama A, Ginja M. 2015. *N*-methyl-*N*-nitrosourea as a mammary carcinogenic agent. *Tumor Biology* 36 (12): 9095-9117. DOI: 10.1007/s13277-015-3973-2. *Review*. (Times cited: 8)

- **Faustino-Rocha AI**, Oliveira PA, Duarte JA, Ferreira R, Ginja M. 2013. Ultrasonographic evaluation of *gastrocnemius* muscle in a rat model of *N*-methyl-*N*-nitrosourea-induced mammary tumor. *In vivo* 27 (6): 803-807. (Times cited: 5)

- **Faustino-Rocha AI**, Silva A, Gabriel J, Teixeira-Guedes CI, Lopes C, Gil da Costa R, Gama A, Ferreira R, Oliveira PA, Ginja M. 2013. Ultrasonographic, thermographic and histologic evaluation of MNU-induced mammary tumors in female Sprague-Dawley rats. *Biomedicine & Pharmacotherapy* 67 (8): 771-776. DOI: 10.1016/j.biopha.2013.06.011. (Times cited: 18)

2. Abstracts published in SCI indexed journals

- **Faustino-Rocha AI**, Gama A, Oliveira PA, Ferreira R, Ginja M. 2017. Mast cells as targets on mammary carcinogenesis. *Journal of Comparative Pathology* 156 (1): 63.
- **Faustino-Rocha AI**, Silva A, Gabriel J, Gil da Costa RM, Oliveira PA, Gama A, Ferreira R, Ginja M. 2017. Long-term exercise training and mammary tumors' vascularization: thermography, ultrasonography and immunohistochemistry. *Journal of Comparative Pathology* 156 (1): 119.
- **Faustino-Rocha AI**, Calado AM, Gama A, Ferreira R, Ginja M, Oliveira PA. 2016. MNU-induced mammary tumors: transmission electron microscopy. *Microscopy and Microanalysis*. (Accepted for publication)
- **Faustino-Rocha AI**, Gama A, Oliveira PA, Alvarado A, Ferreira R, Ginja M. 2015. Effects of lifelong exercise training on the expression of estrogen receptors α and β in rat mammary tumors. *Laboratory Animals* 49 (Suppl 3): 40. DOI: 10.1177/0023677215601807.
- **Faustino-Rocha AI**, Gama A, Oliveira PA, Ferreira R, Ginja M. 2015. Inflammation in healthy animals and animals with mammary tumors: effects of lifelong exercise training. *Laboratory Animals* 49 (Suppl 3): 59. DOI: 10.1177/0023677215601807.
- **Faustino-Rocha AI**, Gama A, Oliveira PA, Alvarado A, Vala H, Ferreira R, Ginja M. 2015. Expression of estrogen receptors-alpha and beta in chemically-induced mammary tumors. *Virchows Archiv* 467 (Suppl 1): S51. DOI: 10.1007/s00428-015-1805-9.
- **Faustino-Rocha AI**, Gama A, Oliveira PA, Vala H, Ferreira R, Ginja M. 2015. Effects of histamine on the development of MNU-induced mammary tumors. *Virchows Archiv* 467 (Suppl 1): 51. DOI: 10.1007/s00428-015-1805-9.
- **Faustino-Rocha AI**, Oliveira PA, Pinto C, Gil da Costa RM, Duarte JA, Ferreira R, Ginja M. 2015. Effects of physical exercise on *gastrocnemius* muscle in a rat model

of mammary cancer. *Journal of Comparative Pathology* 152 (1): 78. DOI: 10.1016/j.jcpa.2014.10.148.

- **Faustino-Rocha AI**, Gama A, Pires MJ, Oliveira PA, Ginja M. 2014. Effects of a mast cell stabilizer on the vascularization of mammary tumors: ultrasonographic evaluation. *Anticancer Research* 34 (2014): 5901.
- **Faustino-Rocha AI**, Pinto C, Gama A, Oliveira PA. 2014. Effects of ketotifen on mammary tumors volume and weight. *Anticancer Research* 34 (2014): 5902.
- **Faustino-Rocha AI**, Talhada D, Andrade A, Teixeira-Guedes CI, Ferreira R, Gama A, Oliveira PA, Ginja M. 2014. Evaluation of MNU-induced mammary tumours in female Sprague-Dawley rats by histology and contrast enhanced ultrasound. *Journal of Comparative Pathology* 150 (1): 110. DOI: 10.1016/j.jcpa.2013.11.141.
- **Faustino-Rocha AI**, Silva A, Gabriel J, Talhada D, Andrade A, Teixeira-Guedes CI, Gil da Costa RM, Ferreira R, Oliveira PA, Ginja M. 2014. A new approach to evaluate mammary tumours in female Sprague-Dawley rats: thermography. *Journal of Comparative Pathology* 150 (1): 108. DOI: 10.1016/j.jcpa.2013.11.135.

TABLE OF CONTENTS

LIST OF FIGURES	xxxiii
LIST OF TABLES	xxxvii
LIST OF ABBREVIATURES AND SYMBOLS	xli
CHAPTER 1	1
1. General introduction	3
1.1. Cancer	3
1.2. Breast cancer.....	4
1.2.1. <i>Risk factors and prevention</i>	5
1.2.2. <i>Diagnosis and treatment</i>	6
1.2.3. <i>Animal models</i>	7
1.3. Aims.....	8
1.4. References.....	8
CHAPTER 2	13
2. <i>N</i>-methyl-<i>N</i>-nitrosourea as a mammary carcinogenic agent: a review	17
Abstract.....	17
2.1. Chemical induction.....	17
2.2. The potential of <i>N</i> -nitroso compounds as carcinogenic agents	18
2.3. Application of MNU and available animal models for the study of carcinogenesis.....	22
2.4. MNU administration.....	32
2.5. MNU-induced mammary tumors.....	33
2.6. Signaling pathways in MNU-induced rat mammary tumors: a homology with human cancer	37
2.7. Applications of MNU-induced mammary carcinogenesis	44
2.8. Transition of breast cancer therapies from female rats to human patients ..	51
2.9. Conclusion	52
2.10. References	52

CHAPTER 3.....	81
3. Antihistamines as promising drugs in cancer therapy: a review	85
.....	85
Abstract.....	85
3.1. Cancer.....	85
3.2. Mast cells.....	88
3.2.1. <i>Mast cells' maturation</i>	88
3.2.2. <i>Granules' content and release</i>	90
3.2.3. <i>Mast cells' classes</i>	93
3.3. Mast cells and disease.....	93
3.4. Cancer and inflammation.....	97
3.5. Histamine.....	99
3.6. Histamine receptors.....	100
3.7. Histamine and allergic diseases.....	102
3.8. Mast cells and histamine in cancer.....	102
3.9. Antihistamines.....	104
3.9.1. <i>Pharmacodynamics</i>	108
3.9.2. <i>Pharmacokinetics</i>	108
3.10. Antihistamines and cancer risk.....	108
3.11. Conclusion.....	118
3.12. References.....	118
 CHAPTER 4.....	 139
4. Ultrasonography as the gold standard for <i>in vivo</i> volumetric determination of chemically-induced mammary tumors.....	143
Abstract.....	143
4.1. Introduction.....	143
4.2. Material and Methods.....	144
4.2.1. <i>Animals</i>	144
4.2.2. <i>Chemicals</i>	145
4.2.3. <i>Animal experiments</i>	145
4.2.4. <i>Mammary tumor evaluation</i>	146
4.2.5. <i>Animal sacrifice and necropsy</i>	147
4.2.6. <i>Histology</i>	148

4.2.7. <i>Data analysis</i>	148
4.3. Results	149
4.3.1. <i>General observations</i>	149
4.3.2. <i>Mammary tumors number and histological evaluation</i>	149
4.3.3. <i>Tumor dimension</i>	151
4.3.4. <i>Tumor volume and weight</i>	152
4.3.5. <i>Invasive and non-invasive mammary tumors</i>	153
4.4. Discussion.....	154
4.5. Conclusion	157
4.6. References.....	157

CHAPTER 5..... 161

5. Ultrasonographic, thermographic and histologic evaluation of MNU-induced mammary tumors in female Sprague-Dawley rats	165
Abstract.....	165
5.1. Introduction.....	165
5.2. Material and Methods	167
5.2.1. <i>Animals</i>	167
5.2.2. <i>Chemicals</i>	167
5.2.3. <i>Animal experiments</i>	167
5.2.4. <i>Mammary tumors</i>	168
5.2.5. <i>Thermographic examination</i>	168
5.2.6. <i>Ultrasonographic examination</i>	169
5.2.7. <i>Necropsy</i>	169
5.2.8. <i>Histology</i>	170
5.2.9. <i>Statistics</i>	170
5.3. Results	171
5.3.1. <i>General findings</i>	171
5.3.2. <i>Macroscopic evaluation of mammary tumors</i>	171
5.3.3. <i>Mammary tumors</i>	171
5.3.4. <i>Mammary tumors histology</i>	174
5.4. Discussion.....	176
5.5. Conclusion	178
5.6. References.....	179

CHAPTER 6.....	183
6. Electron microscopy findings in MNU-induced mammary tumors	187
.....	187
Abstract.....	187
6.1. Introduction.....	187
6.2. Material and Methods	188
6.2.1. <i>Animals</i>	188
6.2.2. <i>Animal experiments</i>	188
6.2.3. <i>Animals' sacrifice and samples</i>	188
6.2.4. <i>Histological analysis</i>	189
6.2.5. <i>Transmission electron microscopy</i>	189
6.3. Results	190
6.3.1. <i>Animals</i>	190
6.3.2. <i>Mammary tumors</i>	190
6.3.3. <i>Histological classification</i>	190
6.3.4. <i>Transmission electron microscopy</i>	191
6.4. Discussion.....	194
6.5. Conclusion	196
6.6. References.....	196
 CHAPTER 7.....	 201
7. Effects of lifelong exercise training on mammary tumorigenesis induced by MNU in female Sprague-Dawley rats	205
Abstract.....	205
7.1. Introduction.....	206
7.2. Material and Methods	207
7.2.1. <i>Animals</i>	207
7.2.2. <i>Experimental design</i>	207
7.2.3. <i>Animals' killing</i>	208
7.2.4. <i>Blood samples analysis</i>	209
7.2.5. <i>Histological and immunohistochemical analysis</i>	209
7.2.6. <i>Statistical analysis</i>	210
7.3. Results	210
7.3.1. <i>Animals</i>	210

7.3.2. <i>Blood samples analysis</i>	212
7.3.3. <i>Mammary tumors</i>	213
7.3.4. <i>Histological and immunohistochemical analysis</i>	215
7.4. Discussion.....	218
7.5. Conclusion	221
7.6. References.....	221

CHAPTER 8..... 227

8. Long-term exercise training as a modulator of mammary cancer vascularization	231
Abstract.....	231
8.1. Introduction.....	231
8.2. Material and Methods	233
8.2.1. <i>Animals</i>	233
8.2.2. <i>Animal experiments</i>	233
8.2.3. <i>Mammary tumors evaluation</i>	234
8.2.4. <i>Thermographic evaluation</i>	234
8.2.5. <i>Ultrasonographic evaluation</i>	235
8.2.6. <i>Necropsy</i>	235
8.2.7. <i>Histology and immunohistochemistry</i>	235
8.2.8. <i>Statistical analysis</i>	236
8.3. Results	237
8.3.1. <i>General findings</i>	237
8.3.2. <i>Mammary tumors</i>	237
8.3.3. <i>Thermographic and ultrasonographic analysis</i>	239
8.3.4. <i>Mammary tumors histology</i>	241
8.3.5. <i>Correlations between data</i>	243
8.4. Discussion.....	244
8.5. Conclusion	246
8.6. References.....	246

CHAPTER 9..... 253

9. A contrast-enhanced ultrasonographic study about the impact of long-term exercise training on mammary tumors vascularization.....	257
---	------------

Abstract.....	257
9.1. Introduction.....	257
9.2. Material and Methods	258
9.2.1. <i>Animals</i>	258
9.2.2. <i>Experimental protocol</i>	259
9.2.3. <i>Animal experiments</i>	259
9.2.4. <i>CEUS</i>	260
9.2.5. <i>Statistical analysis</i>	261
9.3. Results	261
9.3.1. <i>General findings</i>	261
9.3.2. <i>Mammary tumors' development</i>	262
9.3.3. <i>Mammary tumors' vascularization</i>	262
9.4. Discussion.....	265
9.5. Conclusion	267
9.6. References.....	267

CHAPTER 10..... 271

10. Effects of long-term exercise training in <i>gastrocnemius</i> muscle in a rat model of <i>N</i>-methyl-<i>N</i>-nitrosourea-induced mammary tumors: ultrasonographic evaluation	275
Abstract.....	275
10.1. Introduction	275
10.2. Material and Methods.....	277
10.2.1. <i>Animals</i>	277
10.2.2. <i>Animal experiments</i>	277
10.2.3. <i>Evaluation of MNU effects</i>	278
10.2.4. <i>Ultrasound examination</i>	278
10.2.5. <i>Necropsy, sample collection and serum analysis</i>	279
10.2.6. <i>Statistics</i>	280
10.3. Results	280
10.3.1. <i>General observations</i>	280
10.3.2. <i>Body weight</i>	280
10.3.3. <i>Mammary tumors</i>	281
10.3.4. <i>Gastrocnemius muscle</i>	281

10.3.5. Echogenicity of muscle and fibrous tissue between muscle and tibia	282
10.3.6. Serum analysis	284
10.4. Discussion	284
10.5. Conclusion	286
10.6. References	286

CHAPTER 11..... 289

11. Mast cells on mammary carcinogenesis: host or tumor supporters?

..... 293

Abstract	293
----------	-----

11.1. Introduction	293
--------------------	-----

11.2. Material and Methods	295
----------------------------	-----

11.2.1. Animals	295
-----------------	-----

11.2.2. Experimental protocol	295
-------------------------------	-----

11.2.3. Sample collection	296
---------------------------	-----

11.2.4. Sacrifice	297
-------------------	-----

11.2.5. Blood samples analysis	297
--------------------------------	-----

11.2.6. Histology and immunohistochemistry	298
--	-----

11.2.7. Statistical analysis	298
------------------------------	-----

11.3. Results	298
---------------	-----

11.3.1. General data	298
----------------------	-----

11.3.2. Mammary tumors	300
------------------------	-----

11.3.3. Blood and urine samples analysis	301
--	-----

11.3.4. Histological analysis	302
-------------------------------	-----

11.3.5. Immunohistochemistry	305
------------------------------	-----

11.4. Discussion	307
------------------	-----

11.5. Conclusion	310
------------------	-----

11.6. References	310
------------------	-----

CHAPTER 12..... 315

**12. Modulation of mammary tumors vascularization by mast cells:
ultrasonographic and histopathological approaches..... 319**

12.1. Introduction	319
--------------------	-----

12.2. Material and Methods	321
----------------------------	-----

12.2.1. <i>Animals</i>	321
12.2.2. <i>Experimental protocol</i>	321
12.2.3. <i>Ultrasonographic evaluation</i>	322
12.2.4. <i>CEUS</i>	322
12.2.5. <i>Animals' sacrifice and necropsy</i>	323
12.2.6. <i>Histology and immunohistochemistry</i>	323
12.2.7. <i>Statistical analysis</i>	324
12.3. <i>Results</i>	324
12.3.1. <i>General findings and mammary tumor development</i>	324
12.3.2. <i>Histological classification of mammary tumors</i>	325
12.3.3. <i>Mammary tumor vascularization</i>	326
12.4. <i>Discussion</i>	331
12.5. <i>Conclusion</i>	334
12.6. <i>References</i>	334
CHAPTER 13	341
13. General discussion	343
13.1. <i>References</i>	348
CHAPTER 14	353
14. Final conclusions	355
14.1. <i>References</i>	356

LIST OF FIGURES

CHAPTER 2

- Figure 2.1.** Chemical structure of *N*-methyl-*N*-nitrosourea (MNU)..... 25
- Figure 2.2.** Decomposition of the chemical carcinogen *N*-methyl-*N*-nitrosourea (MNU) in water (pH>5) 26
- Figure 2.3.** Different macroscopic appearance of MNU-induced mammary tumors in female Sprague-Dawley rats 35 weeks after the administration of the carcinogen agent 37
- Figure 2.4.** Predicted interactions of the carcinogen agent MNU 44
- Figure 2.5.** MNU-induced mammary tumor in Sprague-Dawley female rats evaluated by ultrasonography (B mode) (A) and thermography (B)..... 51

CHAPTER 3

- Figure 3.1.** Schematic representation of carcinogenesis stages..... 87
- Figure 3.2.** Schematic representation of mast cells' maturation and activation 92
- Figure 3.3.** Bivalent role of mast cells on tumor progression..... 96

CHAPTER 4

- Figure 4.1.** Number of mammary tumors in animals from MNU-treated group (n=6) during the experimental protocol..... 150
- Figure 4.2.** Mammary tumor in an animal from MNU-treated group. 152

CHAPTER 5

- Figure 5.1.** Thermographic evaluation of a rat mammary tumor.....172
- Figure 5.2.** Comparison of mammary tumors evaluated by PDI (A) and B Flow (B) ultrasonographic modes 172
- Figure 5.3.** Color pixel density in PDI and B Flow ultrasonographic modes..... 173

CHAPTER 6

- Figure 6.1.** Semithin sections of mammary tumors stained with methylene blue and azur II (2:1) by light microscopy 191
- Figure 6.2.** Ultrastructural findings in MNU-induced cribriform and papillary carcinomas 1943

CHAPTER 7

Figure 7.1. Effects of exercise training on carcinogenic response of the mammary gland: cumulative number of mammary tumors in MNU sedentary and MNU exercised groups during the experimental protocol..... 214

Figure 7.2. Immunohistochemical staining for ERs α (A and C) and β (B and D) in mammary tumors from sedentary (A and B) and exercised (C and D) animals 217

CHAPTER 8

Figure 8.1. Visible image (A) and thermographic analysis (B) of a MNU-induced mammary tumor (temperature range 30-38°C)..... 240

Figure 8.2. Evaluation of mammary tumors from MNU sedentary (A and B) and MNU exercised (C and D) groups by Power Doppler (A and C) and B Flow (B and D) 241

Figure 8.3. Immunoexpression of VEGF-A in mammary tumors from MNU sedentary (A) and MNU exercised (B) animals..... 242

CHAPTER 9

Figure 9.1. Evaluation of a mammary tumor from MNU exercised group by Pulsed Doppler 264

Figure 9.2. Mathematical representation of the evaluation of the vascularization of a mammary tumor from MNU exercised group by CEUS after gamma variate curve fitting 265

CHAPTER 10

Figure 10.1. Measurement of length (1) and width (2) of *gastrocnemius* muscle..... 279

Figure 10.2. Measurement of mean pixels using Adobe Photoshop® in the lateral *gastrocnemius* muscle (A) and in the tissue between muscle and the tibia (B) 279

Figure 10.3. Optical density measurements for myostatin. 284

CHAPTER 11

Figure 11.1. Schematic representation of the experimental protocol 296

Figure 11.2. Graphic representation of the number of mammary tumors in Groups I, II and III and the respective week of appearance..... 300

Figure 11.3. Mean number of mast cells in mammary tumors from animals that received the carcinogen agent MNU and in the normal mammary gland..... 305

Figure 11.4. Mast cells stained with toluidine blue appearing purple in color in a papillary carcinoma induced by MNU (A). Immunohistochemical staining for Ki-67 (B), caspase-3 (C) and caspase-9 (D) in a mammary cribriform carcinoma induced by MNU in female rats. 307

CHAPTER 12

Figure 12.1. Evaluation of mammary tumors by PDI (A), B Flow (B) and Pulsed Doppler (C). Graphic representation of contrast intensity in each moment after its administration (TIC analysis) (D)..... 330

Figure 12.2. Immunoexpression of VEGF-A in a cribriform carcinoma. 331

LIST OF TABLES

CHAPTER 2

Table 2.1. List of <i>N</i> -nitroso-compounds and its sources of exposure.....	20
Table 2.2. <i>In vivo</i> studies using <i>N</i> -methyl- <i>N</i> -nitrosourea (MNU) as a carcinogenic agent	27
Table 2.3. Data from two experimental protocols of mammary carcinogenesis MNU-induced in female Sprague-Dawley rats performed by our research team.....	36
Table 2.4. Therapeutic approaches evaluated in MNU-induced mammary tumors.	46

CHAPTER 3

Table 3.1. Distribution of histamine receptors in all cells and tissues.....	101
Table 3.2. Most frequently used H1, H2, H3 and H4 antihistamines	107
Table 3.3. <i>In vitro</i> and <i>in vivo</i> studies to assess the efficacy of antihistamines in cancer therapy	112

CHAPTER 4

Table 4.1. Initial and final body weight (g) and body weight gain (%) in animals from both MNU-treated and control groups.....	149
Table 4.2. Histological classification of mammary tumors identified in animals from MNU-treated group	150
Table 4.3. Measurement of length, width and depth by caliper (before and after necropsy) and ultrasonography in 13 mammary tumors identified in animals from group MNU.	151
Table 4.4. Volume and weight of 13 mammary tumors calculated using different formulas	153
Table 4.5. Comparison of tumor length, width, depth, volume and weight between non-invasive and invasive mammary tumors	154

CHAPTER 5

Table 5.1. Correlation between ultrasonographic methods and thermography	174
Table 5.2. Histological classification of mammary tumors	175
Table 5.3. Characterization of histological lesions by CEUS.....	176

CHAPTER 7

Table 7.1. Final body weight, tumor weight and accurate body weight.....	211
Table 7.2. Organs' weight in all groups at the end of the experiment.....	211
Table 7.3. Characterization of animals' response to the MNU-induced mammary tumors and physical exercise: biochemical profile.....	213
Table 7.4. Histological classification of mammary tumors developed by animals from MNU sedentary and exercised groups.....	216
Table 7.5. Immunohistochemical expression of estrogen receptors α and β in MNU groups (% of immunopositive cells).....	218

CHAPTER 8

Table 8.1. Histological classification, weight, volume and area of necrosis of mammary tumors identified in both MNU sedentary and exercised groups taking into account the predominant histological pattern	238
Table 8.2. Thermographic, ultrasonographic and immunohistochemical evaluation of mammary tumors in both groups MNU sedentary and MNU exercised.....	240
Table 8.3. Semi-quantitative evaluation of VEGF-A immunoeexpression in neoplastic cells of MNU-induced mammary tumors from sedentary and exercised animals	243
Table 8.4. Correlation between data from thermography, ultrasonography and immunohistochemistry	244

CHAPTER 9

Table 9.1. Evaluation of mammary tumors vascularization by Pulsed Doppler and CEUS	263
Table 9.2. Qualitative evaluation of CEUS of mammary tumors in both MNU-exposed experimental groups	264

CHAPTER 10

Table 10.1. Mean \pm S.D. of body weight, tumor weight and accurate body weight ...	281
Table 10.2. Mean \pm S.D. of <i>gastrocnemius</i> muscle weight at necropsy, and its length and width measured by ultrasonography.....	282
Table 10.3. Echogenicity of <i>gastrocnemius</i> muscle	283

Table 10.4. Echogenicity of fibrous tissue between muscle and tibia	283
--	-----

CHAPTER 11

Table 11.1. Initial and final accurate body weight (g) and ponderal gain (%), and mammary tumor volume and weight in all experimental groups	299
---	-----

Table 11.2. Absolute organs' weight (g) in all groups	299
--	-----

Table 11.3. Histamine serum levels (ng/mL) in all groups before the tumors development and at the end of the experimental protocol	301
---	-----

Table 11.4. Characterization of the animal response to the ketotifen administration: biochemical profile	302
---	-----

Table 11.5. Histological classification of mammary tumors developed by animals from experimental groups that received the carcinogen agent MNU	304
---	-----

Table 11.6. Immunohistochemical evaluation of proliferation and apoptois of mammary tumors developed by animals from experimental groups that received the carcinogen agent MNU	306
--	-----

CHAPTER 12

Table 12.1. Histological classification of each mammary tumor according to the predominant histological pattern	326
--	-----

Table 12.2. Evaluation of mammary tumor vascularization by ultrasonography (Doppler, B Flow and CEUS) and immunohistochemistry	328
---	-----

Table 12.3. Qualitative evaluation of CEUS of mammary tumors in all experimental groups	329
--	-----

LIST OF ABBREVIATURES AND SYMBOLS

13cRA	-	13-cis Retinoic acid
3D	-	Three dimensional
ALT	-	Alanine aminotransferase
AMPK	-	Phosphorylated adenosine monophosphate-activated protein kinase
ANOVA	-	Analysis of variance
AT	-	Arrival time
ATP	-	Adenosine triphosphate
AUC	-	Area under the curve
BBN	-	<i>N</i> -butyl- <i>N</i> -(4-hydroxybutyl)nitrosamine
<i>BRCA1</i>	-	Breast cancer gene 1
<i>BRCA2</i>	-	Breast cancer gene 2
b.w.	-	Body weight
CART	-	Amphetamine-regulated transcript peptide
CCL	-	CC-chemokine ligand
CEUS	-	Contrast-enhanced ultrasound
CKs	-	Cytokeratins
CPD	-	Color pixel density
CpG-ODN	-	CpG oligodeoxynucleotides
CRP	-	C-reactive protein
CTMC	-	Connective tissue mast cells
CXCL	-	CXC-chemokine ligand
CYP	-	Cytochrome P450
D	-	Depth
DADS	-	Diallyl disulfide
DMBA	-	7,12-Dimethylbenz(a)anthracene
DNA	-	Deoxyribonucleic acid
Dox	-	Doxorubicin
DPPE	-	<i>N,N</i> -diethyl-2-(4-(phenylmethyl)phenoxy) ethanamine HCl
d.w.	-	Drinking water
ECL	-	Enhanced chemiluminescence
EGFR	-	Epidermal growth factor receptor

EIF4E	-	Eukaryotic translation initiation factor 4E
ELISA	-	Enzyme-linked immunosorbent assay
ER α	-	Estrogen receptor alpha
ER β	-	Estrogen receptor beta
ESR1	-	Estrogen receptor 1
Fc ϵ RI	-	High-affinity receptor for immunoglobulin E
FDA	-	Food and Drug Administration
FGF2	-	Fibroblast growth factor 2
Ge-132	-	Carboxyethyl germanium sesquioxide
GIMP	-	GNU Image Manipulation Program
GM-CSF	-	Granulocyte-macrophage colony-stimulating factor
H1	-	Histamine receptor 1
H2	-	Histamine receptor 2
H3	-	Histamine receptor 3
H4	-	Histamine receptor 4
HDL	-	High-density lipoprotein
HE3235	-	17 α -ethynyl-5 α -androstane-3 α , 17 β -diol
H&E	-	Hematoxylin and eosin
<i>HRAS</i>	-	Harvey rat sarcoma viral oncogene homolog
I2	-	Iodine
ICC	-	Intraclass correlation coefficient
i.c.v.	-	Intracerebroventricular administration
i.d.	-	Intradermal administration
i.duc.	-	Intraductal administration
IFN	-	Interferon
Ig	-	Immunoglobulin
i.g.	-	Intragastric administration
IGF1	-	Insulin-like growth factor 1 (somatomedin C)
IGF1-R	-	Insulin-like growth factor 1 receptor
IL	-	Interleukin
i.m.	-	Intramuscular administration
iNOS	-	Inducible nitric oxide synthase
i.p.	-	Intraperitoneal administration

i.r.	-	Intrarectal administration
IRF1	-	Interferon regulatory factor 1
i.v.	-	Intravenous administration
i.vag.	-	Intravaginal administration
i.ves.	-	Intravesical administration
KCNH1	-	Potassium voltage-gated channel, subfamily H (eag-related), number 1
ket	-	Ketotifen
L	-	Length
LDL	-	Low-density lipoprotein
LIF	-	Leukemia inhibitory factor
LT	-	Leukotrien
MCP	-	Monocyte chemoattractant protein
MC _T	-	Mast cells that only contain tryptase
MC _{TC}	-	Mast cells that contain tryptase and chymase
MGMT	-	O-6-methylguanine-DNA methyltransferase
MI	-	Mortality index
MMC	-	Mucosal mast cells
MMPs	-	Matrix metalloproteinases
MNNG	-	Methylnitrosnitroguanidine
MNU	-	<i>N</i> -methyl- <i>N</i> -nitrosourea
MPG	-	<i>N</i> -methylpurine DNA glycosylase
MRI	-	Magnetic resonance imaging
mTOR	-	Mammalian target of rapamycin
MTT	-	3-(4,5-dimethylthiazol-2-yl)-2,5-diphenyltrazolium bromide
MVD	-	Microvessel density
n	-	Number of samples
NDMA	-	<i>N</i> -nitrosodimethylamine
NF-κB	-	Nuclear factor-kappa B
NGF	-	Nerve growth factor
NNK	-	4-methylnitrosamino-1-3-pyridyl-1-butanone
OPRM1	-	Opioid receptor mu 1
OsO ₄	-	Osmium tetroxide

PBS	-	Phosphate-buffered saline
PDGF	-	Platelet-derived growth factor
PDI	-	Power Doppler
PG	-	Ponderal gain
PI	-	Peak intensity
PMS2	-	Postmeiotic segregation increased 2
p.o.	-	Oral administration
ppm	-	Parts per million
RNA	-	Ribonucleic acid
ROI	-	Region of interest
ROS	-	Reactive oxygen species
SAC	-	S-allyl cysteine
s.c.	-	Subcutaneous administration
SCF	-	Stem cell factor
S.D.	-	Standard deviation
S.E.	-	Standard error
SPSS	-	Statistical Package for the Social Sciences
STZ	-	Streptozotocin
T°	-	Temperature
T4	-	Thyroxine
TBS	-	Tris-buffered saline
TBS-T	-	Tris-buffered saline with Tween
TEM	-	Transmission electron microscopy
TGF- β	-	Transforming growth factor-beta
TIC	-	Time intensity curve
TLR	-	Toll-like receptor
TNF	-	Tumor-necrosis factor
TTP	-	Time to peak
UTAD	-	University of Trás-os-Montes and Alto Douro
V	-	Volume
VEGF	-	Vascular endothelial growth factor
W	-	Width
WHO	-	World Health Organization

CHAPTER 1

GENERAL INTRODUCTION

1. General introduction

The present work intend to contribute to the monitoring and treatment of mammary cancer. For this, two therapeutic approaches were evaluated in two distinct experimental protocols using Sprague-Dawley female rats. In both experiments, mammary tumor development was induced through the administration of the carcinogen agent *N*-methyl-*N*-nitrosourea (MNU); the main physiological variables, like body weight and food and water consumption, were evaluated; and tumor growth and vascularization were non-invasively monitored by employing clinical and imaging methodologies, such as caliper measurement, ultrasonography and thermography. In order to evaluate the therapeutic approaches, it was promoted the practice of moderate exercised training for a long period of time in the first experimental protocol and the second-generation noncompetitive H1-antihistamine and mast cell stabilizer drug ketotifen was administered to the animals in the second experiment. Both experimental protocols were performed in the University of Trás-os-Montes and Alto Douro (UTAD). Despite this, four months were spent in the Faculty of Veterinary Medicine of the University of Ghent under the supervision of Professor Jimmy Saunders and Professor Katrien Vanderperren in order to evaluate the contrast-enhanced ultrasound (CEUS) of the mammary tumors.

The present thesis is divided into chapters. A general introduction of the main subject of the thesis is provided in the first chapter (Chapter 1), followed by two review works (Chapter 2 and 3) about the use of MNU as a mammary carcinogenic agent and the antihistamines as promising drugs in cancer therapy, respectively. Following these, three chapters (Chapter 4 to 6) about the monitoring of mammary tumors are presented. Subsequently, four chapters (Chapter 7 to 10) on the effects of long-term moderate exercise training on mammary carcinogenesis and in other systems, like skeletal muscle, and two chapters (Chapter 11 and 12) about the effects of ketotifen on mammary tumor progression and vascularization are displayed. A general discussion and the main conclusions are presented in the last two chapters (Chapters 13 and 14).

1.1. Cancer

Cancer is a major public health concern, figuring among the leading causes of morbidity and mortality worldwide [1]. Approximately 14 million new cases and 8.2 million deaths from cancer were recorded in 2012. About 70% of all cancer deaths occur

in low- and middle-income countries. Disappointing projections are being pointed for the next years, with an increase in the number of new cancer cases *per* year to 22 million over the next two decades [2]. Although more than 100 types of cancers were described and any part of the body can be affected, the most frequent types of cancer in men are lung, prostate, colorectal, stomach and liver. Breast, colorectal, lung, cervix and stomach cancer are the most frequently found in women [1].

Cancer is a complex and multistage biological process that progresses over several years [3–5]. It comprises four different but linked stages: initiation, promotion, progression and metastization. The carcinogenesis begins with an irreversible alteration (deoxyribonucleic acid (DNA)-damage) in a cell that leads to the conversion of a normal cell into an initiated one. This DNA-damage may occur spontaneously or may be induced by physical agents (X-rays, gamma radiation), chemical carcinogens (asbestos, tobacco, arsenic, MNU; 7,12-Dimethylbenz(a)anthracene (DMBA), *N*-butyl-*N*-(4-hydroxybutyl)nitrosamine (BBN), Diethylnitrosamine) or biological agents (infection by papillomavirus, hepatitis virus, *Schistosoma haematobium*, *Helicobacter pylori*, *Clonorchis sinensis*). Then, during promotion the initiated cells grow and divide in an uncontrolled way as a consequence of accumulated abnormalities, originating a population of preneoplastic cells. The promotion is a relatively long process that may be reversible (tumor growth rate may be modulated). During progression, a fast increase in tumor size and conversion of preneoplastic cells into neoplastic ones as a consequence of additional genetic changes are observed. Metastization is characterized by spread of cancer cells from primary tumor to distant organs through blood or lymphatic system. Although the ability to metastasize is exclusive of malignant tumors, not all malignant tumor metastasize [6,7].

1.2. Breast cancer

Breast cancer is the most frequent cancer in women, being traditionally considered a female-specific disease [8]. According to the World Health Organization (WHO), this type of cancer was responsible for more than a half a million of deaths worldwide in the year 2012. The incidence of breast cancer varies according to geographical regions, with a higher incidence recorded in North America, Western Europe and Oceania when compared with middle- and low-income countries [9]. Concerning to our pets, mammary

cancer constitutes the most frequent cancer in intact female dogs and the third most frequent in female cats [10,11].

1.2.1. Risk factors and prevention

Several factors, namely age, sex, race, reproductive factors, estrogens exposure, body weight, genetic mutations and lifestyle, have been associated with the risk of breast cancer development [12,13].

Breast cancer development is age-dependent, being extremely rare before 30 years of age and a higher incidence observed in women older than 55 years of age. The risk of developing breast cancer is 1/53 for women before 49 years of age, rising to 1/43 for women between 50 and 59 years of age, and to 1/23 for women between 60 and 69 years of age. It is probably associated with the less effectiveness of cellular repair mechanisms in older people when compared with younger people [14].

Breast cancer development is predominantly diagnosed in women. Inversely, it is only sporadically detected in men constituting less than 1% of all diagnosed breast cancers. The frequency of occurrence of this kind of cancer is higher in Caucasian women (127.4 in 100 000 individuals) when compared with Black women (121.4 in 100 000 individuals) [15].

The longer the estrogens exposure, higher is the breast cancer risk development. Women with early menarche (before 12 years old) and those that did not reach the menopause until 55 years of age or used hormone replacement therapy have higher risk of breast cancer development when compared with those that menstruated by the first time after 15 years old or those that experienced menopause before the age of 45 [12,16]. Furthermore, it was demonstrated that nulliparous women and those that experienced the first full-term pregnancy after 30 years of age have a higher risk of breast cancer development. This may be related with the differentiation of epithelial cells that occurs in the breast during the last part of pregnancy and lactation, decreasing their susceptibility to carcinogenesis [17].

High body mass index is considered a risk factor for breast cancer development due to the increase of insulin and insulin like factors that have been associated with an increase in breast cancer risk development. Furthermore, high body mass index is commonly

associated with the accumulation of abdominal fat that is an extragonadal source of estrogens [18,19].

Mutations in Breast Cancer gene (*BRCA*) 1 and *BRCA2* are associated with an inherited susceptibility for breast cancer development. These genes codify tumor suppressor proteins that are responsible for repairing DNA damage and ensure the stability of genetic material. The risk of breast cancer development is increased in 65% in individuals carrying mutations in *BRCA1* or *BRCA2* [20].

Concerning to lifestyle, alcohol use, unhealthy diet and physical inactivity are the main cancer risk factors. The alcohol consumption may increase the breast cancer risk due to the stimulation of metabolism of carcinogens such as acetaldehyde, by decreasing the efficiency of DNA repair or reducing intake of protective nutrients [13]. Unhealthy food supplemented with chemical substances to enhance flavor or preserve food that may act as promoters of neoplastic transformation in mammary gland cells increase the risk of breast cancer development [12]. It was also suggested that regular physical activity with a frequency of 3-5 times a week reduces the breast cancer risk by 20-40% due to the reinforcement of immune system. Additionally, physical activity improves general fitness and quality of life [21].

Taking into account all the factors that influence breast cancer risk development, the number of cancers may be reduced by avoiding exposure to them and maintaining a healthy lifestyle.

1.2.2. Diagnosis and treatment

The early detection of breast cancer is intimately related to the success of the treatments and prognosis. Breast cancer screening programs are running in more than 26 countries around the world [22,23] and they have greatly contributed to increase the early detection of breast cancer and consequent reduction of mortality [24]. Although mammography is considered the gold standard for breast cancer screening, other imaging modalities like ultrasonography, magnetic resonance, computed tomography and thermography are available [25]. Furthermore, the self-examination and clinical examination of the breasts are also considered methods for the detection of breast alterations [26].

Despite several therapeutic approaches are available, namely surgery, radiotherapy, chemotherapy, hormone therapy and immunotherapy, the distinct response of cancer to the therapies, the devastating effects of some of these therapies for patients and their ineffectiveness are the major concerns about cancer. Additionally to these, skeletal muscle wasting also constitutes a great concern on cancer treatment. According to several authors, it is a major factor involved in cancer cachexia contributing to physical disability, weakness, reduced tolerance to anticancer therapies and decreased survival [27–29]. Cancer-induced cachexia has been implicated in up to 20% of cancer-related deaths [30]. In order to increase the lifespan and improve the quality of life of oncologic patients, it is important to search for new or at least adjuvant therapies that may improve the lifespan and quality of life of oncologic patients.

1.2.3. Animal models

Intensive research has been carried out in breast cancer, aiming to better understand the reasons for tumor development and progression, and to develop new preventive and/or therapeutic strategies more effective and with less side effects for patients. In this way, animal models have been intensively used for the study of mammary carcinogenesis. Although *in vitro* models may be used to study cancer, *in vivo* models are the link between experimental and clinical research. Indeed, animals allow a better understanding of several aspects of mammary carcinogenesis, namely genetic and molecular basis, pathogenesis, and the evaluation of several preventive and therapeutic approaches [31,32].

Although different species may be used for *in vivo* experiments, rats and mice are those most frequently used in research protocols [33]. When compared with other species, they have several advantages: their physiology and genetic are well-known, they are small animals and consequently they are easily accommodated and manipulated, they are relatively cheap, and they are mammals with several anatomical, physiological, genetic and biochemical similarities with humans [34,35].

Distinct rat models of mammary cancer may be used, namely mammary cancer induction by the administration of carcinogenic agents, exposition to radiation, hormone administration, implantation of cancer cells or use of genetically engineered animals. Among these, the rat model of mammary cancer chemically-induced by the

administration of carcinogenic agents MNU or DMBA are the most frequently used for the study of mammary carcinogenesis. When compared with DMBA, MNU has the advantage to be a direct alkylating agent that does not require prior metabolic activation to exert carcinogenic effects [36,37]. Additionally, MNU-induced mammary tumors are similar to those developed by women in terms of their histopathology, hormone dependency, genetic alterations and ability to metastasize [38].

1.3. Aims

Breast cancer is one of the most frequent cancers among women worldwide. Regardless all the research in this field, the devastating effects of chemotherapy for patients remain a great problem in cancer treatment which has motivated the researchers on the search of new therapeutic (alternative or at least adjuvant) approaches that may improve the quality of life of oncologic patients.

In this way, the present work had as mains goals:

- i) To monitor mammary tumor growth and vascularization by employing non-invasive methodologies.
- ii) To evaluate the effects of long-term moderate exercise training on mammary cancer progression and vascularization, and in other biological systems, namely in skeletal muscle.
- iii) To assess the role of the second-generation H1-antihistamine and mast cell stabilizer drug ketotifen on mammary carcinogenesis.

1.4. References

- [1] World Health Organization (WHO). Cancer - Fact sheet n° 297. *WHO*, **2015**.
- [2] Stewart, B.; Wild, C. World cancer report. *WHO*, **2014**.
- [3] Frank, LM.; Knowles, MA. What is cancer? In *Introduction to the cellular and molecular biology of cancer* (Knowles, M. and Selby, P., eds), **2005**, pp. 1–24, Oxford University Press.

- [4] Hall, EJ.; Giaccia, AJ. Cancer biology. In *Radiobiology for the radiologist* (Hall, E. J. and Giaccia, A. J., eds), **2006**, pp. 274–302, Lippincott Williams & Wilkins.
- [5] Hanahan, D.; Weinberg, RA. The hallmarks of cancer. *Cell*, **2000**, 100, 57–70.
- [6] Eickmeyer, SM.; Gamble, GL.; Shahpar, S.; Do, KD. The role and efficacy of exercise in persons with cancer. *PMR: J. Inj. Funct. Rehabil.*, **2012**, 4, 874–881.
- [7] Siddiqui, IA.; Sanna, V.; Ahmad, N.; Sechi, M.; Mukhtar, H. Resveratrol nanoformulation for cancer prevention and therapy. *Ann. N.Y. Acad. Sci.*, **2015**, 1348, 20–31.
- [8] Ly, D.; Forman, D.; Ferlay, J.; Brinton, LA.; Cook, MB. An international comparison of male and female breast cancer incidence rates. *Int. J. Cancer*, **2013**, 132, 1918–1926.
- [9] International Agency for Research on Cancer. Globocan 2012: estimated cancer incidence, mortality and prevalence worldwide in 2012. *WHO*, **2015**.
- [10] Viste, JR.; Myers, SL.; Singh, B.; Simko, E. Feline mammary adenocarcinoma: tumor size as a prognostic indicator. *Can. Vet. J.*, **2002**, 43, 33–37.
- [11] Moe, L. Population-based incidence of mammary tumours in some dog breeds. *J. Reprod. Fertil. Suppl.*, **2001**, 57, 439–443.
- [12] Kamińska, M.; Ciszewski, T.; Łopacka-Szatan, K.; Miotła, P.; Starosławska, E. Breast cancer risk factors. *Menopause Rev.*, **2015**, 14, 196–202.
- [13] Singletary, SE. Rating the risk factors for breast cancer. *Ann. Surg.*, **2003**, 237, 474–482.
- [14] Siegel, R.; Naishadham, D.; Jemal, A. Cancer statistics, 2012. *CA Cancer J. Clin.*, **2012**, 62, 10–29.
- [15] Gnerlich, JL.; Deshpande, AD.; Jeffe, DB.; Seelam, S.; Kimbuende, E.; Margenthaler, JA. Poorer survival outcomes for male breast cancer compared with female breast cancer may be attributable to in-stage migration. *Ann. Surg. Oncol.*, **2011**, 18, 1837–1844.
- [16] Brinton, LA.; Schairer, C.; Hoover, RN.; Fraumeni, JF. Menstrual factors and risk of breast cancer. *Cancer Invest.*, **1988**, 6, 245–254.
- [17] Sharpe, CR. A developmental hypothesis to explain the multicentricity of breast cancer. *CMAJ*, **1998**, 159, 55–59.
- [18] Clemons, M.; Goss, P. Estrogen and the risk of breast cancer. *N. Engl. J. Med.*, **2001**, 344, 276–285.

- [19] Suga, K.; Imai, K.; Eguchi, H.; Hayashi, S.; Higashi, Y.; Nakachi, K. Molecular significance of excess body weight in postmenopausal breast cancer patients, in relation to expression of insulin-like growth factor I receptor and insulin-like growth factor II genes. *Jpn. J. Cancer Res.*, **2001**, 92, 127–134.
- [20] Antoniou, A.; Pharoah, PDP.; Narod, S.; Risch, HA.; Eyfjord, JE.; Hopper, JL.; Loman, N.; Olsson, H.; Johannsson, O.; Borg, A.; Pasini, B.; Radice, P.; Manoukian, S.; Eccles, DM.; Tang, N.; Olah, E.; Anton-Culver, H.; Warner, E.; Lubinski, J.; Gronwald, J.; Gorski, B.; Tulinius, H.; Thorlacius, S.; Eerola, H.; Nevanlinna, H.; Syrjäkoski, K.; Kallioniemi, O-P.; Thompson, D.; Evans, C.; Peto, J.; Lalloo, F.; Evans, DG.; Easton, DF. Average risks of breast and ovarian cancer associated with *BRCA1* or *BRCA2* mutations detected in case series unselected for family history: a combined analysis of 22 studies. *Am. J. Hum. Genet.*, **2003**, 72, 1117–1130.
- [21] Lynch, BM.; Neilson, HK.; Friedenreich, CM. Physical activity and breast cancer prevention. *Recent Results Cancer Res.*, **2011**, 186, 13–42.
- [22] Paap, E.; Verbeek, ALM.; Botterweck, AAM.; Van Doorne-Nagtegaal, HJ.; Imhof-Tas, M.; De Koning, HJ.; Otto, SJ.; De Munck, L.; Van der Steen, A.; Holland, R.; Den Heeten, GJ.; Broeders, MJM. Breast cancer screening halves the risk of breast cancer death: a case-referent study. *Breast*, **2014**, 23, 439–444.
- [23] National Cancer Institute (NCI). Breast cancer screening programs in 26 ICSN countries, 2012: organization, policies, and program reach. *NCI*, **2015**.
- [24] Gøtzsche, PC.; Jørgensen, KJ. Screening for breast cancer with mammography. *Cochrane Database Syst. Rev.*, **2013**, 4, CD001877.
- [25] Kösters, JP.; Gøtzsche, PC. Regular self-examination or clinical examination for early detection of breast cancer. *Cochrane Database Syst. Rev.*, **2003**, 2, CD003373.
- [26] Güleser, GN.; Unalan, D.; Akyldz, HY. The knowledge and practice of breast self-examination among healthcare workers in Kayseri, Turkey. *Cancer Nurs.*, 32, E1–7.
- [27] Argilés, JM.; Busquets, S.; Stemmler, B.; López-Soriano, FJ. Cancer cachexia: understanding the molecular basis. *Nat. Rev. Cancer*, **2014**, 14, 754–762.
- [28] Julienne, CM.; Dumas, J-F.; Goupille, C.; Pinault, M.; Berri, C.; Collin, A.; Tesseraud, S.; Couet, C.; Servais, S. Cancer cachexia is associated with a decrease

- in skeletal muscle mitochondrial oxidative capacities without alteration of ATP production efficiency. *J. Cachexia. Sarcopenia Muscle*, **2012**, 3, 265–275.
- [29] Fearon, K.; Strasser, F.; Anker, SD.; Bosaeus, I.; Bruera, E.; Fainsinger, RL.; Jatoi, A.; Loprinzi, C.; MacDonald, N.; Mantovani, G.; Davis, M.; Muscaritoli, M.; Ottery, F.; Radbruch, L.; Ravasco, P.; Walsh, D.; Wilcock, A.; Kaasa, S.; Baracos, VE. Definition and classification of cancer cachexia: an international consensus. *Lancet Oncol.*, **2011**, 12, 489–495.
- [30] MacDonald, N.; Easson, AM.; Mazurak, VC.; Dunn, GP.; Baracos, VE. Understanding and managing cancer cachexia. *J. Am. Coll. Surg.*, **2003**, 197, 143–161.
- [31] Clarke, R. Animal models of breast cancer: their diversity and role in biomedical research. *Breast Cancer Res. Treat.*, **1996**, 39, 1–6.
- [32] Iannaccone, PM.; Jacob, HJ. Rats! *Dis. Model. Mech.*, **2009**, 2, 206–210.
- [33] European Commission. Seventh report on the statistics on the number of animals used for experimental and other scientific purposes in the member states of the European Union. *European Commission*, **2013**, 1–40.
- [34] Kararli, TT. Comparison of the gastrointestinal anatomy, physiology, and biochemistry of humans and commonly used laboratory animals. *Biopharm. Drug Dispos.*, **1995**, 16, 351–380.
- [35] National Research Council of The National Academies. *Guide for the care and use of laboratory animals*. **2011**, The National Academies Press.
- [36] Faustino-Rocha, AI.; Ferreira, R.; Oliveira, PA.; Gama, A.; Ginja, M. *N*-methyl-*N*-nitrosourea as a mammary carcinogenic agent. *Tumor Biol.*, **2015**, 36, 9095–9117.
- [37] Murray, TJ.; Ucci, AA.; Maffini, M V.; Sonnenschein, C.; Soto, AM. Histological analysis of low dose NMU effects in the rat mammary gland. *BMC Cancer*, **2009**, 9, 267.
- [38] Steele, VE.; Lubet, RA. The use of animal models for cancer chemoprevention drug development. *Semin. Oncol.*, **2010**, 37, 327–238.

CHAPTER 2

***N*-METHYL-*N*-NITROSOUREA AS A MAMMARY CARCINOGENIC AGENT: A REVIEW**

THE CONTENT OF THIS CHAPTER WAS PUBLISHED IN:

Faustino-Rocha AI, Ferreira R, Oliveira PA, Gama A, Ginja M. 2015. *N*-methyl-*N*-nitrosourea as a mammary carcinogenic agent. *Tumor Biology* 36 (12): 9095-9117.
DOI: 10.1007/s13277-015-3973-2. *Review*. (Full paper)

2. *N*-methyl-*N*-nitrosourea as a mammary carcinogenic agent: a review

Abstract

Administration of chemical carcinogens is one of the most commonly used methods to induce tumors in several organs in laboratory animals, in order to study human oncologic diseases. The carcinogen agent *N*-methyl-*N*-nitrosourea (MNU) is the oldest member of nitroso compounds that has the ability to alkylate deoxyribonucleic acid (DNA). MNU is classified as a complete, potent, and direct alkylating compound. Depending on animal species and strains, dose, route, and age at the administration, MNU may induce tumor development in several organs. The aim of this manuscript was to review MNU as a carcinogenic agent, taking into account that this carcinogen has been frequently used in experimental protocols to study the carcinogenesis in several tissues, namely breast, ovary, uterus, prostate, liver, spleen, kidney, stomach, small intestine, colon, hematopoietic system, lung, skin, retina, and urinary bladder. In this paper, we also reviewed the experimental conditions to chemical induction of tumors in different organs with this carcinogen agent, with a special emphasis on mammary carcinogenesis.

Keywords: animal models, carcinogen agent, mammary cancer, MNU

2.1. Chemical induction

From the biological point of view, cancer is a complex disease. Since the beginning of the development of modern medicine, this disease encouraged researchers to use animal models, in order to better study and understand it. In 1915, the Japanese scientist Katsusaburō Yamagiwa and his assistant Kōichi Ichikawa performed the first studies regarding carcinogenic agents. Using four experimental protocols, based on the application of a simple coal tar painting on different locations in rabbits' ears, they induced papillomas, demonstrating the coal tar painting carcinogenic properties [1]. After these researches, there was a great investment in the research of other carcinogen agents to induce tumors in other tissues, and animals started to be used to the study of several human oncologic diseases. From the 60s of the last century, there was a great investment in the research of carcinogenic compounds whereby new carcinogen agents were gradually discovered with specific tropism for different target tissues [2].

In a general way, carcinogenic agents have the ability to induce tumors in several locations, depending on application site (i.e., urinary bladder, skin), absorption site (i.e., forestomach using oral administration), organ of metabolism (i.e., liver), and excretory organs (i.e., ureters, urinary bladder, urethra) [2]. When compared with other animal models, namely genetically modified, xenograft and syngeneic models, the chemically induced tumors have some advantages, namely their short period of latency and high reproducibility. Attending to the similarities with the carcinogenesis process that occurs in humans, like tumor development through a series of progressive steps including initiation, promotion, progression, and metastasis, these *in vivo* systems provide more relevant information about the carcinogenesis process in a target organ and the possibility to evaluate new preventive and therapeutic agents [3,4]. However, these chemically-induced models have also some limitations, such as the high costs to obtain and maintain the animals, the need of use carcinogenic agents in high doses to induce cancer development, application of the carcinogenic agents during a long-time period, toxicity of the carcinogenic compounds that may cause harm to people that handle the animals and to the environment, and the lack of organ specificity of the carcinogenic compounds, since several carcinogens have the capacity to induce tumor development in more than one organ [3,4].

2.2. The potential of *N*-nitroso compounds as carcinogenic agents

N-nitroso compounds are a vast group of chemical compounds easily produced by the reaction of nitrogen oxides with secondary and tertiary amines or amides [5–8] (Table 2.1). Nitroso compounds act as carcinogenic agents inducing tumor development in several experimental animal models, being also possible that these agents may be associated with the development of some human cancers [6]. Humans are frequently exposed to these compounds through diet (cured meats, bacon, smoked and fried fish, beer, butter, sausages, cheese, ham, Thai fish, dried milk, and pickles), occupation (hairdresser; rubber, metal, and leather industry; and agriculture), social addictions (tobacco smoke), and minor sources of exposure like pharmaceutical products, cosmetics, and indoor and outdoor air [7,9–13]. The accumulation of these compounds in food is associated with the processing conditions, such as pickled foods, stored under humid

conditions, smoked in air saturated with nitrogen, dried at high temperatures, and cured with nitrate or nitrite [14].

Some of these nitroso-compounds, namely *N*-methyl-*N*-nitrosourea (MNU), *N*-nitrosodimethylamine (NDMA), streptozotocin (STZ), 4-methylnitrosamino-1-3-pyridyl-1-butanone (NNK), and methylnitrosnitroguanidine (MNNG), are alkylating agents able to react with biomolecules, like nucleic acids of deoxyribonucleic acid (DNA) and ribonucleic acid (RNA), and although it was not fully understood, they have also the ability to react with proteins (Deshpande, 2002; Kyrtopoulos, 1998; Lijinski, 1981). Some of these alkylating agents, namely MNU, STZ and MNNG, have been used with carcinogenic, mutagenic, teratogenic, and immunosuppressant purposes, but they were also used as antineoplastic agents to treat L1210 leukemia cells implanted in a mice model [18,19].

Alkylating agents are also used for military purposes (chemical weapons) in poison gases [20] or sulfur mustard (mustard gas) [21]. Mustard gas was first produced by Despretz in 1822 and used in the World War I in 1917 by the Germans against the British in a field near Ypres in Belgium, where during a period of ten days, more than one million of mustard shells were used [21]. After this, a campaign in order to interdict chemical weapons began, and in the year 1925, the Geneva Protocol for the prohibition of the use of asphyxiating and poisonous gases and bacteriological methods in war was promulgated [22]. However, in the years 1935 and 1936, Italian troops used mustard gas in combat with native forces during the campaign in Ethiopia [23]; between 1963 and 1967, it was also used by Egyptian forces in Yemen and, between 1983 and 1988, by the Iraqi army against Iranian soldiers where approximately 5,000 citizens were killed [24].

The agents that react with DNA causing DNA damages are considered genotoxic chemicals [15]. They transfer an alkyl group and react with nucleophilic nitrogen and oxygen atoms in the purine and pyrimidine bases, and phosphate group of DNA producing a wide range of DNA adducts, namely N^7 and N^3 alkylpurines, and O^6 -alkylguanine and O^4 -alkylthymine [16,17,25–27]. Although O^6 -alkylguanine is a minor alkylation product, it is considered to be responsible for the mutagenic and carcinogenic actions of these alkylating agents [28]. The O^6 -alkylguanine is produced by the alkylation of the DNA molecule at O^6 position of guanine. This alteration in the DNA structure will create a wrong nucleotide incorporation during the replication of DNA and consequently in the transcription of RNA that has an important role in mutagenesis and carcinogenesis

processes [6,29,30]. Among the nitroso compounds mentioned above, the MNU is one of the most frequently used in assays of chemically-induced carcinogenesis [13,31,32].

Table 2.1. List of *N*-nitroso-compounds and their sources of exposure (adapted from [7,8,10,11]).

<i>N</i> -nitroso compound	Sources of exposure
1-nitroso-2-naphthol	Gasoline
4-methylnitrosamino-1-3-pyridyl-1-butanone	Tobacco leaves, tobacco smoke
4-nitrosophenol	Dyes, metal complexes
5-nitroso-2,4,6-triaminopyrimidine	Agrochemicals
5-nitroso-8-quinolinol	Laboratory utilization
6-nitroso-1,2-benzopyrone	Food, cosmetics
Methylnitrosnitroguanidine	Laboratory utilization
<i>N</i> -butyl- <i>N</i> -nitroso- <i>N</i> -butamine	Laboratory utilization
<i>N</i> -diethylnitrosamine	Laboratory utilization
<i>N</i> -methyl- <i>N</i> -nitrosourea	Air
<i>N</i> -nitrosarcosine	Laboratory utilization
<i>N</i> -nitroso-thiazolidine	Food (sausage, ham, bacon, cured lunch meat, fresh seafood, beef, smoked seafood, smoked meat, dried meat)
<i>N</i> -nitroso-2-hydroxymethylthiazolidine	Food (bacon)
<i>N</i> -nitroso-2-hydroxymethylthiazolidine-4-carboxylic acid	Food (smoked meat)
<i>N</i> -nitrosodibutylamine	Tobacco smoke, water, food (soya bean oil, cheese, ham, bacon, cured meat, fresh seafood, beef)
<i>N</i> -nitroso- <i>N</i> -(1-methylacetyl)-3-methylbutylamine	Food (grain)

<i>N</i> -nitrosodiethanolamine	Tobacco, cutting fluids, pesticides, cosmetics
<i>N</i> -nitrosodiethylamine	Tobacco smoke, air, gasoline, plastics, water, food (cheese, vegetables, vegetable oils, cereal products, fish, sausage, ham, bacon, cured lunch meat, hotdog, fresh seafood, cooked meats, grain, smoked meat), alcoholic drinks (apple brandy, ciders, cognac, armagnac, rum, whisky)
<i>N</i> -nitrosodimethylamine	Tobacco smoke, air, water, soil, food (cheese, sausages, ham, bacon, cured lunch meat, beef, smoked meat, hotdog, organ meats, cured meat, vegetables (beans), vegetable oils, fresh seafood, smoked seafood, eggs, solid fat, roots, spices used for meat curing), alcoholic beverages (ciders, cognacs, beer, wine), pesticides
<i>N</i> -nitrosodiphenylamine	Air (from sludge incinerators), water (waste water from factories), soil
<i>N</i> -nitrosodipropylamine	Waste-water from chemical factories, food (cheese, fresh seafood), alcoholic drinks (cognac, rum, whisky), pesticides
<i>N</i> -nitrosofolic acid	Laboratory utilization
<i>N</i> -nitrosohydroxyproline	Food (sausage, bacon, cured lunch meat)
<i>N</i> -nitrosodilbenzylamine	Food (ham, cured lunch meat)
<i>N</i> -nitrosomethylethylamine	Tobacco smoke, food (luncheon meats, bacon, chicken, meals with mushrooms, cured meats)
<i>N</i> -nitrosomethylvinylamine	Alcoholic drinks (apple brandy)
<i>N</i> -nitrosomorpholine	Food (sausage, ham, cured lunch meat, solid fat)
<i>N</i> -nitroso- <i>N</i> -ethylurea	Air
<i>N</i> -nitroso- <i>N</i> -methyl-3-aminopropionic acid	Laboratory utilization
<i>N</i> -nitrosornicotine	Tobacco, tobacco smoke

<i>N</i> -nitrosopiperidine	Tobacco smoke, water, food (cheese, smoked cod, fried bacon, spices, bologna, sausage, ham, bacon, cured lunch meat, cooked meats, smoked meat)
<i>N</i> -nitrosoproline	Food (bacon and smoked meat, ham, boiled ham, bologna, meatloaf, sausage, fried bacon, cured meats, fresh seafood, cooked meats)
<i>N</i> -nitrosopyrrolidine	Tobacco smoke, air, waste-water from chemical factories, food (cheese, grilled and fried bacon, spices, sausage, ham, cured lunch meat, fresh seafood, eggs, cooked meats, grain, roots, smoked meat), alcoholic drinks (liquor, wine)
<i>N</i> -nitrososarcosine	Food (smoked meat, cured lunch meat, boiled ham, bologna, meatloaf, sausage, ham)
<i>N</i> -nitrosothioazolidine	Food (sausage, ham, bacon, cured lunch meat, hotdog, fresh seafood, beef, smoked meat, green leafy)
<i>N</i> -nitrosothioazolidine-4-carboxylic acid	Food (smoked meats, sausage, ham, bacon, hotdog, cured lunch meat, fresh seafood, beef, cheese, smoked seafood, dried meats, beans)
<i>S</i> -nitroso- <i>N</i> -acetylpenicillamine	Tobacco smoke
Streptozotocin	Soil

2.3. Application of MNU and available animal models for the study of carcinogenesis

MNU was first prepared by Gustave Von Brüning in 1889 by the reaction of sodium nitrate with an aqueous solution of methylurea [33,34]. Afterwards, this agent was extensively studied, and its strong mutagenic effects were first reported by Rapoport in *Drosophila* spp. [35]. Subsequently, several investigators reported the carcinogenic effects of MNU in experimental protocols using different animal species and even in humans. Although today it is fully unconceivable due to ethical reasons, Kolaric used humans to evaluate the effects of intravenous administration of MNU and verified that

patients that had received a MNU injection at the concentration of 4 mg/kg of body weight exhibited signs of nausea and emesis [36]. Nowadays, MNU is still used in studies of chemical carcinogenesis of breast, spleen, kidney, uterus, ovary, hematopoietic system, liver, small intestine, colon, stomach, skin, prostate, retina, and urinary bladder [37] (Table 2.2).

MNU is represented by the molecular formula $C_2H_5N_3O_2$ (Figure 2.1) and has a molecular weight of 103.08 g/mol [19,20]. It is commercialized as pale yellow crystals that are soluble in water, polar organic solvents, alcohol, ether, acetone benzene, and chloroform [20]. MNU crystals should be stored at $-20\text{ }^\circ\text{C}$ [38]. MNU dissolution is not easy. It requires more than 30 min and it is difficult to exceed the concentration of 10 mg/mL [38]. The stability of MNU in aqueous solutions is favored at a pH of 4 (half-life 125 hours) and disfavored at a pH of 9 (half-life of 1 min and 48 s) at the temperature of $20\text{ }^\circ\text{C}$ [20]. Usually, MNU is dissolved in aqueous vehicle acidified to a pH of about 5, and the solution should be used within 3 hours after its preparation [38]. At high values of pH, the MNU solution is very reactive with water, which facilitates decontamination [20].

MNU was categorized by the National Center for Biotechnology Information as a potent mutagen and carcinogen agent that has the ability to introduce alkyl radicals into the biologically active molecules, namely DNA of most body tissues, inhibiting their normal functioning [6,30,39,40]. It is classified as a direct-acting alkylating agent, since it does not require metabolic activation. The mutagenic ability of MNU was previously evaluated by Yano and Isobe [41] and Brundrett *et al.* [42] through the use of Ames test. They concluded that MNU has a strong mutagenic potency *in vitro*. MNU has the ability to act as initiator in several tissues, namely breast, ovary, hematopoietic system, spleen, kidney, uterus, liver, colon, small intestine, large bowel, stomach, lung, skin, prostate, retina, urinary bladder, nervous system, eyes, and oral cavity [43–45] (Table 2.2).

The antineoplastic activity of MNU is associated with an apoptotic mechanism that is initiated when there is an excessive accumulation of DNA damages in cells that are highly sensitive to its action; MNU acts like a cell-disrupting agent [3,39,46]. To better understand the molecular basis of the carcinogenic and chemotherapeutic effects of MNU, it is necessary to know its mechanisms of decomposition in water at $\text{pH}>5$ (Figure 2.2) [47].

As MNU is a potent carcinogenic agent, all operations involving the handling and the topical application of the solid compound or the administration of its solutions should be

carried out taking appropriate safety measures: use two pairs of gloves, a mask, a lab coat, and a fume cupboard reserved for their manipulations. MNU can be destroyed by the mixture with saturated aqueous sodium bicarbonate [38,48,49].

An ideal animal model should develop tumors within a short period of latency, allowing the evaluation of tumor progression. The model should also mimic a range of pathobiologic, genetic, etiologic, and therapeutic characteristics of human tumors. Since there is not a model that has all of these characteristics, the researchers should select the best suitable model for answering to the aims of their studies [2].

Several animal models such as rats, hamsters, mice, rabbits, birds, shrews, fishes, and gerbils have been used in experimental protocols of chemically-induced carcinogenesis using the carcinogen agent MNU [50,51] (Table 2.2). In the past, also monkeys [52,53], pigs [54], and dogs [55] were used to investigate MNU effects.

Due to ethical reasons, economical issues, and conditions of animals' facilities, nowadays, it is not recommended to use dogs and mentally more developed animals like monkeys, as animal models in experimental protocols of carcinogenesis.

Every year, a great number of animals are sacrificed, from these stands out the rats and mice. Some investigators questioned if these sacrifices and the money dispended to maintain these animals are useful [56]. The answer to this question seems obvious, since biological functions of rodents and humans are acceptably similar, and it is difficult to use other animals that are mentally more developed (i.e., monkeys) to study human diseases [57].

The main advantages of using small rodents are their easy accommodation, cheap maintenance, behavioral, biological, physiological and genetic characteristics, and well-described carcinogenesis process. They are mammals like humans and the latency period in carcinogenesis process is relatively short [58,59]. However, it is also necessary to take into account some important differences such as lifespan, body weight, intestinal morphology, and diet that may have a substantial interference in the carcinogenesis process [57].

Many mice strains such as Swiss, ICR, C3H, B6C3F1, C57BL, BALB/c, MSM, p53^{+/-} knockout, and INS-GAS wild type, and rat strains such as Wistar, Zucker, Sprague-Dawley, Copenhagen, and Fischer are among the most frequently used rodents in carcinogenesis assays with the chemical carcinogen MNU (Table 2.2).

Among all rat strains, the Sprague-Dawley female rats have been universally recommended for use in experimental protocols to study MNU-induced mammary carcinogenesis. Sprague-Dawley is an outbred strain sensible to the MNU administration; the spontaneous development of tumors in this rat strain is age-related, being their occurrence extremely rare during the first year of life [60]. Although the Sprague-Dawley female rats are the most commonly used in the research of mammary carcinogenesis, there are several works in this field that used other rat strains, namely Copenhagen, Fischer and Wistar [61–64]. The use of outbred animals ensures the heterogeneity of the tumors, while when used inbred animals, they develop identical tumors at the same stage of growth but the tumor heterogeneity is lost. This is one more reason that makes the outbred Sprague-Dawley rats the most commonly used rat strain in the study of mammary carcinogenesis [65].

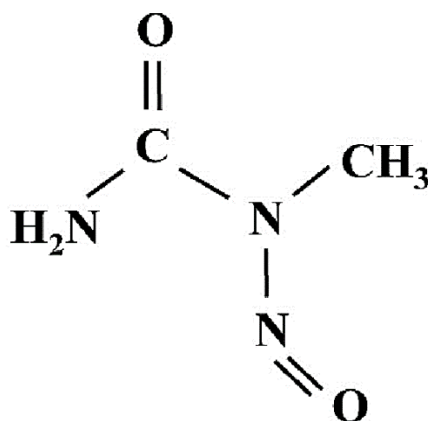


Figure 2.1. Chemical structure of *N*-methyl-*N*-nitrosourea (MNU) (adapted from Tsubura *et al.* [39]).

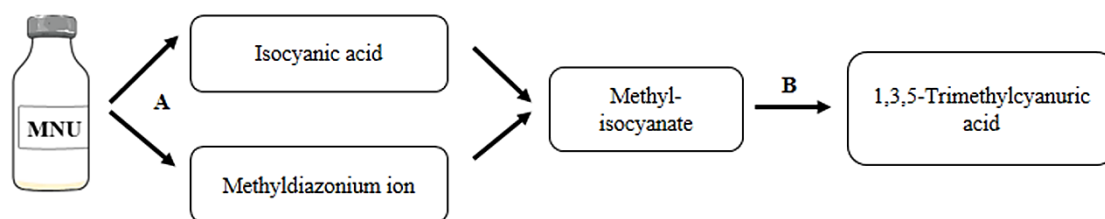


Figure 2.2. Decomposition of the chemical carcinogen *N*-methyl-*N*-nitrosourea (MNU) in water (pH>5). **A.** Fragmentation. **B.** Trimerisation.

Table 2.2. *In vivo* studies using *N*-methyl-*N*-nitrosourea (MNU) as a carcinogenic agent.

Target organ	Animals' strain and gender	Animals' age at MNU administration (weeks)	MNU dose and route of administration	Duration of the experimental protocol (after the beginning of the MNU administration) (weeks)	Incidence of tumors (%)	Histological classification	References
Breast	♀ Sprague-Dawley rat	7-15	12.5-60 mg/kg/b.w.; i.v.	14-35	33.3-100	Adenocarcinoma, carcinoma, sarcoma, fibroadenoma, fibroma, tubular, cystic and lactating adenoma	[64,66–81]
		6	50 mg/kg/b.w.; s.c.	30	95	Carcinoma, proliferative ductal processes	[82]
		7	10 mg, topic (dusting)	30	100	Adenocarcinoma, fibroadenoma, trichoepithelioma	[64]
	♀ Zucker rat	7	37.5 mg/kg/b.w.; i.p.	29	76.7	Carcinoma, intraductal papilloma, sarcoma, fibroadenoma	[83]
	♀ Copenhagen rat	7	50 mg/kg/b.w.; s.c.	52	10	Adenocarcinoma	[61]
			10 mg, topic (dusting)	30	45	Adenocarcinoma, fibroadenoma, trichoepithelioma	[64]
	♀ Fischer 344 rat	7	50 mg/kg/b.w.; s.c.	52	10	Adenocarcinoma	[61]

Breast; ovary	♀ Syrian hamsters	6	50 mg/kg/b.w.; i.p.	-	80, 30	Papillary lesions, atypical ductal hyperplasia, ductal carcinoma <i>in situ</i> , adenocarcinoma, sex cord-stromal tumors	[84]
Endometrium	♀ ICR mice	10-12	1 mg/100g; i.vag.	19-30	15-20	Adenocarcinoma	[85,86]
Prostate	♂ Gerbils	13	30 mg/kg/b.w.; s.c.	12	20	Adenocarcinoma	[87]
Prostate and seminal vesicle	♂ Wistar rat	12	50 mg/kg/b.w.; i.v.	16	-	Hyperplastic prostatic acini, malignant proliferation of ductal epithelial cells (prostate and seminal vesicle)	[62]
Hematopoietic system	♀ BALB/c mice	10	0.92 mg; i.v.	12	50	Lymphoma	[88]
		8	50 mg/kg/b.w.; i.p	43	65	Lymphoma	[89]
	♂ and ♀ C57BL/6/129 mice	2	50 mg/kg/b.w.; i.p.	16	14	Thymic lymphoma	[90]
Hematopoietic system, kidney, breast	♀ Copenhagen rat	7	50 mg/kg/b.w.; i.v.	52	10-20	Leukemia, adenocarcinoma	[61]
Hematopoietic system, stomach	♀ Fischer 344 rat p53+/- knockout mice	-	90 mg/kg/b.w.; i.g.	13	-	Lymphoma, squamous cell carcinoma, leiomyosarcoma	[91]
Stomach	♂ Wistar rat	10	200 ppm; d.w.	70	-	Sarcoma, squamous carcinoma, adenocarcinoma	[92]
	♀ Wistar rat	8	0.03-4.5 mg/kg/b.w.; i.g.	38	22.2	Squamous cell carcinoma, squamous cell papilloma, adenocarcinoma	[93]
	♂ Fischer 344 rat	6	400 ppm; d.w.	36	-	Adenocarcinoma	[94]

	♂ INS-GAS wild-type mice	8-10	240 ppm; d.w.	36	≈ 98	Hyperplastic foci, adenoma, adenocarcinoma	[95]
	♂ C57BL/6 wild-type mice	6	240 ppm; d.w.	40	86	Adenocarcinoma	[96]
	♂ MSM mice	6-8	0.03-4.5	38-46	70-100	Carcinoma, papilloma	[97]
	♂ C3H mice		mg/kg/b.w.; i.g.				
	♂ C3HxMSM mice						
	♂ Mongolian gerbils	7	10 ppm; d.w.	41	0	-	[98]
	♂ Syrian golden hamsters	12-15	1%; intratracheal	28	94	Carcinoma, papilloma	[99]
Stomach, spleen, liver, kidney, lung	♂ C3H mice	6	120 ppm; d.w.	42	3.7-66.7	Adenocarcinoma, sarcoma, hemangioendothelial sarcoma, neoplastic nodule, adenoma	[100]
Colon	Swiss mice	12	1 ml; i.p.	8	-	Preneoplastic changes	[101]
Colon, small intestine	♂ Fischer 344 rat	7	2.5 mg; i.r.	35	23.3-73.3	Adenoma, adenocarcinoma	[63]
Colon, small intestine, uterine cervical	♀ house musk shrew	6	0.5-1.5 mg; i.r.	31	23-100	Adenocarcinoma, carcinoma, squamous cell carcinoma	[102]
Large bowel	♀ CD-Fischer rat	7-9	0.5 ml or 2 mg; i.r.	26	67-85	Adenocarcinoma	[103,104]

Spleen, kidney, uterus, hematopoietic system, liver	♀ Sprague- Dawley rat	7	12.5-50 mg/kg/b.w.; i.p.	28	3.3-13.3	Fibrosaroma, mesenchymal tumor, leiomyoma, rhabdomyosarcoma, hemangiosarcoma, angiolioma, non-Hodgkin's lymphoma, hemangiosarcoma	[66]
Liver	♀ Sprague- Dawley rat	7	50 mg/kg/b.w.; i.p.	15	-	Schwannoma	[105]
	♀ B6C3F1 mice	2	25 mg/kg/b.w.; i.p.	52	10-17.5	Carcinoma, adenoma	[106]
Lung	♀ BALB/c mice	8	50 mg/kg/b.w.; i.p.	43	86	-	[89]
	♂ BALB/c mice	6	120 ppm: d.w.	50	23	Adenocarcinoma	[107]
Oral cavity	♂ Wistar rat	5	300 mg/kg/b.w.; injected into the periostium of the left mandibule	32	-	Odontogenic tumor, squamous cell carcinoma, malignant fibrous histiocytoma	[108]
Retina	♂ and ♀ Sprague- Dawley rat	6-10	40-60 mg/kg/b.w.; i.p.	24 hours-20	-	Retinal degeneration	[109–112]
Skin	<i>Xiphophorus</i> fish	5	1 mM	24	21.7-36.	Melanoma	[111,113]
Nervous, eyes, mesenchymal tumor	<i>Xiphophorus</i> fish	5	1 mM	56	2.8-6.6	Schwannoma, retinoblastoma, fibrosarcoma	[114]
Urinary bladder	♀ Fischer 344 rat	4-7	0.5-1.5 mg/kg/b.w.; i.ves.	20-33	40-80	Papillary carcinoma, papilloma, papillary transitional cell carcinoma, transitional cell carcinoma	[115–117]

	♂ Wistar rat	7	20 mg/kg/b.w.; i.p.	26	25	Hyperplasia (simple, papillary or nodular)	[44]
Urinary bladder, uterus	♀ Wistar rat	-	7.5 mg/kg/b.w.; i.ves.	60	29.3	Papillary transitional cell carcinoma, exophytic papilloma, fibrous histiocytoma	[118]

b.w. body weight; **d.w.** drinking water; **i.g.** intragastric; **i.p.** intraperitoneal; **i.r.** intrarectal; **i.v.** intravenous; **i. vag.** intravaginal; **i.ves.** intravesical; **s.c.** subcutaneous

2.4. MNU administration

This nitroso-compound may act as a carcinogenic agent in rats, mice, hamsters, gerbils, fishes and shrews, inducing the development of cancer in breast, ovary, uterus, prostate, hematopoietic organs, kidney, urinary bladder, liver, intestine, spleen and retina. The development of a wide spectrum of lesions in different tissues depends on the animal species, strains and age, and the dose, frequency and route of administration of the carcinogen agent (Table 2.2).

MNU may be administered in drinking water, intraperitoneally, subcutaneously, orally, intravenously, intragastrically, topically (dusting), intrarectally, intrauterinely, intratracheally, intravesically, and intravaginally (Table 2.2). When animals are not familiar with manipulation, it is advised to use chemical restraint (sedation) to increase the safety of administration to the manipulator [38]. After its administration, MNU has an *in vivo* half-life of approximately 30 min [38]. By the decomposition at physiological pH, MNU produces the ion cyanate that has the ability to react with proteins by carbamylation; in a study performed by Knox [119], it was observed that this reaction with serum proteins was responsible for the toxic effects of MNU on the growth of fetal rat brain cells in culture.

The researchers should be conscious that when they administer the carcinogen agent in order to induce carcinogenesis in a target organ, the animals may simultaneously develop lesions in the target organ and in other organs. Esendagli *et al.* [120] reported the coexistence of carcinogenesis in different non-mammary tissues in an experimental protocol where female Sprague-Dawley rats were intraperitoneally injected with the carcinogen agent MNU (50 mg/kg). Additionally, it is known that the MNU has also the ability to induce the development of cataracts by the cytotoxic effects in epithelial cells of lens [121]. Cataracts are defined as the opacity of the lens that can affect vision and conduct to blindness [122]. In female Sprague-Dawley rats, MNU starts damaging the DNA of the epithelial cells of lens leading to apoptosis, through the up-regulation of *BAX*, down-regulation of *BCL-2*, and activation of caspase-3 [123]. The development of cataracts in these animals is inversely related with their age; the cataract development occurs more quickly in young animals when compared with older ones [39]. In a study performed by Tsubura and collaborators [39], a single intraperitoneal administration of the carcinogen agent MNU at a concentration of 100 mg/kg to male and female Sprague-

Dawley rats with zero, five and ten days of age induced the appearance of bilateral cataracts seven days (young animals) and 14 days after MNU administration.

In an experimental protocol of mammary carcinogenesis performed by our research team, where female Sprague-Dawley rats with 50 days of age received a single intraperitoneal administration of the carcinogen agent MNU at a concentration of 50 mg/kg, we verified that some of our animals developed cataracts in the last two weeks of the experimental protocol that finished 35 weeks after the MNU administration (data not published). Previously, Roy and colleagues [124] had described that development of cataracts in adult rats requires a long period of time, approximately six to eight months, after MNU administration. So, according to our experience and the analysis of results of other researches, the development of cataracts is age-dependent.

2.5. MNU-induced mammary tumors

MNU-induced mammary tumors in rodents is a well-established animal model for breast cancer research that resembles woman mammary tumors and simple mammary tumors of female dog in their morphologic, pathobiologic, genetic, and etiologic characteristics and response to therapeutic approaches [125,126]. In 1975, Gullino and collaborators [127] described this model as “a simplest method for inducing in rats a most nearly complete model for human mammary carcinomas.” However, susceptibility to MNU-induced mammary tumors differs significantly among mouse and rat strains. Our research group induced mammary carcinogenesis using the intraperitoneal administration of MNU (50 mg/kg) within 1 hour after its preparation, in female Sprague-Dawley rats at 50 days of age in two experimental protocols. In the first experimental protocol, the MNU (50 mg/kg) was also administered intraperitoneally to female Sprague-Dawley rats with 50 days of age, four days after its preparation (data not published).

In both protocols, the MNU preparation and its administration to animals were made by the same researcher. Animals were maintained under similar conditions of humidity, temperature, ventilation, and light/dark cycle, and they were fed with the same diet. All animals were palpated once a week in order to detect mammary tumor development. Despite similar conditions in both studies, the latency period, incidence and number of tumors *per* animal were very different between experimental protocols. As expected, the latency period was higher, and the incidence and number of mammary tumors *per* animal

were lower in animals that received MNU four days after its preparation (Table 2.3). Looking to our results, we can say that the use of the same rat strain, carcinogen dosage, and route of administration does not guarantee equivalent results.

There are few reports concerning to the induction of mammary tumors by the carcinogen agent MNU in mice. However, published works indicate that the MNU administration at a concentration of 50 mg/kg to young mice induces a low number of mammary tumors (an incidence between 15 and 20%). Additionally, while rats exhibited a latency period of approximately 10-12 weeks, mice showed a higher latency period (approximately 25 weeks) [128,129]. Our research team performed a small experimental protocol using nine female albino mice. All animals received an intraperitoneal injection of the carcinogen agent MNU at a concentration of 50 mg/kg, and the protocol finished 28 weeks after the carcinogen administration. Four animals died during the experiment; only one mammary tumor was detected 24 weeks after the MNU administration (incidence of 20%) (data not published), confirming the data previously described, which indicate that the mice are less susceptible than rats to the development of MNU-induced mammary tumors.

Macroscopically, rat mammary tumors seem to take an oblate spheroid geometry [130]. Tumor dimensions are variable, ranging from few millimeters to approximately 5 cm (Figure 2.3). Microscopically, a wide range of mammary lesions can be observed, such as epithelial, stromal and epithelial-stromal neoplasms, and non-neoplastic lesions that may be classified according to the classification of chemically-induced mammary tumors previously established by Russo and Russo [131]. This spectrum of mammary tumors is similar to that observed in women and female dog [131–133].

Chemically-induced mammary cancer by the carcinogen agent MNU may also be used as a model of cachexia. Cachexia is defined as a multifactorial metabolic syndrome characterized by a loss of skeletal muscle with or without loss of fat mass, anorexia, metabolic alterations and asthenia [134,135]. It may be associated with a high number of diseases, namely congestive heart failure, acquired immunodeficiency syndrome, chronic kidney diseases, tuberculosis, malabsorption syndromes, sepsis and cancer [136–138]. Cachexia occurs in about half of all oncologic patients, decreasing their survival rate; since the current therapeutic approaches are largely ineffective, this metabolic syndrome is responsible for approximately 20% of deaths among patients with cancer [139–142]. The mechanisms of cachexia development are not fully elucidated; however, it has been

suggested that it results from a balance between tumor and host-released factors, reduced food intake by patients and increased metabolism [142,143]. Several *in vitro* (cancer cell lines: C2C12 myoblasts and L6 myoblasts) and *in vivo* models may be used to study cancer cachexia. Relatively to *in vivo* models, it is possible to use syngeneic (Walker 256, Yoshida sarcoma, Lewis lung carcinoma, Yoshida AH-130, MAC 16 ADK, MCG 101, Prostate ADK), xenograft (XK1), genetically engineered and carcinogen-induced models [135]. In 1975, Gullino and co-workers [127] verified that female BUF/N, Sprague-Dawley and F344 female rats developed cachexia 5 weeks after appearance of the first chemically-induced mammary tumor by the intravenous administration of MNU; these animals developed the first mammary tumor 77, 86 and 94 days after administration of the carcinogen agent, respectively [127]. In one of the experimental protocols of mammary carcinogenesis performed by our research team described above, we aimed to better understand the mechanisms underlying cancer-induced muscle wasting, and we observed that animals MNU-exposed showed a lower body weight when compared with those from control group that were not exposed to the carcinogen agent, being these data an indicator of cancer-induced cachexia.

Table 2.3. Data from two experimental protocols of mammary carcinogenesis MNU-induced in female Sprague-Dawley rats performed by our research team.

Parameter	First protocol		Second protocol (n=10)
	MNU administration immediately after its preparation (n=11)	MNU administration four days after its preparation (n=14)	
First mammary tumor appearance (after MNU administration)	10 weeks	16 weeks	8 weeks
End of the experiment (after MNU administration)	35 weeks	35 weeks	18 weeks
Number of mammary tumors	28	8	21
Tumor incidence (%)	100	57	60
Number of mammary tumors <i>per</i> animal	2.5	1.0	3.5

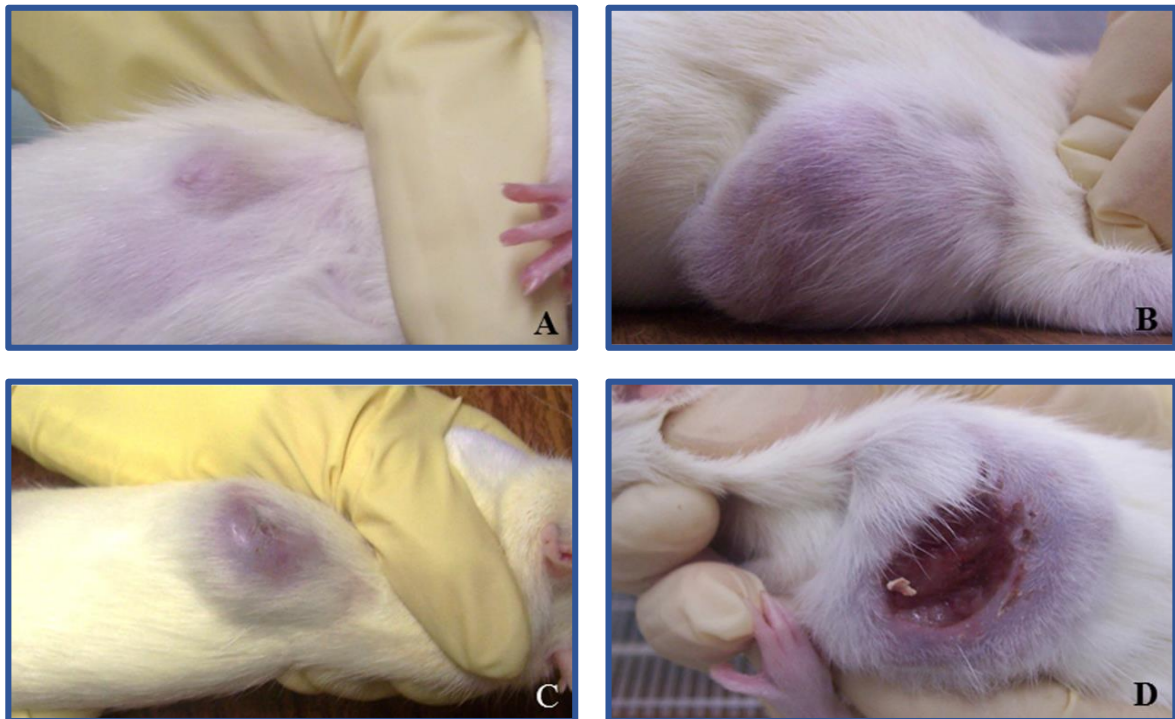


Figure 2.3. Different macroscopic appearance of MNU-induced mammary tumors in female Sprague-Dawley rats 35 weeks after administration of the carcinogen agent. Small mammary tumor (approximately 1 cm in diameter) (A). Mammary tumor of large dimensions (approximately 4.5 cm in diameter) (B). Mammary tumor with eroded surface (C). Ulcerated mammary tumor (D).

2.6. Signaling pathways in MNU-induced rat mammary tumors: a homology with human cancer

Cancer is characterized by several genetic alterations that define its behavior [144]. Advances in molecular biology have allowed the identification of markers in breast cancer that may be used as indicators of therapeutic response and prognosis, as well as, used as therapeutic targets [145].

MNU-induced mammary tumors in female Sprague-Dawley rats are a recognized model to better understand mammary carcinogenesis and its treatment [146–148]. This model displays similarities with human breast cancer in terms of tumor origin (transition duct/lobular epithelial cells), aggressiveness, local invasiveness, relationship with steroid hormones and the expression of their receptors, alterations in the Ras/Raf/MAPK and PI3K/Akt pathways, and in the expression of several genes (*p53*, *c-kit*, *mTOR*, and *c-myc*) [66,146,149,150] (Figure 2.4).

Sex steroid hormones have an important role in breast cancer development and progression, since it is an endocrine-dependent disease [151]. These hormones act by linkage with two different isoforms of estrogen receptors (ERs): ER α and ER β . According to some authors, activation of these receptors has opposite roles in breast cancer proliferation and differentiation; ER α has promoting effects while ER β acts as tumor suppressor by anti-proliferative and pro-apoptotic activities, inhibiting tumor growth and invasion [152–154]. However, according to other authors, ER β may have a dual role in breast cancer, being its role still controversial [152]. Nowadays, ER α expression is recognized as a marker in oncologic clinical practice, being used as an indicator of tumor biology, prognosis and predictor of tumor response to endocrine therapy [155,156]. The presence of ER α in breast tumors is associated with better response to hormonal therapy and consequently better prognosis [157]. The high expression of ER β is controversial. Some authors associated it with a good prognostic and clinical outcome [158–160], while other authors indicated that ER β expression is an indicator of poor prognosis [161–164].

Lu and collaborators concluded that MNU-induced rat mammary tumors also express ERs α and β and are a good model to study ER-positive human breast cancer [165]. ER α was also identified in all MNU-induced mammary tumors in Sprague-Dawley female rats in an experimental protocol performed by our research team [146].

HER family, also known as ErbB or epidermal growth factor receptor (EGFR) family, is constituted by four transmembrane receptor tyrosine kinases: EGFR also called HER1, HER2 or ErbB2, HER3 or ErbB3, and HER4 or ErbB4 [166]. The signaling of these receptors induces cell proliferation, motility and invasion. The abnormal expression and activity of these HER family receptors occurs frequently in human cancers [167]. More than 30% of breast carcinomas overexpress HER2 as a consequence of genomic amplification of a region of the long arm of chromosome 17 that included the HER2 locus [166]. Generally, the overexpression of HER2 is associated with a low or absence expression of ERs and aggressive behavior of tumors in both humans and animals [168,169].

Ras/Raf/MAPK is one of the most frequently deregulated signaling pathways in human breast cancer [170,171]. *Ras* is a cellular proto-oncogene that is activated in more than 15% of all human cancers [172]. McLaughlin and collaborators [173] verified that activation of Ras pathway in breast cancer acts as a suppressor of tumor growth and

metastasis. Molecular techniques allowed the identification of genetic alterations in the codon 12 of Ha-*ras* proto-oncogene in carcinomas [174–176]. Raf is one of the most studied Ras effectors that after phosphorylation activates MEK and ERK, leading to the increase of cell proliferation and survival [172]. Similarly to that occurs in human breast cancer, this signaling pathway is also frequently deregulated in MNU-induced rat mammary cancer [172]. Most of MNU-induced mammary tumors in female Sprague-Dawley rats contain a guanine to adenine transition at the second base of Ha-*ras* codon 12 [174,175,177]. Since this mutation may be observed in normal mammary tissues, some authors consider that this mutation alone is not sufficient for the transformation of normal mammary epithelial cells into neoplastic cells [177]. Asamoto and collaborators [178] observed that Sprague-Dawley rats carrying the transduced human H-*ras* proto-oncogene are highly susceptible to the development of mammary tumors after administration of the carcinogen agent MNU. Kito and collaborators [179] also identified mutation in Ha-*ras* gene in 79% (27 of 34 mammary tumors) of MNU-induced mammary tumors in female Sprague-Dawley rats. Ras/Raf/MAPK pathway interacts with PI3K/Akt pathway in the regulation of cell growth, contributing to tumorigenesis [172]. Similarly to that occurs with the Ras/Raf/MAPK pathway, the PI3K/Akt is other signaling cascade frequently deregulated in breast cancer [170,171]. This pathway may be activated by two different ways: by binding with the phosphorylated tyrosine residues of receptor tyrosine kinases via p85 or by Ras protein [172]. Activation of Akt signaling pathway plays an important role in the development and progression of breast cancer, being associated with poor prognosis and resistance to hormonal and chemical therapy [180]. Similarly to that occurs in human breast cancer, this signaling pathway is also frequently deregulated in MNU-induced rat mammary cancer [172].

Mammalian target of rapamycin (mTOR) has been classified as a member of the phosphatidylinositol 3-kinase-related protein kinase [181]. mTOR is composed by two complexes: mTORC1 and mTORC2. mTORC1 regulates glycolysis, protein synthesis, lipid metabolism, cell proliferation and autophagy [182,183], while mTORC2 regulates cell proliferation, survival and cytoskeleton [184,185]. Preclinical studies have suggested that mTOR plays a role in the resistance of human breast cancer patients to hormonal and chemical therapy [181]. mTOR may be up-regulated in breast cancer due to the genetic alterations or aberrant activation of the components of PI3K/ Akt pathway [186]. mTOR expression contributes to deregulation of cell proliferation, growth, differentiation and

survival [187–190]. Arumugan and co-workers [191] also observed the activation of mTOR signaling in MNU-induced mammary tumors in female Copenhagen rats.

Phosphorylated adenosine monophosphate-activated protein kinase (AMPK) is a component of a regulatory network (AMPK, mTOR, Akt) that integrates signals from the extracellular and intracellular environments to maintain tissue homeostasis [192–195]. This network is frequently deregulated during carcinogenesis [196,197]. AMPK is activated in situations of cellular stress, namely glucose deprivation, tissue ischemia, hyperosmotic stress, hypoxia, and oxidative stress [198,199]. AMPK activation may be used as therapeutic target in cancer with activated Akt signaling pathway, since AMPK inhibits mTOR signaling pathway by Akt [200]. Zhu and co-workers [201] verified that the activation of AMPK in MNU-induced mammary cancer in female Sprague-Dawley rats by metformin administration decreased mammary tumors incidence and multiplicity, and increased latency period.

c-kit is a proto-oncogene that encodes a transmembrane tyrosine kinase receptor [202]. It is expressed in several cells during development, such as epithelial, endocrine and endothelial cells. *c-kit* has been associated with promotion of cellular migration, proliferation and/or survival of melanoblasts, hematopoietic progenitors and primordial germ cells [203]. Some studies have demonstrated that the product of *c-kit* is expressed in normal adult tissues, such as basal portion of renal distal tubules, acinar cells of parotid, spermatogonia, thyrocytes, melanocytes, alveolar and ductal cells of mammary epithelium, astrocytes, Purkinje cells and small size vessels, and in solid tumors, namely small cell carcinoma and squamous cell carcinoma of lung, glioblastoma in the brain, breast cancer, seminoma in genitourinary tract, and pheochromocytoma in adrenal gland [204,205]. Natali and colleagues [206] observed a homogeneous and large expression of this oncogene in normal epithelium of breast tissues; they also observed the lack of expression of this oncogene in human breast cancer. Chui and collaborators [207] observed a uniform expression of *c-kit* in normal human breast tissues, a heterogeneous expression in benign human breast cancer, and a lack of expression in malignant human breast cancer. These results suggest that the deletion of *c-kit* occurs in the early phase of malignant transformation of breast mammary epithelia [207]. Maffini and collaborators [208] also verified that the lack of *c-kit* in genetically modified Ws/Ws rats obtained from the Brown Norway and Donryu rats genetic background is permissive for the development of mammary tumors in female rats treated with the carcinogen agent MNU,

while the wild-type animals of the genetic background from the same rats (animals with the *c-kit*) treated with the same carcinogen agent did not develop any neoplasia [208].

Angiogenesis is a crucial phenomenon for tumor growth and metastasis [209,210]. Tumor angiogenesis is frequently associated with the overexpression of the vascular endothelial growth factor (VEGF) [211]. This factor is overexpressed in human breast cancer [212,213], being used as an indicator of poor prognosis in this type of cancer [214]. Saminathan and collaborators [215] also identified this factor in MNU-induced mammary tumors in female Sprague-Dawley rats.

Transforming growth factor-beta (TGF- β) is a multifunctional cytokine that has the ability to inhibit mammary tumorigenesis by inducing apoptosis, inhibiting cell cycle progression, and maintaining cellular and tissue homeostasis [216,217]. The cytostatic activity in normal mammary epithelial cells is often inactivated in human malignant mammary epithelial cells; this cytokine acquires oncogenic activity, contributing to the development and progression of mammary tumors [218,219]. This aberrant expression of the TGF- β in human mammary tumors is positively correlated with enhanced breast cancer progression, angiogenesis and metastasis, contributing to poor prognosis [218,220]. Similarly to that occurs with human breast cancer, MNU-induced mammary tumors may also carry altered expression of the TGF- β [221].

Insulin-like growth factor 1 receptor (IGF1-R) is a homodimeric receptor that may be found in normal and malignant breast tissue [222]. Although this receptor has been associated with cell survival and resistance, the prognostic value associated with this receptor is not fully understood [223,224]. IGF1-R has the capacity to the aberrant activation of the PI3K/Akt pathway in breast cancer cells, which increases cell proliferation and cancer progression [190]. Arumugan and co-workers [191] also observed an enhancement in IGF1-R in MNU-induced mammary tumors in female Copenhagen rats.

p53 is a tumor suppressor gene, being one of the most frequently mutated genes in human cancers [176,225,226]. However, the frequency of mutation of this gene in breast cancer is lower when compared with other cancers, being present in only 20% of human breast cancer patients [227]. Some investigators identified a higher frequency of mutations in this gene in patients with mutations in breast cancer gene (*BRCA*) 1 and *BRCA2* [228,229]. *BRCA1* and *BRCA2* are also tumor suppressor genes [230]. Mutations in these genes are associated with a high risk of breast cancer development [231,232].

Although the mechanisms of their activity are not fully understood, the role of these genes in transcriptional regulation, check-point control in cell cycle and repair of DNA damage has been described [233]. Wild-type *p53* acts to eliminate and inhibit the proliferation of abnormal cells, avoiding the neoplastic development [225]. In both humans and rats, the mutations in the gene *p53* are clustered in exons 5 through 8 that includes evolutionarily conserved domains [177,234]. *p53* mutations induce the neoplastic transformation through several mechanisms, namely changes in DNA repair, apoptosis, cell cycle regulation, angiogenesis and metastasis [176,235–237]. In human breast cancer, mutation in this gene is associated with more aggressive and therapeutically refractory tumors and consequently patients with lower survival rate [144,227]. Ogawa and collaborators [177] studied this gene in nine MNU-induced mammary tumors in female F344 rats and did not identify any mutation, concluding that *p53* mutations are not involved in MNU-induced rat mammary carcinogenesis. Similarly, Kito and collaborators [179] did not identify any *p53* mutation in 34 MNU-induced mammary tumors in female Sprague-Dawley rats. This may be due to the narrow spectrum of mammary lesions that were identified, since all the mammary tumors were histologically classified as adenocarcinomas.

c-myc is one of the first oncogenes to be overexpressed in breast cancer [238]. It is involved in the regulation of cell cycle, metabolism, biosynthesis, architecture and survival, tissue remodeling and angiogenesis, being an essential factor for the proliferation of normal and cancer cells [239]. Cellular response to the overexpression of *c-myc* depends on the cellular context; *c-myc* may increase proliferation rate and induce oncogenic transformation but may also induce cell apoptosis [240]. In human mammary gland, *c-myc* acts as a potent transforming gene for epithelial mammary cells, supporting observations that the gene amplification is a contributory factor in breast carcinogenesis [241]. Similarly to that occurs in human breast cancers, *c-myc* oncogene is frequently overexpressed in MNU-induced mammary tumors in female Sprague-Dawley rats [242].

Cyclin D1 is a member of cyclin protein family that has an important role in the transition from G1 to S phase of cellular cycle; consequently, changes in this protein may lead to neoplastic transformation [243]. Cyclin D1 overexpression has been described in both human and rat mammary tumors [244,245]. Russo and Russo [246] observed that overexpression of cyclin D1 occurs frequently in early lesions of human mammary gland that ultimately form malignant breast cancers, concluding that cyclin D1 overexpression may be a critical step in human breast cancer development. Zhu and co-workers [247]

evaluated the expression of cyclin D1 in normal mammary tissue, preneoplastic lesions, and mammary tumors MNU-induced in Wistar-Furth rats. They observed that the percentage of positive cells was very low in normal mammary gland, increasing with each subsequent stage of tumorigenesis [247]. Similarly to that occurs with human breast cancer, mammary tumors MNU-induced may also carry altered expression of cyclin D1 [221].

Cytokeratins (CKs) are intermediate filaments that constitute mammalian cell cytoskeleton [248]. In normal breast tissue, luminal cells express CKs 7, 8, 18, and 19, and myoepithelial/basal cells express CKs 5, 14, and 17 [249,250]. Some authors verified that human breast cancer predominantly expresses CKs 7, 8, 18, and 19 [251,252]. Other studies also verified that 4 to 16% of invasive breast carcinomas express basal CKs 5 and 14 [249,253–256]. El-Rehim and colleagues [257] concluded that the expression of CKs is associated with different clinical and pathological parameters; the expression of luminal CKs is associated with better patients' survival, while the expression of basal CKs is associated with poor tumor behavior and prognosis. Lu and co-workers [258] identified the CK 18 gene in MNU-induced mammary tumors in female Sprague-Dawley rats. CKs 8 and 14 were also identified by immunohistochemistry in MNU-induced mammary tumors in female Wistar-Furth rats; epithelial cells stained positive for the CK 8 and basal carcinoma cells stained positive for the CK 14 [259,260]. CK 14 was also detected by immunohistochemistry in basal cells of MNU-induced mammary tumors in female Lewis rats [261] and CK 19 was identified in luminal cells of mammary gland in Wistar-Furth rats [260].

Expression of metalloproteinases (MMPs) is associated with the growth and invasiveness of human breast cancer [262–265]. MMPs have the ability to degrade the macromolecules of the extracellular matrix of supporting stroma, allowing the metastasis of mammary tumors [266]. Human breast cancer constitutively expresses some types of MMPs, namely MMP-1, MMP-2, MMP-7, MMP-11, MMP-13, MMP-14 and MMP-16; these MMPs are not expressed in normal mammary cells [267]. Roomi and co-workers [268] verified that the inhibition of MMPs in MNU-induced mammary tumors in female Sprague-Dawley rats by natural inhibitors reduced the incidence and growth of induced mammary tumors.

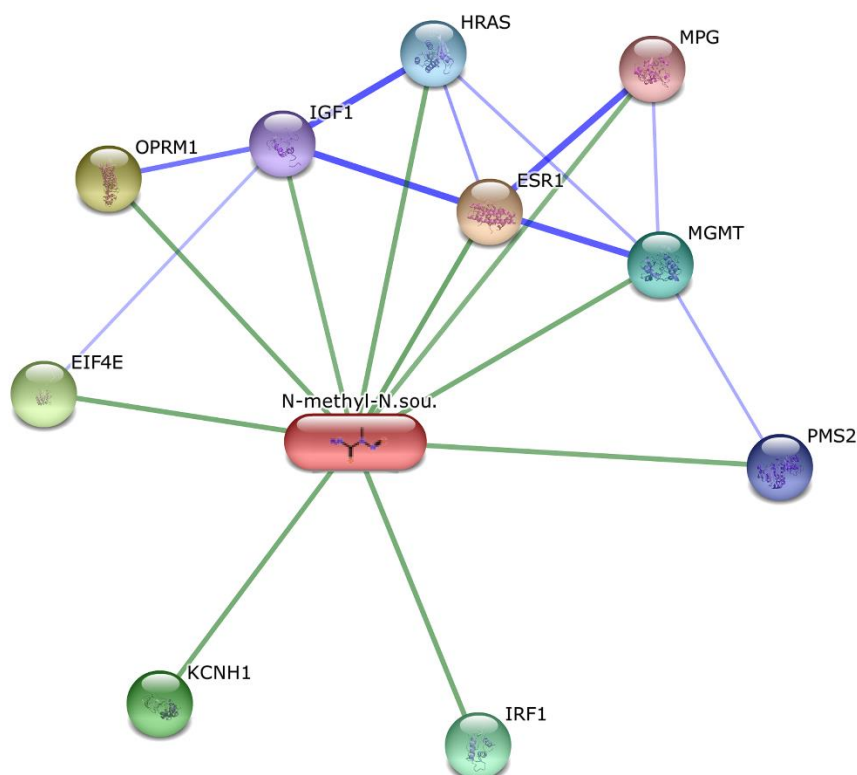


Figure 2.4. Predicted interactions of the carcinogen agent MNU. *ESR1* estrogen receptor 1; *OPRM1* opioid receptor; *EIF4E* eukaryotic translation initiation factor 4E; *KCNHI* potassium voltage-gated channel, subfamily H (eag-related), number 1; *IRF1* interferon regulatory factor 1; *MGMT* O-6-methylguanine-DNA methyltransferase; *HRAS* v-Ha-ras Harvey rat sarcoma viral oncogene homolog; *PMS2* postmeiotic segregation increased 2; *IGF1* insulin-like growth factor 1 (somatomedin C); *MPG* N-methylpurine-DNA glycosylase. These predictions were made using the STITCH 4.0 online database.

2.7. Applications of MNU-induced mammary carcinogenesis

Animal models have been used to assess the efficacy of synthetic and natural agents, and combination of several compounds, using different doses and routes of administration [269] (Table 2.4). Data obtained from experimental protocols using these animal models are essential to determine if the chemical compounds will be evaluated in clinical chemoprevention trials [269].

An ideal animal model to evaluate the chemopreventive effects of a compound should exhibit genetic abnormalities, and be histologically and molecularly similar to human tumors. These models should also exhibit a high incidence and number of tumors *per* animal; efficient agents in animals should also show efficiency in clinical trials and the inverse should also happen [269].

The MNU-induced mammary tumors in female rats are considered an ideal model as it meets all the mentioned advantages. This model is also estrogen-dependent and has some genetic alterations similar to human mammary tumors [270,271].

In addition to the evaluation of drug efficacy in mammary cancer prevention or treatment, this model provides data about the dose-response, toxicity and pharmacokinetic that are essential before clinical testing of the chemicals [269]. This model has also allowed the *in vivo* study of mammary tumor morphology, vascularization, progression and response to drug administration using imaging modalities, such as ultrasonography, magnetic resonance imaging, elastography, computed tomography and thermography [67]. Since these imaging methods are non-invasive, they allow the mammary tumor evaluation without animals' sacrifice reducing the number of animals used in experimental protocols. We used ultrasonography and thermography in the evaluation of MNU-induced mammary tumors in female Sprague-Dawley rats (Figure 2.5) [67]. B Flow ultrasonographic mode shows more sensitivity than Power Doppler (PDI) in the detection of tumor vascularization. Mammary tumors exhibited a centripetal enhancement order of contrast agent and clear margins in contrast-enhanced ultrasound analysis. Maximum superficial temperature of mammary tumors and thermal amplitude determined by thermography were significantly correlated with tumor volume and color pixel density determined by PDI [67].

Table 2.4. Therapeutic approaches evaluated in MNU-induced mammary tumors.

Animals' strain and gender	Compound	Therapeutic approach	Duration of the treatment	Conclusion	Reference
♀ Lewis rat	Anastrozole Docetaxel 17 α -ethynyl-5 α -androstane-3 α , 17 β -diol (HE3235) + Docetaxel HE3235 Tamoxifen	2.5 mg/day; i.p. 1.5 mg; once a week; i.p. 6.6 mg/day + 1.5 mg; once a week; i.p. 4-6.6 mg/day; i.p. 0.25 mg; s.c.; once a week	4 weeks	All compounds decreased incidence and number of mammary tumors; the highest dose of HE3235 in combination with docetaxel was the most efficient treatment	[270]
♀ Wistar rat	Carboxy ethyl germanium sesquioxide (Ge-132) Green tea extract	1500 mg/kg/day; i.p. 30 mg in the diet	34 weeks 9 weeks	Ge-132 reduced tumor growth Tumor multiplicity was lower in animals that received green tea extract	[272] [273]
♀ Ludwig/Wistar/Olac rat	Pamidronate	0.4 mg/kg/b.w.; s.c.	4 weeks	Pamidronate reduced tumor volume	[274]
♀ rat	Potato (<i>Solanum tuberosum</i> L.)	5-50% of potato in the diet	5 weeks	A reduction in the cancer incidence was observed	[275]

♀ Sprague-Dawley rat	Amphetamine-regulated transcript peptide (CART)	1 µg/rat/day, i.c.v.	5 days	CART inhibition may have a role in the reversion of cancer cachexia	[77]
	CART-antibody	5 µl (1:500)/rat/day, i.c.v.			
	Anastrozole	0.05-0.5 mg/kg/diet	15 weeks	Anastrozole at high concentration reduced mammary tumor incidence and number of tumors <i>per</i> animal	[276]
	Carboplatin	6 mg/rat; i.duc.	Single	Carboplatin was the most efficient agent in the inhibition of mammary carcinogenesis	[277]
	Methotrexate	4-10 mg/rat; i.duc.	administration		
	Paclitaxel	60 mg/rat; i.duc.			
	Celecoxib	1500 ppm in the diet	7-24 weeks	Celecoxib suppressed mammary carcinogenesis	[258,278]
	13-cis retinoic acid (13cRA)	1 mg/kg; 3 times a week; i.g.	15 weeks	CpG-ODN reduced the number of mammary tumors	[74]
	CpG oligodeoxynucleotides (CpG-ODN)	CpG-ODN motifs; i.d.	2 administrations		
	13-cis retinoic acid (13cRA) + CpG oligodeoxynucleotides	1 mg/kg; 3 times a week; i.g.	15 weeks + 2 administration		
Curcumin	168 µg encapsulated drug/teat; i.duc.	2-3 administrations	Curcumin reduced the incidence of mammary tumors	[279]	

	200 mg/kg/b.w.; gavage			
Doxorubicin (DOX)	4-16 mg/kg; i.p.	1 day	I ₂ may be used as adjuvant of doxorubicin in	[280]
DOX + Iodine (I ₂)	4-16 mg/kg; i.p. + 0.05% in drinking water	1 day + 7 days	cancer therapy	
Exemestane	1-10 mg/kg in the diet	13 weeks	Exemestane administration in premenopausal animals induced mammary carcinogenesis	[276]
Fluorouracil	12 mg/rat; i.v. 12 mg/rat; i.duc.	4 administrations	I. duc. administration was effective in the inhibition of mammary carcinogenesis	[277]
Flurbiprofen	31.25-62.5 mg/kg diet	26 weeks	Inhibited mammary carcinogenesis induced by the low dose of MNU (25 mg/kg/b.w.) but not induced by high dose (50 mg/kg/b.w.)	[75]
Garlic powder	20 g/kg diet	27 weeks	Garlic powder, alkyl sulfur component SAC and	[78]
S-allyl cysteine (SAC)	57 nmol/kg diet		DADS inhibited mammary carcinogenesis	
Diallyl disulfide (DADS)	57 µmol/kg diet			
Genistein	12.5 mg/day; s.c.	3 days	Increased tumor multiplicity	[81]
High fat, low fiber diet + phytic acid	2% phytic acid in the diet	9-30 weeks	Phytic acid contributed to the reduction of mammary tumor incidence	[82]
1 α -Hydroxyvitamin D ₅	25-50 µg/kg diet	18 weeks	Reduced the incidence	[76]

			of mammary carcinogenesis	
Keoxifene	20-500 µg; s.c.	13 weeks	Keoxifene reduced mammary tumors incidence and number of tumors <i>per</i> animal	[281]
Lapatinib	25-75 mg/kg/b.w.; gavage	21 weeks	High dose of lapatinib reduced mammary tumors incidence and multiplicity	[73]
Letrozole	1-10 mg/kg in the diet	18 weeks	Letrozole at 0.001% suppressed mammary carcinogenesis	[282]
Mango (<i>Mangifera indica</i> L.)	0.02-0.06 g/ml of drinking water	2 weeks 23 weeks	Mango consumption did not inhibit mammary carcinogenesis	[283]
2-methoxyestradiol	1-5 mg/kg/day; s.c.	4 weeks	2-methoxyestradiol did not inhibit mammary carcinogenesis	[284]
Paclitaxel	10-25 mg/kg; i.duc 25 mg/kg; i.p.	8 weeks	Local administration of paclitaxel may be useful for breast cancer treatment	[285]
Potassium iodide Iodine (I ₂)	0.05% in drinking water	3-18 weeks	Long term I ₂ treatment was the only effective in the inhibition of mammary carcinogenesis	[70]
Thyroxine (T4)	3 µg/ml in drinking water	18 weeks		
Raloxifene	20-60 mg/kg/diet	19 weeks		[286]

Keoxifen (9-cis-retinoic acid + raloxifene)	60 mg/kg/diet + 20-60 mg/kg/diet		Raloxifene and keoxifene suppressed mammary carcinogenesis	
Resveratrol (trans-3,4',5-trihydroxystilbene)	10-100 mg/kg/day; s.c.	5 days	Prepubertal treatment with resveratrol induced mammary carcinogenesis	[287]
Retinoid 9cUAB30 + Tamoxifen	150 mg/kg diet + 0.4 mg/kg diet	21 weeks	Combination of the agents resulted in an increased effect in preventing mammary cancers	[71]
Supplementation with lysine, arginine, proline, ascorbic acid and green tea extract	0.5% in the diet	24 weeks	The combination of supplements inhibited incidence and number of mammary tumors	[268]
Tamoxifen	6.25-500 µg; s.c.	8 weeks	Tamoxifen reduced mammary tumors incidence	[281,288]
	1 mg/kg; i.p.	21 weeks	and number of tumors <i>per</i> animal	
Targretin	6.7-60 mg/kg/day; gavage 92-275 mg/kg diet	17 weeks	Targretin reduced cancer multiplicity, the highest reduction was observed in high dose	[289]

b.w. body weight; **i.c.v.** intracerebroventricular; **i.d.** intradermal; **i.duc.** intraductal; **i.g.** intragastric; **i.p.** intraperitoneal; **i.v.** intravenous; **s.c.** subcutaneous

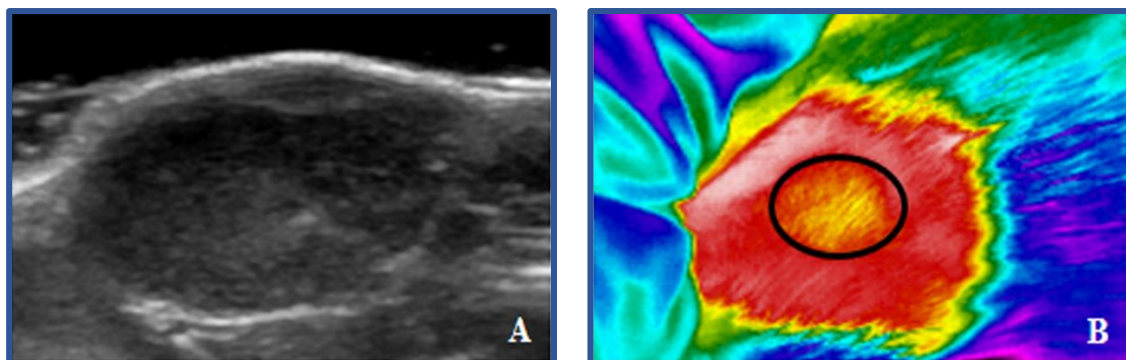


Figure 2.5. MNU-induced mammary tumor in Sprague-Dawley female rats evaluated by ultrasonography (B mode) (A) and thermography (tumor is delimited by the black circle) (B) 35 weeks after administration of the carcinogen agent MNU.

2.8. Transition of breast cancer therapies from female rats to human patients

In the 1960s, Calvin Schwabe developed the concept of one medicine stating that the human and animal medicines are linked and should grow together [290,291]. Study of breast cancer is one of the examples of involvement of comparative pathology between humans and animals [292]. As mentioned above, the model of MNU-induced mammary tumors in female rats has been used to develop new therapeutic agents and search for new targets in cancer therapy [132,149,268,278,293–297], being the main goal the transposition of data obtained in these animals to humans [39,270].

In Table 2.4, it is possible to observe several therapeutic approaches evaluated in the MNU-induced mammary cancer in female rats of Lewis, Sprague-Dawley, Ludwig, Wistar and Olac strains. MNU-induced mammary tumors in female rats have been used to evaluate the effects of several drugs and dietary compounds in mammary carcinogenesis, using different doses, routes and periods of administration.

Some of the compounds that were evaluated in this model of MNU-induced mammary tumors, such as anastrozole, docetaxel, doxorubicin, exemestane, fluorouracil, keoxifene, lapatinib, letrozole, methotrexate, paclitaxel, pamidronate, raloxifene and tamoxifen, are nowadays approved for breast cancer treatment in humans [298] and are being used in clinical practice to treat human patients with cancer. This fact highlights the importance of animal models in humans' health and welfare.

2.9. Conclusion

MNU is a universally used chemical carcinogen agent that may induce tumors in several organs. MNU-induced mammary tumors in Sprague-Dawley female rats is one of the best models for mammary cancer research, since this orthotopic model exhibits a short latency period and high reproducibility, and allow the analysis of different carcinogenesis steps (initiation, promotion, progression and metastasis). In addition to this, animals are easily housed and manipulated, they are cheap to maintain, and their use allow the research of novel potential therapeutic drugs. This *in vivo* experimental model of mammary tumors chemically-induced also allows the study of biology and evolution of tumors using imaging, genetic, molecular and histological techniques, and the most important one, the transposition of therapies from animals to humans.

2.10. References

- [1] Fujiki, H. Gist of Dr. Katsusaburo Yamagiwa's papers entitled "Experimental study on the pathogenesis of epithelial tumors" (I to VI reports). *Cancer Sci.*, **2014**, 105, 143–149.
- [2] Jonkers, J.; Berns, A. Animal models of cancer. In *Introduction to the cellular and molecular biology of cancer* (Knowles, M. and Selby, P., eds), **2005**, pp. 317–336, Oxford University Press.
- [3] Lijinski, W. Carcinogenicity and mutagenicity of *N*-nitroso compounds. *Mol. Toxicol.*, **1987**, 1, 107–119.
- [4] Steele, VE.; Lubet, RA.; Moon, RC. Preclinical animal models for the development of cancer chemoprevention drugs. In *Cancer chemoprevention* (Kelloff, G., Hawk, E. T., and Sigman, C. C., eds), **2004**, Humana Press.
- [5] Aucher, MC. Hazards of nitrate, nitrite and *N*-nitrosocompounds in human nutrition. In *Nutritional Toxicology* (Hathcock, J. N., ed), **1982**, pp. 328–367, Academic Press.
- [6] Saffhill, R.; Margison, GP.; Oconnor, PJ. Mechanisms of carcinogenesis induced by alkylating agents. *Biochim. Biophys. Acta*, **1985**, 823, 111–145.
- [7] Lijinsky, W. *N*-nitroso compounds in the diet. *Mutat. Res. Toxicol. Environ. Mutagen.*, **1999**, 443, 129–138.
- [8] International Agency for Research on Cancer (IARC). Evaluation of the

- carcinogenic risk of chemicals to humans: some *N*-nitroso compounds. *IARC*, **1978**.
- [9] Raj, A.; Mayberry, JF.; Podas, T. Occupation and gastric cancer. *Postgrad. Med. J.*, **2003**, 79, 252–258.
- [10] Rappe, C.; Buser, HR. Occupational exposure to polychlorinated dioxins and dibenzofurans. *Abstr. Pap. Am. Chem. Soc.*, **1980**, 180, 21.
- [11] Stuff, JE.; Goh, ET.; Barrera, SL.; Bondy, ML.; Forman, MR. Construction of an *N*-nitroso database for assessing dietary intake. *J. Food Compos. Anal.*, **2009**, 22, S42–47.
- [12] Tricker, AR. *N*-nitroso compounds and man: sources of exposure, endogenous formation and occurrence in body fluids. *Eur. J. Cancer Prev.*, **1997**, 6, 226–268.
- [13] Wynder, EL.; Hoffman, D. Biological testes for tumorigenic and cilia-toxic activity. In *Tobacco and tobacco smoke: studies in experimental carcinogenesis* (Wynder, E. L. and Hoffman, D., eds), **1967**, pp. 179, Academic Press.
- [14] Reed, PI. *N*-nitroso compounds, their relevance to human cancer and further prospects for prevention. *Eur. J. Cancer Prev.*, **1996**, 5, 137–147.
- [15] Kyrtopoulos, SA. DNA adducts in humans after exposure to methylating agents. *Mutat. Res. Mol. Mech. Mutagen.*, **1998**, 405, 135–143.
- [16] Lijinski, W. Interaction with nucleic acids of carcinogenic and mutagenic *N*-nitroso compounds. In *Progress in nucleic acid & molecular biology* (Cohn, W. E., ed), **1981**, pp. 247–270, Academic Press
- [17] Deshpande, SS. Principles of toxicology. In *Handbook of food toxicology*, **2002**, pp. 11–40, Marcel Dekker.
- [18] Montgomery, JA. The design of chemotherapeutic agents. *Acc. Chem. Res.*, **1986**, 19, 293–300.
- [19] International Agency for Research on Cancer (IARC). Evaluation of the carcinogenic risk of chemicals to humans: some *N*-nitroso compounds. *IARC*, **1978**.
- [20] National Center for Biotechnology Information: PubChem Substance Database; CID=12699, Source=Scripps Research Institute Molecular Screening Center. http://pubchem.ncbi.nlm.nih.gov/summary/summary.cgi?cid=12699&loc=ec_rcs, **2014**.
- [21] Prentiss, AM. Vesicant agents. In *Chemicals in welfare: a treatise on chemical*

- warfare*, **1937**, pp. 177–300, McGraw-Hill.
- [22] Reutter, S. Hazards of chemical weapons release during war: new perspectives. *Environ. Health Perspect.*, **1999**, 107, 985–990.
- [23] Alexander, SF. Medical report of the Bari Harbor mustard casualties. *Mil. Surg.*, **1947**, 101, 1–17.
- [24] United Nations, Security Council. Report of the mission dispatched by the Secretary General to investigate allegations of the use of chemical weapons in the conflict between the Islamic Republic of Iran and Iraq. *United Nations*, **1988**.
- [25] Margison, GP.; O'Connor, PJ. Nucleic acid modification by *N*-nitroso compounds. In *Chemical carcinogens and DNA* (Grover, P. L., ed), **1979**, pp. 111–159, CRC Press
- [26] Magee, PN.; Montesano, R.; Preussman, R. *N-Nitroso compounds and related carcinogenesis*. **1976**, ACS Press.
- [27] Singer, B.; Kusmierk, JT. Chemical mutagenesis. *Annu. Rev. Biochem.*, **1982**, 51, 655–693.
- [28] Beranek, DT. Distribution of methyl and ethyl adducts following alkylation with monofunctional alkylating agents. *Mutat. Res.*, **1990**, 231, 11–30.
- [29] Ellison, KS.; Dogliotti, E.; Connors, TD.; Basu, AK.; Essigmann, JM. Site-specific mutagenesis by O-6-alkylguanines located in the chromosomes of mammalian cells: influence of the mammalian O-6-alkylguanine-DNA alkyltransferase. *Proc. Natl. Acad. Sci. U.S.A.*, **1989**, 86, 8620–8624.
- [30] Loveless, A. Possible relevance of O-6 alkylation of deoxyguanosine to mutagenicity and carcinogenicity of nitrosamines and nitrosamides. *Nature*, **1969**, 223, 206–207.
- [31] Stephanou, G.; Vlastos, D.; Vlachodimitropoulos, D.; Demopoulos, NA. A comparative study on the effect of MNU on human lymphocyte cultures *in vitro* evaluated by O-6-mdG formation, micronuclei and sister chromatid exchanges induction. *Cancer Lett.*, **1996**, 109, 109–114.
- [32] Wurdeman, RL.; Church, KM.; Gold, B. DNA methylation by *N*-methyl-*N*-nitrosourea, *N*-methyl-*N'*-nitro-*N*-nitrosoguanidine, *N*-nitroso (1-acetoxyethyl) methylamine, and Diazomethane - mechanism for the formation of N⁷-methylguanine in sequence-characterized 5'-P-32-end-labeled DNA. *J. Am. Chem. Soc.*, **1989**, 111, 6408–6412.

- [33] Prager, B.; Jacobson, P.; Schmidt, P.; Stern, D. *Beilsteins handbuch der organischen chemie*. **1922**, Springer.
- [34] Von Brüning, G. Ueber das methylhydrazin. *Liebigs Ann. der Chemie*, **1889**, 253, 5–14.
- [35] Rapoport, IA. 85-percent of mutations in sex chromosome under influence of nitrosoethylurea. *Dokl. Akad. Nauk Sssr*, **1962**, 146, 1418–1421.
- [36] Kolaric, K. Combination chemotherapy with *N*-methyl-*N*-nitrosourea (MNU) and cyclophosphamide in solid tumors. *Zeitschrift für Krebsforsch. und Klin. Onkol.*, **1977**, 89, 311–319.
- [37] Sendowski, K.; Rajewsky, MF. DNA sequence dependence of Guanine-O⁶ alkylation by the *N*-nitroso carcinogens *N*-methyl-*N*-nitrosourea and *N*-ethyl-*N*-nitrosourea. *Mutat. Res.*, **1991**, 250, 153–160.
- [38] Bosland, MC. Chemical and hormonal induction of prostate cancer in animal models. *Urol. Oncol.*, **1996**, 2, 103–110.
- [39] Tsubura, A.; Lai, YC.; Miki, H.; Sasaki, T.; Uehara, N.; Yuri, T.; Yoshizawa, K. Animal models of *N*-methyl-*N*-nitrosourea-induced mammary cancer and retinal degeneration with special emphasis on therapeutic trials. *In vivo*, **2011**, 25, 11–22.
- [40] O'Connor, PJ.; Saffhil, R.; Margison, GP. *N*-nitrosocompounds: biochemical mechanisms of action. In *Environmental carcinogens, occurrence, risk evaluation and mechanisms* (Emmelot, P. and Kriek, E., eds), **1979**, pp. 73–96, Elsevier/North Holland Press.
- [41] Yano, K.; Isobe, M. Mutagenicity of *N*-methyl-*N'*-aryl-*N*-nitrosoureas and *N*-methyl-*N'*-aryl-*N'*-methyl-*N*-nitrosoureas in relation to their alkylating activity. *Cancer Res.*, **1979**, 39, 5147–5149.
- [42] Brundrett, RB.; Colvin, M.; White, EH.; Mckee, J.; Hartman, PE.; Brown, DL. Comparison of mutagenicity, anti-tumor activity, and chemical properties of selected nitrosoureas and nitrosoamides. *Cancer Res.*, **1979**, 39, 1328–1333.
- [43] Reis, LO.; Favaro, WJ.; Ferreira, U.; Billis, A.; Fazuoli, MG.; Cagnon, VHA. Evolution on experimental animal model for upper urothelium carcinogenesis. *World J. Urol.*, **2010**, 28, 499–505.
- [44] Cui, LB.; Yuan, S.; Dai, GD.; Pan, HX.; Chen, JF.; Song, L.; Wang, SL.; Chang, HC.; Sheng, HB.; Wang, XR. Modification of *N*-methyl-*N*-nitrosourea initiated bladder carcinogenesis in Wistar rats by terephthalic acid. *Toxicol. Appl.*

- Pharmacol.*, **2006**, 210, 24–31.
- [45] Lijinsky, W. Species-differences in nitrosamine carcinogenesis. *J. Cancer Res. Clin. Oncol.*, **1984**, 108, 46–55.
- [46] Wijnhoven, SWP.; Van Steeg, H. Transgenic and knockout mice for DNA repair functions in carcinogenesis and mutagenesis. *Toxicology*, **2003**, 193, 171–187.
- [47] Naghipur, A.; Ikonomou, MG.; Kebarle, P.; Lown, JW. Mechanism of action of (2-Haloethyl)nitrosoureas on DNA - discrimination between alternative pathways of DNA-base modification by 1,3-bis(2-fluoroethyl)-1-nitrosourea by using specific deuterium labeling and identification of reaction-products by Hplc Tan. *J. Am. Chem. Soc.*, **1990**, 112, 3178–3187.
- [48] Lunn, G.; Sansone, EB. Dealing with spills of hazardous chemicals: some nitrosamides. *Food Chem. Toxicol.*, **1988**, 26, 481–484.
- [49] Lunn, G.; Sansone, EB.; Andrews, AW.; Keefer, LK. Decontamination and disposal of nitrosoureas and related *N*-nitroso compounds. *Cancer Res.*, **1988**, 48, 522–526.
- [50] Lukasova, E.; Palecek, E.; Kruglyakova, KE.; Zhizhina, GP.; Smotryaeva, MA. Properties of DNA modified with -nitrosourea. *Radiat. Environ. Biophys.*, **1977**, 14, 231–238.
- [51] Druckrey, H.; Schmahl, D.; Muller, M.; Preussmann, R. Erzeugung von magenkrebs durch nitrosamide an ratten. *Naturwissenschaften*, **1961**, 48, 165.
- [52] Janisch, W.; Schreiber, D.; Warzok, R.; Scholtze, P. Experiments on rhesus-monkeys (*Macaca mulatta*) with carcinogens methylnitrosourea and ethylnitrosourea. *Arch. Geschwulstforsch.*, **1977**, 47, 123–126.
- [53] Adamson, RH.; Krolkowski, FJ.; Correa, P.; Sieber, SM.; Dalgard, DW. Carcinogenicity of 1-methyl-1-nitrosourea in nonhuman-primates. *J. Natl. Cancer Inst.*, **1977**, 59, 415–422.
- [54] Stavrou, D.; Dahme, E.; Kalich, J. Induction of tumors of stomach in mini pigs by methylnitrosourea administration. *Res. Exp. Med.*, **1976**, 169, 33–43.
- [55] Warzok, R.; Schneide, J.; Schreibe, D.; Janisch, W. Experimental brain tumours in dogs. *Experientia*, **1970**, 26, 303–304.
- [56] Corpet, DE.; Pierre, F. How good are rodent models of carcinogenesis in predicting efficacy in humans? A systematic review and meta-analysis of colon chemoprevention in rats, mice and men. *Eur. J. Cancer*, **2005**, 41, 1911–1922.

- [57] Gescher, AJ.; Steward, WP. Relationship between mechanisms, bioavailability, and preclinical chemopreventive efficacy of resveratrol: a conundrum. *Cancer Epidemiol. Biomarkers Prev.*, **2003**, 12, 953–957.
- [58] Okajima, E.; Hiramatsu, T.; Hirao, K.; Ijuin, M.; Hirao, Y.; Babaya, K.; Ikuma, S.; Ohara, S.; Shiomi, T.; Hijioka, T.; Ohishi, H. Urinary bladder tumors induced by *N*-butyl-*N*-(4-hydroxybutyl)nitrosamine in dogs. *Cancer Res.*, **1981**, 41, 1958–1966.
- [59] Oliveira, PA.; Colaco, A.; De la Cruz P, LF.; Lopes, C. Experimental bladder carcinogenesis - rodent models. *Exp. Oncol.*, **2006**, 28, 2–11.
- [60] Son, WC.; Gopinath, C. Early occurrence of spontaneous tumors in CD-1 mice and Sprague-Dawley rats. *Toxicol. Pathol.*, **2004**, 32, 371–374.
- [61] Isaacs, JT. Genetic control of resistance to chemically-induced mammary adenocarcinogenesis in the rat. *Cancer Res.*, **1986**, 46, 3958–3963.
- [62] Kumar, DG.; Parvathi, V.; Meenakshi, P.; Rathi, MA.; Gopalakrishnan, VK. Anticancer activity of the ethanolic extract of *Crateva nurvala* bark against testosterone and MNU-induced prostate cancer in rats. *Chin. J. Nat. Med.*, **2012**, 10, 334–338.
- [63] Reddy, BS.; Watanabe, K.; Weisburger, JH. Effect of high-fat diet on colon carcinogenesis in F344 rats treated with 1,2-Dimethylhydrazine, Methylazoxymethanol acetate, or Methylnitrosourea. *Cancer Res.*, **1977**, 37, 4156–4159.
- [64] Takahashi, H.; Uemura, Y.; Nakao, I.; Tsubura, A. Induction of mammary carcinomas by the direct application of crystalline *N*-methyl-*N*-nitrosourea onto rat mammary gland. *Cancer Lett.*, **1995**, 92, 105–111.
- [65] Raghavan, D.; Debruyne, F.; Herr, H.; Jocham, D.; Kakizoe, T.; Okajima, E.; Sandberg, A.; Tannock, I. Developments in bladder cancer. In *Experimental models of bladder cancer: a critical review* (Allen, R., ed), **1986**, pp. 171–208, Liss.
- [66] Thompson, HJ.; Adlakha, H. Dose-responsive induction of mammary gland carcinomas by the intraperitoneal injection of *l*-methyl-*l*-nitrosourea. *Cancer Res.*, **1991**, 51, 3411–3415.
- [67] Faustino-Rocha, AI.; Silva, A.; Gabriel, J.; Teixeira-Guedes, CI.; Lopes, C.; Gil da Costa, R.; Gama, A.; Ferreira, R.; Oliveira, PA.; Ginja, M. Ultrasonographic,

- thermographic and histologic evaluation of MNU-induced mammary tumors in female Sprague-Dawley rats. *Biomed. Pharmacother.*, **2013**, 67, 771–776.
- [68] Bera, TK.; Tsukamoto, T.; Panda, DK.; Huang, T.; Guzman, RC.; Hwang, SI.; Nandi, S. Defective retrovirus insertion activates c-Ha-ras protooncogene in an MNU-induced rat mammary carcinoma. *Biochem. Biophys. Res. Commun.*, **1998**, 248, 835–840.
- [69] Bigsby, RA. Synergistic tumor promoter effects of estrone and progesterone in methylnitrosourea-induced rat mammary cancer. *Cancer Lett.*, **2002**, 179, 113–119.
- [70] Garcia-Solis, P.; Alfaro, Y.; Anguiano, B.; Delgado, G.; Guzman, RC.; Nandi, S.; Diaz-Munoz, M.; Vazquez-Martinez, O.; Aceves, C. Inhibition of *N*-methyl-*N*-nitrosourea-induced mammary carcinogenesis by molecular iodine (I-2) but not by iodide (I) treatment evidence that I-2 prevents cancer promotion. *Mol. Cell. Endocrinol.*, **2005**, 236, 49–57.
- [71] Grubbs, CJ.; Hill, DL.; Bland, KI.; Beenken, SW.; Lin, TH.; Eto, I.; Atigadda, VR.; Vines, KK.; Brouillette, WJ.; Muccio, DD. 9cUAB30, an RXR specific retinoid, and/or tamoxifen in the prevention of methylnitrosourea-induced mammary cancers. *Cancer Lett.*, **2003**, 201, 17–24.
- [72] Imai, T.; Cho, YM.; Hasumura, M.; Hirose, M. Enhancement by acrylamide of *N*-methyl-*N*-nitrosourea-induced rat mammary tumor development - possible application for a model to detect co-modifiers of carcinogenesis. *Cancer Lett.*, **2005**, 230, 25–32.
- [73] Li, JX.; Cho, YY.; Langfald, A.; Carper, A.; Lubet, RA.; Grubbs, CJ.; Ericson, ME.; Bode, AM. Lapatinib, a preventive/therapeutic agent against mammary cancer, suppresses RTK-mediated signaling through multiple signaling pathways. *Cancer Prev. Res.*, **2011**, 4, 1190–1197.
- [74] Liska, J.; Macejova, D.; Galbavy, S.; Baranova, M.; Zlatos, J.; Stvrtina, S.; Mostbock, S.; Weiss, R.; Scheiblhofer, S.; Thalhamer, J.; Brtko, J. Treatment of *I*-methyl-*I*-nitrosourea-induced mammary tumours with immunostimulatory CpG motifs and 13-*cis* retinoic acid in female rats: histopathological study. *Exp. Toxicol. Pathol.*, **2003**, 55, 173–179.
- [75] McCormick, DL.; Moon, RC. Inhibition of mammary carcinogenesis by flurbiprofen, a non-steroidal anti-inflammatory agent. *Br. J. Cancer*, **1983**, 48,

- 859–861.
- [76] Mehta, R.; Hawthorne, M.; Uselding, L.; Albinescu, D.; Moriarty, R.; Christov, K.; Mehta, R. Prevention of *N*-methyl-*N*-nitrosourea-induced mammary carcinogenesis in rats by 1 alpha-hydroxyvitamin D-5. *J. Natl. Cancer Inst.*, **2000**, 92, 1836–1840.
- [77] Nakhate, KT.; Kokare, DM.; Singru, PS.; Taksande, AG.; Kotwal, SD.; Subhedar, NK. Hypothalamic cocaine- and amphetamine-regulated transcript peptide is reduced and fails to modulate feeding behavior in rats with chemically-induced mammary carcinogenesis. *Pharmacol. Biochem. Behav.*, **2010**, 97, 340–349.
- [78] Schaffer, EM.; Liu, JZ.; Green, J.; Dangler, CA.; Milner, JA. Garlic and associated allyl sulfur components inhibit *N*-methyl-*N*-nitrosourea induced rat mammary carcinogenesis. *Cancer Lett.*, **1996**, 102, 199–204.
- [79] Shirai, K.; Uemura, Y.; Fukumoto, M.; Tsukamoto, T.; Pascual, R.; Nandi, S.; Tsubura, A. Synergistic effect of MNU and DMBA in mammary carcinogenesis and H-ras activation in female Sprague-Dawley rats. *Cancer Lett.*, **1997**, 120, 87–93.
- [80] Thompson, HJ.; Meeker, LD. Induction of mammary gland carcinomas by the subcutaneous injection of *l*-methyl-*l*-nitrosourea. *Cancer Res.*, **1983**, 43, 1628–1629.
- [81] Yang, JH.; Nakagawa, H.; Tsuta, K.; Tsubura, A. Influence of perinatal genistein exposure on the development of MNU-induced mammary carcinoma in female Sprague-Dawley rats. *Cancer Lett.*, **2000**, 149, 171–179.
- [82] Shivapurkar, N.; Tang, ZC.; Frost, A.; Alabaster, O. A rapid dual organ rat carcinogenesis bioassay for evaluating the chemoprevention of breast and colon cancer. *Cancer Lett.*, **1996**, 100, 169–179.
- [83] Lee, WM.; Lu, SY.; Medline, A.; Archer, MC. Susceptibility of lean and obese Zucker rats to tumorigenesis induced by *N*-methyl-*N*-nitrosourea. *Cancer Lett.*, **2001**, 162, 155–160.
- [84] Coburn, MA.; Brueggemann, S.; Bhatia, S.; Cheng, B.; Li, BDL.; Li, XL.; Luraguiz, N.; Maxuitenko, YY.; Orchard, EA.; Zhang, SL.; Stoff-Khalili, MA.; Mathis, JM.; Kleiner-Hancock, HE. Establishment of a mammary carcinoma cell line from Syrian hamsters treated with *N*-methyl-*N*-nitrosourea. *Cancer Lett.*, **2011**, 312, 82–90.

- [85] Mori, H.; Niwa, K.; Zheng, Q.; Yamada, Y.; Sakata, K.; Yoshimi, N. Cell proliferation in cancer prevention; effects of preventive agents on estrogen-related endometrial carcinogenesis model and on an *in vitro* model in human colorectal cells. *Mutat. Res. Mol. Mech. Mutagen.*, **2001**, 480, 201–207.
- [86] Niwa, K.; Morishita, S.; Murase, T.; Mudigdo, A.; Tanaka, T.; Mori, H.; Tamaya, T. Chronological observation of mouse endometrial carcinogenesis induced by *N*-methyl-*N*-nitrosourea and 17 beta-estradiol. *Cancer Lett.*, **1996**, 104, 115–119.
- [87] Gonçalves, BF.; Zanetoni, C.; Scarano, WR.; Góes, RM.; Vilamaior, PSL.; Taboga, SR.; Campos, SGP. Prostate carcinogenesis induced by *N*-methyl-*N*-nitrosourea (MNU) in gerbils: histopathological diagnosis and potential invasiveness mediated by extracellular matrix components. *Exp. Mol. Pathol.*, **2010**, 88, 96–106.
- [88] Ordóñez, G.; Rembao, D.; Sotelo, J. *Taenia crassiceps* cysticercosis in mice does not increase the carcinogenic effect of methyl-nitrosourea. *Exp. Parasitol.*, **2003**, 103, 169–170.
- [89] Pazos, P.; Lanari, C.; Molinolo, AA. Protective role of medroxyprogesterone acetate on *N*-methyl-*N*-nitrosourea-induced lymphomas in BALB/c female mice. *Leuk. Res.*, **2001**, 25, 165–167.
- [90] Zhang, SSM.; Welte, T.; Fu, XY. Dysfunction of Stat4 leads to accelerated incidence of chemical-induced thymic lymphomas in mice. *Exp. Mol. Pathol.*, **2001**, 70, 231–238.
- [91] Hoivik, DJ.; Allen, JS.; Wall, HG.; Nold, JB.; Miller, RT.; Santostefano, MJ. Studies evaluating the utility of *N*-methyl-*N*-nitrosourea as a positive control in carcinogenicity studies in the p53(+/-) mouse. *Int. J. Toxicol.*, **2005**, 24, 349–356.
- [92] Tarso, L.; Meyer, FS.; Cioato, MG.; Meurer, L.; Schirmer, CC. Experimental model of gastric carcinogenesis with *N*-methyl-*N*-nitrosourea for F344 rats and CH3 mice is valid for Wistar rats? *Arq. Bras. Cir. Dig.*, **2011**, 24, 55–58.
- [93] Iatropoulos, MJ.; Jeffrey, AM.; Enzmann, HG.; Von Keutz, E.; Schlueter, G.; Williams, GM. Assessment of chronic toxicity and carcinogenicity in an accelerated cancer bioassay in rats of moxifloxacin, a quinolone antibiotic. *Exp. Toxicol. Pathol.*, **2001**, 53, 345–357.
- [94] Shimizu, M.; Suzui, M.; Moriwaki, H.; Mori, H.; Yoshimi, N. No involvement of beta-catenin gene mutation in gastric carcinomas induced by *N*-methyl-*N*-

- nitrosourea in male F344 rats. *Cancer Lett.*, **2003**, 195, 147–152.
- [95] Tomita, H.; Takaishi, S.; Menheniott, TR.; Yang, XD.; Shibata, W.; Jin, GC.; Betz, KS.; Kawakami, K.; Minamoto, T.; Tomasetto, C.; Rio, MC.; Lerkowit, N.; Varro, A.; Giraud, AS.; Wang, TC. Inhibition of gastric carcinogenesis by the hormone gastrin is mediated by suppression of TFF1 epigenetic silencing. *Gastroenterology*, **2011**, 140, 879–891.
- [96] Sakamoto, K.; Hikiba, Y.; Nakagawa, H.; Hayakawa, Y.; Yanai, A.; Akanuma, M.; Ogura, K.; Hirata, Y.; Kaestner, KH.; Omata, M.; Maeda, S. Inhibitor of kappa B kinase beta regulates gastric carcinogenesis via interleukin-1 alpha expression. *Gastroenterology*, **2010**, 139, 226–238.
- [97] Masui, T.; Tezuka, N.; Nakanishi, H.; Inada, K.; Miyashita, N.; Tatematsu, M. Induction of invasive squamous cell carcinomas in the forestomach of (C3HxMSM)F1, MSM, and C3H mice by *N-methyl-N-nitrosourea* and mutational analysis of the H-ras and p53 genes. *Cancer Lett.*, **1997**, 111, 97–104.
- [98] Maruta, F.; Sugiyama, A.; Ishida, K.; Ikeno, T.; Murakami, M.; Kawasaki, S.; Ota, H.; Tatematsu, M.; Katsuyama, T. Timing of *N-methyl-N-nitrosourea* administration affects gastric carcinogenesis in Mongolian gerbils infected with *Helicobacter pylori*. *Cancer Lett.*, **2000**, 160, 99–105.
- [99] Yarita, T.; Nettesheim, P.; Williams, ML. Tumor induction in the trachea of hamsters with *N-Nitroso-N-methylurea*. *Cancer Res.*, **1978**, 38, 1667–1676.
- [100] Tatematsu, M.; Yamamoto, M.; Iwata, H.; Fukami, H.; Yuasa, H.; Tezuka, N.; Masui, T.; Nakanishi, H. Induction of glandular stomach cancers in C3H mice treated with *N-methyl-N-nitrosourea* in the drinking water. *Japanese J. Cancer Res.*, **1993**, 84, 1258–1264.
- [101] Shivshankar, P.; Devi, CSS. Evaluation of co-stimulatory effects of *Tamarindus indica L.* on MNU-induced colonic cell proliferation. *Food Chem. Toxicol.*, **2004**, 42, 1237–1244.
- [102] Yang, JH.; Shikata, N.; Mizuoka, H.; Tsubura, A. Colon carcinogenesis in shrews by intrarectal infusion of *N-methyl-N-nitrosourea*. *Cancer Lett.*, **1996**, 110, 105–112.
- [103] Narisawa, T.; Sato, M.; Tani, M.; Kudo, T.; Takahashi, T.; Goto, A. Inhibition of development of methylnitrosourea-induced rat colon tumors by indomethacin treatment. *Cancer Res.*, **1981**, 41, 1954–1957.

- [104] Narisawa, T.; Takahashi, M.; Niwa, M.; Fukaura, Y.; Fujiki, H. Inhibition of methylnitrosourea-induced large bowel cancer development in rats by sarcophytol-A, a product from a marine soft coral *Sarcophyton glaucum*. *Cancer Res.*, **1989**, 49, 3287–3289.
- [105] Teixeira-Guedes, CI.; Faustino-Rocha, AI.; Talhada, D.; Duarte, JA.; Ferreira, R.; Seixas, F.; Oliveira, PA. A liver schwannoma observed in a female Sprague-Dawley rat treated with MNU. *Exp. Toxicol. Pathol.*, **2014**, 66, 125–128.
- [106] Pereira, MA.; Phelps, JB. Promotion by dichloroacetic acid and trichloroacetic acid of *N*-methyl-*N*-nitrosourea-initiated cancer in the liver of female B6C3F1 mice. *Cancer Lett.*, **1996**, 102, 133–141.
- [107] Kobayashi, K.; Inada, K.; Furihata, C.; Tsukamoto, T.; Ikehara, Y.; Yamamoto, M.; Tatematsu, M. Effects of low dose catechol on glandular stomach carcinogenesis in BALB/c mice initiated with *N*-methyl-*N*-nitrosourea. *Cancer Lett.*, **1999**, 139, 167–172.
- [108] Hamamoto, Y.; Hamamoto, N.; Nakajima, T.; Ozawa, H. Morphological changes of epithelial rests of Malassez in rat molars induced by local administration of *N*-methylnitrosourea. *Arch. Oral Biol.*, **1998**, 43, 899–906.
- [109] Moriguchi, K.; Yuri, T.; Yoshizawa, K.; Kiuchi, K.; Takada, H.; Inoue, Y.; Hada, T.; Matsumura, M.; Tsubura, A. Dietary docosahexaenoic acid protects against *N*-methyl-*N*-nitrosourea-induced retinal degeneration in rats. *Exp. Eye Res.*, **2003**, 77, 167–173.
- [110] Paik, SS.; Jeong, E.; Jung, SW.; Ha, TJ.; Kang, S.; Sim, S.; Jeon, JH.; Chun, MH.; Kim, IB. Anthocyanins from the seed coat of black soybean reduce retinal degeneration induced by *N*-methyl-*N*-nitrosourea. *Exp. Eye Res.*, **2012**, 97, 55–62.
- [111] Wan, J.; Zheng, H.; Chen, ZL.; Xiao, HL.; Shen, ZJ.; Zhou, GM. Preferential regeneration of photoreceptor from Muller glia after retinal degeneration in adult rat. *Vision Res.*, **2008**, 48, 223–234.
- [112] Yang, L.; Li, D.; Chen, JM.; Yang, JN.; Xue, LP.; Hu, SX.; Wu, KL. Microarray expression analysis of the early *N*-methyl-*N*-nitrosourea-induced retinal degeneration in rat. *Neurosci. Lett.*, **2007**, 418, 38–43.
- [113] Rahn, JJ.; Trono, D.; Gimenez-Conti, I.; Butler, AP.; Nairn, RS. Etiology of MNU-induced melanomas in *Xiphophorus hybrids*. *Comp. Biochem. Physiol. C-Toxicology Pharmacol.*, **2009**, 149, 129–133.

- [114] Kazianis, S.; Gimenez-Conti, I.; Setlow, RB.; Woodhead, AD.; Harshbarger, JC.; Trono, D.; Ledesma, M.; Nairn, RS.; Walter, RB. MNU induction of neoplasia in a platyfish model. *Lab. Investig.*, **2001**, 81, 1191–1198.
- [115] Graham, SD.; Napalkov, P.; Oladele, A.; Keane, TE.; Petros, JA.; Clarke, HS.; Kassabian, VS.; Dillehay, DL. Intravesical suramin in the prevention of transitional cell carcinoma. *Urology*, **1995**, 45, 59–63.
- [116] Reis, LO.; Ferreira, U.; Billis, A.; Cagnon, VHA.; Favaro, WJ. Anti-angiogenic effects of the superantigen staphylococcal enterotoxin B and bacillus Calmette-Guérin immunotherapy for nonmuscle invasive bladder cancer. *J. Urol.*, **2012**, 187, 438–445.
- [117] Wang, ZG.; Durand, DB.; Schoenberg, M.; Pan, YT. Fluorescence guided optical coherence tomography for the diagnosis of early bladder cancer in a rat model. *J. Urol.*, **2005**, 174, 2376–2381.
- [118] Kunze, E.; Schulz, H.; Ahrens, H.; Gabius, HJ. Lack of an antitumoral effect of immunomodulatory galactoside-specific mistletoe lectin on *N*-methyl-*N*-nitrosourea-induced urinary bladder carcinogenesis in rats. *Exp. Toxicol. Pathol.*, **1997**, 49, 167–180.
- [119] Knox, P. Carcinogenic nitrosamides and cell cultures. *Nature*, **1976**, 259, 671–673.
- [120] Esendagli, G.; Yilmaz, G.; Canpinar, H.; Gunel-Ozcan, A.; Guc, MO.; Guc, D. Coexistence of different tissue tumorigenesis in an *N*-methyl-*N*-nitrosourea-induced mammary carcinoma model: a histopathological report in Sprague-Dawley rats. *Lab. Anim.*, **2009**, 43, 60–64.
- [121] Miyazono, Y.; Harada, K.; Sugiyama, K.; Ueno, M.; Torii, M.; Kato, I.; Matsuura, H.; Hirata, K. Toxicological characterization of *N*-methyl-*N*-nitrosourea-induced cataract in rats by LC/MS-based metabonomic analysis. *J. Appl. Toxicol.*, **2011**, 31, 655–662.
- [122] Kiuchi, K.; Yoshizawa, K.; Moriguchi, K.; Tsubura, A. Rapid induction of cataract by a single intraperitoneal administration of *N*-methyl-*N*-nitrosourea in 15-day-old Sprague-Dawley (Jcl:SD) rats. *Exp. Toxicol. Pathol.*, **2002**, 54, 181–186.
- [123] Yoshizawa, K.; Oishi, Y.; Nambu, H.; Yamamoto, D.; Yang, JH.; Senzaki, H.; Miki, H.; Tsubura, A. Cataractogenesis in neonatal Sprague-Dawley rats by *N*-methyl-*N*-nitrosourea. *Toxicol. Pathol.*, **2000**, 28, 555–564.
- [124] Roy, B.; Fujimoto, N.; Watanabe, H.; Ito, A. Induction of cataract in

- methylnitrosourea treated Fisher (F344) rats. *Hiroshima J. Med. Sci.*, **1989**, 38, 95–98.
- [125] Steele, VE.; Moon, RC.; Lubet, RA.; Grubbs, CJ.; Reddy, BS.; Wargovich, M.; McCormick, DL.; Pereira, MA.; Crowell, JA.; Bagheri, D.; Sigman, CC.; Boone, CW.; Kelloff, GJ. Preclinical efficacy evaluation of potential chemopreventive agents in animal carcinogenesis models - methods and results from the NCI chemoprevention drug development program. *J. Cell. Biochem.*, **1994**, 20, 32-54.
- [126] Gal, A.; Baba, A.; Miclaus, V.; Bouari, C.; Taulescu, M.; Bolf, P.; Borza, G.; Catoi, C. Comparative aspects regarding MNU-induced mammary carcinogenesis in immature Spague-Dawley and Wistar rats. *Bull. UASVM, Vet. Med.*, **2011**, 68, 159–163.
- [127] Gullino, PM.; Pettigrew, HM.; Grantham, FH. *N*-nitrosomethylurea as mammary gland carcinogen in rats. *J. Natl. Cancer Inst.*, **1975**, 54, 401–414.
- [128] International Agency for Research on Cancer (IARC). Hormonal contraception and post-menopausal hormonal therapy. *IARC*, **1999**.
- [129] Pazos, P.; Lanari, C.; Meissm, R.; Charreau, E.; Pasqualini, CD. Mammary carcinogenesis induced by *N*-methyl-*N*-nitrosourea (MNU) and medroxyprogesterone acetate (MPA) in BALB/c mice. *Breast Cancer Res. Treat.*, **1991**, 20, 133–138.
- [130] Faustino-Rocha, A.; Oliveira, PA.; Pinho-Oliveira, J.; Teixeira-Guedes, C.; Soares-Maia, R.; Gil da Costa, R.; Colaço, B.; Pires, MJ.; Colaço, J.; Ferreira, R.; Ginja, M. Estimation of rat mammary tumor volume using caliper and ultrasonography measurements. *Lab. Anim. (NY)*, **2013**, 42, 217–24.
- [131] Russo, J.; Russo, IH. Atlas and histologic classification of tumors of the rat mammary gland. *J. Mammary Gland Biol. Neoplasia*, **2000**, 5, 187–200.
- [132] Russo, J.; Gusterson, BA.; Rogers, AE.; Russo, IH.; Wellings, SR.; Vanzwieten, MJ. Biology of disease - comparative study of human and rat mammary tumorigenesis. *Lab. Investig.*, **1990**, 62, 244–278.
- [133] Shafiee, R.; Javanbakht, J.; Atyabi, N.; Kheradmand, P.; Kheradmand, D.; Bahrami, A.; Daraei, H.; Khadivar, F. Diagnosis, classification and grading of canine mammary tumours as a model to study human breast cancer: an clinico-cytopathological study with environmental factors influencing public health and medicine. *Cancer Cell Int.*, **2013**, 13, 79.

- [134] Deboer, MD. Animal models of anorexia and cachexia. *Expert Opin. Drug Discov.*, **2009**, 4, 1145–1155.
- [135] Bennani-Baiti, N.; Walsh, D. Animal models of the cancer anorexia-cachexia syndrome. *Support. Care Cancer*, **2011**, 19, 1451–1463.
- [136] Tisdale, MJ. Biology of cachexia. *J. Natl. Cancer Inst.*, **1997**, 89, 1763–1773.
- [137] Tisdale, MJ. Cancer cachexia. *Curr. Opin. Gastroenterol.*, **2010**, 26, 146–151.
- [138] Morley, JE.; Thomas, DR.; Wilson, MMG. Cachexia: pathophysiology and clinical relevance. *Am. J. Clin. Nutr.*, **2006**, 83, 735–743.
- [139] Dewys, WD.; Begg, C.; Lavin, PT.; Band, PR.; Bennett, JM.; Bertino, JR.; Cohen, MH.; Douglass, HO.; Engstrom, PF.; Ezdinli, EZ.; Horton, J.; Johnson, GJ.; Moertel, CG.; Oken, MM.; Perlia, C.; Rosenbaum, C.; Silverstein, MN.; Skeel, RT. Prognostic effect of weight-loss prior to chemotherapy in cancer patients. *Am. J. Med.*, **1980**, 69, 491–497.
- [140] Tan, BHL.; Fearon, KCH. Cachexia: prevalence and impact in medicine. *Curr. Opin. Clin. Nutr. Metab. Care*, **2008**, 11, 400–407.
- [141] MacDonald, N.; Easson, AM.; Mazurak, VC.; Dunn, GP.; Baracos, VE. Understanding and managing cancer cachexia. *J. Am. Coll. Surg.*, **2003**, 197, 143–161.
- [142] Stewart, GD.; Skipworth, RJE.; Fearon, KCH. Cancer cachexia and fatigue. *Clin. Med. (Northfield. Il.)*, **2006**, 6, 140–143.
- [143] Fearon, KCH. Cancer cachexia: developing multimodal therapy for a multidimensional problem. *Eur. J. Cancer*, **2008**, 44, 1124–1132.
- [144] Miller, LD.; Smeds, J.; George, J.; Vega, VB.; Vergara, L.; Ploner, A.; Pawitan, Y.; Hall, P.; Klaar, S.; Liu, ET.; Bergh, J. An expression signature for p53 status in human breast cancer predicts mutation status, transcriptional effects, and patient survival. *Proc. Natl. Acad. Sci. U.S.A.*, **2005**, 102, 17882.
- [145] Milanezi, F.; Carvalho, S.; Schmitt, FC. EGFR/HER2 in breast cancer: a biological approach for molecular diagnosis and therapy. *Expert Rev. Mol. Diagn.*, **2008**, 8, 417–434.
- [146] Soares-Maia, R.; Faustino-Rocha, AI.; Teixeira-Guedes, CI.; Pinho-Oliveira, J.; Talhada, D.; Rema, A.; Faria, F.; Ginja, M.; Ferreira, R.; Gil da Costa, RM.; Oliveira, PA.; Lopes, C. MNU-induced rat mammary carcinomas: immunohistology and estrogen receptor expression. *J. Environ. Pathol. Toxicol.*

- Oncol.*, **2013**, 32, 157–163.
- [147] Thompson, HJ.; McGinley, JN.; Rothhammer, K.; Singh, M. Rapid induction of mammary intraductal proliferations, ductal carcinoma *in situ* and carcinomas by the injection of sexually immature female rats with *l*-methyl-*l*-nitrosourea. *Carcinogenesis*, **1995**, 16, 2407–2411.
- [148] Welsch, CW. Host factors affecting the growth of carcinogen-induced rat mammary carcinomas - a review and tribute to Charles Brenton Huggins. *Cancer Res.*, **1985**, 45, 3415–3443.
- [149] Rivera, ES.; Andrade, N.; Martin, G.; Melito, G.; Cricco, G.; Mohamad, N.; Davio, C.; Caro, R.; Bergoc, RM. Induction of mammary tumors in rat by intraperitoneal injection of NMU: histopathology and estral cycle influence. *Cancer Lett.*, **1994**, 86, 223–228.
- [150] Rose, DP.; Pruitt, B.; Stauber, P.; Erturk, E.; Bryan, GT. Influence of dosage schedule on the biological characteristics of *N*-nitrosomethylurea-induced rat mammary tumors. *Cancer Res.*, **1980**, 40, 235–239.
- [151] Rizza, P.; Barone, I.; Zito, D.; Giordano, F.; Lanzino, M.; De Amicis, F.; Mauro, L.; Sisci, D.; Catalano, S.; Wright, KD.; Gustafsson, JA.; Ando, S. Estrogen receptor beta as a novel target of androgen receptor action in breast cancer cell lines. *Breast Cancer Res.*, **2014**, 16, R21.
- [152] Leygue, E.; Murphy, LC. A bi-faceted role of estrogen receptor beta in breast cancer. *Endocr. Relat. Cancer*, **2013**, 20, R127–139.
- [153] Powell, E.; Shanle, E.; Brinkman, A.; Li, J.; Keles, S.; Wisinski, KB.; Huang, W.; Xu, W. Identification of estrogen receptor dimer selective ligands reveals growth-inhibitory effects on cells that co-express ER alpha and ER beta. *Plos One*, **2012**, 7.
- [154] Shanle, EK.; Xu, W. Selectively targeting estrogen receptors for cancer treatment. *Adv. Drug Deliv. Rev.*, **2010**, 62, 1265–1276.
- [155] Rastelli, F.; Crispino, S. Factors predictive of response to hormone therapy in breast cancer. *Tumori*, **2008**, 94, 370–383.
- [156] Ma, CX.; Sanchez, CG.; Ellis, MJ. Predicting endocrine therapy responsiveness in breast cancer. *Oncol. York*, **2009**, 23, 133–142.
- [157] Ali, SH.; O'Donnell, AL.; Balu, D.; Pohl, MB.; Seyler, MJ.; Mohamed, S.; Mousa, S.; Dandona, P. Estrogen receptor-alpha in the inhibition of cancer growth and

- angiogenesis. *Cancer Res.*, **2000**, 60, 7094–7098.
- [158] Gruvberger-Saal, SK.; Bendahl, PO.; Saal, LH.; Laakso, M.; Hegardt, C.; Eden, P.; Peterson, C.; Malmstrom, P.; Isola, J.; Borg, A.; Ferno, M. Estrogen receptor beta expression is associated with tamoxifen response in ER alpha-negative breast carcinoma. *Clin. Cancer Res.*, **2007**, 13, 1987–1994.
- [159] Fleming, FJ.; Hill, ADK.; McDermott, EW.; O’Higgins, NJ.; Young, LS. Differential recruitment of coregulator proteins steroid receptor coactivator-1 and silencing mediator for retinoid and thyroid receptors to the estrogen receptor-estrogen response element by beta-estradiol and 4-hydroxytamoxifen in human breast cancer. *J. Clin. Endocrinol. Metab.*, **2004**, 89, 375–383.
- [160] Esslimani-Sahla, M.; Simony-Lafontaine, J.; Kramar, A.; Lavaill, R.; Mollevi, C.; Warner, M.; Gustallsson, JA.; Rochefort, H. Estrogen receptor beta (ER beta) level but not its ER beta cx variant helps to predict tamoxifen resistance in breast cancer. *Clin. Cancer Res.*, **2004**, 10, 5769–5776.
- [161] Shaaban, AM.; Green, AR.; Karthik, S.; Alizadeh, Y.; Hughes, TA.; Harkins, L.; Ellis, IO.; Robertson, JF.; Paish, EC.; Saunders, PTK.; Groome, NP.; Speirs, V. Nuclear and cytoplasmic expression of ER beta 1, ER beta 2, and ER beta 5 identifies distinct prognostic outcome for breast cancer patients. *Clin. Cancer Res.*, **2008**, 14, 5228–5235.
- [162] Saji, S.; Omoto, Y.; Shimizu, C.; Warner, M.; Hayashi, Y.; Horiguchi, S.; Watanabe, T.; Hayashi, S.; Gustafsson, JA.; Toi, M. Expression of estrogen receptor (ER) beta cx protein in ER alpha-positive breast cancer: specific correlation with progesterone receptor. *Cancer Res.*, **2002**, 62, 4849–4853.
- [163] O’Neill, PA.; Davies, MPA.; Shaaban, AM.; Innes, H.; Torevell, A.; Sibson, DR.; Foster, CS. Wild-type oestrogen receptor beta (ERb1) mRNA and protein expression in tamoxifen-treated post-menopausal breast cancers. *Br. J. Cancer*, **2004**, 91, 1694–1702.
- [164] Novelli, F.; Milella, M.; Melucci, E.; Di Benedetto, A.; Sperduti, I.; Perrone-Donnorso, R.; Perracchio, L.; Ventura, I.; Nistico, C.; Fabi, A.; Buglioni, S.; Natali, PG.; Mottolese, M. A divergent role for estrogen receptor-beta in node-positive and node-negative breast cancer classified according to molecular subtypes: an observational prospective study. *Breast Cancer Res.*, **2008**, 10,74.
- [165] Lu, Y.; You, M.; Ghazoui, Z.; Liu, PY.; Vedell, PT.; Wen, WD.; Bode, AM.;

- Grubbs, CJ.; Lubet, RA. Concordant effects of aromatase inhibitors on gene expression in ER+ rat and human mammary cancers and modulation of the proteins coded by these genes. *Cancer Prev. Res.*, **2013**, 6, 1151–1161.
- [166] Howe, LR.; Brown, PH. Targeting the HER/EGFR/ErbB family to prevent breast cancer. *Cancer Prev. Res.*, **2011**, 4, 1149–1157.
- [167] Arteaga, CL.; Moulder, SL.; Yakes, FM. HER (ErbB) tyrosine kinase inhibitors in the treatment of breast cancer. *Semin. Oncol.*, **2002**, 29, 4–10.
- [168] Slamon, DJ.; Clark, GM.; Wong, SG.; Levin, WJ.; Ullrich, A.; Mcguire, WL. Human breast cancer: correlation of relapse and survival with amplification of the Her-2/neu oncogene. *Science*, **1987**, 235, 177–182.
- [169] Sorlie, T.; Perou, CM.; Tibshirani, R.; Aas, T.; Geisler, S.; Johnsen, H.; Hastie, T.; Eisen, MB.; van de Rijn, M.; Jeffrey, SS.; Thorsen, T.; Quist, H.; Matese, JC.; Brown, PO.; Botstein, D.; Lonning, PE.; Borresen-Dale, AL. Gene expression patterns of breast carcinomas distinguish tumor subclasses with clinical implications. *Proc. Natl. Acad. Sci. U.S.A.*, **2001**, 98, 10869–10874.
- [170] Grant, S. Cotargeting survival signaling pathways in cancer. *J. Clin. Invest.*, **2008**, 118, 3003–3006.
- [171] McCubrey, JA.; Steelman, LS.; Chappell, WH.; Abrams, SL.; Wong, EWT.; Chang, F.; Lehmann, B.; Terrian, DM.; Milella, M.; Tafuri, A.; Stivala, F.; Libra, M.; Basecke, J.; Evangelisti, C.; Martelli, AM.; Franklin, RA. Roles of the Raf/MEK/ERK pathway in cell growth, malignant transformation and drug resistance. *Biochim. Biophys. Acta-Molecular Cell Res.*, **2007**, 1773, 1263–1284.
- [172] Dineva, IK.; Zaharieva, MM.; Konstantinov, SM.; Eibl, H.; Berger, MR. Erufosine suppresses breast cancer *in vitro* and *in vivo* for its activity on PI3K, c-Raf and Akt proteins. *J. Cancer Res. Clin. Oncol.*, **2012**, 138, 1909–1917.
- [173] McLaughlin, SK.; Olsen, SN.; Dake, B.; De Raedt, T.; Lim, E.; Bronson, RT.; Beroukhi, R.; Polyak, K.; Brown, M.; Kuperwasser, C.; Cichowski, K. The RasGAP gene, RASAL2, is a tumor and metastasis suppressor. *Cancer Cell*, **2013**, 24, 365–378.
- [174] Zarbl, H.; Sukumar, S.; Arthur, A V.; Martinzanca, D.; Barbacid, M. Direct mutagenesis of Ha-Ras-oncogenes by *N*-nitroso-*N*-methylurea during initiation of mammary carcinogenesis in rats. *Nature*, **1985**, 315, 382–385.
- [175] Sukumar, S.; Notario, V.; Martinzanca, D.; Barbacid, M. Induction of mammary

- carcinomas in rats by nitroso-methylurea involves malignant activation of H-Ras-1 locus by single point mutations. *Nature*, **1983**, 306, 658–661.
- [176] Lacroix, M.; Linares, LK.; Le Cam, L. Role of the p53 tumor suppressor in metabolism. *M S-Medecine Sci.*, **2013**, 29, 1125–1130.
- [177] Ogawa, K.; Tokusashi, Y.; Fukuda, I. Absence of p53 mutations in methylnitrosourea-induced mammary tumors in rats. *Cancer Detect. Prev.*, **1996**, 20, 214–217.
- [178] Asamoto, M.; Ochiya, T.; Toriyama-Baba, H.; Ota, T.; Sekiya, T.; Terada, M.; Tsuda, H. Transgenic rats carrying human c-Ha-ras proto-oncogenes are highly susceptible to *N*-methyl-*N*-nitrosourea mammary carcinogenesis. *Carcinogenesis*, **2000**, 21, 243–249.
- [179] Kito, K.; Kihana, T.; Sugita, A.; Murao, S.; Akehi, S.; Sato, M.; Tachibana, M.; Kimura, S.; Ueda, N. Incidence of p53 and Ha-ras gene mutations in chemically induced rat mammary carcinomas. *Mol. Carcinog.*, **1996**, 17, 78–83.
- [180] Toker, A.; Yoeli-Lerner, M. Akt signaling and cancer: surviving but not moving on. *Cancer Res.*, **2006**, 66, 3963–3966.
- [181] Wazir, U.; Wazir, A.; Khanzada, ZS.; Jiang, WG.; Sharma, AK.; Mokbel, K. Current state of mTOR targeting in human breast cancer. *Cancer Genomics Proteomics*, **2014**, 11, 167–174.
- [182] Toschi, A.; Lee, E.; Thompson, S.; Gadir, N.; Yellen, P.; Drain, CM.; Ohh, M.; Foster, DA. Phospholipase D-mTOR requirement for the Warburg effect in human cancer cells. *Cancer Lett.*, **2010**, 299, 72–79.
- [183] Laplante, M.; Sabatini, DM. mTOR signaling in growth control and disease. *Cell*, **2012**, 149, 274–293.
- [184] McDonald, PC.; Oloumi, A.; Mills, J.; Dobрева, I.; Maidan, M.; Gray, V.; Wederell, ED.; Bally, MB.; Foster, LJ.; Dedhar, S. Rictor and integrin-linked kinase interact and regulate Akt phosphorylation and cancer cell survival. *Cancer Res.*, **2008**, 68, 1618–1624.
- [185] Sarbassov, DD.; Guertin, DA.; Ali, SM.; Sabatini, DM. Phosphorylation and regulation of Akt/PKB by the rictor-mTOR complex. *Science*, **2005**, 307, 1098–1101.
- [186] Feng, ZH.; Zhang, H.; Levine, AJ.; Jin, S. The coordinate regulation of the p53 and mTOR pathways in cells. *Proc. Natl. Acad. Sci. U.S.A.*, **2005**, 102, 8204–8209.

- [187] Sabatini, DM. mTOR and cancer: insights into a complex relationship. *Nat. Rev. Cancer*, **2006**, 6, 729–734.
- [188] Schmelzle, T.; Hall, MN. TOR, a central controller of cell growth. *Cell*, **2000**, 103, 253–262.
- [189] Inoki, K.; Corradetti, MN.; Guan, KL. Dysregulation of the TSC-mTOR pathway in human disease. *Nat. Genet.*, **2005**, 37, 19–24.
- [190] Mita, MM.; Mita, A.; Rowinsky, EK. Mammalian target of rapamycin: a new molecular target for breast cancer. *Clin. Breast Cancer*, **2003**, 4, 126–137.
- [191] Arumugam, A.; Parada, J.; Rajkumar, L. Mammary cancer promotion by ovarian hormones involves IGFR/AKT/mTOR signaling. *Steroids*, **2012**, 77, 791–797.
- [192] Hardie, DG. AMP-activated protein kinase: the guardian of cardiac energy status. *J. Clin. Invest.*, **2004**, 114, 465–468.
- [193] Hardie, DG. The AMP-activated protein kinase pathway: new players upstream and downstream. *J. Cell Sci.*, **2004**, 117, 5479–5487.
- [194] Hardie, DG. New roles for the LKB1 - AMPK pathway. *Curr. Opin. Cell Biol.*, **2005**, 17, 167–173.
- [195] Hardie, DG. AMPK: a key regulator of energy balance in the single cell and the whole organism. *Int. J. Obes.*, **2008**, 32, S7–12.
- [196] Zoncu, R.; Efeyan, A.; Sabatini, DM. mTOR: from growth signal integration to cancer, diabetes and ageing. *Nat. Rev. Mol. Cell Biol.*, **2011**, 12, 21–35.
- [197] Efeyan, A.; Sabatini, DM. mTOR and cancer: many loops in one pathway. *Curr. Opin. Cell Biol.*, **2010**, 22, 169–176.
- [198] Kahn, BB.; Alquier, T.; Carling, D.; Hardie, DG. AMP-activated protein kinase: ancient energy gauge provides clues to modern understanding of metabolism. *Cell Metab.*, **2005**, 1, 15–25.
- [199] Kemp, BE.; Stapleton, D.; Campbell, DJ.; Chen, ZP.; Murthy, S.; Walter, M.; Gupta, A.; Adams, JJ.; Katsis, F.; van Denderen, B.; Jennings, IG.; Iseli, T.; Michell, BJ.; Witters, LA. AMP-activated protein kinase, super metabolic regulator. *Biochem. Soc. Trans.*, **2003**, 31, 162–168.
- [200] Motoshima, H.; Goldstein, BJ.; Igata, M.; Araki, E. AMPK and cell proliferation - AMPK as a therapeutic target for atherosclerosis and cancer. *J. Physiol.*, **2006**, 574, 63–71.
- [201] Zhu, Z.; iang, W.; Thompson, MD.; McGinley, JN.; Thompson, HJ. Metformin as

- an energy restriction mimetic agent for breast cancer prevention. *J. Carcinog.*, **2011**, 10, 17.
- [202] Qiu, F.; Ray, P.; Brown, K.; Barker, PE.; Jhanwar, S.; Ruddle, FH.; Besmer, P. Primary structure of c-kit: relationship with the CSF-1/PDGF receptor kinase family - oncogenic activation of v-kit involves deletion of extracellular domain and C terminus. *Embo J.*, **1988**, 7, 1003–1011.
- [203] Bernex, F.; DeSepulveda, P.; Kress, C.; Elbaz, C.; Delouis, C.; Panthier, JJ. Spatial and temporal patterns of c-kit-expressing cells in $W^{lacZ/+}$ and W^{lacZ}/W^{lacZ} mouse embryos. *Development*, **1996**, 122, 3023–3033.
- [204] Natali, PG.; Nicotra, MR.; Sures, I.; Santoro, E.; Bigotti, A.; Ullrich, A. Expression of c-kit receptor in normal and transformed human nonlymphoid tissues. *Cancer Res.*, **1992**, 52, 6139–6143.
- [205] Matsuda, R.; Takahashi, T.; Nakamura, S.; Sekido, Y.; Nishida, K.; Seto, M.; Seito, T.; Sugiura, T.; Ariyoshi, Y.; Takahashi, T.; Ueda, R. Expression of the c-kit protein in human solid tumors and in corresponding fetal and adult normal tissues. *Am. J. Pathol.*, **1993**, 142, 339–346.
- [206] Natali, PG.; Nicotra, MR.; Sures, I.; Mottolese, M.; Botti, C.; Ullrich, A. Breast cancer is associated with loss of the c-kit oncogene product. *Int. J. Cancer*, **1992**, 52, 713–717.
- [207] Chui, X.; Egami, H.; Yamashita, J.; Kurizaki, T.; Ohmachi, H.; Yamamoto, S.; Ogawa, M. Immunohistochemical expression of the c-kit proto-oncogene product in human malignant and non-malignant breast tissues. *Br. J. Cancer*, **1996**, 73, 1233–1236.
- [208] Maffini, M V.; Soto, AM.; Sonnenschein, C.; Papadopoulos, N.; Theoharides, TC. Lack of c-kit receptor promotes mammary tumors in *N*-nitrosomethylurea-treated *Ws/Ws* rats. *Cancer Cell Int.*, **2008**, 8, 5.
- [209] Folkman, J. What is the evidence that tumors are angiogenesis dependent. *J. Natl. Cancer Inst.*, **1990**, 82, 4–6.
- [210] Folkman, J.; Bach, M.; Rowe, JW.; Davidoff, F.; Lambert, P.; Hirsch, C.; Goldberg, A.; Hiatt, HH.; Glass, J.; Henshaw, E. Tumor angiogenesis - therapeutic implications. *N. Engl. J. Med.*, **1971**, 285, 1182–1186.
- [211] Weidner, N. Tumor angiogenesis - review of current applications in tumor prognostication. *Semin. Diagn. Pathol.*, **1993**, 10, 302–313.

- [212] Relf, M.; LeJeune, S.; Scott, PAE.; Fox, S.; Smith, K.; Leek, R.; Moghaddam, A.; Whitehouse, R.; Bicknell, R.; Harris, AL. Expression of the angiogenic factors vascular endothelial cell growth factor, acidic and basic fibroblast growth factor, tumor growth factor beta-1, platelet-derived endothelial cell growth factor, placenta growth factor, and pleiotrophin in human primary. *Cancer Res.*, **1997**, *57*, 963–969.
- [213] Yoshiji, H.; Gomez, DE.; Shibuya, M.; Thorgeirsson, UP. Expression of vascular endothelial growth factor, its receptor, and other angiogenic factors in human breast cancer. *Cancer Res.*, **1996**, *56*, 2013–2016.
- [214] Obermair, A.; Obruca, A.; Pohl, M.; Kaider, A.; Vales, A.; Leodolter, S.; Wojta, J.; Feichtinger, W. Vascular endothelial growth factor and its receptors in male fertility. *Fertil. Steril.*, **1999**, *72*, 269–275.
- [215] Saminathan, M.; Rai, RB.; Dhama, K.; Ranganath, GJ.; Murugesan, V.; Kannan, K.; Pavulraj, S.; Gopalakrishnan, A.; Suresh, C. Histopathology and immunohistochemical expression of *N*-methyl-*N*-nitrosourea (NMU) induced mammary tumours in Sprague-Dawley rats. *Asian J. Anim. Vet. Adv.*, **2014**, *9*, 621–640.
- [216] Massague, J.; Gomis, RR. The logic of TGF beta signaling. *Febs Lett.*, **2006**, *580*, 2811–2820.
- [217] Taylor, MA.; Lee, YH.; Schiemann, WP. Role of TGF-beta and the tumor microenvironment during mammary tumorigenesis. *Gene Expr.*, **2011**, *15*, 117–132.
- [218] Massague, J. TGF beta in cancer. *Cell*, **2008**, *134*, 215–230.
- [219] Tian, MZ.; Neil, JR.; Schiemann, WP. Transforming growth factor-beta and the hallmarks of cancer. *Cell. Signal.*, **2011**, *23*, 951–962.
- [220] Bierie, B.; Moses, HL. Tumour microenvironment. TGF beta: the molecular jekyll and hyde of cancer. *Nat. Rev. Cancer*, **2006**, *6*, 506–520.
- [221] Thompson, HJ.; Singh, M. Rat models of premalignant breast disease. *J. Mammary Gland Biol. Neoplasia*, **2000**, *5*, 409–420.
- [222] Ouban, A.; Muraca, P.; Yeatman, T.; Coppola, D. Expression and distribution of insulin-like growth factor-1 receptor in human carcinomas. *Hum. Pathol.*, **2003**, *34*, 803–808.
- [223] Shimizu, C.; Hasegawa, T.; Tani, Y.; Takahashi, F.; Takeuchi, M.; Watanabe, T.;

- Ando, M.; Katsumata, N.; Fujiwara, Y. Expression of insulin-like growth factor 1 receptor in primary breast cancer: immunohistochemical analysis. *Hum. Pathol.*, **2004**, 35, 1537–1542.
- [224] Yerushalmi, R.; Gelmon, KA.; Leung, S.; Gao, DX.; Cheang, M.; Pollak, M.; Turashvili, G.; Gilks, BC.; Kennecke, H. Insulin-like growth factor receptor (IGF-1R) in breast cancer subtypes. *Breast Cancer Res. Treat.*, **2012**, 132, 131–142.
- [225] Gasco, M.; Shami, S.; Crook, T. The p53 pathway in breast cancer. *Breast Cancer Res.*, **2002**, 4, 70–76.
- [226] Hollstein, M.; Sidransky, D.; Vogelstein, B.; Harris, CC. p53 mutations in human cancers. *Science (80-.)*, **1991**, 253, 49–53.
- [227] Pharoah, PDP.; Day, NE.; Caldas, C. Somatic mutations in the p53 gene and prognosis in breast cancer: a meta-analysis. *Br. J. Cancer*, **1999**, 80, 1968–1973.
- [228] Phillips, KA.; Nichol, K.; Ozcelik, H.; Knight, J.; Done, SJ.; Goodwin, PJ.; Andrulis, IL. Frequency of p53 mutations in breast carcinomas from Ashkenazi Jewish carriers of *BRCA1* mutations. *J. Natl. Cancer Inst.*, **1999**, 91, 469–473.
- [229] Smith, PD.; Crossland, S.; Parker, G.; Osin, P.; Brooks, L.; Waller, J.; Philp, E.; Crompton, MR.; Gusterson, BA.; Allday, MJ.; Crook, T. Novel p53 mutants selected in *BRCA*-associated tumours which dissociate transformation suppression from other wild-type p53 functions. *Oncogene*, **1999**, 18, 2451–2459.
- [230] Antoniou, AC.; Easton, DF. Models of genetic susceptibility to breast cancer. *Oncogene*, **2006**, 25, 5898–5905.
- [231] Levy-Lahad, E.; Plon, SE. A risky business - assessing breast cancer risk. *Science*, **2003**, 302, 574–575.
- [232] King, MC.; Marks, JH.; Mandell, JB. Breast and ovarian cancer risks due to inherited mutations in *BRCA1* and *BRCA2*. *Science*, **2003**, 302, 643–646.
- [233] Narod, SA.; Foulkes, WD. *BRCA1* and *BRCA2*: 1994 and beyond. *Nat. Rev. Cancer*, **2004**, 4, 665–676.
- [234] Greenblatt, MS.; Bennett, WP.; Hollstein, M.; Harris, CC. Mutations in the p53 tumor suppressor gene: clues to cancer etiology and molecular pathogenesis. *Cancer Res.*, **1994**, 54, 4855–4878.
- [235] Lloyd, DR.; Hanawalt, PC. p53-dependent global genomic repair of benzo[a]pyrene-7,8-diol-9,10-epoxide adducts in human cells. *Cancer Res.*, **2000**, 60, 517–521.

- [236] Miyashita, T.; Krajewski, S.; Krajewska, M.; Wang, HG.; Lin, HK.; Liebermann, DA.; Hoffman, B.; Reed, JC. Tumor suppressor p53 is a regulator of bcl-2 and bax gene expression *in vitro* and *in vivo*. *Oncogene*, **1994**, 9, 1799–1805.
- [237] Yonishrouach, E.; Resnitzky, D.; Lotem, J.; Sachs, L.; Kimchi, A.; Oren, M. Wild-type p53 induces apoptosis of myeloid leukemic cells that is inhibited by interleukin-6. *Nature*, **1991**, 352, 345–347.
- [238] Oster, SK.; Ho, CSW.; Soucie, EL.; Penn, LZ. The myc oncogene: marvelously complex. *Adv. Cancer Res.*, **2002**, 84, 81–154.
- [239] Evan, G. Taking a back door to target Myc. *Science*, **2012**, 335, 293–294.
- [240] Eisenman, RN. *The Myc oncogene*. **2006**, Springer-Verlag.
- [241] Cowling, VH.; D’Cruz, CM.; Chodosh, LA.; Cole, MD. c-Myc transforms human mammary epithelial cells through repression of the Wnt inhibitors DKK1 and SFRP1. *Mol. Cell. Biol.*, **2007**, 27, 5135–5146.
- [242] Barathidasan, R.; Pawaiya, RS.; Rai, RB.; Dhama, K. Upregulated Myc expression in *N*-methyl nitrosourea (MNU)-induced rat mammary tumours. *Asian Pacific J. Cancer Prev.*, **2013**, 14, 4883–4889.
- [243] Hunter, T.; Pines, J. Cyclins and cancer. II: Cyclin D and CDK inhibitors come of age. *Cell*, **1994**, 79, 573–582.
- [244] Sgambato, A.; Han, EKH.; Zhang, YJ.; Moon, RC.; Santella, RM.; Weinstein, IB. Deregulated expression of cyclin D1 and other cell cycle-related genes in carcinogen-Induced rat mammary tumors. *Carcinogenesis*, **1995**, 16, 2193–2198.
- [245] Devilee, P.; Schuurin, E.; Vandevijver, MJ.; Cornelisse, CJ. Recent developments in the molecular genetic understanding of breast cancer. *Crit. Rev. Oncog.*, **1994**, 5, 247–270.
- [246] Russo, J.; Russo, IH. Mammary tumorigenesis. *Prog. Exp. Tumor Res.*, **1991**, 33, 175–191.
- [247] Zhu, ZJ.; Jiang, WQ.; Thompson, HJ. Effect of energy restriction on the expression of cyclin D1 and p27 during premalignant and malignant stages of chemically induced mammary carcinogenesis. *Mol. Carcinog.*, **1999**, 24, 241–245.
- [248] Cooper, D.; Schermer, A.; Sun, TT. Classification of human epithelia and their neoplasms using monoclonal antibodies to keratins - strategies, applications, and limitations. *Lab. Invest.*, **1985**, 52, 243–256.
- [249] Nagle, RB.; Bocker, W.; Davis, JR.; Heid, HW.; Kaufmann, M.; Lucas, DO.;

- Jarasch, ED. Characterization of breast carcinomas by two monoclonal antibodies distinguishing myoepithelial from luminal epithelial cells. *J. Histochem. Cytochem.*, **1986**, 34, 869–881.
- [250] Debus, E.; Weber, K.; Osborn, M. Monoclonal cytokeratin antibodies that distinguish simple from stratified squamous epithelia - characterization on human tissues. *Embo J.*, **1982**, 1, 1641–1647.
- [251] Malzahn, K.; Mitze, M.; Thoenes, M.; Moll, R. Biological and prognostic significance of stratified epithelial cytokeratins in infiltrating ductal breast carcinomas. *Virchows Arch. Int. J. Pathol.*, **1998**, 433, 119–129.
- [252] Rejthar, A.; Nenutil, R. The intermediate filaments and prognostically oriented morphological classification in ductal breast carcinoma. *Neoplasma*, **1997**, 44, 370–373.
- [253] Van de Rijn, M.; Perou, CM.; Tibshirani, R.; Haas, P.; Kallioniemi, C.; Kononen, J.; Torhorst, J.; Sauter, G.; Zuber, M.; Kochli, OR.; Mross, F.; Dieterich, H.; Seitz, R.; Ross, D.; Botstein, D.; Brown, P. Expression of cytokeratins 17 and 5 identifies a group of breast carcinomas with poor clinical outcome. *Am. J. Pathol.*, **2002**, 161, 1991–1996.
- [254] Santini, D.; Ceccarelli, C.; Taffurelli, M.; Pileri, S.; Marrano, D. Differentiation pathways in primary invasive breast carcinoma as suggested by intermediate filament and biopathological marker expression. *J. Pathol.*, **1996**, 179, 386–391.
- [255] Wetzels, RHW.; Kuijpers, HJH.; Lane, EB.; Leigh, IM.; Troyanovsky, SM.; Holland, R.; Vanhaelst, UJGM.; Ramaekers, FCS. Basal cell-specific and hyperproliferation-related keratins in human breast cancer. *Am. J. Pathol.*, **1991**, 138, 751–763.
- [256] Altmannsberger, M.; Dirk, T.; Droese, M.; Weber, K.; Osborn, M. Keratin polypeptide distribution in benign and malignant breast tumors - subdivision of ductal carcinomas using monoclonal antibodies. *Virchows Arch. B Cell Pathol. Incl. Mol. Pathol.*, **1986**, 51, 265–275.
- [257] El-Rehim, DMA.; Pinder, SE.; Paish, CE.; Bell, J.; Blamey, R.; Robertson, JFR.; Nicholson, RI.; Ellis, IO. Expression of luminal and basal cytokeratins in human breast carcinoma. *J. Pathol.*, **2004**, 203, 661–671.
- [258] Lu, JX.; Pei, HY.; Kaeck, M.; Thompson, HJ. Gene expression changes associated with chemically induced rat mammary carcinogenesis. *Mol. Carcinog.*, **1997**, 20,

- 204–215.
- [259] Goepfert, TM.; Moreno-Smith, M.; Edwards, DG.; Pathak, S.; Medina, D.; Brinkley, WR. Loss of chromosomal integrity drives rat mammary tumorigenesis. *Int. J. Cancer*, **2007**, 120, 985–994.
- [260] Sharma, D.; Smits, BMG.; Eichelberg, MR.; Meilahn, AL.; Muelbl, MJ.; Haag, JD.; Gould, MN. Quantification of epithelial cell differentiation in mammary glands and carcinomas from DMBA- and MNU-exposed rats. *Plos One*, **2011**, 6, e26145.
- [261] Tsukamoto, R.; Mikami, T.; Miki, K.; Uehara, N.; Yuri, T.; Matsuoka, Y.; Okazaki, K.; Tsubura, A. *N*-methyl-*N*-nitrosourea-induced mammary carcinogenesis is promoted by short-term treatment with estrogen and progesterone mimicking pregnancy in aged female Lewis rats. *Oncol. Rep.*, **2007**, 18, 337–342.
- [262] Sreenath, T.; Matrisian, LM.; Stetlerstevenson, W.; Gattonicelli, S.; Pozzatti, RO. Expression of matrix metalloproteinase genes in transformed rat cell lines of high and low metastatic potential. *Cancer Res.*, **1992**, 52, 4942–4947.
- [263] Duffy, MJ. The role of proteolytic-enzymes in cancer invasion and metastasis. *Clin. Exp. Metastasis*, **1992**, 10, 145–155.
- [264] Nagase, H.; Woessner, JF. Matrix metalloproteinases. *J. Biol. Chem.*, **1999**, 274, 21491–21494.
- [265] Nabeshima, K.; Inoue, T.; Shima, Y.; Sameshima, T. Matrix metalloproteinases in tumor invasion: role for cell migration. *Pathol. Int.*, **2002**, 52, 255–264.
- [266] Kousidou, OC.; Roussidis, AE.; Theocharis, AD.; Karamanos, NK. Expression of MMPs and TIMPs genes in human breast cancer epithelial cells depends on cell culture conditions and is associated with their invasive potential. *Anticancer Res.*, **2004**, 24, 4025–4030.
- [267] Bartsch, JE.; Staren, ED.; Appert, HE. Matrix metalloproteinase expression in breast cancer. *J. Surg. Res.*, **2003**, 110, 383–392.
- [268] Roomi, MW.; Roomi, NW.; Ivanov, V.; Kalinovskiy, T.; Niedzwiecki, A.; Rath, M. Modulation of *N*-methyl-*N*-nitrosourea induced mammary tumors in Sprague-Dawley rats by combination of lysine, proline, arginine, ascorbic acid and green tea extract. *Breast Cancer Res.*, **2005**, 7, R291–295.
- [269] Steele, VE.; Lubet, RA. The use of animal models for cancer chemoprevention

- drug development. *Semin. Oncol.*, **2010**, 37, 327–338.
- [270] Ahelm, CN.; Frincke, JM.; White, SK.; Reading, CL.; TRauger, RJ.; Lakshmanaswamy, R. 17 α -ethynyl-5 α -androstane-3 α , 17 β -diol treatment of MNU-induced mammary cancer in rats. *Int. J. Breast Cancer*, **2011**, 2011, 1–9.
- [271] Moon, RC.; Mehta, RG. Chemoprevention of experimental carcinogenesis in animals. *Prev. Med.*, **1989**, 18, 576–591.
- [272] Vinodhini, J.; Sudha, S. Effect of bis-carboxy ethyl germanium sesquioxide on *N*-nitroso-*N*-methylurea-induced rat mammary carcinoma. *Asian J. Pharm. Clin. Res.*, **2013**, 6, 242–244.
- [273] Kale, A.; Gawande, S.; Kotwal, S.; Netke, S.; Roomi, MW.; Ivanov, V.; Niedzwecki, A.; Rath, M. A combination of green tea extract, specific nutrient mixture and quercetin: an effective intervention treatment for the regression of *N*-methyl-*N*-nitrosourea (MNU)-induced mammary tumors in Wistar rats. *Oncol. Lett.*, **2010**, 1, 313–317.
- [274] Colston, KW.; Pirianov, G.; Bramm, E.; Hamberg, J.; Binderup, L. Effects of Seocalcitol (EB1089) on nitrosomethyl urea-induced rat mammary tumors. *Breast Cancer Res. Treat.*, **2003**, 80, 303–311.
- [275] Thompson, MD.; Thompson, HJ.; McGinley, JN.; Neil, ES.; Rush, DK.; Holm, DG.; Stushnoff, C. Functional food characteristics of potato cultivars (*Solanum tuberosum* L.): phytochemical composition and inhibition of 1-methyl-1-nitrosourea induced breast cancer in rats. *J. Food Compos. Anal.*, **2009**, 22, 571–576.
- [276] Kubatka, P.; Sadlonova, V.; Kajo, K.; Machalekova, K.; Ostatnikova, D.; Nosalova, G.; Fetisovova, Z. Neoplastic effects of exemestane in premenopausal breast cancer model. *Neoplasma*, **2008**, 55, 538–543.
- [277] Stearns, V.; Mori, T.; Jacobs, LK.; Khouri, NF.; Gabrielson, E.; Yoshida, T.; Kominsky, SL.; Huso, DL.; Jeter, S.; Powers, P.; Tarpinian, K.; Brown, RJ.; Lange, JR.; Rudek, MA.; Zhang, Z.; Tsangaris, TN.; Sukumar, S. Preclinical and clinical evaluation of intraductally administered agents in early breast cancer. *Sci. Transl. Med.*, **2011**, 3,
- [278] Badawi, AF.; Eldeen, MB.; Liu, YY.; Ross, EA.; Badr, MZ. Inhibition of rat mammary gland carcinogenesis by simultaneous targeting of cyclooxygenase-2 and peroxisome proliferator-activated receptor gamma. *Cancer Res.*, **2004**, 64,

- 1181–1189.
- [279] Chun, YS.; Bisht, S.; Chenna, V.; Pramanik, D.; Yoshida, T.; Hong, SM.; de Wilde, RF.; Zhang, Z.; Huso, DL.; Zhao, M.; Rudek, MA.; Stearns, V.; Maitra, A.; Sukumar, S. Intraductal administration of a polymeric nanoparticle formulation of curcumin (NanoCurc) significantly attenuates incidence of mammary tumors in a rodent chemical carcinogenesis model: implications for breast cancer chemoprevention in at-risk populations. *Carcinogenesis*, **2012**, 33, 2242–2249.
- [280] Alfaro, Y.; Delgado, G.; Cárabez, A.; Anguiano, B.; Aceves, C. Iodine and doxorubicin, a good combination for mammary cancer treatment: antineoplastic adjuvancy, chemoresistance inhibition, and cardioprotection. *Mol. Cancer*, **2013**, 12, 1–11.
- [281] Gottardis, MM.; Jordan, C. Antitumor actions of keoxifene and tamoxifen in the *N*-nitrosomethylurea-induced rat mammary carcinoma model. *Cancer Res.*, **1987**, 47, 4020–4024.
- [282] Kubatka, P.; Sadlonova, V.; Kajo, K.; Nosalova, G.; Fetisovova, Z. Preventive effects of letrozole in the model of premenopausal mammary carcinogenesis. *Neoplasma*, **2008**, 55, 42–46.
- [283] Garcia-Solis, P.; Yahia, EM.; Aceves, C. Study of the effect of “Ataulfo” mango (*Mangifera indica* L.) intake on mammary carcinogenesis and antioxidant capacity in plasma of *N*-methyl-*N*-nitrosourea (MNU)-treated rats. *Food Chem.*, **2008**, 111, 309–315.
- [284] Lippert, TH.; Adlercreutz, H.; Berger, MR.; Seeger, H.; Elger, W.; Mueck, AO. Effect of 2-methoxyestradiol on the growth of methyl-nitroso-urea (MNU)-induced rat mammary carcinoma. *J. Steroid Biochem. Mol. Biol.*, **2003**, 84, 51–56.
- [285] Okugawa, H.; Yamamoto, D.; Uemura, Y.; Sakaida, N.; Tanano, A.; Tanaka, K.; Kamiyama, Y. Effect of periductal paclitaxel exposure on the development of MNU-induced mammary carcinoma in female S-D rats. *Breast Cancer Res. Treat.*, **2005**, 91, 29–34.
- [286] Anzano, MA.; Peer, CW.; Smith, JM.; Mullen, LT.; Shrader, MW.; Logsdon, DL.; Driver, CL.; Brown, CC.; Roberts, AB.; Sporn, MB. Chemoprevention of mammary carcinogenesis in the rat: combined use of raloxifene and 9-cis-retinoic acid. *J. Natl. Cancer Inst.*, **1996**, 88, 123–125.
- [287] Sato, M.; Pei, RJ.; Yuri, T.; Danbara, N.; Nakane, Y.; Tsubura, A. Prepubertal

- resveratrol exposure accelerates *N*-methyl-*N*-nitrosourea-induced mammary carcinoma in female Sprague-Dawley rats. *Cancer Lett.*, **2003**, 202, 137–145.
- [288] Martin, G.; Melito, G.; Rivera, E.; Levin, E.; Davio, C.; Cricco, G.; Andrade, N.; Caro, R.; Bergoc, R. Effect of tamoxifen on intraperitoneal *N*-nitroso-*N*-methylurea induced tumors. *Cancer Lett.*, **1996**, 100, 227–234.
- [289] Lubet, RA.; Christov, K.; Nunez, NP.; Hursting, SD.; Steele, VE.; Juliana, MM.; Eto, I.; Grubbs, CJ. Efficacy of targretin on methylnitrosourea-induced mammary cancers: prevention and therapy dose-response curves and effects on proliferation and apoptosis. *Carcinogenesis*, **2005**, 26, 441–448.
- [290] Kahn, LH. Confronting zoonoses, linking human and veterinary medicine. *Emerg. Infect. Dis.*, **2006**, 12, 556–561.
- [291] Enserink, M. Medicine - initiative aims to merge animal and human health science to benefit both. *Science*, **2007**, 316, 1553.
- [292] Cardiff, RD. Epilog: comparative medicine, one medicine and genomic pathology. *Breast Dis.*, **2007**, 28, 107–110.
- [293] Kubatka, P.; Ahlers, I.; Ahlersova, E.; Adamekova, E.; Luk, P.; Bojkova, B.; Markova, M. Chemoprevention of mammary carcinogenesis in female rats by rofecoxib. *Cancer Lett.*, **2003**, 202, 131–136.
- [294] McCormick, DL.; Adamowski, CB.; Fiks, A.; Moon, RC. Lifetime dose-response relationships for mammary tumor induction by a single administration of *N*-methyl-*N*-nitrosourea. *Cancer Res.*, **1981**, 41, 1690–1694.
- [295] Mehta, RG. Experimental basis for the prevention of breast cancer. *Eur. J. Cancer*, **2000**, 36, 1275–1282.
- [296] Singh, M.; McGinley, JN.; Thompson, HJ. A comparison of the histopathology of premalignant and malignant mammary gland lesions induced in sexually immature rats with those occurring in the human. *Lab. Investig.*, **2000**, 80, 221–231.
- [297] Thompson, HJ.; McGinley, J.; Rothhammer, K.; Singh, M. Ovarian hormone dependence of pre-malignant and malignant mammary gland lesions induced in pre-pubertal rats by *l*-methyl-*l*-nitrosourea. *Carcinogenesis*, **1998**, 19, 383–386.
- [298] National Cancer Institute (NCI). Drugs approved for breast cancer. *NCI*, **2014**.

CHAPTER 3

ANTIHISTAMINES AS PROMISING DRUGS IN CANCER THERAPY: A REVIEW

THE CONTENT OF THIS CHAPTER WAS PUBLISHED IN:

Faustino-Rocha AI, Gama A, Oliveira PA, Ferreira R, Ginja M. 2016. Antihistamines as promising drugs in cancer therapy. *Life Sciences* 172 (2017): 27-41. *Review*. (Full paper)

3. Antihistamines as promising drugs in cancer therapy: a review

Abstract

Histamine is a biogenic amine, synthesized and released by mast cells, which acts as a vasodilator in several pathologic processes, namely in allergies and conjunctivitis. Its role on cancer is not fully understood. High levels of histamine have been associated with a bivalent behavior in regulation of several tumors (i.e. cervical, ovarian, vaginal, uterine, vulvar, colorectal cancer, and melanoma), promoting or inhibiting their growth. Histamine receptors (H1, H2, H3 and H4) are present in a vast group of cells, including tumor cells, making them sensitive to histamine variations. In this work, we review the role of mast cells and histamine on cancer development and the possibility of using antihistamines in the clinical management of this disease.

Keywords: cancer therapy, histamine, histamine receptors, mast cell, microenvironment, tumor

3.1. Cancer

Cancer is one of the most important public health problems in many countries around the world. Despite all advances in the diagnosis and treatment of this disease, it is still one of the principal causes of death globally [1]. Cancer is a multistage process that arises from genetic and epigenetic alterations responsible for the transformation of normal cells into neoplastic cells [2–4] (Figure 3.1). Cancers are not only proliferations of malignant cells but complex “rogue” organs, to which many other cells are recruited and potentially changed by the transformed cells. The interactions between the malignant and non-transformed cells constitute the tumor microenvironment [5]. Lymphatic and vascular endothelial cells, pericytes, adipocytes, mesenchymal stem cells, smooth muscle cells, fibroblasts, myofibroblasts, myeloid cells and inflammatory cells (B and T lymphocytes, neutrophils, dendritic cells, eosinophils, basophils, natural killer cells, macrophages and mast cells) are among the cells of tumor microenvironment [4,6]. These cells may be identified in the tumor microenvironment by their specific cell surface molecules and may act as tumor-promoting at all stages of carcinogenesis [7]. Each of them have the capacity to synthesize cytokines, reactive oxygen species (ROS), serine and cysteine proteases,

metalloproteinases, growth and pro-angiogenic factors, inflammatory and matrix remodeling enzymes, chemokines, and adhesion molecules that interact among them and with tumor cells promoting tumor growth, invasion and dissemination to other organs (metastization) [8–11]. The evolution, structure and activities of cells in tumor microenvironment have many parallels with the processes of wound healing and inflammation; however, cells such as macrophages may be found in cancers that have no known association with chronic inflammatory conditions [12–14]. Now, it is known that targeting the non-malignant cells of tumor microenvironment or mediators of communication among them could complement other cancer therapeutic approaches, such as chemotherapy and radiotherapy. However, questions about the similarity of tumor microenvironment among different types of cancer, and between primary cancers and metastasis remain unclear.

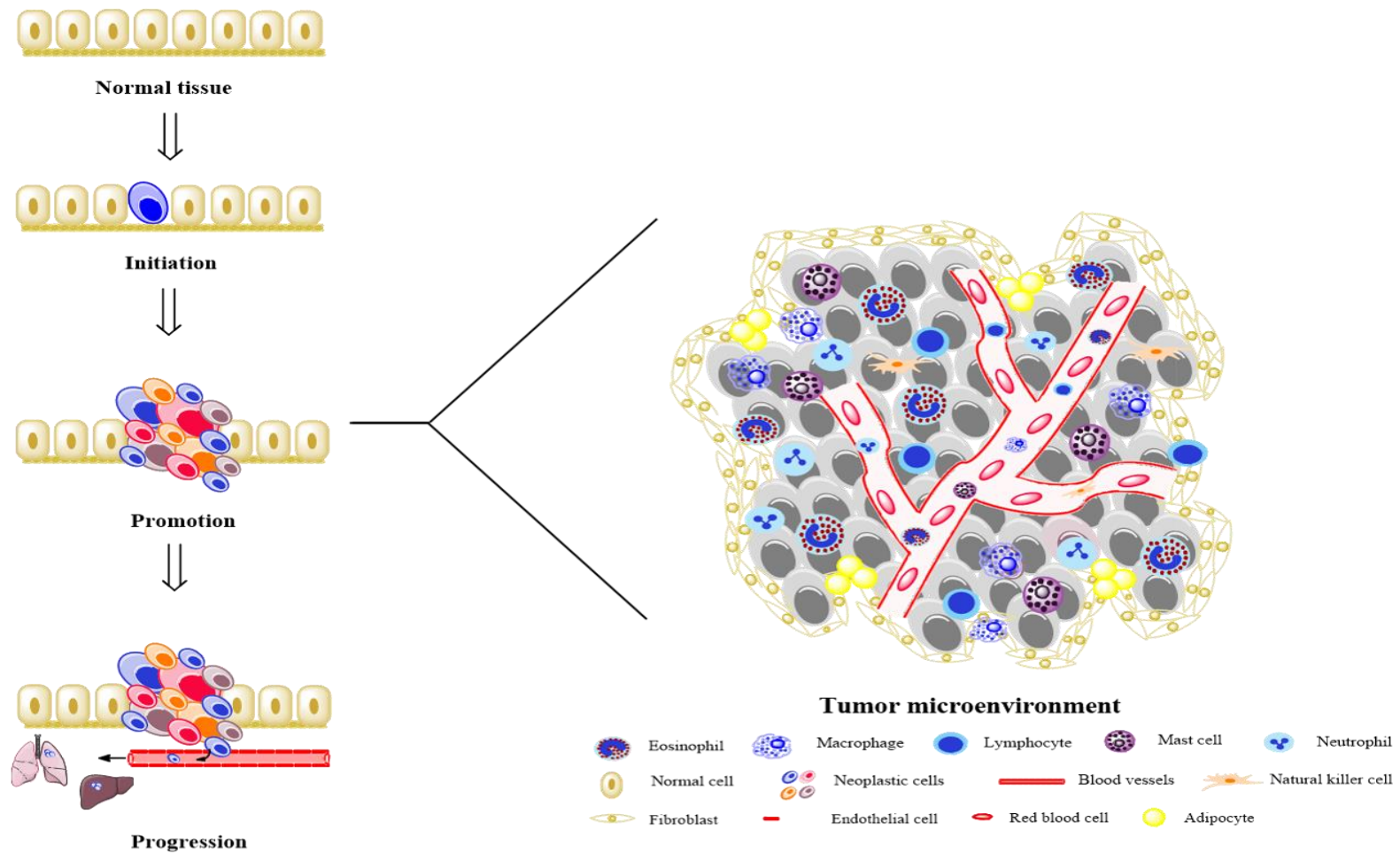


Figure 3.1. Schematic representation of carcinogenesis stages and tumor microenvironment. Cancer begins with the mutation of one cell (Initiation), then this cell divides itself originating other mutated cells (Promotion). During this process, tumor is reached by several inflammatory and non-inflammatory cells that constitute tumor microenvironment. As last step, tumor cells go to other tissues, originating a new tumor in distant organs (Progression and Metastization).

3.2. Mast cells

Mast cells are bone-marrow derived leukocytes that were first described by Paul Ehrlich more than 130 years ago in his PhD thesis [15]. Mast cells were identified in all vertebrates [16] and some authors consider that they may be primitive cells, maybe the surviving remnant of an ancient model of the immune system [17]. Actually, mast cells are strategically placed at the host/environment interfaces. They may be found in proximity to surfaces that are common portals of infection, namely in mucosa of the respiratory, digestive and urogenital tracts, and in the dermis of the skin. Mast cells may also be found in the connective tissue near vessels and nerves, making them key elements in processes of tissue remodelling, wound healing, fibrosis and angiogenesis, and in the central nervous system where the histamine acts as a neurotransmitter [18,19]. Mast cells are not found in avascular tissues, namely mineralized bone, cartilage and cornea [20]. At histological analysis, mast cells appear as round or elongated cells with a diameter ranging from 8 to 20 μm . They have a non-segmented monolobed nucleus with peripherally condensed chromatin [16] and may be easily recognized by their toluidine blue positive granules that fill the cytoplasm. The fully granulated mast cells contain up to 1000 secretory granules (also known as secretory lysosomes) of 60-80 nm that occupy more than 40% of cytoplasm volume [21]. These granules are the functional cell organelles and they are composed by several substances, namely histamine, serotonin, proteases, cytokines and growth factors [22]. Beyond the secretory granules, in the mast cells' cytoplasm there are also lipid bodies that are a source of triglyceride-derived arachidonic acid [23]. At electron microscopy, it was observed that mast cells' cytoplasm also contains some mitochondria and rough endoplasmic reticulum, and several free ribosomes [16].

3.2.1. Mast cells' maturation

Enerback *et al.* [24] verified that mast cells have a long half-life, they observed that rodent intestinal mast cells have a half-life of at least 40 days. In another study, Ekoff *et al.* [25] concluded that mast cells normally survive within tissues for several months and their number kept relatively constant. Unlike other cells that leave the bone marrow as fully matured cells, mast cells stem from immature precursors (non-granulated cells) that leave the bone marrow to circulate in the blood [26–28]. Then these precursors migrate

into different tissues and under the influence of the microenvironmental growth factors such as the stem cell factor (SCF) that is synthesized by fibroblasts, stromal cells and endothelial cells of each tissue, they proliferate and differentiate into fully mature granulated cells (granulated mast cells) [29,30] (Figure 3.2). Since the progression of mast cells' precursors to fully mature mast cells depends on c-kit activation that occurs as a consequence of c-kit dimerization and auto-phosphorylation by the SCF, the SCF is also known as c-kit ligand. The SCF also regulates mast cell survival by inhibiting FOXO3a and down regulating the pro-apoptotic BH3 protein [25]. It was observed that mice with a defective surface expression or catalytic activity of c-kit have lower number of mast cells in tissues when compared with animals without any alteration [31]. It was also observed that the inhibition of c-kit catalytic activity by specific tyrosine kinase inhibitor, such as imatinib, induced human mast cell apoptosis [25]. Although the SCF and its receptor (c-kit) are essential for the differentiation, proliferation and survival of mast cells, there are other factors, namely cytokines and growth factors such as immunoglobulin E (IgE) that are involved in the differentiation, proliferation and survival of mast cells [32] (Figure 3.2). The IgE acts on mast cells progenitors to induce differentiation into mature mast cells. The linkage of different IgE subtypes to the surface mast cells tetrameric $\alpha\beta\gamma_2$ form of the high-affinity receptor for IgE (Fc ϵ RI) in early stages of mast cell differentiation change the expression of various genes, mainly those essential to the differentiation, and contributes to the mast cells heterogeneity [32]. Activated mast cells have also the ability to release mediators that induce activation of themselves and their neighboring mast cells. Additionally, the IgE in absence of antigen promotes mast cell survival as mentioned above (the IgE reduced the mast cell apoptosis in the absence of growth factors and promoted their survival by Fc ϵ RI stimulation) and amplifies the inflammatory response in allergic tissues (the accumulation of mast cell Fc ϵ RI may amplify the inflammatory reactions via molecules such as histamine, leukotrienes, chemokines and cytokines released during their degranulation). These molecules will recruit other immune cells, such as T cells, eosinophils, monocytes and neutrophils, and induce the synthesis of other pro-inflammatory effector molecules [32].

3.2.2. Granules' content and release

Mast cells have the ability to produce, store and release immune-modulatory molecules upon activation. Depending on the agent responsible for the infection (bacteria, virus or parasite), the mediators released by mast cells are different. They produce three main classes of mediators: **1)** granule associated substances: histamine, serotonin, heparin, chondroitin sulphate peptidoglycans, tryptase, chymase, carboxypeptidase, tumor-necrosis factor (TNF), vascular endothelial growth factor (VEGF), fibroblast growth factor 2 (FGF2), **2)** newly generated lipid-derived substances: leukotriene (LT) C₄, LTB₄, prostaglandin D₂, prostaglandin E₂ and platelet-activating factor, and **3)** a wide variety of cytokines [TNF, interleukin (IL)-1 α , IL-1 β , IL-3, IL-4, IL-5, IL-6, IL-9, IL-10, IL-12, IL-13, IL-15, IL-16, IL-18, interferon (IFN)- α , IFN- β , IFN- γ , leukemia inhibitory factor (LIF), granulocyte/macrophage colony-stimulating factor (GM-CSF), transforming growth factor (TGF)- β and VEGF], chemokines [CC-chemokine ligand (CCL) 2, CCL3, CCL4, CCL5, CCL11, CCL20, CXC-chemokine ligand (CXCL) 1, CXCL 2, CXCL 8, CXCL 9, CXCL 10, CXCL 11], nitric oxide, oxide radicals and antimicrobial peptides [33,34]. The granules' content is extruded to the cell exterior upon cell activation under the form of massive (exocytosis or anaphylactic degranulation) or limited degranulation (piecemeal degranulation) [23] (Figure 3.2). The first one is characterized by a quick and generalized release of the granules content and occurs during type I allergic reactions. Conversely, the piecemeal degranulation is a selective process (the mast cells may release subtle amounts of granule-stored mediators) and occurs for a long period of time, namely in chronic inflammatory processes, such as cancer [22]. The regeneration of a granular compartment may take up to 72 hours [21].

Mast cells' responses are governed by their wide range of cell surface receptors which regulate the selective release of mediators. On their surface, they express the Fc ϵ RI that is crucial to the activation of their anaphylactic degranulation [35]. For a long period of time, it was thought that two steps were necessary for the mast cell activation. In the first one, denominated sensitization, the monomeric IgE binds to Fc ϵ RI on the mast cell surface. In the second one, the antigen binds to the IgE that had previously bound with mast cell receptors. However, recent findings demonstrated that the monomeric IgE has the ability to activate mast cells in the absence of antigen, for this the IgE concentrations should be 2-3 log higher when compared with the situation where the antigen is present

(Figure 3.2). In this way, the allergic symptoms may also occur in patients not exposed to allergens [32]. Upon activation via cross-linking of FcεRI, phosphorylation cascades are activated, leading to calcium influx, nuclear importation of transcriptase factors and the mast cells may release all pre-formed granule-associated mediators (degranulation), and they also produce *de novo* synthesized lipid mediators (namely prostaglandins and leukotriens) within minutes after activation, and a wide range of growth factors (such as cytokines and chemokines) over a more sustained time period [36]. Mast cells may also be activated by other pathways, such as aggregation of FcγRIII by IgG/antigen complexes, c-kit and toll-like receptor (TLR) mechanisms, exposure to chemokines, anaphylatoxins C3a and C5a, fragments of fibrinogen and fibronectin, and via hypoxia-inducible factor 1α [34,37,38].

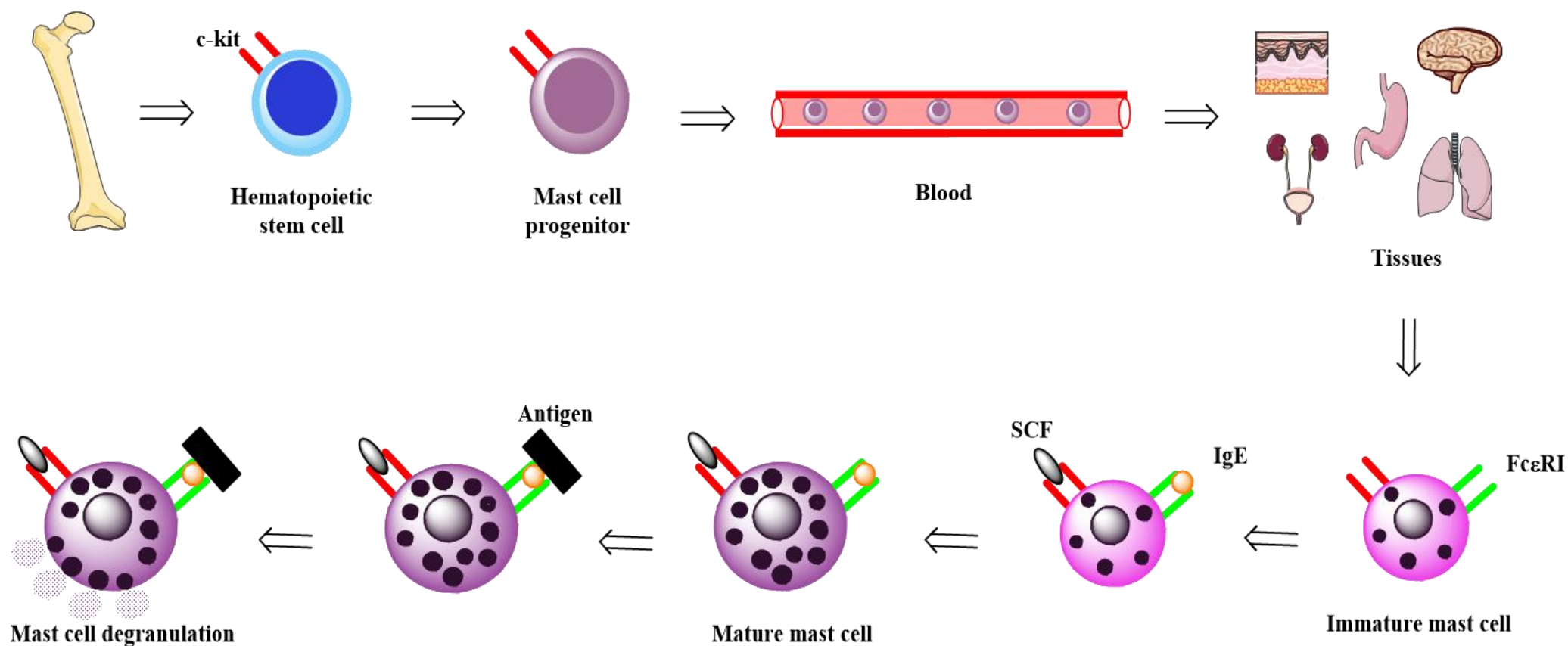


Figure 3.2. Schematic representation of mast cells' maturation and activation. Mast cells derived from non-granulated immature precursors (hematopoietic stem cells) that originate in bone marrow. These stem cells give rise to mast cell progenitors that circulate in the blood and migrate into different tissues. In tissues, under the influence of several factors, namely stem cell factor (SCF) that links with c-kit receptor and immunoglobulin (Ig) E that links with high-affinity receptor for IgE (FcεRI), they undergo differentiation and maturation becoming mature granulated mast cells. After a contact with an antigen, mast cell degranulation is promoted and the substances contained in the cytoplasmic granules are released.

3.2.3. Mast cells' classes

In spite of common characteristics, mast cells phenotype differs among species and anatomical locations, being this phenomenon known as “mast cells heterogeneity” [39,40]. Depending on what tissue and species they are derived from, the mast cells may exhibit differences in lifespan, morphology, development, expression of proteases and proteoglycans, and sensitivity to immunologic and non-immunologic stimuli [32]. Rodent mast cells may be classified into two main groups according to their placement: connective tissue mast cells (CTMC) and mucosal mast cells (MMC). The CTMCs only require SCF for their persistence, while MMCs, additionally to the SCF, also require the T cell derived cytokines [32]. Accordingly, a reduced number of MMCs was observed in a T cell deficient mice model, while the number of CTMCs remained normal. Human mast cells are classified according to their granules' proteases content into three different classes. Mast cells that only contain tryptase are denominated as mast cells T (MC_T) and may be found in respiratory and intestinal tracts. Mast cells that contain both tryptase and chymase (MC_{TC}) mainly reside in connective tissues in the stomach, in the intestine mucosa, in the skin, in the parenchyma of the mammary gland, in the myocardium, in the cornea and in the lymph nodes. Comparing humans and rodents, in terms of localization in tissues, the human MC_T correspond to rodent MMC that are mainly found in mucosal tissues, and the MC_{TC} correspond to rodent CTMC that are mainly located in connective tissues. Similarly to that was observed in the T cells deficient mice model, the humans with a T cells immunodeficiency lack MC_T , while the MC_{TC} appeared at normal numbers [25].

3.3. Mast cells and disease

Historically, the role of mast cells has been focused on atopic disorders, pathogenesis of allergic reactions, response to parasites and bacteria, and anaphylaxis [41,42]. Mast cells are among the first inflammatory cells that interact with invading pathogenic agents, acting as important sentinels of the immune system [41,43]. They have the ability to recognize, attach to, phagocyte and kill Gram-negative and Gram-positive bacteria (innate immunity). By the interaction with B and T cells, and interference in the migration, maturation and function of dendritic cells, mast cells contribute to the initiation of acquired immune response [33,34]. The initiation of innate and adaptive immune

response during an infection depends on a rapid burst of pro-inflammatory mediators at the site of infection. Previous studies suggested that the mast cells may be involved in the creation of this pro-inflammatory environment [44]. The mast cells location, expression of diverse receptors that facilitate the pathogens recognition, and the pro-inflammatory mediators (cytokines and chemokines) released by them support this hypothesis [44].

The knowledge about mast cells was changing over the years, and nowadays they appear as highly versatile tissue elements that play an important role in several biological settings, namely autoimmune diseases (multiple sclerosis and rheumatoid arthritis), angiogenesis, immune modulation, tissue repair and remodeling, and cancer [45,46]. However, their role in these diseases and mainly in cancer is not fully understood [47,48]. Although the dense infiltration of mast cells at the periphery of carcinomatous tumors had been described in 1891 by Westphal, the studies about the role of these cells in tumor immunity are very limited [49,50]. Previous studies concluded that mast cells number increase in inflammatory conditions, such as allergy, asthma, skin and autoimmune diseases, and cancer, and they accumulate inside the tissues and orchestrate the inflammatory response [25]. This increased number of mast cells may occur not only due to the increase in the migration of mast cells precursors from the blood, but also due to the *in situ* division of few mature mast cells. Indeed, mast cells and their precursors express several chemokine and growth factors that in response to chemotactic stimuli lead to their migration to inflamed or damaged tissues [51]. It was observed that SCF overexpression in mammary tumors increases mast cell accumulation at sites of tumor growth, while the inhibition of SCF expression results in decreased mast cell accumulation and angiogenesis [52]. A correlation between mast cells number and severity of these diseases was previously reported [31]. The ability of mast cells to synthesize and release potent angiogenic compounds, such as FGF, VEGF, tryptase and chymase is the major point that links them to cancer [53]. Actually, mast cells are among the first immune cells recruited to solid tumors. In the context of tumor environment, several stimuli such as anti-tumor antibodies, hypoxia, alarmins, cytokines and chemokine may activate mast cell degranulation [54]. The role of mast cells on tumor development is yet contradictory, mast cells and their mediators may exert both pro-tumor (angiogenesis, extracellular matrix degradation and immune suppression) and anti-tumorigenic effects (cytotoxic activity, immune cell recruitment and activation) [54] (Figure 3.3). Although the overall impact in tumor microenvironment is contradictory,

the mast cells density was described as an indicator of poor prognosis in Hodgkin's lymphoma, melanoma, endometrial, cervical, esophageal, lung, gastric, colorectal and prostate carcinomas. Since the mast cells are involved in several diseases, their use as a target for new therapeutic approaches seems very attractive. Their control may be done by the regulation of their number or activity (inhibiting the release of substances or inhibiting their linkage with respective receptors, such as inhibition of histamine linkage to their receptors). The mast cell activity may be directly suppressed by the use of mast cell stabilizer agents or indirectly by targeting mast cell mediators. As example, the TNF may be targeted by anti-TNF monoclonal antibody and antihistaminic drugs may inhibit the histamine action [55].

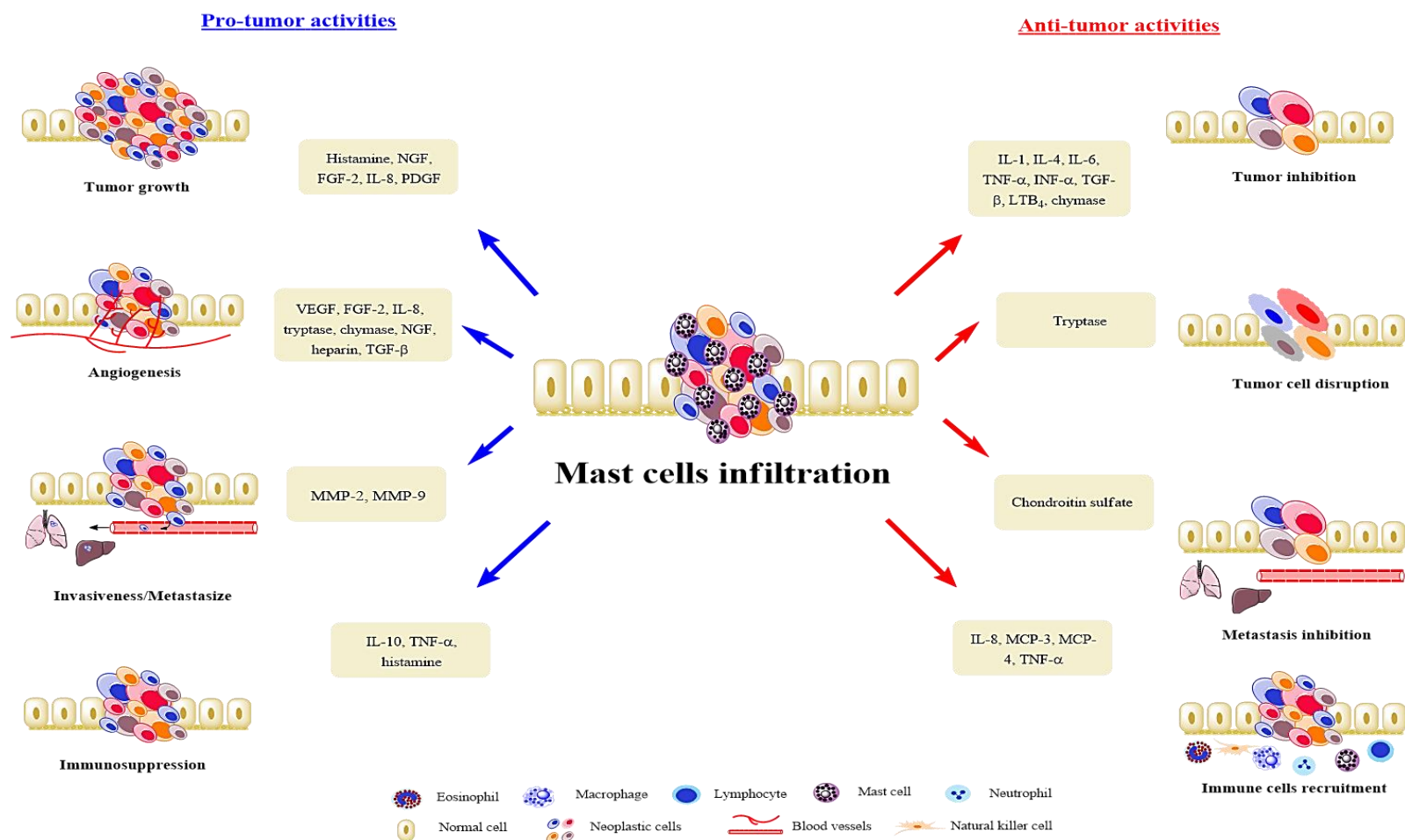


Figure 3.3. Bivalent role of mast cells on tumor progression. Mast cells may promote or inhibit tumor growth by the synthesis and release of several granule compound. FGF2 - fibroblast growth factor 2; IL - interleukin; INF- α – interferon- α ; LTB₄ - leukotriene B₄; MCP - monocyte chemoattractant protein; MMP - matrix metalloproteinases; NGF - nerve growth factor ; PDGF - platelet-derived growth factor; TGF- β - transforming growth factor β ; TNF- α - tumor necrosis factor- α (Adapted from Ribatti and Crivellato, [17]).

3.4. Cancer and inflammation

Since 1863, when Virchow hypothesized that cancer arises from sites of chronic inflammation, a possible link between chronic inflammation and cancer has been recognized. Inflammation is defined as a physiological process in response to tissue damage by microbial pathogen infection (virus, bacteria or parasite), chemical irritation or wounding [56]. Since chronic inflammation is characterized by several processes that have been implicated in cancer initiation and progression, such as infiltration of mononuclear immune cells (macrophages, lymphocytes), up-regulation of pro-inflammatory molecules (cytokines, ROS, inducible nitric oxide synthase (iNOS) and nuclear factor-kappa B (NF-kB)), tissue destruction, fibrosis, increased angiogenesis, promotion of invasion, increased genomic damage, deoxyribonucleic acid (DNA) synthesis, increased cellular proliferation, disruption of DNA repair pathways and inhibition of apoptosis; it is reasonable to consider that inflammation provides the key mutations and a favorable microenvironment for cancer development [57,58]. Indeed, most tumors are infiltrated by several inflammatory cells [6,56,59–61]. Chronic inflammation induces both proliferation of resident mast cells and recruitment of mast cells and their precursors [62], and they have been associated with angiogenesis, tumor growth and metastasis [32]. These facts suggest that mast cells may participate in tumorigenesis rather than providing a defense against the tumors [32]. Numerous epidemiologic, research and clinical studies verified that an association exists between chronic inflammation and cancer development in several organs, namely breast, urinary bladder, ovary, liver, stomach, intestine, prostate and skin [49,50,63–66]. According to some authors, tumor cells express phenotypes similar to inflammatory cells, expressing cytokines, chemokines and their receptors that have an important role on cancer angiogenesis, migration and metastasis. Some authors also verified that the expression of referred mediators is higher in high-grade mammary tumors when compared with low-grade mammary tumors [6,67,68].

The gastric infection by *Helicobacter pylori* is the leading cause of gastric adenocarcinoma [6,60]. The chronic inflammation of biliary tract by *Clonorchis sinensis* is associated with the development of cholangiocarcinoma [6]. The chronic hepatitis by hepatitis B and C viruses predisposes to the development of hepatocellular carcinoma [69]. Infection by human papillomavirus is the main cause of penile and anogenital (anal

and cervical) cancers in humans [56,70]. *Schistosoma haematobium*'s chronic infection is a factor that contributes to increase the incidence of urinary bladder cancer [71] and the infection by this agent represents the main risk factor for the development of urinary bladder squamous cell carcinoma in several schistosomal endemic countries in Africa [72]. Human herpesvirus 8 is associated with high risk of developing Kaposi's sarcoma [56,70]. The risk of colorectal cancer was higher in people with inflammatory bowel disease, such as Crohn's disease and ulcerative colitis [73,74]. A higher risk of esophageal and pancreatic cancer was also observed in people with esophagitis and Barrett's metaplasia, and chronic pancreatitis, respectively [60,75]. An association between Marjolin's ulcer and skin carcinoma was also observed [60], asbestos exposure and mesothelioma [60], chronic asthma and lung cancer [76,77], silica exposure and bronchial cancer [60], sarcoidosis and lung, skin and liver cancer [78], ulcerative lichen planus and verrucous carcinoma [79,80], foreskin inflammation and penile cancer [81], pelvic inflammatory disease or ovarian epithelial inflammation and ovarian cancer [60,82], chronic prostatitis and prostate cancer [83]. Allergies are also responsible by chronic inflammation. Although several researchers have studied the association between cancer risk and allergies, this association remains unclear and contradictory [84,85]. As mentioned above, some investigators have reported that the development of cancer in several organs is positively influenced by the inflammation [86–88]; according to the other authors the inflammation does not exert any kind of influence [89,90]; and for other investigators the inflammation associated with allergies seems to have a negative influence on cancer development [91–93]. According to some authors, allergy may confer protective effects to cancer development due to the hyperstimulation of the immune system [91,94,95], with a consequent better response of a stimulated immune system to an initiated cell when compared with a non-stimulated immune system. Inversely, other investigators suggest that allergies are permanent state of inflammation associated with the release of several inflammation mediators, such as cytokines that increase the risk of cancer development [88]. Over the last years, researchers have focused their attention on the development of new drugs for cancer therapy, however poor response and severe toxicity of these drugs remain as a main problem in the treatment of oncologic patients. Besides to the development of new drugs, it is important to improve the cancer therapeutic strategies with the existing ones [96]. One of the therapeutic approaches used in oncology that has been used from several years in the treatment of allergic diseases is

immunotherapy; through the stimulation of the immune system, it intends that inflammatory cells phagocyte neoplastic cells [97–100]. Due to their abundance at tumor periphery, their proximity to blood vessel, their radiation resistance and ability to change tumor microenvironment, mast cells represent an important target for tumor immunotherapy [96].

3.5. Histamine

Histamine, also known as 2-(4-imidazolyl)ethylamine or 5b-amino-ethylimidazole, is an endogenous physiological active substance that was discovered and chemically classified as a biogenic amine in 1910 by Henry Dale and Patrick Laidlaw [101–104]. They observed that histamine promoted the contraction of smooth muscle from the gut and respiratory tract, vasodilation, increased vasopermeabilization, increased mucous production, stimulated cardiac contraction and induced shock-like syndrome when injected in animals [102,105]. Some years later, in 1920, histamine was recognized as a stimulator of the acid secretion in the stomach and proposed as mediator of anaphylactic and allergic reactions [106–108]. Histamine is synthesized by the enzyme L-histidine decarboxylase from the amino acid histidine [107]. It is synthesized and stored within cytoplasmic granules or vesicles of several cells, namely mast cells (they are the main source of histamine), basophils, lymphocytes, platelets, enterochromaffin cells and histaminergic neurons, acting as a neurotransmitter in the central nervous system [17,109]. Histamine is the major and the most important bioactive amine released by degranulation of mast cells. Upon release into the extracellular microenvironment, it has a half-life of around one minute in the extracellular fluid and it is degraded by the enzymes *N*-methyltransferase and diamine oxidase [16]. Serum and tissue histamine levels may be measured by fluorometric and radio-enzymatic techniques [110]. Histamine is present in all tissues of mammals, ranging from less than 1 µg/g to higher than 100 µg/g. The histamine is present in higher concentration in skin, connective tissue, lung and gastrointestinal tract [110].

Histamine has a crucial role in several physiological and pathophysiological processes, namely conjunctivitis, allergic rhinitis, urticaria, atopic dermatitis, anaphylaxis, bronchoconstriction, mucus secretion, asthma and gastric acid secretion [111–114]. *In vivo* and *in vitro* studies with human cell lines of breast cancer, lymphoma, leukemia,

cervical, ovarian, vaginal, uterine, vulvar and colorectal cancer, and melanoma showed the positive involvement of histamine in cancer cell proliferation, migration and invasion [96].

3.6. Histamine receptors

Histamine exerts its effects by binding to and activating histamine receptors [111,115]. Up to now, four different types of histamine receptors have been identified: H1, H2, H3 and H4 [116]. All of these receptors belong to the family of heptahelical G protein-coupled receptors family [96,116] and are expressed by several cells and tissues (Table 3.1). These histamine receptors were also identified by genomics-based approaches (reverse transcription polymerase chain reaction) in several human tumors, namely breast cancer, lymphoma, leukemia, cervical, ovarian, vaginal, uterine, vulvar, and colorectal cancer and melanoma [96].

Depending on the binding of histamine to each receptor, the induced physiological response will be different. The activation of H1-receptors is responsible by the activation of pathways that trigger many symptoms of allergy, namely vasodilatation, bronchoconstriction, pruritus, rhinorrhea, oedema and smooth muscle contraction [110,117]. H2-receptors are the main responsible by the regulation of gastric secretion and in low grade by the control of arterial blood pressure and bronchoconstriction, when activated these receptors stimulate gastric acid secretion and promote vasodilation [96,118]. H3-receptors inhibit excessive bronchoconstriction and regulate pruritus. They also act as presynaptic autoreceptors in central and peripheral nervous system, controlling release and synthesis of histamine and other neurotransmitters, such as dopamine, serotonin, noradrenaline, γ -aminobutyric acid and acetylcholine [110,119–122]. H4-receptors show significant homology with H3-receptors [110]. They regulate the differentiation of myeloblasts and promyelocytes, induce chemotaxis and have an important role in chronic inflammatory skin diseases [110,123–125].

Table 3.1. Distribution of histamine receptors in all cells and tissues [96,103,110,123,124,126–136].

H1	H2	H3	H4
Adrenal medulla	Chondrocytes	Eosinophils	Basophils
Cardiovascular system	Dendritic cells	Histaminergic neurons	Bone marrow
Chondrocytes	Endothelial cells	Monocytes	Colon
Dendritic cells	Eosinophils		Dendritic cells
Endothelial cells	Epithelial cells		Eosinophils
Eosinophils	Gastric parietal cells		Heart
Epithelial cells	Heart		Hematopoietic cells
Gastrointestinal tract	Hepatocytes		Hepatocytes
Genitourinary system	Monocytes		Lung
Hepatocytes	Nerve cells		Mast cells
Monocytes	Neutrophils		Monocytes
Nerve cells	Smooth muscle		Nerve cells
Neutrophils	T and B cells		Neutrophils
Smooth muscle			Small intestine
T and B cells			Spleen
			Stomach
			T cells
			Thymus

3.7. Histamine and allergic diseases

Although it is not the purpose of this work, the role of histamine in allergic reactions is essential to understand its role in cancer. During the acute phase of allergic reactions, histamine is released in high quantities by mast cells [111–114,137]. Activation of histamine receptors promotes smooth muscle constriction, vasodilation, endothelial permeability and stimulates sensory nerves. These alterations promote clinical manifestations that are characteristic signs or symptoms of allergic diseases [115]. In the nose, histamine stimulates the sensory nerve endings and increases vascular permeability and glandular secretions, causing itching, sneezing, edema, obstruction, rhinitis and rhinorrhoea [111–115]. Similar to that occurs in the nose, the histamine also increases vascular permeability in the skin, promotes vasodilation and stimulates sensory nerve endings, causing erythema, pruritus, urticaria, edema and itching. In chronic allergic inflammation, histamine released by mast cells is responsible for the activation of inflammatory cells, such as basophils and eosinophils, and the release of proinflammatory mediators, such as leukotriens and cytokines [111].

3.8. Mast cells and histamine in cancer

During the tumor development, mast cells precursors migrate into the tumor and constitute one of the major stromal cell populations [62]. Some studies suggest that the mediators released by mast cells have both detrimental (promote tumor growth, neovascularization, immunosuppression and tumor invasion) and beneficial effects for the host (inhibit tumor growth, induce apoptosis, stimulate inflammation, inhibit metastasis) [17]. So, the involvement of mast cells in tumor onset and progression is far from being fully understood [17] (Figure 3.3). If in one hand, some authors observed a correlation between the progressive increase in mast cell number and poor prognosis in human melanoma, oral squamous carcinoma and prostate cancer; in the other hand, other studies observed a positive correlation between mast cell infiltration and prognosis in women with breast cancer [62]. A positive correlation between mast cell density and microvessel density was also observed in esophageal squamous cell carcinoma, gastric cancer, colorectal cancer, hepatocellular carcinoma, pancreatic adenocarcinoma, renal cell carcinoma, melanoma and oral squamous cell carcinoma [138]. If proved the positive role of mast cells on cancer progression, they may be a new target for the adjuvant

treatment of tumors by inhibiting angiogenesis, tissue remodeling and tumor promoting molecules [62].

Despite firstly hypothesized in 1960's that histamine may be involved in carcinogenesis process, nowadays this issue still remains in discussion [139]. Some researchers observed high activity of the enzyme L-histidine decarboxylase by immunohistochemistry and reverse transcription-polymerase chain reaction, and high levels of histamine by radioimmunoassay in some tumors, namely colon, breast and endometrial cancers, melanoma and small cell lung carcinoma [140–147]. It was also observed that blood levels of histamine in human patients with breast, prostate and lung malignant tumors were two or three times higher when compared with healthy ones and they remained high for two months after surgery and dropped close to normal levels three months after surgery [148]. According to some authors, the effects of histamine on tumor growth depends on histamine concentration, the tumor cell type and the receptor subtype to which it binds [149,150]. Rivera and colleagues [151] studied the mammary adenocarcinoma chemically-induced by the carcinogen agent *N*-methyl-*N*-nitrosourea (MNU) in female rats and observed that the activation of histamine receptors with concentrations of histamine up to 50 nM increased tumor cells proliferation while the use of higher concentrations inhibited tumor cells growth. Likewise, the stimulation of human pancreatic carcinoma PANC-1 cells with low levels of histamine (0.01 μM) increased tumor cells proliferation and the stimulation with higher concentrations (10 μM) decreased tumor cells proliferation [152]. According to an *in vivo* study performed on a melanoma xenograft model and an *in vitro* study using cells from mice spleen, histamine promotes cancer growth by stimulating cell division and activating suppressor T cells that are responsible by the down regulation of immune system [153,154]. Lawson *et al.* [155] observed a high number of mast cells in colorectal cancer tissue. They also observed that cancer cells that are near to the histamine-producing cells are highly proliferative, affecting negatively the prognosis. Our research team also identified a mixed inflammatory infiltrate composed of numerous mast cells and less abundant lymphocytes in mammary tumors and urinary bladder tumors chemically-induced by carcinogen agents MNU and *N*-butyl-*N*-(4-hydroxybutyl)nitrosamine in a rodent model, respectively [156,157].

As mentioned above, histamine acts by binding with different receptors [149,158]. Histamine may exert angiogenic effects through the interaction with H1 and H2 receptors [62]. It may also induce tumor cell proliferation through H1 receptors and the suppression of immune system through H2 receptors [62]. Different histamine receptors were found in several cancer cell lines and human neoplastic lesions. H1 and H2 receptors were identified in breast cancer [151,159,160], lymphoma, leukemia [161], melanoma [162], cervical, ovarian, vaginal, vulvar [163] and colorectal cancer [164]. H3 receptors were identified in breast cancer [165] and melanoma [162]. H4 receptors were identified in breast [165], cervical, ovarian, vaginal, vulvar [166] and colorectal cancer by genomics-based approaches [164]. H3 and H4-receptors are the main receptors in human neoplasias, controlling the metabolic pathways responsible for the tumor growth and progression [96].

3.9. Antihistamines

The term antihistamine is frequently used to define only substances that act as inverse agonists of H1-receptors [111,167], however the other substances that act as inverse agonists of H2, H3 and H4-receptors are also considered antihistamines. The first antihistamine was synthesized by Staub and Bovet in 1937 [168]. Antihistamines have a molecular structure similar to the histamine with which they compete [169]. The first antihistamine applied in humans was phenbenzamine in 1942 to treat allergies and skin conditions, such as pruritus and irritation [110]. Since then, the antihistamines have been used for many years as the main treatment for the relief of allergic signs or symptoms caused by histamine release [111,170,171]. They are frequently used in several clinical conditions, including allergic conditions (rhinitis, dermatoses, atopic dermatitis, contact dermatitis, allergic conjunctivitis, hypersensitivity reactions to drugs, mild transfusion reactions and urticaria), motion sickness, vertigo and insomnia [109].

According to their chemical structure, H1-antihistamines may be classified into six groups: alkylamines, ethanolamines, ethylenediamines, phenotiazines, piperazines and piperidines [109,115,172–174] (Table 3.2). Based on antihistamines pharmacological and toxic properties and their side-effects in central nervous system, these H1 antihistamines may also be divided into two distinct groups: the first-generation and the second-generation antihistamines [111,175] (Table 3.2). The first-generation antihistamines, also

called classic antihistamines, have a low molecular weight, are highly liposoluble, easily cross the blood-brain barrier and show high affinity to the H₁-receptors of the brain, causing sedation, incoordination, vertigo, lack of concentration and in some cases, agitation and excitability [111,173]. The sedative effects reflect not only in sleepiness, they also affect the cognitive performance that may prejudice several daytime activities that require high concentration [111]. These first-generation antihistamines have short half-life, being necessary multiple daily doses [173,174]. They are less expensive when compared with the second-generation ones [176]. Beyond their inhibition of central and peripheral H₁-receptors, H₁ antihistamines also inhibit muscarinic and adrenergic receptors, causing drying of nasal secretions and mouth, urinary retention, tachycardia, blurred vision and hypotension [111,124].

The second-generation antihistamines, also called newer antihistamines, were developed in the early 1980's to minimize the adverse effects of first-generation antihistamines mentioned above [173]. They have high specificity to H₁-receptors and low affinity to non-histamine receptors, namely to the muscarinic and adrenergic receptors [111,173,177,178]. Contrary to the first-generation antihistamines, the second-generation antihistamines have high molecular weight, are low liposoluble and have low affinity to the cerebral H₁-receptors, being unprovided of effects on central nervous system when administered at therapeutic doses [111]. These antihistamines have longer half-life, allowing the administration of only one or two doses *per day* [173,177,178]. Although the second-generation antihistamines were designed to overcome the sedative effects of the first-generation antihistamines, some of them show sedative effects when used in high doses [111]. In the last years emerged a new class of antihistamines, the third-generation antihistamines. Third generation antihistamines are active metabolites of first-generation antihistamines that were developed with the aim of improving clinical efficacy and minimizing adverse effects [172]. The definition of this class is not consensual among the scientific community. So, the Consensus Group on New Generation Antihistamines concluded that a new class of antihistamines must demonstrate clinical advantages over present compounds and must be free of cardiotoxicity, drug interactions and central nervous system effects [111]. The cardiotoxic effects of antihistamines, namely arrhythmia and prolongation of the QT interval, are

associated with the use of excessive doses or when they are simultaneously administered with other drugs [111].

The most frequently used H3 and H4 antihistamines may be consulted in Table 3.2. H2 antihistamines or H2 blocker drugs are frequently used in the treatment of duodenal ulcers, gastroesophageal reflux disease and in the prophylaxis of conditions where there is high gastric acidity [158]. Due to their interaction with H2-receptors, these drugs may also have a modulatory effect on immune system [158]. The effects of antihistamines vary from patient to patient [111]. It is necessary to adjust the dose of antihistamines in patients with renal or hepatic insufficiency [175]. Similar to that occurs in all medicines, the knowledge of pharmacodynamics and pharmacokinetics is essential to the correct use of these drugs [111,175,176]. Although the antihistamines' safety and appropriate use is not fully clarified, they are among the most frequently prescribed drugs in both children and adults [111,175,176]. Even though the role of mast cells is not fully understood, they have been generally considered protumorigenic cells; their inhibition by the use of frequently used and well-known antihistamine drugs, namely the ketotifen that not only acts as antihistamine drug but also stabilizes mast cells' membranes inhibiting their degranulation, would be a promising therapeutic approach.

Table 3.2. Most frequently used H1, H2, H3 and H4 antihistamines [109,111,115,118,124,172–175,179].

H1 antihistamines	First generation	Alkylamines	Brompheniramine; Chlorpheniramine; Dexbrompheniramine; Dexchlorpheniramine; Dimethindene; Pheniramine; Triprolidine
		Ethanolamines	Bromazine; Carbinoxamine; Clemastine; Dimenhydrinate; Diphenhydramine; Doxylamine; Ophenadrine; Phenyltoloxamine
		Ethylenediamines	Antazoline; Mepyramine; Pyrilamine; Tripeleennamine
		Phenothiazins	Methdilazine; Promethazine; Trimeprazine
		Piperazines	Buclizine; Chlorcyclizine; Cyclizine; Hydroxyzine; Mebhydrolin; Meclizine; Oxatomide
		Piperidines	Azatadine; Cyproheptadine; Diphenylpyraline
H1 antihistamines	Second generation	Alkylamines	Acrivastine
		Piperazines	Cetirizine; Levocetirizine
		Piperidines	Astemizole; Bilastine; Desloratadine; Ebastine; Fexofenadine; Ketotifen; Levocabastine; Loratadine; Mizolastine; Olopatadine; Terfenadine; Rupatadine
H2 antihistamines		Burimamide; Cimetidine; Dimaprid; Famotidine; Lafutidine; Nizatidine; Pibutidine; Ranitidine; Zolantidine	
H3 antihistamines		Ciproxifan; Imoproxifan; Impromidine	
H4 antihistamines		Alobenpropit; Clobenpropit; Thioperamide	

3.9.1. Pharmacodynamics

Antihistamines are a class of pharmacological agents that may inhibit the action of histamine by different ways: blocking histamine receptors (acting as inverse agonists) or inhibiting the activity of the enzyme L-histidine decarboxylase [180]. Besides their capacity to interact with histamine receptors and enzyme L-histidine decarboxylase, some antihistamines, namely ketotifen and desloratadine, have the capacity to inhibit the release of histamine by mast cells and consequently the mast cell activity. They inhibit mast cell degranulation by stabilizing their membranes, presenting antiallergic and anti-inflammatory effects [111,181–184]. Antihistamines also exerts an anti-inflammatory activity by inhibiting the accumulation of inflammatory cells and their activation, probably by the suppression of NF- κ B [185].

3.9.2. Pharmacokinetics

Nowadays, antihistamines are available as both prescription and non-prescription drugs [170]. Antihistamines may be administered by different routes, namely orally and topically [170,186]. When administered by oral route, antihistamines show a good absorption and reach the plasma concentration within three hours after administration [124]. The simultaneous administration of antihistamines and some food, namely grapefruit juice, change plasmatic concentration of antihistamines due to the blockage of action of cytochrome P450 (CYP) 3A4. This may also occur due to the interaction between antihistamines and some drugs [124,177]. Although the biotransformation of antihistamines is not clearly understood, it is known that they are predominantly biotransformed in the liver by the CYP enzyme system, mainly by CYP3A4 isoenzyme. Other isoenzymes, namely CYP1A2 and CYP2D6 may be involved in antihistamines metabolism [177,187–190]. The metabolic breakdown products, mainly inactivated, are excreted by the kidneys and eliminated in the urine [111,175]. Some antihistamines are eliminated in the feces after biliary excretion, without metabolic alterations [175].

3.10. Antihistamines and cancer risk

Several investigators have studied the relationship between cancer risk development and the use of antihistamines in humans. The results of the studies are complex and contradictory [149]. Nadalin and collaborators [170] performed a study where they

evaluated the relationship between antihistamines use and development of breast cancer. In this study, they enquired a total of 3,133 women with breast cancer and 3,062 without the disease with age ranging from 25 to 74 years-old, about the regular use of antihistamines at any time of their lives; they found no association between antihistamines use and the risk of breast cancer development. In another study, Kelly and colleagues [191] studied the association between antihistamines use and breast cancer risk in 5,814 women with invasive breast cancer and in 5,095 healthy women between 18 and 69 years of age; similarly to that was observed by Nadalin and collaborators, their findings did not support any association between the antihistamines use and breast cancer development. Some studies suggest that the use of antihistamines is not associated with a risk for cancer development, cancer recurrence or occurrence of metastases [170,191–193]. The opinions regarding to the association between the exposition of antihistamines for a long period of time (ten years or more) and the development of glioma are also divergent. According to some investigators, the exposition to these compounds is favorable [95,194–197]; based on epidemiological studies, Scheurer and colleagues [198] verified that the risk of glioma development is reduced with the exposition of antihistamines. It was also observed that antihistamines inhibit the growth of human melanoma [199], colorectal [200] and leukemic [201] cell lines. Several researchers observed that the aminoethyl ether group of antihistamines is structurally similar to *N,N*-diethyl-2-(4-(phenylmethyl)phenoxy) ethanamine HCl (DPPE) that is a tamoxifen derivative known to inhibit the *in vitro* growth of MCF-7 breast cancer cells by binding with intracellular histamine receptors [170,202,203]. Brandes and collaborators [203] observed that B16F10 melanoma and C-3 fibrosarcoma cell lines injected in a syngeneic mice model grown quickly after the administration of human equivalent doses of the H1 antihistamines loratadine and astemizole (for both tumors) and hydroxyzine (for melanoma only), they also verified that doxylamine and cetirizine did not change the growth of any cell lines. In an *in vitro* study performed by Brandes and co-workers [202] in MCF-7 and EVSA-T human breast cancer cell lines, it was observed that hydroxyzine was cytotoxic against these human breast cancer cells. Hadzijusufovic and colleagues [204] reported that H1 antihistamines terfenadine and loratadine inhibited the *in vitro* growth of HMC-1 human leukemia cell line, and C2 and NI-1 canine mastocytoma cell lines.

The H₂ antihistamine cimetidine remains as one of the most commonly prescribed medicines around the world [205]. It was first proposed as an anti-cancer drug in 1979 [206], but its effects are not consensual. It was observed that cimetidine has positive effects in patients with renal cell carcinoma [207], malignant melanoma [208] and glioblastoma [209]. Jiang and collaborators [210] performed a study where they evaluated the *in vitro* and *in vivo* effects of the H₂ antihistamine cimetidine. By 3-(4,5-dimethylthiazol-2-yl)-2,5-diphenyltrazolium bromide (MTT) assay, they evaluated the growth inhibitory effects of different concentrations of cimetidine after 24 and 48 hours of exposition in SGC-7901 human gastric carcinoma metastatic lymph node cell line, in MGC-803 human gastric mucinous adenocarcinoma cell line and in GES-1 normal human gastric epithelial cell line. They verified that cimetidine induced apoptosis in neoplastic cells and had almost no effect in the normal gastric cells. In the same work, they performed a xenograft model by subcutaneous injection of SGC-7901 cell line in the dorsal region of three groups of BALB/c nude female mice; when tumors reached 100 mm³, tumors from group one were injected with cimetidine at a concentration of 100 mg/kg, tumors from group two were injected with cimetidine at a concentration of 200 mg/kg, and tumors from group three did not receive any treatment. The treatment was performed two times a week, during four consecutive weeks. At the end of the experiment, they observed that tumor volume and weight were lower in cimetidine treated animals when compared with non-treated animals, being this reduction higher in the group that received the highest concentration of cimetidine. However, Brandes and collaborators [203] observed that the daily intraperitoneal injection of the well-known H₂ antihistamine cimetidine for 18 days did not have any effect in B16F10 melanoma and C-3 fibrosarcoma cell lines subcutaneously injected in C57BL and C3H female mice. Takahashi and colleagues [211] evaluated the effects of cimetidine in a syngeneic model. CT-26 mouse colon adenocarcinoma cell line was intradermally injected in the lumbar region of BALB/c female mice. Rats were daily treated with a subcutaneous injection of cimetidine at a concentration of 0.12 mg/kg or with saline during consecutive 14 days. During the experiment they observed that the tumor volume and weight were lower in treated animals when compared with non-treated animals.

Cimetidine inhibits tumor growth and metastasis by different ways. It inhibits cell adhesion of tumor cells, exerts antiangiogenic effects by the inhibition of VEGF that has been recognized as an important angiogenic factor, induces apoptosis, activates

macrophages, activates the immune system through the increase of interleukin levels, increases infiltration of tumors by immune cells and inhibits immunosuppression [158]. Several *in vitro* studies with cell lines of different types of cancer, namely mammary, colon, prostate, ovarian, liver and Ehrlich ascites cancer, melanoma, glioblastoma, leukemia, mastocytosis and lymphoma have been employed to evaluate the effects of several antihistamines in cancer development. Furthermore, *in vivo* studies in humans, and in syngeneic, xenograft and chemically-induced animal models of cancer have also been employed to assess the influence of antihistamines in carcinogenesis. These studies may be consulted in Table 3.3.

In a study performed by our research team, where the role of mast cells was evaluated in the initiation and progression of mammary tumors chemically-induced by the carcinogen agent MNU in Sprague-Dawley female rats, through the inhibition of mast cell degranulation by the administration of ketotifen, we observed that animals from ketotifen-treated groups developed less number of mammary tumors (palpable masses) but higher number of mammary lesions when compared with non-treated animals. A lower proliferation (Ki-67 immunoexpression) and apoptotic index (caspase-3 and -9 immunoexpression) in ketotifen-exposed animals was also observed. The main positive effect of ketotifen administration seemed to be the reduction of tumor proliferation when the mast cell degranulation was inhibited before tumor development (submitted for publication).

Table 3.3. *In vitro* and *in vivo* studies to assess the efficacy of antihistamines in cancer therapy.

Model	Drug	Dose	Effects	Reference	
<i>In vitro</i>	Tumors <i>N</i> -methyl- <i>N</i> -nitrosourea induced in ♀ Sprague-Dawley rats	Ranitidine	Concentration of 10 µM	Inhibited tumor cell proliferation	[159]
	HT29 (human colon carcinoma); DU145 (human prostate carcinoma); SF295 (human glioblastoma)	Loratadine followed by radiation treatment	Concentration of 75 µM	Pre-treatment with loratadine increased radiation-induced cytotoxicity	[212]
	SUM-229PE and T-47D (human invasive ductal carcinoma cell lines)	Astemizole	Concentration of 0.5-4.5 µM, for 6 days	Inhibited tumor cell proliferation	[213]
	A375, HT144, HSs294T and MJOI (human melanoma cell lines)	Terfenadine, astemizole, diphenhydramine, triprolidine	Concentration of 0.1-1 mM for diphenhydramine and triprolidine; 1-10 µM for terfenadine and astemizole, for 6 to 24 hours	All drugs induced apoptotic cell death in all cell lines	[199]
	HMC-1 (human mast cells leukemic cell line)	Terfenadine, loratadine	Concentration of 10 µM, for 6, 12, 24, 48 or 72 hours	Both drugs induced apoptosis in neoplastic mast cells	[204]

HT29 and COLO 205 (human colon adenocarcinoma cell lines)	Meclizine	Concentration of 10-100 μM , for 24 hours	Induced a dose-dependent decrease in cell number	[214]
MDA-MB231 and MCF-7 (human breast cancer cells)	Chlorpheniramine	Concentration of 250 μM , for 48 hours	Induced a dose-dependent decrease in cell number	[215]
A375, HT144, Hs294T (human melanoma cell lines)	Terfenadine	Concentration of 0-20 μM ; for 24 hours	Induced apoptosis	[216]
A375 (human melanoma cell lines)	Cimetidine, Terfenadine	Concentration of 0-10 μM ; for 2-10 hours	Cimetidine did not show effects on cells; terfenadine induced a dose and time-dependent cytotoxicity	[217]
HBL-2, Granta-519 and Leko-1 (human lymphoma cell lines)	Cyproheptadine	Concentration of 25 $\mu\text{mol/L}$, 30 $\mu\text{mol/L}$ and 40 $\mu\text{mol/L}$	Decreased mitochondrial membrane potential at high concentrations; induced apoptosis	[218]
Mz-ChA-1; SG-231; HuCCT-1; CCLP-1; HuH-28; TFK-1 (human cholangiocarcinoma cell lines)	Clobenpropit	Concentration from 1-50 μM ; for 48 hours	Inhibited cell proliferation in a dose-dependent manner	[219]

Human	Colorectal cancer	Cimetidine	(1) p.o.; 400 mg/kg; for 2 years after surgery (2) p.o.; 400 mg/kg; for 5 days before surgery (3) p.o.; 800 mg/kg; for 5 years before surgery	(1) Increased patients surveillance in 40 months (1) or 14 months (2 and 3)	[220,221]
		Ranitidine	i.v.; 100 mg intra-operatively followed by 150 mg/kg p.o. for 5 years	Increased patients surveillance in 80 months	[222]
		Mastocytosis	Cyproheptadine	0.38 mg/kg/day; for 33 months	Reduced degree of blistering; child grown and developed normally without sign of disease
Ruptadine	Concentration of 20 mg/day; for 28 days		Controlled symptoms and improved quality of life	[224]	
50 Grey horses	Melanoma	Cimetidine	p.o.; 3.5 mg/kg/2 times days or 7.5 mg/kg/day; for 60 days	It was not effective in the treatment of horses melanoma	[225]
Sprague-Dawley rats		Cimetidine; Diphenhydramine	p.o. in drinking water; 100 mg/kg/day; for 26 weeks	Cimetidine did not reduce the incidence of colon	[226]

	Colonic tumors chemically-induced by 1,2-dimethylhydrazine	Cyproheptadine	i.p.; 1 mg/kg; single doses	tumors; none of the drugs affected the staging and degree of differentiation of tumor Reduced number of tumors; increased necrosis in neoplastic cells	[227]
♀ C57BL mice/ ♀ C3H mice	<i>Syngeneic</i> ; B16F10 melanoma cells and C-3 fibrosarcoma cells; s.c. injection	Loratadine, astemizole, cetirizine, hydroxyzine	i.p. administration; human-equivalent dose; once a day; for 18-21 days	Loratadine and astemizole promoted the growth of both tumors Hydroxyzine promoted the growth of melanoma Cetirizine did not have any effects	[203]
BALB/c nude mice	♀ <i>Xenograft</i> ; SGC-7901 (human gastric carcinoma metastatic lymph node cells) ♂ <i>Xenograft</i> ; C170 and LIM2412 (human colon adenocarcinoma cell lines)	Cimetidine	Intratumoral injection; 100 mg/kg for 2 days; 200 mg/kg for 2 days; for 4 weeks Subcutaneously implanted; 100 mg/kg/day; for 21 or 28 days	Decreased tumor volume and weight Inhibited tumor growth (lower number and volume of tumors)	[210] [140]

	<i>Xenograft</i> ; KK (ovarian carcinoma cell lines)		p.o. in drinking water; 25, 50 or 100 mg/kg/day; for 20 days	Decreased tumor growth	[228]
C57BL mice	♀ LL57B004 (mice Lewis lung carcinoma); s.c. or i.m. injection	Cimetidine	p.o. in drinking water; 100 mg/kg/day; for 20 days	Decreased cell growth	[141]
	♂ <i>Syngeneic</i> ; McB6-1 (mice fibrosarcoma cell line); s.c. injection	Mepyramine	i.p.; 0.2mg; 7days/week; for 35 days	Induced a slight increase in tumor growth; decreased animals' survival	[229]
Immunodeficient nude mice	<i>Xenograft</i> ; Mz-ChA-1 (human cholangiocarcinoma cell lines); s.c. injection	Clobenpropit	i.p.; 20 mmol/kg/day; for 39 days	Inhibited tumor progression and decreased tumor volume	[219]
Immunodeficient SCID mice	<i>Xenograft</i> ; HT168 (human melanoma cell line); i.d. injection	Ranitidine, cimetidine	p.o. in drinking water; 50 mg/kg/day	Both drugs inhibited tumor growth	[230]
♂ nude mice	<i>Xenograft</i> ; C170 and LIM2412 (human colonic adenocarcinoma cell lines)	Ranitidine	p.o. in drinking water; 25, 50 or 100 mg/kg/day (C170); 10, 25 or 50mg/Kg/day (LIM2412); for 28 days	Ranitidine had no effect in C170 cell line. Ranitidine stimulated tumor growth in LIM2412 cell line	[155]

	<i>Xenograft</i> ; MKN45G (gastric adenocarcinoma cell line); s.c. injection	Cimetidine	p.o. in drinking water; 100 mg/kg/day; for 20 days	Inhibited proliferation of tumor cells	[231]
DBA2 mice	<i>Syngeneic</i> ; MDAY-D2 (mouse leukemic cells); s.c. injection	Cyproheptadine	i.p.; 10 mg/kg/day; for 5 or 10 days	Abolished formation of malignant ascites; inhibited tumor growth; induced apoptosis of tumor cells	[232]
Sublethally irradiated NOD/SCID mice	<i>Xenograft</i> ; LP-1(human multiple myeloma line); s.c. injection			Delayed tumor growth; decreased tumor volume; induced apoptosis of tumor cells	[232]
Mice	<i>Syngeneic</i> ; Ehrlich carcinoma cells	Chlorpheniramine	i.p.; 0.2 mL/day of 6.4 mM chlorpheniramine solution; for 7 or 11 days	Decreased tumor growth	[233]

i.d. intradermal injection; **i.m.** intramuscular injection, **i.p.** intraperitoneal injection, **i.v.** intravenous administration, **p.o.** oral administration, **s.c.** subcutaneous injection

3.11. Conclusion

Histamine receptors were identified in several cancers, namely in mammary, cervical, ovarian, vaginal, uterine, vulvar, colorectal cancer, and melanoma. The results of some studies that evaluated the effects of mast cell mediators on cancer development suggest that they may be potential targets in new cancer therapies, since the inhibition of their degranulation avoid the release of pro-tumor mediators. Since monotherapy is typically insufficient to completely eradicate cancer, combination therapy is generally administered. Given that antihistamines toxicity is lower when compared with conventional chemotherapeutic agents used in cancer, the study of their use as adjuvants for conventional therapy is warranted. However, before recommending the use of antihistamines as new cancer agents, it is necessary to clarify the exact level of histamine receptors in different types of tumors and the effects of the activation of each one on cancer growth, evaluating them *in vitro* and *in vivo*.

3.12. References

- [1] Herbst, RS.; Bajorin, DF.; Bleiberg, H.; Blum, D.; Hao, D.; Johnson, BE.; Ozols, RF.; Demetri, GD.; Ganz, PA.; Kris, MG.; Levin, B.; Markman, M.; Raghavan, D.; Reaman, GH.; Sawaya, R.; Schuchter, LM.; Sweetenham, JW.; Vahdat, LT.; Vokes, EE.; Winn, RJ.; Mayer, RJ. Clinical cancer advances 2005: major research advances in cancer treatment, prevention, and screening - a report from the American Society of Clinical Oncology. *J. Clin. Oncol.*, **2006**, 24, 190–205.
- [2] Hall, EJ.; Giaccia, AJ. Cancer biology. In *Radiobiology for the radiologist* (Hall, E. J. and Giaccia, A. J., eds), **2006**, pp. 274–302, Lippincott Williams & Wilkins.
- [3] Frank, LM.; Knowles, MA. What is cancer? In *Introduction to the cellular and molecular biology of cancer* (Knowles, M. and Selby, P., eds), **2005**, pp. 1–24, Oxford University Press.
- [4] Hanahan, D.; Weinberg, RA. The hallmarks of cancer. *Cell*, **2000**, 100, 57–70.
- [5] Balkwill, F.; Capasso, M.; Hagemann, T. The tumor microenvironment at a glance. *J. Cell Sci.*, **2012**, 125, 5591–5596.
- [6] Coussens, LM.; Werb, Z. Inflammatory cells and cancer: Think different! *J. Exp. Med.*, **2001**, 193, F23–26.
- [7] Hanahan, D.; Weinberg, RA. Accessories to the crime: functions of cells recruited

- to the tumor microenvironment. *Cancer Cell*, **2012**, 21, 309–322.
- [8] Ungefroren, H.; Sebens, S.; Seidl, D.; Lehnert, H.; Hass, R. Interaction of tumor cells with the microenvironment. *Cell Commun. Signal.*, **2011**, 9, 18.
- [9] Tan, W.; Zhang, WZ.; Strasner, A.; Grivennikov, S.; Cheng, JQ.; Hoffman, RM.; Karin, M. Tumour-infiltrating regulatory T cells stimulate mammary cancer metastasis through RANKL-RANK signalling. *Nature*, **2011**, 470, 548–553.
- [10] Daniel, D.; Chiu, C.; Giraud, E.; Inoue, M.; Mizzen, LA.; Chu, NR.; Hanahan, D. CD4+ T cell-mediated antigen-specific immunotherapy in a mouse model of cervical cancer. *Cancer Res.*, **2005**, 65, 2018–2025.
- [11] Jiang, YF.; Goldberg, ID.; Shi, YE. Complex roles of tissue inhibitors of metalloproteinases in cancer. *Oncogene*, **2002**, 21, 2245–2252.
- [12] Mantovani, A.; Allavena, P.; Sica, A.; Balkwill, F. Cancer-related inflammation. *Nature*, **2008**, 454, 436–444.
- [13] Hanahan, D.; Weinberg, RA. Hallmarks of cancer: the next generation. *Cell*, **2011**, 144, 646–674.
- [14] Grivennikov, SI.; Greten, FR.; Karin, M. Immunity, inflammation, and cancer. *Cell*, **2010**, 140, 883–899.
- [15] Ehrlich, P. Beiträge zur theorie und praxis der histologischen färbung. **1878**.
- [16] Ribatti, D.; Crivellato, E. The mast cell. In *Mast cells and tumors: from biology to clinic* (Ribatti, D. and Crivellato, E, eds), **2011**, pp. 3–48, Springer.
- [17] Ribatti, D.; Crivellato, E. (2011) Mast cells and tumors. In *Mast cells and tumors: from biology to clinic* (Ribatti, D. and Crivellato, E, eds), **2011**, pp. 83–88, Springer.
- [18] Grimbaldston, MA.; Nakae, S.; Kalesnikoff, J.; Tsai, M.; Galli, SJ. Mast cell-derived interleukin 10 limits skin pathology in contact dermatitis and chronic irradiation with ultraviolet B. *Nat. Immunol.*, **2007**, 8, 1095–1104.
- [19] Weller, K.; Foitzik, K.; Paus, R.; Syska, W.; Maurer, M. Mast cells are required for normal healing of skin wounds in mice. *Faseb J.*, **2006**, 20, 2366–2388.
- [20] Silver, R.; Silverman, AJ.; Vitkovic, L.; Lederhendler, II. Mast cells in the brain: evidence and functional significance. *Trends Neurosci.*, **1996**, 19, 25–31.
- [21] Blank, U. The mechanism of exocytosis in mast cells. In *Mast cell biology: contemporary and emerging topics* (Gilfillan, A. M. and Metcalfe, D. D., eds), **2011**, pp. 107–122, Springer.

- [22] Crivellato, E.; Ribatti, D. The mast cell: an evolutionary perspective. *Biol. Rev.*, **2010**, 85, 347–360.
- [23] Dvorak, AM. Ultrastructural studies of human basophils and mast cells. *J. Histochem. Cytochem.*, **2005**, 53, 1043–1070.
- [24] Enerback, L.; Lowhagen, GB. Long term increase of mucosal mast-cells in the rat induced by administration of compound 48/80. *Cell Tissue Res.*, **1979**, 198, 209–215.
- [25] Ekoff, M.; Nilsson, G. Mast cell apoptosis and survival. In *Mast cell biology: contemporary and emerging topics* (Gilfillan, A. M. and Metcalfe, D. D., eds), **2011**, pp. 47–61, Springer
- [26] Kirshenbaum, AS.; Metcalfe, DD. Growth of human mast cells from bone marrow and peripheral blood-derived CD34+ pluripotent progenitor cells. *Methods Mol. Biol.*, **2006**, 315, 105–112.
- [27] Gurish, M.; Austen, KF. The diverse role of mast cells. *J. Exp. Med.*, **2001**, 194, 1–5.
- [28] Okayama, Y.; Kawakami, T. Development migration, and survival of mast cells. *Immunol. Res.*, **2006**, 34, 97–115.
- [29] Kitamura, Y.; Go, S.; Hatanaka, K. Decrease of mast cells in W/W^v mice and their increase by bone marrow transplantation. *Blood*, **1978**, 52, 447–452.
- [30] Kitamura, Y.; Hirotab, S. Kit as a human oncogenic tyrosine kinase. *Cell. Mol. Life Sci.*, **2004**, 61, 2924–2931.
- [31] Gilfillan, AM.; Austin, SJ.; Metcalfe, DD. Mast cell biology: introduction and overview. In *Mast cell biology: contemporary and emerging topics* (Gilfillan, A. M. and Metcalfe, D. D., eds), **2011**, pp. 2–13, Springer.
- [32] Kashiwakura, J.; Otani, I.; Kawakami, T. Monomeric IgE and mast cell development, survival and function. In *Mast cell biology: contemporary and emerging topics* (Gilfillan, A. M. and Metcalfe, D. D., eds), **2011**, pp. 29–46, Springer.
- [33] Bachelet, I.; Levi-Schaffer, F. Mast cells as effector cells: a co-stimulating question. *Trends Immunol.*, **2007**, 28, 360–365.
- [34] Marshall, JS. Mast-cell responses to pathogens. *Nat. Rev. Immunol.*, **2004**, 4, 787–799.
- [35] Galli, SJ.; Tsai, M.; Piliponsky, AM. The development of allergic inflammation.

- Nature*, **2008**, 454, 445–454.
- [36] Blank, U.; Rivera, J. The ins and outs of IgE-dependent mast-cell exocytosis. *Trends Immunol.*, **2004**, 25, 266–273.
- [37] Gommerman, JL.; Oh, DY.; Zhou, XN.; Tedder, TF.; Maurer, M.; Galli, SJ.; Carroll, MC. A role for CD21/CD35 and CD19 in responses to acute septic peritonitis: a potential mechanism for mast cell activation. *J. Immunol.*, **2000**, 165, 6915–6921.
- [38] Talkington, J.; Nickell, SP. Role of Fc gamma receptors in triggering host cell activation and cytokine release by *Borrelia burgdorferi*. *Infect. Immun.*, **2001**, 69, 413–419.
- [39] Crivellato, E.; Ribatti, D. The fundamental contribution of William Bate Hardy to shape the concept of mast cell heterogeneity. *Br. J. Haematol.*, **2010**, 150, 152–157.
- [40] Galli, SJ. New insight into “the riddle of mast cells”: microenvironmental regulation of mast cell development and phenotypic heterogeneity. *Lab. Investig.*, **1990**, 62, 5–33.
- [41] Feger, F.; Varadaradjalou, S.; Gao, ZM.; Abraham, SN.; Arock, M. The role of mast cells in host defense and their subversion by bacterial pathogens. *Trends Immunol.*, **2002**, 23, 151–158.
- [42] Gurish, MF.; Boyce, JA. Mast cells: ontogeny, homing, and recruitment of a unique innate effector cell. *J. Allergy Clin. Immunol.*, **2006**, 117, 1285–1291.
- [43] von Kockritz-Blickwede, M.; Goldmann, O.; Thulin, P.; Heinemann, K.; Norrby-Teglund, A.; Rohde, M.; Medina, E. Phagocytosis-independent antimicrobial activity of mast cells by means of extracellular trap formation. *Blood*, **2008**, 111, 3070–3080.
- [44] Shelburne, C.; Abraham, S. The mast cell in innate and adaptative immunity. In *Mast cell biology: contemporary and emerging topics* (Gilfillan, A. and Metcalfe, D., eds), **2011**, pp. 162–185, Springer.
- [45] Beaven, MA. Our perception of the mast cell from Paul Ehrlich to now. *Eur. J. Immunol.*, **2009**, 39, 11–25.
- [46] Galli, SJ.; Kalesnikoff, J.; Grimbaldston, MA.; Piliponsky, AM.; Williams, CMM.; Tsai, M. Mast cells as “tunable” effector and immunoregulatory cells: recent advances. *Annu. Rev. Immunol.*, **2005**, 23, 749–786.

- [47] Burd, PR.; Rogers, HW.; Gordon, JR.; Martin, CA.; Jayaraman, S.; Wilson, SD.; Dvorak, AM.; Galli, SJ.; Dorf, ME. Interleukin-3-dependent and interleukin-3-independent mast cells stimulated with ige and antigen express multiple cytokines. *J. Exp. Med.*, **1989**, 170, 245–257.
- [48] Plaut, M.; Pierce, JH.; Watson, CJ.; Hanleyhyde, J.; Nordan, RP.; Paul, WE. Mast cell lines produce lymphokines in response to cross-linkage of Fc epsilon RI or to calcium ionophores. *Nature*, **1989**, 339, 64–67.
- [49] Kuper, H.; Adami, HO.; Trichopoulos, D. Infections as a major preventable cause of human cancer. *J. Intern. Med.*, **2000**, 248, 171–183.
- [50] De Marzo, AM.; Marchi, VL.; Epstein, JI.; Nelson, WG. Proliferative inflammatory atrophy of the prostate - Implications for prostatic carcinogenesis. *Am. J. Pathol.*, **1999**, 155, 1985–1992.
- [51] Halova, I.; Department, L.; Draber, P. Mast cell chemotaxis - chemoattractants and signaling pathways. *Front. Immunol.*, **2012**, 3,
- [52] Ribatti, D.; Crivellato, E. *Mast cells and tumors: from biology to clinic*. **2011**, Springer.
- [53] Kessler, DA.; Langer, RS.; Pless, NA.; Folkman, J. Mast cells and tumor angiogenesis. *Int. J. Cancer*, **1976**, 18, 703–709.
- [54] Oldford, SA.; Marshall, JS. Mast cells as targets for immunotherapy of solid tumors. *Mol. Immunol.*, **2014**, 63, 113–124.
- [55] Groot, K.; Abudukelimu, A.; Redegeld, FA. Mast cells as target in cancer therapy. *Curr. Pharmaceutical Des.*, **2009**, 15, 5860–5867.
- [56] Balkwill, F.; Mantovani, A. Inflammation and cancer: back to virchow? *Lancet*, **2001**, 357, 539–545.
- [57] Cordon-Cardo, C. At the crossroad of tumorigenesis: drivers and hitchhikers. *Hum. Pathol.*, **1999**, 30, 1001–1003.
- [58] Rayburn, ER.; Ezell, SJ.; Zhang, R. Anti-inflammatory agents for cancer therapy. *Mol. Cell. Pharmacol.*, **2009**, 1, 29–43.
- [59] Coussens, LM.; Werb, Z. Inflammation and cancer. *Nature*, **2002**, 420, 860–867.
- [60] Macarthur, M.; Hold, GL.; El-Omar, EM. Inflammation and cancer II. Role of chronic inflammation and cytokine gene polymorphisms in the pathogenesis of gastrointestinal malignancy. *Am. J. Physiol. Liver Physiol.*, **2004**, 286, G515–520.
- [61] Yang, CR.; Hsieh, SL.; Ho, FM.; Lin, WW. Decoy receptor 3 increases monocyte

- adhesion to endothelial cells via NF-kappa B-dependent up-regulation of intercellular adhesion molecule-1, VCAM-1, and IL-8 expression. *J. Immunol.*, **2005**, 174, 1647–1656.
- [62] Ribatti, D.; Crivellato, E. Mast cells, angiogenesis and cancer. In *Mast cell biology: contemporary and emerging topics* (Gilfillan, A. M. and Metcalfe, D. D., eds), **2011**, pp. 270–288, Springer.
- [63] Brocker, EB.; Zwadlo, G.; Holzmann, B.; Macher, E.; Sorg, C. Inflammatory cell infiltrates in human melanoma at different stages of tumor progression. *Int. J. Cancer*, **1988**, 41, 562–567.
- [64] Ness, RB.; Cottreau, C. Possible role of ovarian epithelial inflammation in ovarian cancer. *J. Natl. Cancer Inst.*, **1999**, 91, 1459–1467.
- [65] Ernst, PB.; Gold, BD. The disease spectrum of *Helicobacter pylori*: the immunopathogenesis of gastroduodenal ulcer and gastric cancer. *Annu. Rev. Microbiol.*, **2000**, 54, 615–640.
- [66] Scholl, SM.; Pallud, C.; Beuvon, F.; Hacene, K.; Stanley, ER.; Rohrschneider, L.; Tang, R.; Pouillart, P.; Lidereau, R. Anti-colony-stimulating factor-1 antibody staining in primary breast adenocarcinomas correlates with marked inflammatory cell infiltrates and prognosis. *J. Natl. Cancer Inst.*, **1994**, 86, 120–126.
- [67] Chavey, C.; Bibeau, F.; Gourgou-Bourgade, S.; Burlincho, S.; Boissiere, F.; Laune, D.; Roques, S.; Lazennec, G. Oestrogen receptor negative breast cancers exhibit high cytokine content. *Breast Cancer Res.*, **2007**, 9, 15.
- [68] Lu, Y.; Cai, Z.; Galson, DL.; Xiao, GZ.; Liu, YL.; George, DE.; Melhem, MF.; Yao, Z.; Zhang, J. Monocyte chemotactic protein-1 (MCP-1) acts as a paracrine and autocrine factor for prostate cancer growth and invasion. *Prostate*, **2006**, 66, 1311–1318.
- [69] Block, TM.; Mehta, AS.; Fimmel, CJ.; Jordan, R. Molecular viral oncology of hepatocellular carcinoma. *Oncogene*, **2003**, 22, 5093–5107.
- [70] Rosin, MP.; Anwar, WA.; Ward, AJ. Inflammation, chromosomal instability, and cancer: the schistosomiasis model. *Cancer Res.*, **1994**, 54, S1929–1933.
- [71] Ketabchi, AA.; Moshtaghi-Kashanian, GR. Urinary schistosomiasis with simultaneous bladder squamous cell carcinoma and transitional cell carcinoma. *Iran. J. Parasitol.*, **2012**, 7, 96–98.
- [72] Rambau, PF.; Chalya, PL.; Jackson, K. Schistosomiasis and urinary bladder cancer

- in North Western Tanzania: a retrospective review of 185 patients. *Infect. Agent. Cancer*, **2013**, 8, 19.
- [73] Itzkowitz, SH.; Yio, XY. Inflammation and cancer IV. Colorectal cancer in inflammatory bowel disease: the role of inflammation. *Am. J. Physiol. Liver Physiol.*, **2004**, 287, G7–17.
- [74] Seril, DN.; Liao, J.; Yang, GY.; Yang, CS. Oxidative stress and ulcerative colitis-associated carcinogenesis: studies in humans and animal models. *Carcinogenesis*, **2003**, 24, 353–362.
- [75] Whitcomb, DC. Inflammation and cancer V. Chronic pancreatitis and pancreatic cancer. *Am. J. Physiol. Liver Physiol.*, **2004**, 287, G315–319.
- [76] Vesterinen, E.; Pukkala, E.; Timonen, T.; Aromaa, A. Cancer incidence among 78,000 asthmatic patients. *Int. J. Epidemiol.*, **1993**, 22, 976–982.
- [77] Wu, AH.; Fontham, ETH.; Reynolds, P.; Greenberg, RS.; Buffler, P.; Liff, J.; Boyd, P.; Henderson, BE.; Correa, P. Previous lung-disease and risk of lung cancer among lifetime nonsmoking women in the United States. *Am. J. Epidemiol.*, **1995**, 141, 1023–1032.
- [78] Askling, J.; Grunewald, J.; Eklund, A.; Hillerdal, G.; Ekblom, A. Increased risk for cancer following sarcoidosis. *Am. J. Respir. Crit. Care Med.*, **1999**, 160, 1668–1672.
- [79] Carlson, JA.; Ambros, R.; Malfetano, J.; Ross, J.; Grabowski, R.; Lamb, P.; Figge, H.; Mihm, MC. Vulvar lichen sclerosus and squamous cell carcinoma: a cohort, case control, and investigational study with historical perspective; implications for chronic inflammation and sclerosis in the development of neoplasia. *Hum. Pathol.*, **1998**, 29, 932–948.
- [80] Mayron, R.; Grimwood, RE.; Siegle, RJ.; Camisa, C. Verrucous carcinoma arising in ulcerative lichen planus of the soles. *J. Dermatol. Surg. Oncol.*, **1988**, 14, 547–551.
- [81] Perky, L. Epidemiology of cancer of the penis. *Recent Results Cancer Res.*, **1977**, 60, 97–109.
- [82] Risch, HA.; Howe, GR. Pelvic Inflammatory disease and the risk of epithelial ovarian cancer. *Cancer Epidemiol. Biomarkers Prev.*, **1995**, 4, 447–451.
- [83] Palapattu, GS.; Sutcliffe, S.; Bastian, PJ.; Platz, EA.; De Marzo, AM.; Isaacs, WB.; Nelson, WG. Prostate carcinogenesis and inflammation: emerging insights.

- Carcinogenesis*, **2005**, 26, 1170–1181.
- [84] Lindelof, B.; Granath, F.; Tengvall-Linder, M.; Ekbom, A. Allergy and cancer. *Allergy*, **2005**, 60, 1116–1120.
- [85] Turner, MC.; Chen, Y.; Krewski, D.; Ghadirian, P. An overview of the association between allergy and cancer. *Int. J. Cancer*, **2006**, 118, 3124–3132.
- [86] Chae, YK.; Neagu, S.; Kim, J.; Smyrlis, A.; Gooptu, M.; Tester, W. Association between common allergic symptoms and cancer in the NHANES III female cohort. *Plos One*, **2012**, 7, e42896.
- [87] Gallagher, RP.; Spinelli, JJ.; Elwood, JM.; Skippen, DH. Allergies and agricultural exposure as risk factors for multiple myeloma. *Br. J. Cancer*, **1983**, 48, 853–857.
- [88] Santillan, AA.; Camargo, CA.; Colditz, GA. A meta-analysis of asthma and risk of lung cancer (United States). *Cancer Causes Control*, **2003**, 14, 327–334.
- [89] Ming, ME.; Levy, R.; Hoffstad, O.; Filip, J.; Abrams, BB.; Fernandez, C.; Margolis, DJ. The lack of a relationship between atopic dermatitis and nonmelanoma skin cancers. *J. Am. Acad. Dermatol.*, **2004**, 50, 357–362.
- [90] Schwartzbaum, J.; Jonsson, F.; Ahlbom, A.; Preston-Martin, S.; Lonn, S.; Soderberg, KC.; Feychting, M. Cohort studies of association between self-reported allergic conditions, immune-related diagnoses and glioma and meningioma risk. *Int. J. Cancer*, **2003**, 106, 423–428.
- [91] Castaing, M.; Youngson, J.; Zaridze, D.; Szeszenia-Dabrowska, N.; Rudnai, P.; Lissowska, J.; Fabianova, E.; Mates, D.; Bencko, V.; Foretova, L.; Navratilova, M.; Janout, V.; Fletcher, T.; Brennan, P.; Boffetta, P. Is the risk of lung cancer reduced among eczema patients? *Am. J. Epidemiol.*, **2005**, 162, 542–547.
- [92] Schuz, J.; Morgan, G.; Bohler, E.; Kaatsch, P.; Michaelis, J. Atopic disease and childhood acute lymphoblastic leukemia. *Int. J. Cancer*, **2003**, 105, 255–260.
- [93] Schuz, J.; Kaletsch, U.; Meinert, R.; Kaatsch, P.; Michaelis, J. Association of childhood leukaemia with factors related to the immune system. *Br. J. Cancer*, **1999**, 80, 585–590.
- [94] Brenner, A V.; Linet, MS.; Fine, HA.; Shapiro, WR.; Selker, RG.; Black, PM.; Inskip, PD. History of allergies and autoimmune diseases and risk of brain tumors in adults. *Int. J. Cancer*, **2002**, 99, 252–259.
- [95] Wigertz, A.; Lonn, S.; Schwartzbaum, J.; Hall, P.; Auvinen, A.; Christensen, HC.; Johansen, C.; Klaeboe, L.; Salminen, T.; Schoemaker, MJ.; Swerdlow, AJ.; Tynes,

- T.; Feychting, M. Allergic conditions and brain tumor risk. *Am. J. Epidemiol.*, **2007**, 166, 941–950.
- [96] Medina, VA.; Lamas, DJM.; Brenzoni, PG.; Massari, N.; Carabajal, E.; Rivera, ES. Histamine receptors as potential therapeutic targets for cancer drug development. In *Drug development - a case study based insight into modern strategies* (Rundfeldt, C., ed), **2011**, pp. 75–100, InTech Europe.
- [97] Kirkwood, JM.; Butterfield, LH.; Tarhini, AA.; Zarour, H.; Kalinski, P.; Ferrone, S. Immunotherapy of cancer in 2012. *CA Cancer J. Clin.*, **2012**, 62, 309–335.
- [98] Cunha, A.; Michelin, MA.; Murta, EFC. Pattern response of dendritic cells in the tumor microenvironment and breast cancer. *World J. Clin. Oncol.*, **2014**, 5, 495–502.
- [99] Till, SJ.; Francis, JN.; Nouri-Aria, K.; Durham, SR. Mechanisms of immunotherapy. *J. Allergy Clin. Immunol.*, **2004**, 111, 1025–1034.
- [100] Frew, AJ. Immunotherapy of allergic disease. *J. Allergy Clin. Immunol.*, **2003**, 111, 712–719.
- [101] Baraniuk, JN. Pathogenesis of allergic rhinitis. *J. Allergy Clin. Immunol.*, **1997**, 99, S763–772.
- [102] Dale, HH.; Laidlaw, PP. The physiological action of beta-iminazolylethylamine. *J. Physiol.*, **1910**, 41, 318–344.
- [103] Dy, M.; Schneider, E. Histamine-cytokine connection in immunity and hematopoiesis. *Cytokine Growth Factor Rev.*, **2004**, 15, 393–410.
- [104] Raphael, GD.; Meredith, SD.; Baraniuk, JN.; Druce, HM.; Banks, SM.; Kaliner, MA. The patho-physiology of rhinitis: II. Assessment of the sources of protein in histamine-induced nasal secretions. *Am. Rev. Respir. Dis.*, **1989**, 139, 791–800.
- [105] Dale, HH.; Laidlaw, PP. Histamine shock. *J. Physiol.*, **1919**, 52, 355–390.
- [106] White, MV. The role of histamine in allergic diseases. *J. Allergy Clin. Immunol.*, **1990**, 28, 599–605.
- [107] Maintz, L.; Novak, N. Histamine and histamine intolerance. *Am. J. Clin. Nutr.*, **2007**, 85, 1185–1196.
- [108] Popielski, L. Beta-imidazol aethyl amines and the organ extracts. First part: beta-imidazol aethyl amine as a powerful stimulant of the stomach glands. *Pflugers Arch. Gesamte Physiol. Menschen Tiere*, **1919**, 177, 214–236.
- [109] Carson, S.; Lee, N.; Thakurta, S. *Drug class review: newer antihistamines*, **2010**,

Oregon Health Science University.

- [110] Parsons, ME.; Ganellin, CR. Histamine and its receptors. *Br. J. Pharmacol.*, **2006**, 147, S127–135.
- [111] Van Schoor, J. Antihistamines: a brief review. *Prof. Nurs. Today*, **2012**, 16, 16–21.
- [112] Beaven, MA. Histamine. *N. Engl. J. Med.*, **1976**, 294, 30–36.
- [113] Code, CF. Histamine and gastric secretion - a later look 1955-1965. *Fed. Proc.*, **1965**, 24, 1311.
- [114] Schwartz, JC.; Pollard, H.; Quach, TT. Histamine as a neurotransmitter in mammalian brain - neurochemical evidence. *J. Neurochem.*, **1980**, 35, 26–33.
- [115] Golightly, LK.; Greos, LS. Second-generation antihistamines: actions and efficacy in the management of allergic disorders. *Drugs*, **2005**, 65, 341–384.
- [116] Jutel, M.; Blaser, K.; Akdis, CA. Histamine in chronic allergic responses. *J. Investig. Allergol. Clin. Immunol.*, **2005**, 15, 1–8.
- [117] Leurs, R.; Church, MK.; Tagliabatella, M. H-1-antihistamines: inverse agonism, anti-inflammatory actions and cardiac effects. *Clin. Exp. Allergy*, **2002**, 32, 489–498.
- [118] Eseverri, JL.; Marín, AM. Proyección de los nuevos antihistamínicos. *Allergol. Immunopathol. (Madr)*, **2000**, 28, 143–152.
- [119] Leurs, R.; Bakker, RA.; Timmerman, H.; De Esch, IJP. The histamine H-3 receptor: from gene cloning to H-3 receptor drugs. *Nat. Rev. Drug Discov.*, **2005**, 4, 107–120.
- [120] Lovenberg, TW.; Roland, BL.; Wilson, SJ.; Jiang, XX.; Pyati, J.; Huvar, A.; Jackson, MR.; Erlander, MG. Cloning and functional expression of the human histamine H-3 receptor. *Mol. Pharmacol.*, **1999**, 55, 1101–1107.
- [121] Arrang, JM.; Garbarg, M.; Schwartz, JC. Auto-inhibition of brain histamine - release mediated by a novel class (H-3) of histamine-receptor. *Nature*, **1983**, 302, 832–837.
- [122] Bongers, G.; Bakker, RA.; Leurs, R. Molecular aspects of the histamine H-3 receptor. *Biochem. Pharmacol.*, **2007**, 73, 1195–1204.
- [123] Zampeli, E.; Tiligada, E. The role of histamine H-4 receptor in immune and inflammatory disorders. *Br. J. Pharmacol.*, **2009**, 157, 24–33.
- [124] Simons, FER. Drug therapy - advances in H-1-antihistamines. *N. Engl. J. Med.*,

- 2004**, 351, 2203–2217.
- [125] Gutzmer, R.; Gschwandtner, M.; Rossbach, K.; Mommert, S.; Werfel, T.; Kietzmann, M.; Baeumer, W. Pathogenetic and therapeutic implications of the histamine H₄ receptor in inflammatory skin diseases and pruritus. *Front. bioscience*, **2011**, 3, 985–994.
- [126] Oda, T.; Morikawa, N.; Saito, Y.; Masuho, Y.; Matsumoto, S. Molecular cloning and characterization of a novel type of histamine receptor preferentially expressed in leukocytes. *J. Biol. Chem.*, **2000**, 275, 36781–36786.
- [127] Nguyen, T.; Shapiro, DA.; George, SR.; Setola, V.; Lee, DK.; Cheng, R.; Rauser, L.; Lee, SP.; Lynch, KR.; Roth, BL.; O'Dowd, BF. Discovery of a novel member of the histamine receptor family. *Mol. Pharmacol.*, **2001**, 59, 427–433.
- [128] Nakamura, Y.; Smith, M.; Krishna, A.; Terranova, PF. Increased number of mast cells in the dominant follicle of the cow - relationships among luteal, stromal, and hilar regions. *Biol. Reprod.*, **1987**, 37, 546–549.
- [129] Morse, KL.; Behan, J.; Laz, TM.; West, RE.; Greenfeder, SA.; Anthes, JC.; Umland, S.; Wan, YT.; Hipkin, RW.; Gonsiorek, W.; Shin, N.; Gustafson, EL.; Qiao, XD.; Wang, SK.; Hedrick, JA.; Greene, J.; Bayne, M.; Monsma, FJ. Cloning and characterization of a novel human histamine receptor. *J. Pharmacol. Exp. Ther.*, **2001**, 296, 1058–1066.
- [130] Medina, V.; Cricco, G.; Nunez, M.; Martin, G.; Mohamad, N.; Correa-Fiz, F.; Sanchez-Jimenez, F.; Bergoc, R.; Rivera, ES. Histamine-mediated signaling processes in human malignant mammary cells. *Cancer Biol. Ther.*, **2006**, 5, 1462–1471.
- [131] Liu, CL.; Ma, XJ.; Jiang, XX.; Wilson, SJ.; Hofstra, CL.; Blevitt, J.; Pyati, J.; Li, XB.; Chai, WY.; Carruthers, N.; Lovenberg, TW. Cloning and pharmacological characterization of a fourth histamine receptor (H-4) expressed in bone marrow. *Mol. Pharmacol.*, **2001**, 59, 420–426.
- [132] Coge, F.; Guenin, SP.; Rique, H.; Boutin, JA.; Galizzi, JP. Structure and expression of the human histamine H-4-receptor gene. *Biochem. Biophys. Res. Commun.*, **2001**, 284, 301–309.
- [133] Coge, F.; Guenin, SP.; Audinot, V.; Renouard-Try, A.; Beauverger, P.; Macia, C.; Ouvry, C.; Nagel, N.; Rique, H.; Boutin, JA.; Galizzi, JP. Genomic organization and characterization of splice variants of the human histamine H-3 receptor.

- Biochem. J.*, **2001**, 355, 279–288.
- [134] Cianchi, F.; Cortesini, C.; Schiavone, N.; Perna, F.; Magnelli, L.; Fanti, E.; Bani, D.; Messerini, L.; Fabbroni, V.; Perigli, G.; Capaccioli, S.; Masini, E. The role of cyclooxygenase-2 in mediating the effects of histamine on cell proliferation and vascular endothelial growth factor production in colorectal cancer. *Clin. Cancer Res.*, **2005**, 11, 6807–6815.
- [135] Leurs, R.; Chazot, PL.; Shenton, FC.; Lim, HD.; de Esch, IJP. Molecular and biochemical pharmacology of the histamine H-4 receptor. *Br. J. Pharmacol.*, **2009**, 157, 14–23.
- [136] Leurs, R.; Smit, MJ.; Timmerman, H. Molecular pharmacological aspects of histamine receptors. *Pharmacol. Ther.*, **1995**, 66, 413–463.
- [137] Janeway, CA.; Travers, P.; Walport, M.; Shlomchik, MJ. *Immunobiology: the immune system in health and disease*. **2001**, Garland Science.
- [138] Ribatti, D.; Crivellato, E. Mast cells and tumor angiogenesis. In *Mast cells and tumors: from biology to clinic* (Ribatti, D. and Crivellato, E, eds), **2011**, pp. 89–102, Springer.
- [139] Kahlson, G.; Rosengren, E. New approaches to the physiology of histamine. *Annu. Rev. Physiol.*, **1965**, 48, 155–196.
- [140] Adams, WJ.; Lawson, JA.; Morris, DL. Cimetidine inhibits *in vivo* growth of human colon-cancer and reverses histamine-stimulated *in vitro* and *in vivo* growth. *Gut*, **1994**, 35, 1632–1636.
- [141] Bartholeyns, J.; Bouclier, M. Involvement of histamine in growth of mouse and rat-tumors - antitumoral properties of monofluoromethylhistidine, an enzyme-activated irreversible inhibitor of histidine decarboxylase. *Cancer Res.*, **1984**, 44, 639–645.
- [142] Grahn, B.; Rosengren, E. Retardation of protein synthesis in rat tumours on inhibiting histamine formation. *Experientia*, **1970**, 26, 125–126.
- [143] Chanda, R.; Ganguly, AK. Diamine-oxidase activity and tissue di- and poly-amine contents of human ovarian, cervical and endometrial carcinoma. *Cancer Lett.*, **2001**, 89, 23–28.
- [144] Garciacaballero, M.; Neugebauer, E.; Campos, R.; Decastro, IN.; Varathorbeck, C. Increased histidine-decarboxylase (HDC) activity in human colorectal cancer: results of a study on ten patients. *Agents Actions*, **1988**, 23, 357–360.

- [145] Garciacaballero, M.; Neugebauer, E.; Rodriguez, F.; Decastro, IN.; Varathorbeck, C. Histamine synthesis and content in benign and malignant breast tumors. Its effects on other host tissues. *Surg. Oncol.*, **1994**, 3, 167–173.
- [146] Graff, L.; Frungieri, M.; Zanner, R.; Pohlinger, A.; Prinz, C.; Gratzl, M. Expression of histidine decarboxylase and synthesis of histamine by human small cell lung carcinoma. *Am. J. Pathol.*, **2002**, 160, 1561–1565.
- [147] Hegyesi, H.; Somlai, B.; Varga, VL.; Toth, G.; Kovacs, P.; Molnar, EL.; Laszlo, V.; Karpati, S.; Rivera, E.; Falus, A.; Darvas, Z. Suppression of melanoma cell proliferation by histidine decarboxylase specific antisense oligonucleotides. *J. Invest. Dermatol.*, **2001**, 117, 151–153.
- [148] Moriarty, CM.; Stucky, JL.; Hamburger, KW.; Patil, KD.; Foley, JF.; Koefoot, RR. Blood histamine and solid malignant tumors. *J. Cancer Res. Clin. Oncol.*, **1988**, 114, 588–592.
- [149] Cianchi, F.; Vinci, MC.; Masini, E. Histamine in cancer - the dual faces of the coin. *Cancer Biol. Ther.*, **2008**, 7, 36–37.
- [150] Lamplasi, N.; Azzolina, A.; Montalto, G.; Cervello, M. Histamine and spontaneously released mast cell granules affect the cell growth of human hepatocellular carcinoma cells. *Exp. Mol. Med.*, **2007**, 39, 284–294.
- [151] Rivera, ES.; Cricco, GP.; Engel, NI.; Fitzsimons, CP.; Martin, GA.; Bergoc, RM. Histamine as an autocrine growth factor: an unusual role for a widespread mediator. *Semin. Cancer Biol.*, **2000**, 10, 15–23.
- [152] Cricco, G.; Martin, G.; Medina, V.; Nunez, M.; Gutierrez, A.; Cocca, C.; Bergoc, R.; Rivera, E. Histamine regulates the MAPK pathway via the H2 receptor in PANC-1 human cells. *Inflamm. Res.*, **2004**, 53, S65–66.
- [153] Nordlund, JJ.; Askenase, PW. The effect of histamine, antihistamines, and a mast-cell stabilizer on the growth of cloudman melanoma-cells in DBA/2 mice. *J. Invest. Dermatol.*, **1983**, 81, 28–31.
- [154] Siegel, JN.; Schwartz, A.; Askenase, PW.; Gershon, RK. T-cell suppression and contrasuppression induced by histamine H2 and H1 receptor agonists, respectively. *Proc. Natl. Acad. Sci. United States Am. Sci.*, **1982**, 79, 5052–5056.
- [155] Lawson, JA.; Adams, WJ.; Morris, DL. Ranitidine and cimetidine differ in their *in vitro* and *in vivo* effects on human colonic cancer growth. *Br. J. Cancer*, **1996**, 73, 872–876.

- [156] Oliveira, PA.; Palmeira, C.; Colaço, A.; De la Cruz, LF.; Lopes, C. DNA content analysis, expression of Ki-67 and p53 in rat urothelial lesions induced by *N*-butyl-*N*-(4-hydroxybutyl) nitrosamine and treated with mitomycin C and bacillus Calmette-Guérin. *Anticancer Res.*, **2006**, 26, 2995–3004.
- [157] Soares-Maia, R.; Faustino-Rocha, AI.; Teixeira-Guedes, CI.; Pinho-Oliveira, J.; Talhada, D.; Rema, A.; Faria, F.; Ginja, M.; Ferreira, R.; Gil da Costa, RM.; Oliveira, PA.; Lopes, C. MNU-induced rat mammary carcinomas: immunohistology and estrogen receptor expression. *J. Environ. Pathol. Toxicol. Oncol.*, **2013**, 32, 157–163.
- [158] Kubecova, M.; Kolostova, K.; Pinterova, D.; Kacprzak, G.; Bobek, V. Cimetidine: an anticancer drug? *Eur. J. Pharm. Sci.*, **2011**, 42, 439–444.
- [159] Cricco, GP.; Davio, CA.; Martin, G.; Engel, N.; Fitzsimons, CP.; Bergoc, RM.; Rivera, ES. Histamine as an autocrine growth factor in experimental mammary carcinomas. *Agents Actions*, **1994**, 43, 17–20.
- [160] Davio, CA.; Cricco, GP.; Bergoc, RM.; Rivera, ES. H1 and H2 histamine receptors in *N*-nitroso-*N*-methylurea (NMU)-induced carcinomas with atypical coupling to signal transducers. *Biochem. Pharmacol.*, **1995**, 50, 91–96.
- [161] Wang, KY.; Arima, N.; Higuchi, S.; Shimajiri, S.; Tanimoto, A.; Murata, Y.; Hamada, T.; Sasaguri, Y. Switch of histamine receptor expression from H2 to H1 during differentiation of monocytes into macrophages. *Febs Lett.*, **2000**, 473, 345–348.
- [162] Lazar-Molnar, E.; Hegyesi, H.; Pallinger, E.; Kovacs, P.; Toth, S.; Fitzsimons, C.; Cricco, G.; Martin, G.; Bergoc, R.; Darvas, Z.; Rivera, ES.; Falus, A. Inhibition of human primary melanoma cell proliferation by histamine is enhanced by interleukin-6. *Eur. J. Clin. Invest.*, **2002**, 32, 743–749.
- [163] Szukiewicz, D.; Klimkiewicz, J.; Pyzlak, M.; Szewczyk, G.; Maslinska, D. Locally secreted histamine may regulate the development of ovarian follicles by apoptosis. *Inflamm. Res.*, **2007**, 56, S33–34.
- [164] Sander, LE.; Lorentz, A.; Sellge, G.; Coeffier, M.; Neipp, M.; Veres, T.; Frieling, T.; Meier, PN.; Manns, MP.; Bischoff, SC. Selective expression of histamine receptors H1R, H2R, and H4R, but not H3R, in the human intestinal tract. *Gut*, **2006**, 55, 498–504.
- [165] Medina, V.; Croci, M.; Crescenti, E.; Mohamad, N.; Sanchez-Jimenez, F.; Massari,

- N.; Nunez, M.; Cricco, G.; Martin, G.; Bergoc, R.; Rivera, E. The role of histamine in human mammary carcinogenesis - H3 and H4 receptors as potential therapeutic targets for breast cancer treatment. *Cancer Biol. Ther.*, **2008**, 7, 28–35.
- [166] Medina, VA.; Rivera, ES. Histamine receptors and cancer pharmacology. *Br. J. Pharmacol.*, **2010**, 161, 755–767.
- [167] Rimmer, SJ.; Church, MK. The pharmacology and mechanisms of action of histamine H1 antagonists. *Clin. Exp. Allergy*, **1990**, 20, 3–17.
- [168] Tickner, A. Inhibition of amine oxidase by antihistamine compounds and related drugs. *Br. J. Pharmacol.*, **1951**, 6, 606–610.
- [169] Sudo, K.; Monsma, FJ.; Katzenellenbogen, BS. Antiestrogen-binding sites distinct from the estrogen receptor - subcellular localization, ligand specificity, and distribution in tissues of the rat. *Endocrinology*, **1983**, 112, 425–434.
- [170] Nadalin, V.; Cotterchio, M.; Kreiger, N. Antihistamine use and breast cancer risk. *Int. J. Cancer*, **2003**, 106, 566–568.
- [171] American Society of Health-System Pharmacists (ASHP). Antihistamine drugs. *ASHP*, **2014**.
- [172] Handley, DA.; Magnetti, A.; Higgins, AJ. Therapeutic advantages of third generation antihistamines. *Expert Opin. Investig. Drugs*, **1998**, 7, 1045–1054.
- [173] Blaiss, MS. Allergic rhinitis and impairment issues in school children: a consensus report. *Curr. Med. Res. Opin.*, **2004**, 20, 1937–1952.
- [174] De Benedictis, FM.; De Benedictis, D.; Canonica, GW. New oral H1 antihistamines in children: facts and unmet needs. *Allergy*, **2008**, 63, 1395–1404.
- [175] Del Cuvillo, A.; Mullol, J.; Bartra, J.; Dávila, I.; Jáuregui, I.; Montoro, J.; Sastre, J.; Valero, AL. Comparative pharmacology of the H1 antihistamines. *J. Investig. Allergol. Clin. Immunol.*, **2006**, 16, 3–12.
- [176] Criado, PR.; Criado, RFJ.; Maruta, CW.; Machado, CD. Histamine, histamine receptors and antihistamines: new concepts. *An. Bras. Dermatol.*, **2010**, 85, 195–210.
- [177] Bartra, J.; Velero, AL.; Del Cuvillo, A.; Dávila, I.; Jáuregui, I.; Montoro, J.; Mullol, J.; Sastre, J. Interactions of the H1 antihistamines. *J. Allergy Clin. Immunol.*, **2006**, 16, 29–36.
- [178] Horak, F.; Stubner, UP. Comparative tolerability of second generation antihistamines. *Drug Saf.*, **1999**, 20, 385–401.

- [179] Repka-Ramirez, MS. New concepts of histamine receptors and actions. *Curr. Allergy Asthma Rep.*, **2003**, 3, 227–231.
- [180] Sicherer, SH. *Understanding and managing your child's food allergies*. **2006**, The Johns Hopkins University Press.
- [181] Brown, JF.; Chafee, KA.; Tepperman, BL. Role of mast cells, neutrophils and nitric oxide in endotoxin-induced damage to the neonatal rat colon. *Br. J. Pharmacol.*, **1998**, 123, 31–38.
- [182] Grant, SM.; Goa, KL.; Fitton, A.; Sorkin, EM. Ketotifen - a review of its pharmacodynamic and pharmacokinetic properties, and therapeutic use in asthma and allergic disorders. *Drugs*, **1990**, 40, 412–448.
- [183] Martin, U.; Baggiolini, M. Dissociation between the anti-anaphylactic and the anti-histaminic actions of ketotifen. *Naunyn-Schmiedebergs Arch. Pharmacol.*, **1981**, 316, 186–189.
- [184] Weller, K.; Maurer, M. Desloratadine inhibits human skin mast cell activation and histamine release. *J. Invest. Dermatol.*, **2009**, 129, 2723–2726.
- [185] Bakker, RA.; Schoonus, SBJ.; Smit, MJ.; Timmerman, H.; Leurs, R. Histamine H(1)-receptor activation of nuclear factor-kappa B: roles for G beta gamma- and G alpha(q/11)-subunits in constitutive and agonist-mediated signaling. *Mol. Pharmacol.*, **2001**, 60, 1133–1142.
- [186] McCarthy, BJ.; Rankin, K.; Il'yasova, D.; Erdal, S.; Vick, N.; Ali-Osman, F.; Bigner, DD.; Davis, F. Assessment of type of allergy and antihistamine use in the development of glioma. *Cancer Epidemiol. Biomarkers Prev.*, **2011**, 20, 370–378.
- [187] Hey, JA.; Affrime, M.; Cobert, B.; Kreutner, W.; Cuss, FM. Cardiovascular profile of loratadine. *Clin. Exp. Allergy*, **1999**, 29, 197–199.
- [188] Chen, CP.; Hanson, E.; Watson, JW.; Lee, JS. P-glycoprotein limits the brain penetration of nonsedating but not sedating H1-antagonists. *Drug Metab. Dispos.*, **2003**, 31, 312–318.
- [189] Hamelin, BA.; Bouayad, A.; Drolet, B.; Gravel, A.; Turgeon, J. *In vitro* characterization of cytochrome P450 2D6 inhibition by classic histamine H-1 receptor antagonists. *Drug Metab. Dispos.*, **1998**, 26, 536–539.
- [190] Simons, FER.; Silver, NA.; Gu, XC.; Simons, KJ. Clinical pharmacology of H-1 antihistamines in the skin. *J. Allergy Clin. Immunol.*, **2002**, 110, 777–783.
- [191] Kelly, JP.; Rosenberg, L.; Palmer, JR.; Rao, RS.; Strom, BL.; Stolley, PD.; Zauber,

- AG.; Shapiro, S. Risk of breast cancer according to use of antidepressants, phenothiazines, and antihistamines. *Am. J. Epidemiol.*, **1999**, 150, 861–868.
- [192] Selby, J V.; Friedman, GD.; Fireman, BH. Screening prescription drugs for possible carcinogenicity - eleven to fifteen years of follow-up. *Cancer Res.*, **1989**, 49, 5736–5747.
- [193] Weiss, SR.; McFarland, BH.; Burkhart, GA.; Ho, PTC. Cancer recurrences and second primary cancers after use of antihistamines or antidepressants. *Clin. Pharmacol. Ther.*, **1998**, 63, 594–599.
- [194] Scheurer, ME.; El-Zein, R.; Thompson, PA.; Aldape, KD.; Levin, VA.; Gilbert, MR.; Weinberg, JS.; Bondy, ML. Long-term anti-inflammatory and antihistamine medication use and adult glioma risk. *Cancer Epidemiol. Biomarkers Prev.*, **2008**, 17, 1277–1281.
- [195] Schlehofer, B.; Blettner, M.; Becker, N.; Martinsohn, C.; Wahrendorf, J. Medical risk-factors and the development of brain tumors. *Cancer*, **1992**, 69, 2541–2547.
- [196] Schlehofer, B.; Blettner, M.; Preston-Martin, S.; Niehoff, D.; Wahrendorf, J.; Arslan, A.; Ahlbom, A.; Choi, WN.; Giles, GG.; Howe, GR.; Little, J.; Menegoz, F.; Ryan, P. Role of medical history in brain tumour development. Results from the international adult brain tumour study. *Int. J. Cancer*, **1999**, 82, 155–160.
- [197] Sivak-Sears, NR.; Schwartzbaum, JA.; Miike, R.; Moghadassi, M.; Wrensch, M. Case-control study of use of nonsteroidal antiinflammatory drugs and glioblastoma multiforme. *Am. J. Epidemiol.*, **2004**, 159, 1131–1139.
- [198] Scheurer, ME.; Amirian, ES.; Davlin, SL.; Rice, T.; Wrensch, M.; Bondy, ML. Effects of antihistamine and anti-inflammatory medication use on risk of specific glioma histologies. *Int. J. Cancer*, **2011**, 129, 2290–2296.
- [199] Jangi, SM.; Diaz-Perez, JL.; Ochoa-Lizarralde, B.; Martin-Ruiz, I.; Asumendi, A.; Perez-Yarza, G.; Gardeazabal, J.; Diaz-Ramon, JL.; Boyano, MD. H1 histamine receptor antagonists induce genotoxic and caspase-2-dependent apoptosis in human melanoma cells. *Carcinogenesis*, **2006**, 27, 1787–1796.
- [200] Rajendra, S.; Mulcahy, H.; Patchett, S.; Kumar, P. The effect of H2 antagonists on proliferation and apoptosis in human colorectal cancer cell lines. *Dig. Dis. Sci.*, **2004**, 49, 1634–1640.
- [201] Aichberger, KJ.; Mayerhofer, M.; Vales, A.; Krauth, MT.; Gleixner, K V.; Bilban, M.; Esterbauer, H.; Sonneck, K.; Florian, S.; Derdak, S.; Pickl, WF.; Agis, H.;

- Falus, A.; Sillaber, C.; Valent, P. The CML-related oncoprotein BCR/ABL induces expression of histidine decarboxylase (HDC) and the synthesis of histamine in leukemic cells. *Blood*, **2006**, 108, 3538–3547.
- [202] Brandes, LJ.; Macdonald, LM. Evidence that the antiestrogen binding site is a histamine or histamine-like receptor. *Biochem. Biophys. Res. Commun.*, **1985**, 126, 905–910.
- [203] Brandes, LJ.; Warrington, RC.; Arron, RJ.; Bogdanovic, RP.; Fang, W.; Queen, GM.; Stein, DA.; Tong, JG.; Zaborniak, CLF.; Labella, FS. Enhanced cancer growth in mice administered daily human-equivalent doses of some H-1 antihistamines - predictive *in vitro* correlates. *J. Natl. Cancer Inst.*, **1994**, 86, 770–775.
- [204] Hadzijusufovic, E.; Peter, B.; Gleixner, K V.; Schuch, K.; Pickl, WF.; Thaiwong, T.; Yuzbasiyan-Gurkan, V.; Mirkina, I.; Willmann, M.; Valent, P. H1-receptor antagonists terfenadine and loratadine inhibit spontaneous growth of neoplastic mast cells. *Exp. Hematol.*, **2010**, 38, 896–907.
- [205] Siegers, CP.; Andresen, S.; Keogh, JP. Does cimetidine improve prospects for cancer patients? A reappraisal of the evidence to date. *Digestion*, **1999**, 60, 415–421.
- [206] Armitage, JO.; Sidner, RD. Anti-tumor effect of cimetidine. *Lancet*, **1979**, 1, 882–883.
- [207] Dexeus, FH.; Logothetis, CJ.; Sella, A.; Fitz, K.; Amato, R.; Reuben, JM.; Dozier, N. Phase-II study of coumarin and cimetidine in patients with metastatic renal cell carcinoma. *J. Clin. Oncol.*, **1990**, 8, 325–329.
- [208] Morton, RF.; Creagan, ET.; Cullinan, SA.; Mailliard, JA.; Ebbert, L.; Veeder, MH.; Chang, M. Phase-II studies of single-agent cimetidine and the combination N-phosphonacetyl-L-aspartate (NSC-224131) plus L-alanosine (NSC-153353) in advanced malignant melanoma. *J. Clin. Oncol.*, **1987**, 5, 1078–1082.
- [209] Lefranc, F.; Yeaton, P.; Brotchi, J.; Kiss, R. Cimetidine, an unexpected anti-tumor agent, and its potential for the treatment of glioblastoma. *Int. J. Oncol.*, **2006**, 28, 1021–1030.
- [210] Jiang, CG.; Liu, FR.; Yu, M.; Li, JB.; Xu, HM. Cimetidine induces apoptosis in gastric cancer cells *in vitro* and inhibits tumor growth *in vivo*. *Oncol. Rep.*, **2010**, 23, 693–700.

- [211] Takahashi, K.; Tanaka, S.; Ichikawa, A. Effect of cimetidine on intratumoral cytokine expression in an experimental tumor. *Biochem. Biophys. Res. Commun.*, **2001**, 281, 1113–1119.
- [212] Soule, BP.; Simone, NL.; DeGraff, WG.; Choudhuri, R.; Cook, JA.; Mitchell, JB. Loratadine dysregulates cell cycle progression and enhances the effect of radiation in human tumor cell lines. *Radiat. Oncol.*, **2010**, 5, 8.
- [213] Garcia-Quiroz, J.; Garcia-Becerra, R.; Barrera, D.; Santos, N.; Avila, E.; Ordaz-Rosado, D.; Rivas-Suarez, M.; Halhali, A.; Rodriguez, P.; Gamboa-Dominguez, A.; Medina-Franco, H.; Camacho, J.; Larrea, F.; Diaz, L. Astemizole synergizes calcitriol antiproliferative activity by inhibiting CYP24A1 and upregulating VDR: a novel approach for breast cancer therapy. *Plos One*, **2012**, 7,
- [214] Lin, JC.; Ho, YS.; Lee, JJ.; Liu, CL.; Yang, TL.; Wu, CH. Induction of apoptosis and cell-cycle arrest in human colon cancer cells by meclizine. *Food Chem. Toxicol.*, **2007**, 45, 935–944.
- [215] GomezFabre, PM.; dePedro, E.; Medina, MA.; Decastro, IN.; Marquez, J. Polyamine contents of human breast cancer cells treated with the cytotoxic agents chlorpheniramine and dehydroidemnin B. *Cancer Lett.*, **1997**, 113, 141–144.
- [216] Nicolau-Galmes, F.; Asumendi, A.; Alonso-Tejerina, E.; Perez-Yarza, G.; Jangi, SM.; Gardezabal, J.; Arroyo-Berdugo, Y.; Careaga, JM.; Diaz-Ramon, JL.; Apraiz, A.; Boyano, MD. Terfenadine induces apoptosis and autophagy in melanoma cells through ROS-dependent and -independent mechanisms. *Apoptosis*, **2011**, 16, 1253–1267.
- [217] Jangi, SM.; Ruiz-Larrea, MB.; Nicolau-Galmes, F.; Andollo, N.; Arroyo-Berdugo, Y.; Ortega-Martinez, I.; Diaz-Perez, JL.; Boyano, MD. Terfenadine-induced apoptosis in human melanoma cells is mediated through Ca²⁺ homeostasis modulation and tyrosine kinase activity, independently of H1 histamine receptors. *Carcinogenesis*, **2008**, 29, 500–509.
- [218] Paoluzzi, L.; Scotto, L.; Marchi, E.; Seshan, VE.; O'Connor, OA. The anti-histaminic cyproheptadine synergizes the antineoplastic activity of bortezomib in mantle cell lymphoma through its effects as a histone deacetylase inhibitor. *Br. J. Haematol.*, **2009**, 146, 656–659.
- [219] Meng, FY.; Han, YY.; Staloch, D.; Francis, T.; Stokes, A.; Francis, H. The H4 histamine receptor agonist, clobenpropit, suppresses human cholangiocarcinoma

- progression by disruption of epithelial mesenchymal transition and tumor metastasis. *Hepatology*, **2011**, 54, 1718–1728.
- [220] Finlay, IG.; Dwerryhouse, SJ.; King, J.; King, DW.; Lubowski, DZ.; Morris, DL. The effect of a short preoperative course of cimetidine on the grade of TIL in primary colorectal cancer - a randomised controlled clinical trial. *Gi Cancer*, **1999**, 3, 121–127.
- [221] Svendsen, LB.; Ross, C.; Knigge, U.; Frederiksen, HJ.; Graversen, P.; Kjaergard, J.; Luke, M.; Stimpel, H.; Sparso, BH. Cimetidine as an adjuvant treatment in colorectal cancer. A double-blind, randomized pilot study. *Dis. Colon Rectum*, **1995**, 38, 514–518.
- [222] Nielsen, HJ.; Christensen, IJ.; Moesgaard, F.; Kehlet, H. Ranitidine as adjuvant treatment in colorectal cancer. *Br. J. Surg.*, **2002**, 89, 1416–1422.
- [223] Enomoto, U.; Kusakabe, H.; Matsumura, T.; Kuno, T.; Tamai, H.; Kiyokane, K. Diffuse cutaneous mastocytosis responding to cyproheptadine. *Clin. Exp. Dermatol.*, **1999**, 24, 16–18.
- [224] Siebenhaar, F.; Fortsch, A.; Krause, K.; Weller, K.; Metz, M.; Magerl, M.; Martus, P.; Church, MK.; Maurer, M. Rupatadine improves quality of life in mastocytosis: a randomized, double-blind, placebo-controlled trial. *Allergy*, **2013**, 68, 949–952.
- [225] Laus, F.; Cerquetella, M.; Paggi, E.; Ippedico, G.; Argentieri, M.; Castellano, G.; Spaterna, A.; Tesei, B. Evaluation of cimetidine as a therapy for dermal melanomatosis in grey horse. *Isr. J. Vet. Med.*, **2010**, 65, 48–52.
- [226] Nee, J.; Ohiggins, N.; Osborne, DH.; Purdy, S. The role of histamine antagonists on the development of experimental cancer in the rat. *Ir. J. Med. Sci.*, **1984**, 153, 332–335.
- [227] Barkla, DH.; Tutton, PJM. Cytotoxicity of cyproheptadine and methysergide to chemically-induced carcinomas of rat colon. *Br. J. Cancer*, **1977**, 36, 814–817.
- [228] Kikuchi, Y.; Oomori, K.; Kizawa, I.; Kato, K. Effects of cimetidine on tumor growth and immune function in nude mice bearing human ovarian carcinoma. *J. Natl. Cancer Inst.*, **1985**, 74, 495–498.
- [229] Burtin, C.; Scheinmann, P.; Salomon, JC.; Lespinats, G.; Canu, P. Decrease in tumor growth by injections of histamine or serotonin in fibrosarcoma-bearing mice: influence of H1 and H2 histamine receptors. *Br. J. Cancer*, **1982**, 45, 54–60.
- [230] Szincsak, N.; Hegyesi, H.; Hunyadi, J.; Falus, A.; Juhasz, I. Different H2 receptor

- antihistamines dissimilarly retard the growth of xenografted human melanoma cells in immunodeficient mice. *Cell Biol. Int.*, **2002**, 26, 833–836.
- [231] Watson, SA.; Wilkinson, LJ.; Robertson, JFR.; Hardcastle, JD. Effect of histamine on the growth of human gastrointestinal tumors - reversal by cimetidine. *Gut*, **1993**, 34, 1091–1096.
- [232] Mao, XL.; Liang, SB.; Hurren, R.; Gronda, M.; Chow, S.; Xu, GW.; Wang, XM.; Zavareh, RB.; Jamal, N.; Messner, H.; Hedley, DW.; Datti, A.; Wrana, JL.; Zhu, YX.; Shi, CX.; Lee, KL.; Tiedemann, R.; Trudel, S.; Stewart, AK.; Schimmer, AD. Cyproheptadine displays preclinical activity in myeloma and leukemia. *Blood*, **2008**, 112, 760–769.
- [233] Urdiales, JL.; Mates, JM.; Decastro, IN.; Sanchezjimenez, FM. Chlorpheniramine inhibits the ornithine decarboxylase induction of ehrlich carcinoma growing *in vivo*. *Febs Lett.*, **1992**, 305, 260–264.

CHAPTER 4

ULTRASONOGRAPHY AS THE GOLD STANDARD FOR *IN VIVO* VOLUMETRIC DETERMINATION OF CHEMICALLY-INDUCED MAMMARY TUMORS

THE CONTENT OF THIS CHAPTER WAS PUBLISHED IN:

Faustino-Rocha AI, Gama A, Oliveira PA, Alvarado A, Fidalgo-Gonçalves L, Ferreira R, Ginja M. 2016. Ultrasonography as the gold standard for *in vivo* volumetric determination of chemically-induced mammary tumor. *In vivo* 30:465-472. (Full paper)

Faustino-Rocha AI, Gama A, Oliveira PA, Alvarado A, Fidalgo-Gonçalves L, Ferreira R, Ginja M. 2015. Dimensions, volume and weight of invasive and non-invasive MNU-induced mammary tumors. *Revista Portuguesa de Ciências Veterinárias*. (Accepted for publication, Abstract)

Faustino-Rocha AI, Gama A, Oliveira PA, Alvarado A, Fidalgo-Gonçalves L, Ferreira R, Ginja M. 2015. Dimensions, volume and weight of invasive and non-invasive MNU-induced mammary tumors. XX Congresso da Sociedade Portuguesa de Patologia Animal. 17th to 18th April, Lisbon, Portugal. (Poster presentation)

4. Ultrasonography as the gold standard for *in vivo* volumetric determination of chemically-induced mammary tumors

Abstract

In this study, we evaluated the dimensions and volume of rat mammary tumors and the association of these variables with tumor invasiveness. Tumors were measured by caliper and ultrasonography. Volume was determined by water displacement and by application of four formulas using tumor length (L), width (W) and depth (D) or tumor weight. Results confirmed the data obtained in our previous work, where we verified that mammary tumors grow as oblate spheroids. Determination of mammary tumor volume by applying the formula $V = \left(\frac{4}{3}\right) \times \pi \times \left(\frac{L}{2}\right) \times \left(\frac{L}{2}\right) \times \left(\frac{D}{2}\right)$ is the best way to evaluate tumor volume *in vivo*. Beyond volume evaluation by water displacement, the determination on the basis of tumor weight is the most accurate way to evaluate tumor volume after animal sacrifice or tumor excision. According to our results, it is not possible to predict if a tumor is invasive or non-invasive by its dimensions, volume or weight. Future work in chemically-induced mammary cancer should use ultrasonography and water displacement or tumor weight to determine tumor volume *in vivo* and after animal sacrifice or tumor excision, respectively.

Keywords: mammary tumors, MNU, ultrasonography, volume, water displacement

4.1. Introduction

Breast is the most common site of cancer development in women [1]. In 2012, breast cancer was responsible for about 521,000 deaths around the world, representing one of the leading causes of death by cancer worldwide [2].

Breast cancer prognosis is based on specific factors, namely on the involvement of axillary lymph nodes and on tumor potential for growth [1]. In 1971, Lala reported that tumor growth is the best parameter for obtaining information about the cell population and the effects of different therapeutic approaches on tumors [3]. Some years later, in 1979, tumor dimension was established by the World Health Organization (WHO) as one of the criteria for grading mammary tumors [4]. Since then, several reports stated that

tumor measurement has an important value in planning and monitoring treatment strategies in patients with cancer [5,6]. In an initial stage of the disease, tumor size is important in choosing the most adequate therapy for each patient [7]; it is an important factor to determine whether a woman is or is not a suitable candidate for a specific modality of treatment, such as surgery (partial resection or mastectomy) or chemotherapy [8]. During treatment, tumor dimensions are important for evaluating if the selected therapy is having the desired effects [7]; a reduction of tumor size (tumor shrinkage) during a treatment suggests that tumor is vulnerable to it [9]. Tumor-growth monitoring is also essential in experimental assays using animal models of different types of cancer for development and evaluation of novel anticancer therapies [10].

Animal models have been widely used in biomedical sciences; they are the intermediate step between *in vitro* cell culture and clinical assays in humans [11]. When compared with *in vitro* cell cultures, animal models provide a three dimensional (3D) view and a realistic microenvironment where it is possible to study tumor growth and its response to therapy [12]. Rodents have an important role on breast cancer study due to the biological similarities of breast cancer in this specie with that in women, namely epithelial origin and hormonal dependence [13]. The model of chemically-induced mammary cancer in Sprague-Dawley female rats by the carcinogenic agent *N*-methyl-*N*-nitrosourea (MNU) is a well-known model for studying this type of cancer [14].

Taking into account the great importance of tumor size measurement, this study intended to verify the shape of chemically-induced mammary tumors in a rat model and correlate it with tumor dimensions, and to compare tumor volume calculated by different formulas with tumor volume as assessed by water displacement. We also aimed to assess the differences in dimensions, volume and weight between invasive and non-invasive mammary tumors.

4.2. Material and Methods

4.2.1. Animals

Thirty-four outbred female Sprague-Dawley rats (*Rattus norvegicus*) of four weeks of age were obtained from Harlan Laboratories Inc. (Barcelona, Spain). Animals were housed in filter capped polycarbonate cages (1500U Eurostandard Type IV S, Tecniplast,

Buguggiate, Italy), using corncob for bedding (Mucedola, Settimo Milanese, Milan, Italy). Cages were kept at the animal facilities of the University of Trás-os-Montes and Alto Douro (UTAD) in a ventilated room with controlled conditions of temperature ($23\pm 2^{\circ}\text{C}$), relative humidity ($50\pm 10\%$), air system filtration (10-20 ventilations/hour) and light:dark cycle (12h:12h). During the experimental protocol, animals had *ad libitum* access to a basic standard diet (4RF21[®], Mucedola, Settimo Milanese, Milan, Italy) and tap water.

4.2.2. Chemicals

The carcinogenic agent MNU (ISOPAC[®]) was purchased from Sigma Aldrich S.A. (Madrid, Spain) and stored according to the manufacturer's instructions.

4.2.3. Animal experiments

Before the beginning of the experimental protocol, animals were submitted to a period of quarantine for one week. After this, we allowed the animals to acclimate to laboratory conditions for two weeks. Then we divided them into five experimental groups: MNU (n=10), MNU + ketotifen-1 (n=10), MNU + ketotifen-2 (n=10), ketotifen (n=2) and control (n=2). However, only two experimental groups (MNU and control) were considered and will be described in the present study. At seven weeks of age with a mean body weight of 184.99 ± 2.95 g, animals from MNU-treated group received a single intraperitoneal injection of MNU at a concentration of 50 mg/kg of body weight. MNU was dissolved in 0.9% saline solution to a concentration of 11 mg/ml and was used within one hour after its preparation. Animals from control group were used as negative control and were not exposed to MNU, they received a single administration of the vehicle (saline solution 0.9%). The MNU administration defined the beginning of the experimental protocol (day zero of the protocol).

Animals were monitored twice a day to check their general health status. Animal body weight was weekly recorded; final body weight was obtained by the subtraction of tumor weight from total body weight. At the end of the experimental protocol (18 weeks after MNU administration), body weight gain was calculated applying the formula previously used by Faustino-Rocha and collaborators [15].

All animal procedures were carried out in accordance with national (Decree-Law 113/2013) and European legislation (European Directive 2010/63/EU) on the protection of animals used for scientific purposes. The experimental protocol was approved by the Ethics Committee of the UTAD (approval CE_12-2013) and by the Portuguese Ethics Committee for Animal Experimentation (approval no. 008961).

4.2.4. Mammary tumor evaluation

After MNU administration, animals were weekly palpated for the detection of mammary tumor development; the time of appearance of the first mammary tumor was recorded. Before animals' sacrifice, the length (longitudinal axis) and width (transversal axis) of mammary tumors identified by palpation were measured by one researcher using a vernier caliper (Vito, Central Lobão S.A., Santa Maria da Feira, Portugal); these measurements were defined as clinical measurements. Tumor volume (V) using these measurements was calculated according to the following formula [16]:

$$V = \frac{W^2 \times L}{2} \text{ (Formula 1),}$$

where W is tumor width and L is tumor length.

Eighteen weeks after MNU administration, all survived animals were anesthetized by intraperitoneal injection of ketamine (75 mg/kg of body weight, Imalgene[®] 1000, Merial S.A.S., Lyon, France) and xylazine (10 mg/kg of body weight, Rompun[®] 2%, Bayer Healthcare S.A., Kiel, Germany). Mammary tumors were evaluated by ultrasonography by two experienced examiners. For ultrasonographic examination, animals were placed in supine position. The skin overlying each mammary tumor was shaved using a machine clipper (Aesculap GT420 Isis, Aesculap Inc., Center Valley, PA, USA) and acoustic gel was applied (Aquasonic, Parker Laboratories Inc., Fairfield, NJ, USA) on mammary tumors. Ultrasonographic evaluation was performed with B mode ultrasound using a real-time Logiq P6[®] scanner (General Electric Healthcare, Milwaukee, WI, USA) with a 10 MHz linear transducer. A standoff pad (Sonokit, MIUS Ltd., Gloucestershire, UK) made of extremely soft polyvinylchloride especially created for skin-contact sonography was used. We used light pressure when scanning the mammary tumors to avoid distorting their shape. During the ultrasonographic examination, sagittal and transverse views of each

mammary tumor were obtained; the probe was rotated until the largest diameter of each view was obtained. Ultrasonographic examinations were recorded in video format. After ultrasonography, the diameter of sagittal (tumor length) and transverse (tumor width) views, and depth of each mammary tumor were measured by one researcher in a frozen image using the integral calipers of the ultrasound apparatus; cursors were set at the borders of the tumor. Tumor volume using these measurements was calculated according to the following formulas [15]:

$$V = \left(\frac{4}{3}\right) \times \pi \times \left(\frac{L}{2}\right) \times \left(\frac{L}{2}\right) \times \left(\frac{D}{2}\right) \text{ (Formula 2),}$$

$$V = \left(\frac{1}{2}\right) \times L \times W \times D \text{ (Formula 3),}$$

where L is the length, W is the width and D is the depth of the tumor.

4.2.5. Animal sacrifice and necropsy

After ultrasonographic examination, anesthetized animals were sacrificed by exsanguination by cardiac puncture as indicated by the Federation of European Laboratory Animal Science Associations [17]. All animals were skinned (all skin was removed) and the skin was carefully observed under a light in order to detect mammary tumors. All mammary tumors were excised and three measurements of each mammary tumor (length, width and depth) were made using a vernier caliper (Vito, Central Lobão S.A.) by one researcher; these measurements were defined as anatomopathological measurements. The volume of mammary tumors was calculated using these measurements according to formulas one and three presented above. Then, mammary tumors were weighed in a top-loading scale (Mettler PM4000, LabWrench, Midland, ON, Canada) and their volume was calculated using the following formula:

$$V = \frac{\textit{Tumor weight}}{1.056} \text{ (Formula 4),}$$

considering tumor density to be similar to that of soft tissue (1.056 g/cm³) [18]. Mammary tumor volume was also determined by water displacement by immersing each tumor in a beaker with saline solution; this volume was defined as the true tumor volume.

Immediately after this procedure, mammary tumors were immersed in phosphate-buffered formaldehyde for 24 hours.

4.2.6. Histology

After fixation, mammary tumors were cut, embedded in paraffin and two μm -thick sections were routinely stained with hematoxylin and eosin (H&E). Histological slides were observed blindly under light microscopy by an experienced pathologist. Mammary tumors were classified according to the classification previously established by Russo and Russo [19]. Each mammary tumor was classified according to the histological pattern with higher proportion in each tumor section.

4.2.7. Data analysis

A descriptive analysis was performed for all variables included in the study. Data were statistically analyzed using Statistical Package for the Social Sciences (SPSS[®] version 23 for Windows, SPSS Inc., IL, USA). Continuous data are expressed as mean \pm standard deviation (S.D.) or mean \pm standard error (S.E.). Independent sample *t*-test was used to compare mean initial and final body weight, and body weight gain between the two groups of rats; and to compare true volume and tumor weight between invasive and non-invasive mammary tumors. Mean initial and final body weight in each group were compared using paired *t*-test. Analysis of variance (ANOVA) with the Bonferroni correction was used to assess the differences in tumor length, width and depth measured using a vernier caliper (clinical and anatomopathological measurements) and by ultrasonography (ultrasonographic measurements); and to compare tumor volume calculated by different formulas. Mean values were considered to be statistically significant when $p < 0.05$. Using Matlab[®] (version 7.12.0.635, The MathWorks Inc., MA, USA), two 3D models of mammary tumors using tumor length, width and depth measured by ultrasonography and by caliper at anatomopathological analysis were created.

4.3. Results

4.3.1. General observations

All animals exhibited a normal health status during the experimental protocol. In both groups, mean initial body weight was statistically different from mean final body weight ($p < 0.05$). The mean initial and final body weight and the body weight gain were similar between MNU and control groups ($p > 0.05$) (Table 4.1).

Table 4.1. Initial and final body weight (g) and body weight gain (%) in animals from both MNU-treated and control groups (mean \pm S.E.).

Group	Body weight		
	Initial (g)	Final (g)	Gain (%)
MNU (n=6)	188.27 \pm 3.78 ^a	304.78 \pm 8.54	38.10 \pm 1.27
Control (n=2)	183.82 \pm 2.84 ^a	295.98 \pm 9.78	37.86 \pm 1.10

^a Statistically different from final body weight ($p < 0.05$).

4.3.2. Mammary tumors number and histological evaluation

At the end of the experimental protocol, 22 masses were palpated in six animals from MNU-treated group (only animals from MNU group that developed mammary tumors were considered in the present study, the group was reduced to six animals). None of the animals from control group developed any mass.

The first mass that was subsequently classified as a mammary tumor by histopathology was palpated in the eighth week of the experimental protocol (Figure 4.1 and 4.2A). At histopathological analysis, we verified that one of the palpated masses was not a mammary tumor, it was histologically classified as a reactive lymph node; this mass was excluded from the study (Table 4.2). Therefore, at the end of the protocol, a total of 21 mammary tumors were counted in six out of ten animals from MNU-treated group (incidence of 60%; mean number of approximately 3.5 mammary tumors *per* animal) (Figure 4.1). Of these tumors, one was classified as a benign lesion (fibroadenoma) and

the remaining were classified as malignant lesions, papillary non-invasive carcinoma being that most frequently identified (Table 4.2).

Table 4.2. Histological classification of mammary tumors identified in animals from MNU-treated group according to the classification established by Russo and Russo [19].

Histological classification		Number of lesions
Benign lesion	Fibroadenoma	1
Malignant lesions	Papillary non-invasive carcinoma	12
	Cribriform non-invasive carcinoma	1
	Papillary invasive carcinoma	3
	Cribriform invasive carcinoma	3
	Comedo carcinoma	1
Total		21

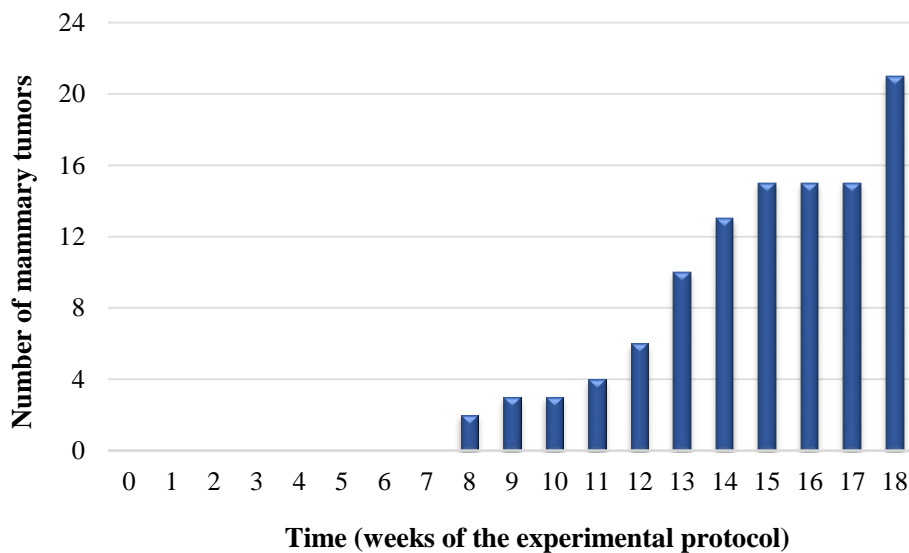


Figure 4.1. Number of mammary tumors in animals from MNU-treated group (n=6) during the experimental protocol; the first mammary tumors was identified by palpation at week eight of the protocol.

4.3.3. Tumor dimension

From the 21 mammary tumors, data were only collected from caliper (clinical and anatomopathological) and ultrasonography in 13 tumors. Although at anatomopathological analysis all tumors were measured using a caliper, not all were previously evaluated by clinical or ultrasonographic analysis. Due to their small size (tumors smaller than 0.5 cm in diameter), some mammary tumors were not identified during clinical palpation and consequently they were not evaluated by ultrasonography; or because of their size exceeded 4 cm we were unable to measure them owing to the size of our probe. The tumors that were not identified by palpation during the experimental protocol due their small size were identified during the observation of the skin under a light after sacrifice.

Looking at the data from these 13 mammary tumors, we verified that the measurement of the length, width and depth was similar using the different methods of measurement employed in this experimental protocol (clinical, ultrasonographic and anatomopathological) ($p>0.05$) (Table 4.3).

In all methods of measurement, we verified that tumor length and width were similar ($p>0.05$). In ultrasonographic and anatomopathological measurements, we also observed that tumor length and width were greater than tumor depth ($p<0.05$) (Table 4.3). These data suggest that mammary tumors grown as oblate spheroids (Figure 4.2B and C).

Table 4.3. Measurement of length, width and depth by caliper (before and after necropsy) and ultrasonography in 13 mammary tumors identified in animals from group MNU (mean \pm S.D.).

Measurement (cm)	Measurement method		
	Clinical	Ultrasonographic	Anatomopathological
Length	2.29 \pm 0.66 ^{a,b}	2.05 \pm 0.75 ^{a,b}	2.12 \pm 0.67 ^{a,b}
Width	1.79 \pm 0.67 ^b	1.98 \pm 0.51 ^{a,b}	1.94 \pm 0.63 ^{a,b}
Depth	-	1.08 \pm 0.43	0.97 \pm 0.33

^a Statistically different from ultrasonographic depth ($p<0.05$); ^b Statistically different from anatomopathological depth ($p<0.05$).

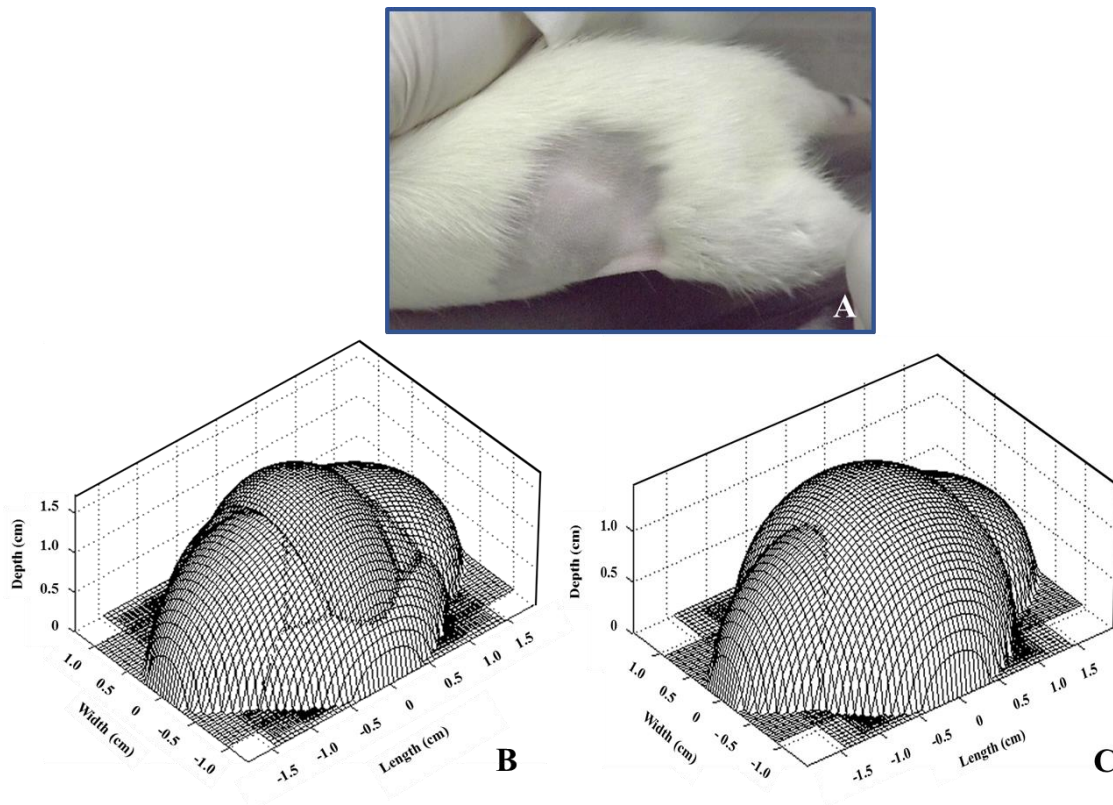


Figure 4.2. Mammary tumor in an animal from MNU-treated group (A). 3D model of mammary tumor as measured by ultrasonography (B). 3D model of mammary tumor as measured by caliper at anatomopathological analysis (C).

4.3.4. Tumor volume and weight

Tumor volume was determined by water displacement and using different formulas previously published by us and by other researchers. In the statistical analysis, we found no statistically significant differences among tumor volume when calculated by different methods ($p > 0.05$) (Table 4.4). However, we verified that the mean tumor volume determined by water displacement, considered as the true volume, was more similar to the tumor volume calculated using formula 2 and formula 4 when compared with that calculated using formulas 1 and 3 (Table 4.4). We also observed that the true tumor volume and tumor volume calculated using formulas 2 and 4 was very similar to tumor weight ($p > 0.05$) (Table 4.4).

Table 4.4. Volume and weight of 13 mammary tumors calculated using different formulas (mean \pm S.D.).

		Mean \pm S.D. (cm ³)	Range (cm ³)
Formula 1	Clinical	4.66 \pm 3.37	0.27-10.48
	Anatomopathological	4.66 \pm 3.23	0.45-11.57
Formula 2	Ultrasonographic	3.40 \pm 3.16	0.23-10.87
Formula 3	Ultrasonographic	2.61 \pm 1.93	0.20-5.65
	Anatomopathological	2.35 \pm 1.74	0.21-5.89
Formula 4		3.49 \pm 2.29	0.40-7.20
True volume		3.63 \pm 2.37	0.50-7.50
Tumor weight (g)		3.68 \pm 2.42	0.38-7.58

Statistically significant differences were not found ($p>0.05$).

4.3.5. Invasive and non-invasive mammary tumors

At the end of the experimental protocol, five invasive and eight non-invasive mammary tumors were compared (Table 4.5). We verified that the length, width and depth of mammary tumors measured by caliper or ultrasonography were similar between invasive and non-invasive mammary tumors ($p>0.05$). Although the differences did not reach the level of statistical significance, we noted that tumor length was slightly greater in non-invasive tumors when compared with the invasive ones ($p>0.05$). We observed the converse for tumor width and depth, where these measurements were higher in invasive tumors than in non-invasive ones ($p>0.05$) (Table 4.5).

Although the mean true tumor volume and tumor weight were slightly higher in non-invasive when compared with invasive mammary tumors, we verified that there were no statistically significant differences between invasive and non-invasive tumors ($p>0.05$) (Table 4.5).

Table 4.5. Comparison of tumor length, width, depth, volume and weight between invasive and non-invasive mammary tumors (mean \pm S.D.).

		Mammary tumors	
		Invasive (n=5)	Non-invasive (n=8)
Length (cm)	Clinical	2.12 \pm 0.41	2.41 \pm 0.81
	Ultrasonographic	1.93 \pm 0.63	2.13 \pm 0.86
	Anatomopathological	1.89 \pm 0.28	2.29 \pm 0.84
Width (cm)	Clinical	1.84 \pm 0.47	1.76 \pm 0.81
	Ultrasonographic	2.01 \pm 0.53	1.96 \pm 0.53
	Anatomopathological	2.07 \pm 0.45	1.84 \pm 0.75
Depth (cm)	Ultrasonographic	1.17 \pm 0.40	1.01 \pm 0.46
	Anatomopathological	1.06 \pm 0.16	0.91 \pm 0.41
True volume (cm³)		3.50 \pm 1.70	3.71 \pm 2.88
Weight (g)		3.56 \pm 1.67	3.76 \pm 2.97

Statistically significant differences were not found ($p > 0.05$).

4.4. Discussion

The accurate and efficient determination of tumor size in experimental protocols using animal models of several types of cancer, namely prostate, skin, mammary and liver, will determine the success of the experiment [20]. Tumor size is also frequently used as an endpoint in experimental protocols aiming to evaluate the efficacy of anticancer drugs [21]. Tumor size may be assessed by different modalities, namely physical examination (measurement with a caliper or a ruler), by mammography, ultrasonography and magnetic resonance. According to Pain and collaborators, the three most used methods of diagnosis (physical examination, mammography and ultrasound) had a similar accuracy for predicting the pathological size [22].

In our study, the mean initial and final body weight were similar between groups; since the animals from MNU-treated group developed mammary tumors, it was expected a lower final body weight in this group. This difference was not observed probably because

the experimental protocol may not have been long enough and animals that developed mammary tumors did not develop cachexia associated with carcinogenesis. These results are in accordance with those observed in a previous protocol of chemically-induced mammary carcinogenesis in female rats performed by our research team [15].

The first mammary tumor was detected eight weeks after MNU injection; in our previous protocol of mammary carcinogenesis [15] where we used the same carcinogen at same dose, in animals of the same strain and age, we detected the first mammary tumor later, at ten weeks after MNU administration. Conversely to our previous study, where all animals exposed to the carcinogen developed mammary tumors, in this protocol, only six animals MNU-exposed developed mammary tumors. At 18 weeks after MNU administration, we counted a total of 21 mammary tumors in six out of ten animals (incidence of 60%; mean number of approximately 3.5 mammary tumors *per* animal); in our previous study, at the same time point, we only observed a total of five mammary tumors in five out of 11 animals (incidence of 45%; mean number of 1.0 mammary tumor *per* animal). Since we used outbred animals, differences in results may be related to the individual differences among animals that were used. As expected and similarly to what was observed in the last experimental protocol of mammary cancer performed by our research team, we did not detect any mass in animals from control group. Contrary to what we would expect when working with the same animal model more than once, the results will always be different among protocols; hence we should be aware that we are working with living experimental animals and not mathematics, and there are many biological factors that may influence the results.

Similarly to what was described by Russo and Russo [19] and in accordance with that previously observed by us [15], it was observed that the number of malignant mammary tumors was higher than the number of the benign ones; of these, the papillary non-invasive carcinoma was the most frequently identified lesion.

Tumor dimensions (length, width and depth) were measured by only one researcher to avoid inter-observer variations. It was previously described that measurements made by more than one person may lead to different results [23]. During the ultrasonographic evaluation, the probe, and consequently the beam, was maintained perpendicular to the skin surface to avoid artifacts and minimize variations in pressure of the transducer which might modify tumor dimensions, especially the depth [24]. We verified that tumor length,

width and depth were similar among the methods employed (caliper before and after animal sacrifice, and ultrasonography). We also observed that the tumor length was similar to tumor width and greater than tumor depth. Taking these data into account, we may state that mammary tumors grown as a circular surface with small depth, resembling the shape of an oblate spheroid, where the length and width are similar and greater than the depth. These data are in accordance with those obtained in our previous study [15]. We suppose that this shape of development of mammary tumors in rats is due to the fact that these animals do not have a developed mammary gland and their skin is thin, with a low quantity of fat, conversely to that in women.

Tumor volume was determined by water displacement similarly to that previously performed by Tomayko and collaborators [25], and using different formulas. Water displacement is a more direct method of volume measurement, but it is difficult to perform when the volume of the tumors is smaller than 0.5 cm^3 [26]. In this work, we used formulas 1 and 2, which according to our previous work [15], are the best formulas for determining tumor volume using two tumor dimensions measured by caliper (length and width) and ultrasonography (length and depth), respectively. We had also used formula 4 to determine tumor volume on the basis of tumor weight. Additionally to our previous work, and in accordance with other investigators [27], which have stated that using the three measurements (length, width and depth) is the most accurate way to determine tumor volume, in this study, we also calculated tumor volume using these three dimensions as obtained by ultrasonography and by using a caliper (anatomopathological measurement). For this, we used formula 3, which was previously used by Tomayko and Reynolds [25] to determine the volume of subcutaneous tumors in a xenograft mouse model. Looking at our results, we may conclude that formula 2 previously developed by us and formula 4 are the most accurate for assessing tumor volume. According to our results, formula 1 overestimates tumor volume, whereas formula 3 underestimates it.

In this work, we also compared tumor dimensions, real volume and weight between invasive and non-invasive mammary tumors, finding no statistically significant differences.

4.5. Conclusion

The results of this work confirm the data obtained in our previous work, where we verified that MNU-induced mammary tumors in female rats grown as oblate spheroids [15]. We may conclude that the determination of mammary tumors volume by the application of formula 2 using two ultrasonographic dimensions (length and depth) is the best way to evaluate tumor dimensions *in vivo*. Beyond the determination of tumor volume by water displacement, the determination of volume on the basis of tumor weight by the application of formula 4 is the best way to evaluate tumor volume after animal sacrifice or after tumor excision. According to our results, it is not possible to predict if a tumor is invasive or non-invasive based on its dimensions, volume or weight.

In future work of chemically-induced mammary cancer, we recommend the following methodology for assessing tumor volume: the use of ultrasonography to assess tumor volume *in vivo* by the application of formula 2; the use of water displacement or tumor weight by the application of formula 4 to determine tumor volume after animal sacrifice or tumor excision.

4.6. References

- [1] Verma, R.; Mathur, R.; Raikwar, R.; Kaushal, M.; Miishra, H.; Shukla, R.; Verma, S.; Bhattacharya, A.; Yashikar, V.; Ratnani, B. Comparison of clinical assessment, mammography and ultrasound in pre-operative estimation of primary breast cancer size: a practical approach. *Internet J. Surg.*, **2008**, 16, 12.
- [2] World Health Organization (WHO). Cancer - Fact sheet n° 297. *WHO*, **2015**.
- [3] Lala, PK. Studies on tumor cell population kinetics. In *Methods in cancer research* (Busch, H., ed), **1971**, pp. 3–95, Academic Press.
- [4] Allen-Auerbach, M.; Weber, WA. Measuring response with FDG-PET: methodological aspects. *Oncologist*, **2009**, 14, 369–377.
- [5] Chen, AM.; Meric-Bernstam, F.; Hunt, KK.; Thames, HD.; Outlaw, ED.; Strom, EA.; McNeese, MD.; Kuerer, HM.; Ross, MI.; Singletary, SE.; Ames, FC.; Feig, BW.; Sahin, AA.; Perkins, GH.; Babiera, G.; Hortobagyi, GN.; Buchholz, TA. Breast conservation after neoadjuvant chemotherapy - a prognostic index for clinical decision-making. *Cancer*, **2005**, 103, 689–695.

- [6] Buchholz, TA.; Tucker, SL.; Masullo, L.; Kuerer, HM.; Erwin, J.; Salas, J.; Frye, D.; Strom, EA.; McNeese, MD.; Perkins, G.; Katz, A.; Singletary, SE.; Hunt, KK.; Buzdar, AU.; Hortobagyi, GN. Predictors of local-regional recurrence after neoadjuvant chemotherapy and mastectomy without radiation. *J. Clin. Oncol.*, **2002**, 20, 17–23.
- [7] Chagpar, AB.; Middleton, LP.; Sahin, AA.; Dempsey, P.; Buzdar, AU.; Mirza, AN.; Ames, FC.; Babiera, G V.; Feig, BW.; Hunt, KK.; Kuerer, HM.; Meric-Bernstam, F.; Ross, MI.; Singletary, SE. Accuracy of physical examination, ultrasonography, and mammography in predicting residual pathologic tumor size in patients treated with neoadjuvant chemotherapy. *Ann. Surg.*, **2006**, 243, 257–264.
- [8] Bonadonna, G.; Veronesi, U.; Brambilla, C.; Ferrari, L.; Luini, A.; Greco, M.; Bartoli, C.; Deyoldi, GC.; Zucali, R.; Rilke, F.; Andreola, S.; Silvestrini, R.; Difronzo, G.; Valagussa, P. Primary chemotherapy to avoid mastectomy in tumors with diameters of three centimeters or more. *J. Natl. Cancer Inst.*, **1990**, 82, 1539–1545.
- [9] Zhao, BS.; Oxnard, GR.; Moskowitz, CS.; Kris, MG.; Pao, W.; Guo, PZ.; Rusch, VM.; Ladanyi, M.; Rizvi, NA.; Schwartz, LH. A pilot study of volume measurement as a method of tumor response evaluation to aid biomarker development. *Clin. Cancer Res.*, **2010**, 16, 4647–4653.
- [10] Saint-Hubert, MD.; Devos, E.; Ibrahim, A.; Debyser, Z.; Mortelmans, L.; Mottaghy, FM. Bioluminescence imaging of therapy response does not correlate with FDG-PET response in a mouse model of Burkitt lymphoma. *Am. J. Nucl. Med. Mol. Imaging*, **2012**, 2, 353–361.
- [11] Kamb, A. What’s wrong with our cancer models? *Nat. Rev. Drug Discov.*, **2005**, 4, 161–165.
- [12] Wirtzfeld, LA.; Graham, KC.; Groom, AC.; MacDonald, IC.; Chambers, AF.; Fenster, A.; Lacefield, JC. Volume measurement variability in three-dimensional high-frequency ultrasound images of murine liver metastases. *Phys. Med. Biol.*, **2006**, 51, 2367–2381.
- [13] Chan, MM.; Lu, X.; Merchant, FM.; Iglehart, JD.; Miron, PL. Gene expression profiling of NMU-induced rat mammary tumors: cross species comparison with

- human breast cancer. *Carcinogenesis*, **2005**, 26, 1343–1353.
- [14] Soares-Maia, R.; Faustino-Rocha, AI.; Teixeira-Guedes, CI.; Pinho-Oliveira, J.; Talhada, D.; Rema, A.; Faria, F.; Ginja, M.; Ferreira, R.; Gil da Costa, RM.; Oliveira, PA.; Lopes, C. MNU-Induced Rat mammary carcinomas: immunohistology and estrogen receptor expression. *J. Environ. Pathol. Toxicol. Oncol.*, **2013**, 32, 157–163.
- [15] Faustino-Rocha, A.; Oliveira, PA.; Pinho-Oliveira, J.; Teixeira-Guedes, C.; Soares-Maia, R.; Gil da Costa, R.; Colaco, B.; Pires, MJ.; Colaco, J.; Ferreira, R.; Ginja, M. Estimation of rat mammary tumor volume using caliper and ultrasonography measurements. *Lab. Anim. (NY)*, **2013**, 42, 217–224.
- [16] Bousquet, PF.; Brana, MF.; Conlon, D.; Fitzgerald, KM.; Perron, D.; Cocchiario, C.; Miller, R.; Moran, M.; George, J.; Qian, XD.; Keilhauer, G.; Romerdahl, CA. Preclinical evaluation of LU 79553 - a novel bis-naphthalimide with potent antitumor activity. *Cancer Res.*, **1995**, 55, 1176–1180.
- [17] Forbes, D.; Blom, H.; Kostomitsopoulos, N.; Moore, G.; Perretta, G. Euroguide: on the accommodation and care of animals used for experimental and other scientific purposes. *Federation of European Laboratory Animal Science Associations*, **2007**.
- [18] Clarys, JP.; Marfelljones, MJ. Soft tissue segmentation of the body and fractionation of the upper and lower limbs. *Ergonomics*, **1994**, 37, 217–229.
- [19] Russo, J.; Russo, IH. Atlas and histologic classification of tumors of the rat mammary gland. *J. Mammary Gland Biol. Neoplasia*, **2000**, 5, 187–200.
- [20] Liao, A-H.; LI, C-H.; Cheng, W-F.; Li, P-C. Non-invasive imaging of small-animal tumors: high-frequency ultrasound vs microPET. *Conf. Proc. IEEE Eng. Med. Biol. Soc.*, **2005**, pp. 5695–5698.
- [21] Girit, IC.; Jure-Kunkel, M.; McIntyre, KW. A structured light-based system for scanning subcutaneous tumors in laboratory animals. *Comp. Med.*, **2008**, 58, 264–270.
- [22] Pain, JA.; Ebbs, SR.; Hern, RPA.; Lowe, S.; Bradbeer, JW. Assessment of breast cancer size - a comparison of methods. *Eur. J. Surg. Oncol.*, **1992**, 18, 44–48.
- [23] Feldman, JP.; Goldwasser, R.; Mark, S.; Schwartz, J.; Orion, I. A mathematical model for tumor volume evaluation using two-dimensions. *J. Appl. Quant. Methods*, **2009**, 4, 455–462.

- [24] Erasmus, JJ.; Gladish, GW.; Broemeling, L.; Sabloff, BS.; Truong, MT.; Herbst, RS.; Munden, RF. Interobserver and intraobserver variability in measurement of non-small cell carcinoma lung lesions: implications for assessment of tumor response. *J. Clin. Oncol.*, **2003**, 21, 2574–2582.
- [25] Tomayko, MM.; Reynolds, CP. Determination of subcutaneous tumor size in athymic (nude) mice. *Cancer Chemother. Pharmacol.*, **1989**, 24, 148–154.
- [26] Gouletsou, PG.; Galatos, AD.; Leontides, LS. Comparison between ultrasonographic and caliper measurements of testicular volume in the dog. *Anim. Reprod. Sci.*, **2008**, 108, 1–12.
- [27] Carlsson, G.; Gullberg, B.; Hafstrom, L. Estimation of liver tumor volume using different formulas - an experimental study in rats. *J. Cancer Res. Clin. Oncol.*, **1983**, 105, 20–23.

CHAPTER 5

ULTRASONOGRAPHIC, THERMOGRAPHIC AND HISTOLOGIC EVALUATION OF MNU-INDUCED MAMMARY TUMORS IN FEMALE SPRAGUE-DAWLEY RATS

THE CONTENT OF THIS CHAPTER WAS PUBLISHED IN:

Faustino-Rocha AI, Silva A, Gabriel J, Teixeira-Guedes CI, Lopes C, Gil da Costa R, Gama A, Ferreira R, Oliveira PA, Ginja M. 2013. Ultrasonographic, thermographic and histologic evaluation of MNU-induced mammary tumors in female Sprague-Dawley rats. *Biomedicine & Pharmacotherapy* 67 (8): 771-776. DOI: 10.1016/j.biopha.2013.06.011. (Full paper)

Faustino-Rocha AI, Silva A, Gabriel J, Talhada D, Andrade A, Teixeira-Guedes CI, Gil da Costa RM, Ferreira R, Oliveira PA, Ginja M. 2014. A new approach to evaluate mammary tumours in female Sprague-Dawley rats: thermography. *Journal of Comparative Pathology* 150 (1): 108. DOI: 10.1016/j.jcpa.2013.11.135. (Abstract)

Faustino-Rocha AI, Oliveira PA, Talhada D, Gama A, Ginja M. 2013. Avaliação ultrassonográfica da vascularização dos tumores da mama quimicamente induzidos em ratos fêmea Sprague-Dawley. 7^{as} Jornadas de Biologia, 21st to 23rd November 2013, Vila Real, Portugal. (Oral presentation)

Faustino-Rocha AI, Silva A, Gabriel J, Talhada D, Andrade A, Teixeira-Guedes CI, Gil da Costa RM, Ferreira R, Oliveira PA, Ginja M. 2013. A new approach to evaluate mammary tumours in female Sprague-Dawley rats: thermography. 31st Meeting of the ESVP and Annual Meeting of ECVP, 4th to 7th September, London, United Kingdom. (Poster presentation)

5. Ultrasonographic, thermographic and histologic evaluation of MNU-induced mammary tumors in female Sprague-Dawley rats

Abstract

As the worldwide breast cancer burden increases, non-invasive tools, such as ultrasonography and thermography are being increasingly sought after. *N*-methyl-*N*-nitrosourea (MNU)-induced rat mammary tumors are important tools to investigate the usefulness of such imaging techniques. This study aimed to integrate both ultrasonographic and thermographic approaches to assess the vascularization and the superficial temperature of chemically-induced rat mammary tumors. Twenty-five female Sprague-Dawley rats were divided into two groups: group I (intraperitoneally administered with MNU) and group II (control group). Thirty-five weeks after administration of the carcinogen, mammary tumors were evaluated using Power Doppler (PDI), B Flow and Contrast-enhanced ultrasound (CEUS), thermography and histology analyses. Animals from group I showed an average of 2.55 mammary tumors *per* animal, mostly papillary and cribriform non-invasive carcinomas. B Flow detected higher counts of color pixels than PDI. CEUS analysis showed a centripetal enhancement order of contrast agent and clear margins. Maximum tumor temperature and thermal amplitude determined by thermography were significantly correlated with tumor volume and with color pixel density (CPD), determined by PDI. B Flow was more sensitive than PDI in detecting tumor vessels, but PDI correlates with thermographic data concerning superficial temperature and may reflect tumor angiogenesis.

Keywords: mammary tumors, rat, vascularization

5.1. Introduction

Breast cancer represents the most common malignancy in women in both developing and developed countries and is the primary cause of death among women worldwide [1]. In 2008, 1.4 million of women were diagnosed with breast cancer and almost 459,000 deaths were recorded [2].

Several animal models have been developed to study varied aspects of breast cancer [3]. Among these, the rat is a well-established model to study the pathogenesis, prevention

and treatment of this disease. The carcinogenic agent *N*-methyl-*N*-nitrosourea (MNU) was recognized in the 1970s as being capable to induce rat mammary tumors [4,5] and has become the most commonly used carcinogen in mammary cancer studies. MNU has the ability to induce multiple mammary carcinomas and early stage mammary lesions in susceptible strains with a single dose administration. Rat mammary carcinomas induced by this chemical carcinogen display many features of human breast cancer, such as histological progression, ovarian hormone dependence [6–8], local aggressiveness and ability to metastasize [9].

In breast cancer, as in other malignancies, angiogenesis plays a crucial role in facilitating tumor growth and metastasis, constituting a significant prognostic indicator [10]. Power Doppler (PDI), B Flow and Contrast-enhanced ultrasound (CEUS) techniques are used to evaluate tumor vascularization and growth. CEUS imaging using second-generation contrast medium and a low-mechanical index may overcome the limitation of the other ultrasonographic techniques, which detect only the fast blood flow of large vessels. Unfortunately, quantification methods for tumor angiogenesis have not yet been established in any rat model [10]. Magnetic resonance imaging (MRI) with dynamic contrast enhancement is the most common non-invasive imaging method for evaluating tumor angiogenesis in humans; however, it is not frequently used in animals [11–13].

Over the years, other imaging techniques have been developed to assess breast tumors in early stages of development; one of these techniques is infrared thermography [14]. In 1982, thermography was established as a non-invasive tool for breast cancer diagnosis by the Food and Drug Administration [15]. One of the first medical applications of thermography was in breast cancer evaluation. However, thermographic techniques study superficial temperature, thereby, providing an indirect measure of tumor vascularization, which may complement information obtained through ultrasonographic methods [16]. Consequently, the aims of this work were to study the vascularization of mammary tumors in a rat model by ultrasonography and to correlate those findings with their superficial temperature, assessed by thermography.

5.2. Material and Methods

5.2.1. Animals

Fifty outbred female Sprague-Dawley rats, four to five weeks-old were obtained from Harlan Laboratories Inc. (Barcelona, Spain), and housed in filter capped polycarbonate cages (1500U Eurostandard Type IV S, Tecniplast, Buguggiate, Italy), with corncob for bedding (Mucedola, Settimo Milanese, Milan, Italy). All cages were kept in a ventilated room with controlled temperature ($23\pm 2^{\circ}\text{C}$), relative humidity ($50\pm 10\%$), and air system filtration (10-20 ventilations/hour) and maintained on a 12h:12h light:dark cycle. Animals had free access to a basic standard laboratory diet (4RF21[®], Mucedola, Settimo Milanese, Milan, Italy), and acidified tap water was supplied through capped water bottles (ACBT0252, Tecniplast, Buguggiate, Italy) *ad libitum* throughout the study. The experimental protocol started after one week of quarantine and two weeks of acclimatization to the laboratory conditions. All the animal procedures were done in accordance with the European Directive 2010/63/EU on the protection of animals used for scientific purposes. The Portuguese Ethics Committee for Animal Experimentation approved all the experiments and procedures carried out on the animals (approval no. 008961).

5.2.2. Chemicals

MNU (ISOPAC[®]) was purchased from Sigma Aldrich S.A. (Madrid, Spain). Contrast agent (SonoVue[®]) was purchased from Bracco (Milan, Italy).

5.2.3. Animal experiments

The rats were randomly divided into four experimental groups: MNU sedentary (n=15), MNU exercised (n=15), control sedentary (n=10) and control exercised (n=10). However, only two experimental groups (MNU sedentary and control sedentary) were considered and will be described in the present study. MNU sedentary group was considered group I and control group was considered group II. Animals from group I received a single MNU intraperitoneal dose (50 mg/kg of body weight) at seven weeks of age; group II was used as negative control and was administered with the vehicle (0.9% saline). The animal's drinking water was changed once a week and the volume drunk was

recorded. Weekly food intake was also noted. All the rats were monitored throughout the experimental protocol for signs of distress or weight loss. Body weights were measured once a week, using a top-loading scale (Mettler PM4000, LabWrench, Midland, ON, Canada). Ponderal gain (PG) was calculated according to the formula [17]:

$$PG = \frac{W2 - W1}{W2} \times 100,$$

where W1 is the initial body weight and W2 the final body weight. At the end of the experimental protocol, mortality index (MI) was also calculated according to the formula:

$$MI = \frac{\text{Number of animals that died during the study}}{\text{Number of animals at the beginning of the study}} \times 100.$$

5.2.4. Mammary tumors

Animals were palpated weekly to detect mammary tumors. The time of appearance of the first tumor (latency period) was recorded. The total number of tumors and the number of tumors/rat was also calculated on a weekly basis and at the end of the study. Mammary tumors were examined by thermography and ultrasonography at the end of the experimental protocol. Twenty-four hours before the examination, the skin overlying the mammary tumors was shaved using a clipper (Aesculap GT420 Isis, Aesculap Inc., Center Valley, PA, USA). Immediately before the examinations, all animals were anesthetized by intraperitoneal administration of ketamine (75 mg/kg of body weight, Imalgene® 1000, Merial S.A.S., Lyon, France) and xylazine (10 mg/kg of body weight, Rompun® 2%, Bayer Healthcare S.A., Kiel, Germany).

5.2.5. Thermographic examination

The thermographic evaluation was performed using a far infrared camera from FLIR® model A325 (FLIR® Systems Inc., Wilsonville, OR, USA), with a sensitivity of 68 mK and a spatial resolution of 320 × 240 pixels. The images were recorded at one frame *per* second for future analyses but the integration time for the micro bolometer was approximately 16.6 ms. The animals were manually held and filmed at a constant distance (0.35 m). The animal emissivity was set to 0.98 and the tumor borders were marked to

overlap with a visible image. Representative frames were selected and analyzed using the ThermaCam Researcher Pro 2.10 (FLIR[®] Systems Inc., Wilsonville, OR, USA) software. In this analysis, the minimum, average and maximum temperatures of each region of interest were obtained.

5.2.6. Ultrasonographic examination

PDI, B Flow and CEUS ultrasonographic images were obtained in sagittal planes with animals in supine position. Acoustic gel (Aquasonic, Parker Laboratories Inc., Fairfield, NJ, USA) was applied and sagittal scanning was performed using light pressure to avoid distortion of tumors shape with a real-time scanner (Logiq P6[®], General Electric Healthcare, Milwaukee, WI, USA) using a 10 MHz linear transducer with a standoff pad (Sonokit, MIUS Ltd., Gloucestershire, UK) made of extremely soft polyvinylchloride, especially created for skin contact sonography. To obtain CEUS images, the contrast agent SonoVue[®] (Bracco, Milan, Italy) was administered through the tail vein.

Color pixels were determined by Adobe Photoshop[®] version 7.0 (Adobe Systems Inc., San Jose, CA, USA) in PDI and B Flow images. The color pixel density (CPD) was calculated according to formula [18]:

$$CPD = \frac{\text{Number of colored pixels in the tumor}}{\text{Number of total pixels of the tumor}} \times 100$$

Two measures of total pixels in ten randomly chosen images were taken, in order to verify reproducibility. Qualitative analysis of images obtained by CEUS was also performed, according to the parameters described by Tuncbilek *et al.* [19] and Liu *et al.* [20]: enhancement order, margin, contrast distribution and penetrating vessels.

5.2.7. Necropsy

After ultrasonographic examination, anesthetized animals were sacrificed by exsanguination by cardiac puncture (method indicated by the Federation of European Laboratory Animal Science Associations) [21]. The animals were skinned and the skin was examined for small tumors. Complete necropsies of all animals were performed. The

tumor volume (V) was calculated based on the next formula $V = \frac{\text{Tumor weight}}{\text{Density}}$, where density was 1.056 g/cm³ [22]. All organs were immersed in phosphate-buffered formaldehyde for 12 hours.

5.2.8. Histology

After fixation, mammary tumors were cut, embedded in paraffin and two μm -thick sections were routinely stained with hematoxylin and eosin (H&E). Histological slides were observed blindly, under a light microscope, by two independent researchers. Histological lesions were classified according to Russo and Russo [23]. Each mammary tumor was classified according to the histological pattern with higher proportion in each tumor section.

5.2.9. Statistics

A descriptive analysis was performed for all the variables included in the study. Data were statistically analyzed using Statistical Package for the Social Sciences (SPSS® version 23 for Windows, SPSS Inc, Chicago, IL, USA). Analysis of variance (ANOVA) with the Bonferroni correction multiple-comparison method was used to determine significant differences concerning food and water consumption, and initial/final mean body weight between the groups. Independent sample *t*-test was used to compare PG between groups. Paired sample *t*-test was used to compare two measures of total pixels measured in ten randomly selected images and the Intraclass correlation coefficient (ICC) was used to quantify the association between these two measures. Paired sample *t*-test was also used to compare the number of color pixels (CPD) in images obtained with PDI and B Flow modes. Linear Pearson correlation was used to assess the correlation between CPD (for PDI and B Flow), tumor volume and temperature. Data from qualitative analysis of CEUS were analyzed using Chi-square test. Data were expressed as mean \pm standard error (S.E.). A *p* value of less than 0.05 was considered to be statistically significant.

5.3. Results

5.3.1. General findings

Five animals were found dead during the course of the experimental protocol: four rats from group I (MI=27%) and one from group II (MI=10%), these animals were excluded from the results. During the experimental procedures, all animals exhibited normal cage activity. The mean food and water intake was constant and similar in both groups throughout the experimental protocol (data not shown). PG was statistically different between the groups, being higher in control group ($p<0.05$) (data not show).

5.3.2. Macroscopic evaluation of mammary tumors

All animals from group I developed mammary tumors (incidence 100%). The tumor volume ranged from 0.30 to 45.14 cm³. The first tumor was detected by palpation ten weeks after MNU administration in animals from group I (MNU). At the end of the experiment, 28 palpable mammary tumors were excised from animals from group I (MNU) (2.55 tumors *per* animal on average) and none from group II (control), as expected from the untreated female Sprague-Dawley rats.

5.3.3. Mammary tumors

Eleven tumors were evaluated by thermography. The temperature of mammary tumors ranged from 32.0°C to 38.6°C (Figure 5.1). The two measures of total pixels detected by PDI and B Flow ultrasonographic modes in ten randomly chosen images were not statistically different ($p>0.05$) and one measure could substitute another [ICC = 0.933, 95% confidence interval, 0.973 to 0.998], demonstrating a high reproducibility. All mammary tumors were evaluated by PDI and B Flow modes, but only sixteen of them showed vascularization (57.1% of all the tumors) (Figures 5.2 and 5.3).

The CPD detected by B Flow was higher than that detected by PDI (Figure 5.3), being statistically significant different ($p<0.05$). Statistically significant correlations ($p<0.05$) were also observed between the CPD (when obtained using PDI) and tumor volume with maximum tumor temperature and thermal amplitude (maximum-minimum) (Table 5.1).

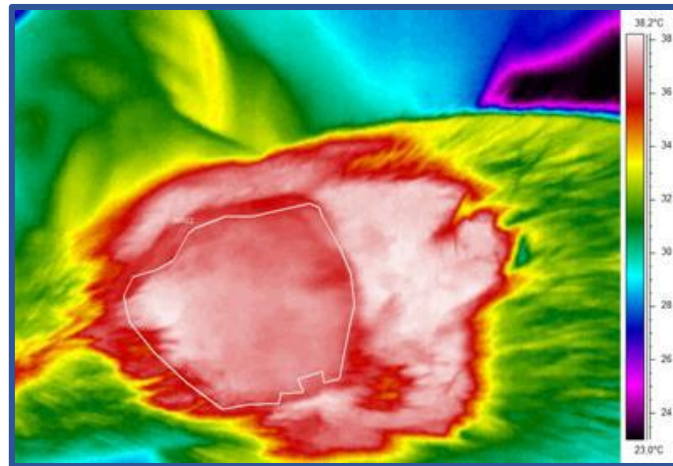


Figure 5.1. Thermographic evaluation of rat mammary tumor.

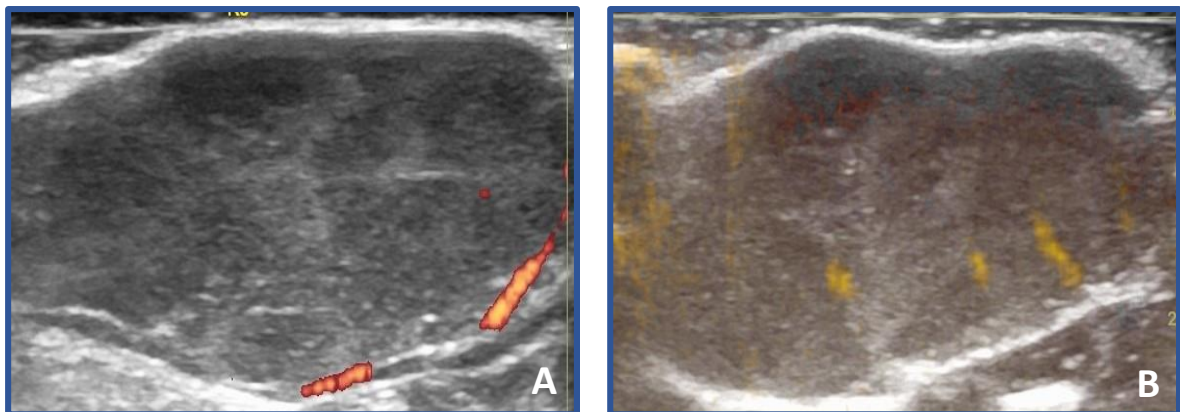


Figure 5.2. Comparison of mammary tumors evaluated by PDI (A) and B Flow (B) ultrasonographic modes.

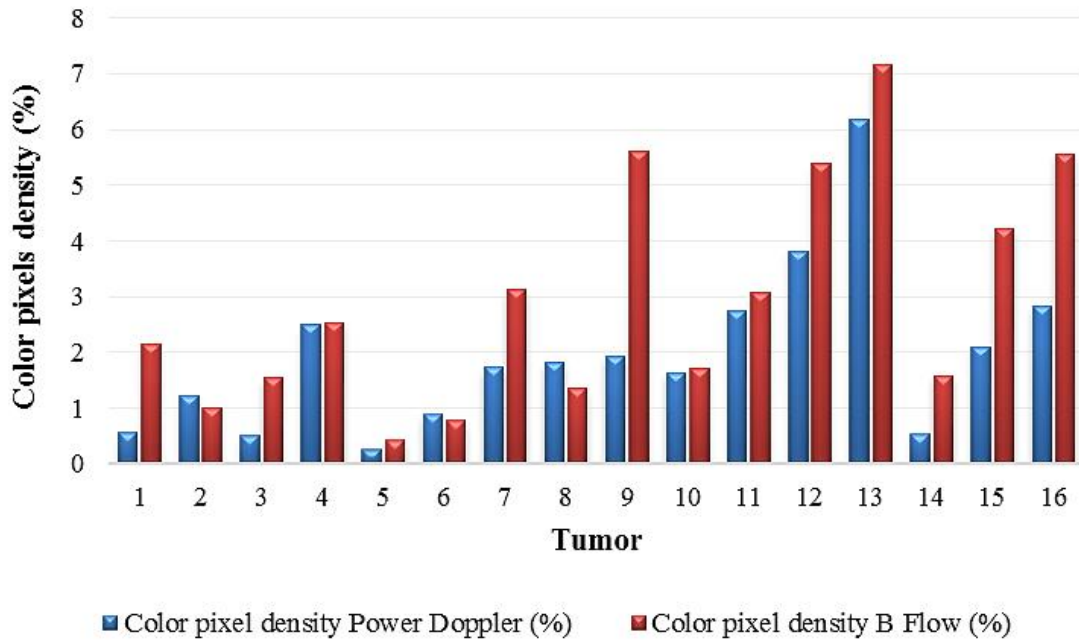


Figure 5.3. Color pixel density in PDI and B Flow ultrasonographic modes.

Table 5.1. Correlation between ultrasonographic methods and thermography.

Parameter	CPD PDI	CPD B Flow	Tumor volume	Minimum temperature	Maximum temperature	Thermal amplitude
CPD PDI	-	0.077 (<i>p</i> =0.822)	-0.451 (<i>p</i> =0.164)	0.562 (<i>p</i> =0.072)	-0.712* (<i>p</i> =0.014)	-0.704* (<i>p</i> =0.016)
CPD B Flow	-	-	-0.227 (<i>p</i> =0.503)	0.313 (<i>p</i> =0.348)	-0.045 (<i>p</i> =0.895)	-0.246 (<i>p</i> =0.466)
Tumor volume	-	-	-	-0.567 (<i>p</i> =0.069)	0.719* (<i>p</i> =0.013)	0.705* (<i>p</i> =0.015)
Minimum temperature	-	-	-	-	-0.477 (<i>p</i> =0.138)	-0.940* (<i>p</i> =0.000)
Maximum temperature	-	-	-	-	-	0.748* (<i>p</i> =0.008)
Thermal amplitude	-	-	-	-	-	-

*These correlations were considered statistically significant (*p*<0.05).

5.3.4. Mammary tumors histology

Palpated tumors were histologically classified as benign and malignant neoplastic lesions. Papillary and cribriform non-invasive carcinomas were the most frequent observed lesions (Table 5.2).

Out of the 28 identified mammary tumors, 15 were selected for CEUS evaluation. This selection was made according to tumor size (> 1.0 cm length). On CEUS analysis, most mammary tumors showed a centripetal order of contrast agent (93.3%) and clear margin

(73.3%). Other analyzed parameters (enhancement degree, enhancement homogeneity and penetrating vessels) showed similar results among different histological types of mammary tumors (Table 5.3).

Table 5.2. Histological classification of mammary tumors.

Histologic lesion		Number of tumors (n)	%
Benign lesion	Tubular adenoma	2	7.14
Malignant lesions	Papillary non-invasive carcinoma	13	46.43
	Cribriform non-invasive carcinoma	5	17.86
	Papillary invasive carcinoma	4	14.29
	Cribriform invasive carcinoma	2	7.14
	Comedo invasive carcinoma	2	7.14
Total		28	100

Table 5.3. Characterization of histological lesions by CEUS.

Parameter	Papillary non-invasive carcinoma (n=6)	Cribriform non-invasive carcinoma (n=5)	Papillary invasive carcinoma (n=3)	Comedo invasive carcinoma (n=1)	
Enhancement order					
Centripetal	6	4	3	1	14 (93.3%) ^a
Centrifugal	0	1	0	0	1 (6.67%)
Margin					
Blurred	1	3	0	0	4 (26.6%)
Clear	5	2	3	1	11 (73.3%)
Contrast distribution					
Homogeneous	4	1	2	0	7 (46.7%)
Heterogeneous	2	4	1	1	8 (53.3%)
Penetrating vessels					
Absent	3	3	1	0	7 (46.7%)
Present	3	2	2	1	8 (53.3%)

^a Statistically different from centrifugal enhancement order ($p < 0.05$).

5.4. Discussion

Breast cancer is the most frequent cancer diagnosed in women [1]. Animal models are crucial tools to understand cancer biology and develop efficient preventive, diagnostic and therapeutic approaches. The dose of MNU used to induce mammary tumors was previously defined by Gullino *et al.* [4] and was well tolerated by animals from group I. The MI in group I (MNU) was higher than in group II (control), which may be due to advanced neoplastic disease that were incompatible with animals' life. This MI was lower than showed by McCormick *et al.* [9].

PG is a realistic measure of how the body weight of the animals evolved along the experimental protocol. The animals from group II (control) showed a higher body weight increase during the experimental protocol when compared with animals from group I (MNU). This result may also be explained because the animals from group I developed

mammary tumors, resulting in a degradation of body condition and consequent weight loss, while animals from group II remained healthy along the experimental protocol. The first mammary tumor was detected by palpation at ten weeks after MNU administration. At the end of the experimental protocol (35 weeks after MNU administration), 28 mammary tumors were palpated (2.55 *per* animal), which is in agreement with reports by other researchers [24,25]. Whittal-Strange *et al.* [26] identified 2.0 tumors *per* animal on average, at 22 weeks. In the present study, at 22 weeks, the number was lower (1.0 tumor *per* animal).

Ultrasound imaging is an accurate technique to measure tumor size at the time of diagnosis [27]. When compared with mammography, ultrasonography is significantly superior for evaluating breast masses [28] and does not impose any radiation that may affect tumor development and harm the patient or the handler [29]. In this study, PDI detected vessels principally at the periphery of tumors, while B Flow mode detected vessels not only at the periphery, but also within the tumor (Figure 5.2). Thus, in accordance with other works [30], the number of color pixels detected by B Flow was significantly higher ($p<0.05$) than that detected by PDI.

Thermography, when compared with other imaging techniques for breast cancer diagnosis, provides additional functional information on vascular condition of the tissues, infections or other conditions that may lead to a change on superficial temperature [31]. As thermography is based on the measurement of infrared radiation emitted by the target (either human or animal), it is perfectly inoffensive and, in addition, it is contactless, being therefore, an interesting complementary method of analysis. Despite this, it has seldom been used in animal models of human oncologic diseases, namely in animal models of breast cancer [32]. For the purposes of cancer diagnosis, the basis of thermography is the detection of heat produced by the metabolic activity of the proliferating tumor cells and the new blood vessels supporting tumor growth [33,34]. Usually in human breast cancer xenografts a 1 to 3°C increase in skin surface temperature is observed at the tumor periphery while the tumor center exhibits a reduced temperature [34], probably due to tumor necrosis [32].

Predictably, in the present work, larger mammary tumors showed higher maximum temperature and thermal amplitude ($p<0.05$) (Table 5.1). Larger mammary tumors require a richer blood supply, resulting in higher temperature values, but also tend to show more

frequent and more extensive necrotic regions which, being devoid of blood vessels, are colder and result in thermal heterogeneity and higher thermal amplitude. Surprisingly, CPD assessed by PDI was negatively correlated with maximum temperature and with thermal amplitude ($p < 0.05$) but, interestingly, only a much weaker trend, without statistical significance, was observed when CPD was assessed by B Flow (Table 5.1). On the one hand, this may indicate that lesions with an overall high CPD are also more homogeneous, with less necrotic regions and, thereby, less reactive angiogenesis in surrounding parts and, consequently, smaller peak temperatures and temperature amplitudes. This is in agreement with the weaker, non-significant correlation between CPD PDI and minimum temperature and the negative correlation with tumor volume. On the other hand, the different results obtained with PDI and B Flow may be associated with the facts that PDI preferentially detects small, peripheral blood vessels and B Flow the deep, larger vessels (as observed in Figure 5.2) and that thermography detects superficial temperature, which is mainly influenced by peripheral vessels located near the tumor surface. Future studies employing larger experimental groups and evaluating temperature variations along the different phases of tumor development should achieve a better understanding of thermal patterns and their significance.

CEUS, as an imaging diagnostic technique, is more accessible than MRI, especially for use in veterinary medicine [10]. In the present work, CEUS was used to characterize the different types of chemically-induced mammary tumors, because it is considered the best ultrasonographic mode to detect tumor vascularization [35]. However, the lesions observed in this study showed a very balanced distribution of ultrasonographic features detected by CEUS, perhaps because they belonged, mostly, to the same histological type. CEUS analysis only showed that the mammary carcinomas evaluated in this study are characterized by a centripetal enhancement order of contrast agent and clear margins.

5.5. Conclusion

The low prevalence of different histological types of mammary tumors in the present sample precluded the study of the ultrasonographic or thermographic features by histological type. Globally, ultrasound and thermographic techniques have shown to be applicable on a relevant animal model of breast cancer and to provide complementary information on the vascularization and thermal status of mammary lesions. These findings

pave the way for a more widespread use of such tools by breast cancer researchers who use animal models, taking advantage of their *in vivo* applicability and non-invasive characteristics.

5.6. References

- [1] Benson, JR.; Jatoi, I. The global breast cancer burden. *Futur. Oncol.*, **2012**, 8, 697–702.
- [2] Youlten, DR.; Cramb, SM.; Dunn, NAM.; Muller, JM.; Pyke, CM.; Baade, PD. The descriptive epidemiology of female breast cancer: an international comparison of screening, incidence, survival and mortality. *Cancer Epidemiol.*, **2012**, 36, 237–248.
- [3] Clarke, R. Animal models of breast cancer: their diversity and role in biomedical research. *Breast Cancer Res. Treat.*, **1996**, 39, 1–6.
- [4] Gullino, PM.; Pettigrew, HM.; Grantham, FH. *N*-nitrosomethylurea as mammary gland carcinogen in rats. *J. Natl. Cancer Inst.*, **1975**, 54, 401–414.
- [5] Huggins, C.; Brillantes, FP.; Grand, LC. Mammary cancer induced by a single feeding of polynuclear hydrocarbons, and its suppression. *Nature*, **1961**, 189, 204–207.
- [6] Russo, J.; Gusterson, BA.; Rogers, AE.; Russo, IH.; Wellings, SR.; Vanzwieten, MJ. Biology of disease - comparative study of human and rat mammary tumorigenesis. *Lab. Investig.*, **1990**, 62, 244–278.
- [7] Singh, M.; McGinley, JN.; Thompson, HJ. A comparison of the histopathology of premalignant and malignant mammary gland lesions induced in sexually immature rats with those occurring in the human. *Lab. Investig.*, **2000**, 80, 221–231.
- [8] Thompson, HJ.; McGinley, J.; Rothhammer, K.; Singh, M. Ovarian hormone dependence of pre-malignant and malignant mammary gland lesions induced in pre-pubertal rats by *I*-methyl-*I*-nitrosourea. *Carcinogenesis*, **1998**, 19, 383–386.
- [9] McCormick, DL.; Adamowski, CB.; Fiks, A.; Moon, RC. Lifetime dose-response relationships for mammary-tumor induction by a single administration of *N*-methyl-*N*-nitrosourea. *Cancer Res.*, **1981**, 41, 1690–1694.
- [10] Ko, EY.; Lee, SH.; Kim, HH.; Kim, SM.; Shin, MJ.; Kim, N.; Gong, G. Evaluation of tumor angiogenesis with a second-generation US contrast medium in a rat breast

- tumor model. *Korean J. Radiol.*, **2008**, 9, 243–249.
- [11] Brix, G.; Kiessling, F.; Lucht, R.; Darai, S.; Wasser, K.; Delorme, S.; Griebel, J. Microcirculation and microvasculature in breast tumors: pharmacokinetic analysis of dynamic MR image series. *Magn. Reson. Med.*, **2004**, 52, 420–429.
- [12] Delille, JP.; Slanetz, PJ.; Yeh, ED.; Kopans, DB.; Garrido, L. Breast cancer: regional blood flow and blood volume measured with magnetic susceptibility-based MR imaging - initial results. *Radiology*, **2002**, 223, 558–565.
- [13] Teifke, A.; Behr, O.; Schmidt, M.; Victor, A.; Vomweg, TW.; Thelen, M.; Lehr, HA. Dynamic MR Imaging of breast lesions: correlation with microvessel distribution pattern and histologic characteristics of prognosis. *Radiology*, **2006**, 239, 351–360.
- [14] Tan, JH.; Ng, EYK.; Acharya, UR.; Chee, C. Infrared thermography on ocular surface temperature: a review. *Infrared Phys. Technol.*, **2009**, 52, 97–108.
- [15] Lahiri, BB.; Bagavathiappan, S.; Jayakumar, T.; Philip, J. Medical applications of infrared thermography: a review. *Infrared Phys. Technol.*, **2012**, 55, 221–235.
- [16] Lawson, R. Implications of surface temperatures in the diagnosis of breast cancer. *Can. Med. Assoc. J.*, **1956**, 75, 309–310.
- [17] Arantes-Rodrigues, R.; Henriques, A.; Pires, MJ.; Colaco, B.; Calado, AM.; Rema, P.; Colaco, A.; Fernandes, T.; De la Cruz, PLF.; Lopes, C.; Fidalgo-Goncalves, L.; Vilela, S.; Pedrosa, T.; Peixoto, F.; Oliveira, PA. High doses of olive leaf extract induce liver changes in mice. *Food Chem. Toxicol.*, **2011**, 49, 1989–1997.
- [18] Denis, F.; Bougnoux, P.; de Poncheville, W.; Prat, M.; Catroux, R.; Tranquart, FO. *In vivo* quantitation of tumour vascularisation assessed by Doppler sonography in rat mammary tumours. *Ultrasound Med. Biol.*, **2002**, 28, 431–437.
- [19] Tuncbilek, N.; Unlu, E.; Karakas, HM.; Cakir, B.; Ozilmaz, F. Evaluation of tumor angiogenesis with contrast-enhanced dynamic magnetic resonance mammography. *Breast J.*, **2003**, 9, 403–408.
- [20] Liu, H.; Jiang, YX.; Liu, JB.; Zhu, QL.; Sun, Q. Evaluation of breast lesions with contrast-enhanced ultrasound using the microvascular imaging technique: initial observations. *Breast*, **2008**, 17, 532–539.
- [21] Forbes, D.; Blom, H.; Kostomitsopoulos, N.; Moore, G.; Perretta, G. Euroguide: on the accommodation and care of animals used for experimental and other scientific

- purposes. *Federation of European Laboratory Animal Science Associations*, **2007**.
- [22] Clarys, JP.; Marfelljones, MJ. Soft-tissue segmentation of the body and fractionation of the upper and lower-limbs. *Ergonomics*, **1994**, 37, 217–229.
- [23] Russo, J.; Russo, IH. Atlas and histologic classification of tumors of the rat mammary gland. *J. Mammary Gland Biol. Neoplasia*, **2000**, 5, 187–200.
- [24] Kubatka, P.; Bojkova, B.; Mocikova-Kalicka, K.; Mnichova-Chamilova, M.; Adamekova, E.; Ahlers, I.; Ahlersova, E.; Cermakova, M. Effects of tamoxifen and melatonin on mammary gland cancer induced by *N*-methyl-*N*-nitrosourea and by 7,12-dimethylbenz(a)anthracene, respectively, in female Sprague-Dawley rats. *Folia Biol. (Praha)*, **2001**, 47, 5–10.
- [25] Perse, M.; Cerar, A.; Injac, R.; Strukelj, B. *N*-methylnitrosourea induced breast cancer in rat, the histopathology of the resulting tumours and its drawbacks as a model. *Pathol. Oncol. Res.*, **2009**, 15, 115–121.
- [26] Whittal-Strange, KS.; Chadau, S.; Parkhouse, WS. Exercise during puberty and NMU induced mammary tumorigenesis in rats. *Breast Cancer Res. Treat.*, **1998**, 47, 1–8.
- [27] Berg, WA.; Gutierrez, L.; NessAiver, MS.; Carter, WB.; Bhargavan, M.; Lewis, RS.; Ioffe, OB. Diagnostic accuracy of mammography, clinical examination, US, and MR imaging in preoperative assessment of breast cancer. *Radiology*, **2004**, 233, 830–849.
- [28] Fornage, B. The role of sonography in staging invasive breast cancer. *Eur. J. Radiol.*, **2012**, 81, 41–44.
- [29] Jensen, MM.; Jorgensen, JT.; Binderup, T.; Kjaer, A. Tumor volume in subcutaneous mouse xenografts measured by microCT is more accurate and reproducible than determined by 18F-FDG-microPET or external caliper. *BMC Med. Imaging*, **2008**, 8,16.
- [30] Fleischer, AC.; Wojcicki, WE.; Donnelly, EF.; Pickens, DR.; Thirsk, G.; Thurman, GB.; Hellerqvist, CG. Quantified color Doppler sonography of tumor vascularity in an animal model. *J. Ultrasound Med.*, **1999**, 18, 547–551.
- [31] Kennedy, DA.; Lee, T.; Seely, D. A comparative review of thermography as a breast cancer screening technique. *Integr. Cancer Ther.*, **2009**, 8, 9–16.
- [32] Poljak-Blazi, M.; Kolaric, D.; Jaganjac, M.; Zarkovic, K.; Skala, K.; Zarkovic, N.

- Specific thermographic changes during Walker 256 carcinoma development: Differential infrared imaging of tumour, inflammation and haematoma. *Cancer Detect. Prev.*, **2009**, 32, 431–436.
- [33] Eddie, Y-K.; Fork, S-C. A framework for early discovery of breast tumor using thermography with artificial neural network. *Breast J.*, **2003**, 9, 341–343.
- [34] Xie, W.; McCahon, P.; Jakobsen, K.; Parish, C. Evaluation of the ability of digital infrared imaging to detect vascular changes in experimental animal tumours. *Int. J. Cancer*, **2004**, 108, 790–794.
- [35] Madjar, H. Improvement in the flow assessment for breast lesions by contrast enhanced Color Doppler imaging . *Echocardiography*, **1993**, 10, 680.

CHAPTER 6

ELECTRON MICROSCOPY FINDINGS IN MNU-INDUCED MAMMARY TUMORS

THE CONTENT OF THIS CHAPTER WAS PUBLISHED IN:

Faustino-Rocha AI, Calado AM, Gama A, Ferreira R, Ginja M, Oliveira PA. 2016. Electron microscopy findings in MNU-induced mammary tumors. *Microscopy and Microanalysis* 22 (5): 1056-1061. DOI: 10.1017/S1431927616011661. (Full paper)

Faustino-Rocha AI, Calado AM, Gama A, Ferreira R, Ginja M, Oliveira PA. 2016. MNU-induced mammary tumors: transmission electron microscopy. *Microscopy and Microanalysis*. (Accepted for publication, Abstract)

Faustino-Rocha AI, Calado AM, Gama A, Ferreira R, Ginja M, Oliveira PA. 2016. MNU-induced mammary tumors: transmission electron microscopy. 50th Meeting of the Portuguese Microscopy Society, 29th to 30th June, Porto, Portugal. (Oral presentation)

6. Electron microscopy findings in MNU-induced mammary tumors

Abstract

Although the rat model of mammary tumors chemically-induced by *N*-methyl-*N*-nitrosourea (MNU) has been frequently used by several research teams, there is a lack of ultrastructural studies in this field. The main aim of this work was to perform an ultrastructural characterization of MNU-induced mammary tumors in female rats. Some alterations previously reported in human mammary tumors, such as nucleus size and shape, accumulation of heterochromatin in perinuclear region and interdigitating cytoplasmic processes between cancer cells were also observed in MNU-induced mammary tumors. Although a low number of samples were analyzed by transmission electron microscopy (TEM) in the present study, we consider that it may contribute to better understand the MNU-induced mammary carcinogenesis in a rat model. The ultrastructural characteristics of the two most frequently diagnosed mammary carcinomas described in the present work may be useful to differentiate them from other histological patterns. In addition, the loss of cytoplasm in neoplastic cells and formation of vacuoles were described.

Keywords: MNU-induced mammary tumor, rat, Sprague-Dawley, transmission electron microscopy, ultrastructure

6.1. Introduction

The rat model of mammary tumors chemically-induced by the carcinogen agent *N*-methyl-*N*-nitrosourea (MNU) has been extensively used by several research groups in order to give new insights on mammary cancer physiopathology, and to develop new preventive and therapeutic strategies [1–4]. Although these tumors have been extensively studied by histopathology, immunohistochemistry and genetic approaches, there is a lack of ultrastructural studies [5–7]. The present work aimed to perform an ultrastructural evaluation of MNU-induced mammary tumors in female rats. Considering that our research team has also been focused on the effects of tumor microenvironment on mammary tumor development, particularly in the role of mast cells, we also examined mast cell infiltration in these tumors.

6.2. Material and Methods

6.2.1. Animals

In total, 50 female Sprague-Dawley rats, 4-5 weeks of age, were obtained from Harlan Laboratories Inc. (Barcelona, Spain). Animals were housed at the facilities of the University of Trás-os-Montes and Alto Douro in filter capped polycarbonate cages (1500U Eurostandard Type IV S, Tecniplast, Buguggiate, Italy) with corncob for bedding (Mucedola, Settimo Milanese, Milan, Italy) under controlled temperature conditions ($23\pm 2^{\circ}\text{C}$), humidity ($50\pm 10\%$), and air filtration system (10-20 ventilations/hour) and on a 12h:12h light:dark cycle. Tap water and a basic standard laboratory diet (4RF21[®], Mucedola, Settimo Milanese, Milan, Italy) were supplied *ad libitum*. Cages were cleaned and water was changed once *per* week. All procedures were done in accordance with European legislation (European Directive 2010/63/EU). The Portuguese Ethics Committee for Animal Experimentation approved all the experiments and procedures carried out on the animals (approval no. 008961).

6.2.2. Animal experiments

Animals were submitted to a period of quarantine for one week and acclimated to laboratory conditions for two weeks. Then they were randomly divided into four experimental groups: MNU sedentary (n=15), MNU exercised (n=15), control sedentary (n=10) and control exercised (n=10). However, only two groups (MNU sedentary and control sedentary) were considered and will be described in this work. Mammary tumor development was induced in animals from MNU group by a single intraperitoneal administration of the carcinogen agent MNU (ISOPAC[®], Sigma Aldrich S.A., Madrid, Spain) at a dose of 50 mg/kg of body weight at seven weeks of age. Animals from control group received a single administration of the vehicle (saline solution 0.9%). All animals were observed twice a day to monitor their general health status. They were palpated weekly for the detection of mammary tumor development.

6.2.3. Animals' sacrifice and samples

After 35 weeks of MNU administration, all survived animals were humanely sacrificed by intraperitoneal administration of ketamine (75 mg/kg of body weight, Imalgene[®] 1000,

Merial S.A.S., Lyon, France) and xylazine (10 mg/kg of body weight, Rompun[®] 2%, Bayer Healthcare S.A., Kiel, Germany) followed by exsanguination by cardiac puncture as indicated by the Federation of European Laboratory Animal Science Associations [8].

All animals were skinned and the skin was carefully observed under a light for the detection of small mammary tumors, and all tumors were removed. Three fragments with less than 1 mm of diameter were randomly taken from the two malignant histological patterns (papillary carcinoma and cribriform carcinoma) most frequently developed by MNU-exposed animals for transmission electron microscopy (TEM) processing. After this, all mammary tumors were immersed in buffered formalin for 12 hours.

6.2.4. Histological analysis

After fixation in buffered formalin, all mammary tumors were routinely processed, embedded in paraffin, and two μm -thick sections were stained with hematoxylin and eosin (H&E). They were histologically classified by a pathologist according to the classification previously established by Russo and Russo [9].

6.2.5. Transmission electron microscopy

The fragments obtained from three mammary tumors from MNU group were fixed with 3% glutaraldehyde in 0.1 M phosphate buffer, pH 7.4, for 2 hours at 4°C [10]. After washing in buffer for 2 hours at 4°C, they were post-fixed in 2% osmium tetroxide (OsO_4) in buffer, dehydrated in an ethanol series followed by propylene oxide and embedded in Epon. Semithin sections with 0.5-1 μm -thick were cut with a glass knife in a RMC Power Tome XL ultramicrotome (Boeckeler Instruments, Tucson, Arizona, USA), stained with a mixture of methylene blue and azur II (2:1), and observed by light microscopy. Ultrathin sections from mammary tumors embedded in Epon were cut in a RMC Power Tome XL ultramicrotome (Boeckeler Instruments, Tucson, Arizona, USA) with a diamond knife (Diatome, Hatfield, Pennsylvania, USA), collected on copper grids (Taab, Aldermaston, Berks, UK), contrasted with uranyl acetate (20 min) and Reynolds lead citrate (10 min), and observed at 60 kV in a LEO 906E transmission electron microscope (Zeiss, Oberkochen, Germany) [11].

6.3. Results

6.3.1. Animals

Five animals died during the course of the experiment: four animals from MNU group and one animal from control group. Data from these animals were excluded from the study.

6.3.2. Mammary tumors

As expected, animals from control group did not develop any mammary tumor. All animals from the MNU group developed mammary tumors (incidence of 100%) and a total of 28 mammary tumors was counted.

6.3.3. Histological classification

At histological analysis of H&E stained mammary tumors, it was observed that each mammary tumor exhibited more than one histological lesion. In this way, a total of 71 lesions were identified in MNU group, as previously published by our research team [6]. The cribriform and papillary carcinomas were the malignant histological patterns most frequently identified [6]. At analysis of mammary tumor sections embedded in Epon, the three tumors from the MNU group sampled for TEM analysis were histologically classified as follows: two of them were classified as cribriform carcinoma and one was classified as papillary carcinoma (Figure 6.1).

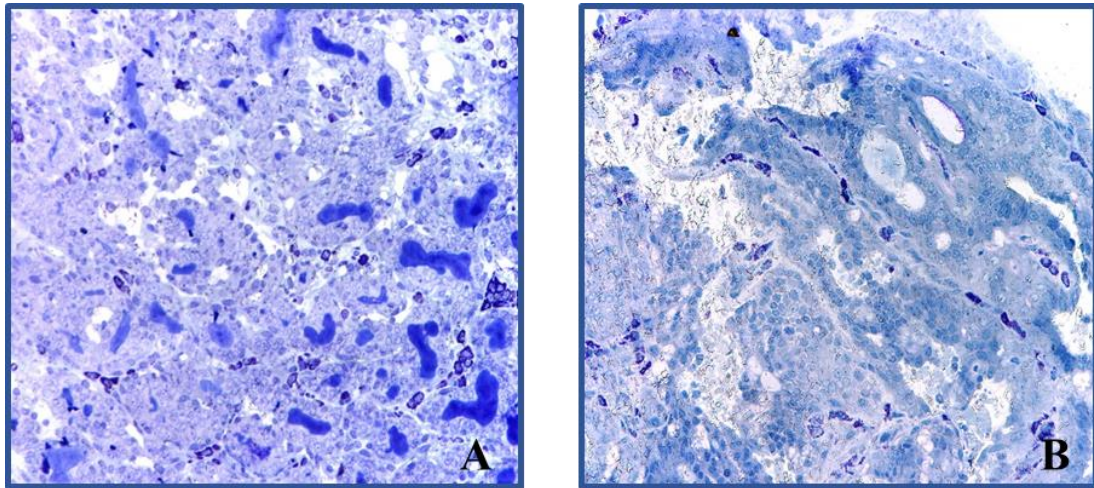


Figure 6.1. Semithin sections of mammary tumors stained with methylene blue and azur II (2:1) observed by light microscopy. The lesions were classified as cribriform carcinoma (A) and papillary carcinoma (B). Magnification of 200 \times .

6.3.4. Transmission electron microscopy

Similar ultrastructural features were found in the two histological patterns (cribriform and papillary carcinomas) analyzed in the present work. Neoplastic cells usually presented a round or elongated regular shaped nucleus, always accompanying a cuboid or a prismatic cell shape. Perinuclear heterochromatin was evident, and uniformly distributed below the entire inner envelope (Figures 6.2A and B). Other cells showed an increased nuclear size, with a very irregular shape and also with numerous folds. In these cells the nucleus had clumps of chromatin (Figure 6.2C). In the cytoplasm, abundant rough endoplasmic reticulum, free ribosomes and Golgi cisterns were observed. Mitochondria were abundant and presented a pleomorphic shape (Figure 6.2D). These cells revealed a clear relationship between Golgi cisterns and mitochondria positions. Some dense vesicles (two or three on each cell section) were also observed. The Golgi apparatus presented a developed lamellar membranous structure with curved parallel series of flattened saccular vesicles (dictyosomes) expanded at their ends. Vesicles of rough endoplasmic reticulum fused on the cis-part of the Golgi apparatus (Figure 6.2D). Cells also presented abundant primary and secondary lysosomes, multivesicular bodies and residual bodies. Some cells were closely embedded between adjacent ones, and showed numerous interdigitating cytoplasmic processes and desmosomes, with very electron-dense plaques attached to the inner side of the cell membrane. Other cells

showed a clear rupture with adjacent cells, and in these regions the plasma membrane developed several long projections (Figures 6.2E and F). These cells, especially those that had lost their contact with the adjacent ones, loose large portions of cytoplasm that were detached from the rest of the cell (Figure 6.2G). Fragmented portions of the cytoplasm were deposited on the extracellular space. These fragments contained several organelles, such as rough endoplasmic reticulum, ribosomes, several cisterns and round mitochondria with visible cristae. Other cells lost large portions of cytoplasm through the formation of large vacuoles just near the nucleus (Figures 6.2H and I). It was also observed in some neoplastic cells that after losing parts of cytoplasm, the remaining part became devoid of plasma membrane (Figures 6.2J and K).

Several mast cells were observed near cells in fragmentation. They appear as round to elongated cells with a diameter of approximately 10 μm . A non-segmented heterochromatic nucleus, abundant granules, elongated mitochondria, free ribosomes and profiles of endoplasmic reticulum were observed in the mast cells cytoplasm (Figure 6.2L).

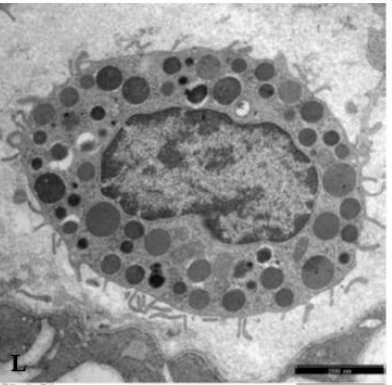
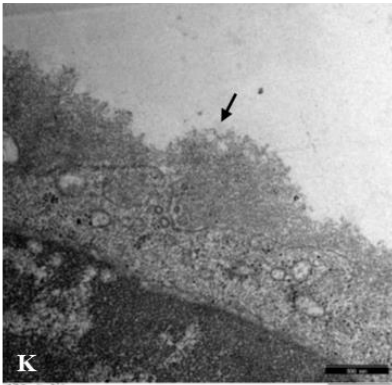
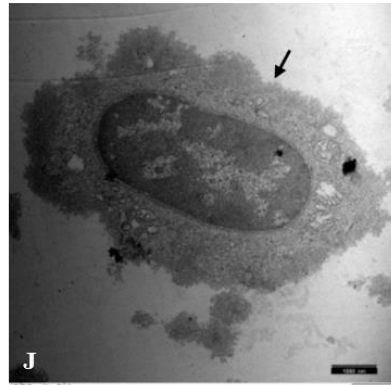
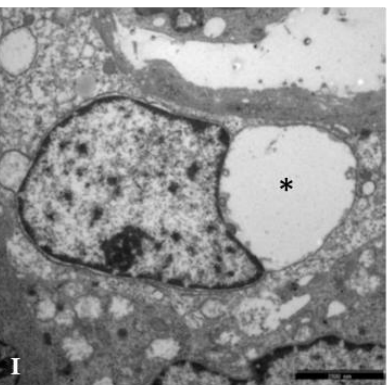
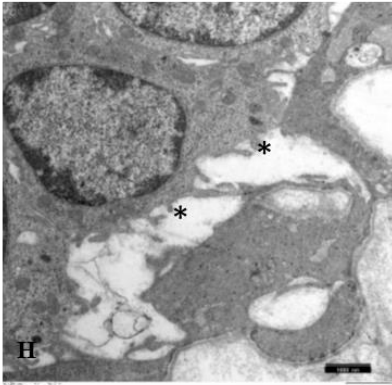
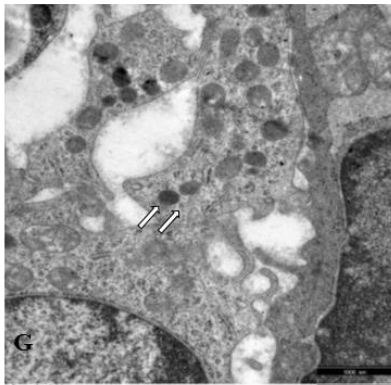
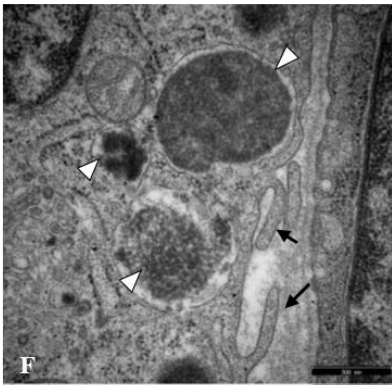
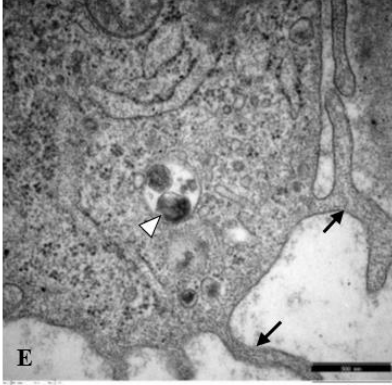
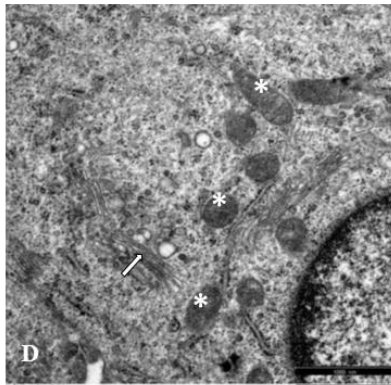
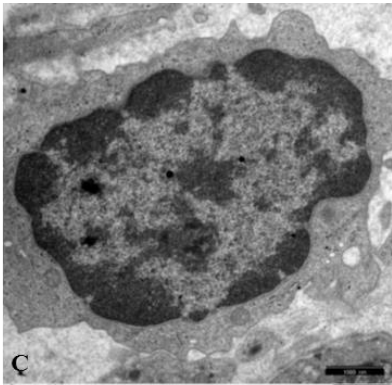
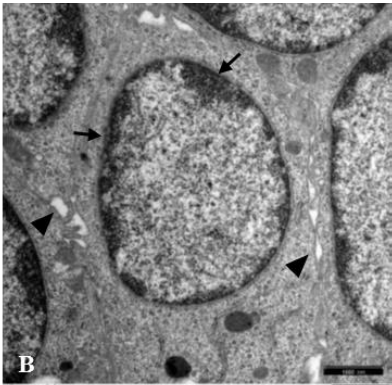
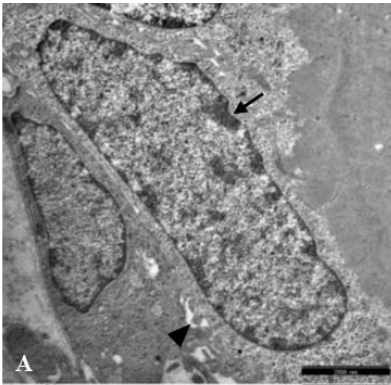


Figure 6.2. Ultrastructural findings in MNU-induced cribriform and papillary carcinomas. Elongated (A) or round (B) nuclei with perinuclear heterochromatin (black arrows) were observed. Several cells are connected with adjacent ones by several interdigitating cytoplasmic processes and desmosomes (black arrow heads) (A and B). Nuclei with an irregular shape and increased size were observed in some cells (C). Golgi cisterns (white arrows) and mitochondria (white asterisks) were closely positioned in cell cytoplasm (D). Abundant lysosomes, multivesicular bodies and residual bodies were observed with different material inside (white arrow heads). Free ribosomes and rough endoplasmic reticulum were abundant. Cells exhibited several long projections of contact with adjacent ones (black arrows) (E and F). Some cells lost large portions of cytoplasm with several organelles by a torsion-like process (white arrows) (G). Other cells formed vacuoles with variable size and shape. These vacuoles increased in size and fused with each other, forming large vacuoles (black asterisks). These vacuoles initiated the separation of cytoplasm portions (H and I). Cells lost parts of cytoplasm and the remaining part became devoid of plasma membrane (black arrows) (J and K). Mast cells were frequently observed, especially near cells in fragmentation (L).

6.4. Discussion

Cancer occurs when a normal cell fails to function properly, leading to abnormalities in cell cycle that induces alterations in a tissue [12]. Some authors consider that several ultrastructural features detected by TEM are useful for the differential diagnosis of breast tumors (benign *versus* malignant tumors), and advise the evaluation of breast lesions using this technique [13]. However, the time consumed for fixation and Epon embedding, as well as advanced skills for preparing ultrathin sections, forces the TEM use for research purposes only [14]. Although the rat model of MNU-induced mammary tumors is one of the most frequently used in breast cancer research, little is known about the ultrastructure of these cancer cells [5]. Since cells undergo transformations during the process of carcinogenesis [15], we consider important to analyze their ultrastructure in order to better understand and justify the observable macroscopic alterations. Thus, TEM was carried out in three samples from MNU-induced mammary tumors in female Sprague-Dawley rats.

TEM analysis revealed similar features between the histological patterns (cribriform and papillary carcinomas) identified in this work. Although a low number of samples (three samples) was used due to the cost, laborious sample preparation and requirement of a specialist to complete the protocol, they were considered representative, given that

the cribriform and papillary carcinomas were the most frequent malignant histological patterns identified in the present protocol [6].

Neoplastic cell nuclei from MNU-induced rat mammary tumors exhibited a round or elongated shape, which is in accordance with that previously reported in human mammary tumors. Cell nuclei from malignant mammary tumors showed an oval or round shape when compared with the nuclei of cells from normal mammary gland [13]. Nuclei were rich in heterochromatin, as previously observed in the nuclei of normal cells from mammary gland and from carcinoid tumors [13]. Although previous works in human mammary tumors concluded that breast cancer cells from both benign and malignant tumors were characterized by absence of atypia [16,17], some cells from MNU-induced rat mammary tumors exhibited cell atypia, characterized by nuclear enlargement, irregular shape, and an increase in heterochromatin. Similar to normal cells from mammary gland, the cytoplasmic organelles appeared to be uniformly distributed throughout the cell [13]. The organelles observed in these cells, namely mitochondria, Golgi complex (composed of few flat saccules and small vesicles), endoplasmic reticulum, free ribosomes, and lysosomes had been previously observed by Russo *et al.* [18] in a work performed in a human breast cancer carcinoma cell line (MCF-7). Mitochondria are essential sources of adenosine triphosphate (ATP) to the cells. Although alterations of mitochondrial morphology were not frequently reported in human mammary cancer cells [19], mitochondria with pleomorphic shape were found in cells from MNU-induced mammary tumors. Rough endoplasmic reticulum and its attached polyribosomes are responsible for the production of secretory proteins. Cells that produce a protein-rich secretion, like hepatocytes, pancreatic cells and fibroblasts, have a well-developed rough endoplasmic reticulum [19]. The reticulum remains in tumors arising in these organs. An inverse relationship was described between the tumor growth rate and the amount of rough endoplasmic reticulum [19]. The Golgi complex is well developed in secretory cells. It is responsible by modifying, condensing and packaging materials to form secretory granules. So, similarly to what occurs with the rough endoplasmic reticulum, the Golgi complex is an indicator of cellular differentiation and functional activity. Immature or undifferentiated cells, like stem cells, have a poorly developed Golgi complex and poor rough endoplasmic reticulum when compared with normal mature cells [19]. Concerning tumors, the Golgi complex is poorly developed in fast-growing tumors. In addition, the less differentiated tumors have smaller Golgi complexes,

in contrast to well-differentiated mammary tumors, which normally present a well-differentiated Golgi complex. In some tumors, it may exhibit hypertrophy, dilation or distortion [19]. Secondary lysosomes were observed in most mammary tumors [20].

The neoplastic cells exhibited several projections from their body that allow them to attach to neighboring/adjacent ones. This contact among cells is established in order to enhance their ability to survive and become more resistant to apoptosis induced by therapeutic approaches, namely administration of anticancer drugs [21,22]. These projections may also be involved in cell migration. Kramer *et al.* [23] verified that the formation of projections maximize the cell membrane surface area and leads to the beginning of tumor cells invasion. Benbow *et al.* [24] described three distinct steps during the process of carcinogenesis: adhesion, invasion and migration. The process begins with attachment between cancer cells, followed by the formation of protrusions, and ends with the movement of cells along the matrix [24]. One of the most interesting phenomena observed in our study was the loss of cytoplasm and the formation of vacuoles. Furthermore, mast cells were also frequently observed near tumor cells in fragmentation, confirming our research team findings in MNU-induced mammary tumors in Sprague-Dawley female rats [1,2,4,25] The characteristics of mast cells observed in the present work were similar to those previously described in mammary tumors [26,27].

6.5. Conclusion

Although a low number of samples (three samples) were analyzed by TEM in the present study, we consider that it may contribute to a better understanding of the carcinogenesis process of MNU-induced mammary tumors in a rat model. Ultrastructural characteristics of the two most common mammary carcinomas MNU-induced in female rats described in the present work may be useful to distinguish them from other histological patterns. In addition, in the present work the loss of cytoplasm in neoplastic cells and formation of vacuoles were described.

6.6. References

- [1] Faustino-Rocha, AI.; Gama, A.; Oliveira, PA.; Vala, H.; Ferreira, R.; Ginja, M. Effects of histamine on the development of MNU-induced mammary tumours. *Virchows Arch.*, **2015**, 467, S51–51.

- [2] Faustino-Rocha, AI.; Gama, A.; Pires, MJ.; Oliveira, PA.; Ginja, M. Effects of a mast cell stabilizer on the vascularization of mammary tumors: ultrasonographic evaluation. *Anticancer Res.*, **2014**, 34, 5901.
- [3] Faustino-Rocha, AI.; Oliveira, PA.; Duarte, JA.; Ferreira, R.; Ginja, M. Ultrasonographic evaluation of gastrocnemius muscle in a rat model of *N*-methyl-*N*-nitrosourea-induced mammary tumor. *In vivo*, **2013**, 27, 803–807.
- [4] Faustino-Rocha, AI.; Pinto, C.; Gama, A.; Oliveira, PA. Effects of ketotifen on mammary tumors volume and weight. *Anticancer Res.*, **2014**, 34, 5902.
- [5] Faustino-Rocha, AI.; Ferreira, R.; Oliveira, PA.; Gama, A.; Ginja, M. *N*-methyl-*N*-nitrosourea as a mammary carcinogenic agent. *Tumor Biol.*, **2015**, 36, 9095–9117.
- [6] Faustino-Rocha, A.; Gama, A.; Oliveira, PA.; Alvarado, A.; Neuparth, MJ.; Ferreira, R.; Ginja, M. Effects of lifelong exercise training on mammary tumorigenesis induced by MNU in female Sprague-Dawley rats. *Clin. Exp. Med.*, **2016**, Epub ahead of print.
- [7] Faustino-Rocha, AI.; Silva, A.; Gabriel, J.; Teixeira-Guedes, CI.; Lopes, C.; Gil da Costa, R.; Gama, A.; Ferreira, R.; Oliveira, PA.; Ginja, M. Ultrasonographic, thermographic and histologic evaluation of MNU-induced mammary tumors in female Sprague-Dawley rats. *Biomed. Pharmacother.*, **2013**, 67, 771–776.
- [8] Forbes, D.; Blom, H.; Kostomitsopulos, N.; Moore, G.; Perretta, G. Euroguide: on the accommodation and care of animals used for experimental and other scientific purposes. *Federation of European Laboratory Animal Science Associations*, **2007**.
- [9] Russo, J.; Russo, IH. Atlas and histologic classification of tumors of the rat mammary gland. *J. Mammary Gland Biol. Neoplasia*, **2000**, 5, 187–200.
- [10] Hyttel, P.; Xu, KP.; Smith, S.; Greve, T. Ultrastructure of *in vitro* oocyte maturation in cattle. *J. Reprod. Fertil.*, **1986**, 78, 615–625.
- [11] Calado, AM.; Oliveira, E.; Colaco, A.; Sousa, M. Ultrastructural and cytochemical characterization of follicular cell types in bovine (*Bos taurus*) cumulus-oocyte complexes aspirated from small and medium antral follicles during the estrus cycle. *Anim. Reprod. Sci.*, **2011**, 123, 23–31.
- [12] Kaul-Ghanekar, R.; Singh, S.; Mamgain, H.; Jalota-Badhwar, A.; Paknikar, KM.; Chattopadhyay, S. Tumor suppressor protein SMAR1 modulates the roughness of cell surface: combined AFM and SEM study. *BMC Cancer*, **2009**, 9, 350.
- [13] Tsuchiya, S.; Li, F. Electron microscopic findings for diagnosis of breast lesions.

Med. Mol. Morphol., **2005**, 38, 216–224.

[14] Winey, M.; Meehl, JB.; O'Toole, ET.; Giddings, TH. Conventional transmission electron microscopy. *Mol. Biol. Cell*, **2014**, 25, 319–323.

[15] Jaafar, H.; Sharif, SET.; Das Murtey, M. Distinctive features of advancing breast cancer cells and interactions with surrounding stroma observed under the scanning electron microscope. *Asian Pacific J. Cancer Prev.*, **2012**, 13, 1305–1310.

[16] Scott, MA.; Lagios, MD.; Axelsson, K.; Rogers, LW.; Anderson, TJ.; Page, DL. Ductal carcinoma in situ of the breast: reproducibility of histological subtype analysis. *Hum. Pathol.*, **1997**, 28, 967–973.

[17] Sloane, JP. *Biopsy pathology of the breast*. **1985**, Chapman & Hall.

[18] Russo, J.; Bradley, RH.; Mcgrath, C.; Russo, IH. Scanning and transmission electron-microscopy study of a human breast carcinoma cell line (MCF-7) cultured in collagen-coated cellulose sponge. *Cancer Res.*, **1977**, 37, 2004–2014.

[19] Ghadially, FN. Differences between normal and neoplastic cells. In *Diagnostic electron microscopy of tumors* (Ghadially, F. N., ed), **1985**, pp. 25–62.

[20] Ghadially, FN.; Parry, EW. Ultrastructure of a human hepatocellular carcinoma and surrounding non-neoplastic liver. *Cancer*, **1966**, 19, 1989–2004.

[21] Kataoka, S.; Tsuruo, T. Physician Education: apoptosis. *Oncologist*, **1996**, 1, 399–401.

[22] Luparello, C.; Sheterline, P.; Pucciminafra, I.; Minafra, S. A comparison of spreading and motility behavior of 8701-BC breast carcinoma cells on type I, I-trimer and type V collagen substrata - evidence for a permissive effect of type I-trimer collagen on cell locomotion. *J. Cell Sci.*, **1991**, 100, 179–185.

[23] Kramer, RH.; Bensch, KG.; Wong, J. Invasion of reconstituted basement membrane matrix by metastatic human-tumor cells. *Cancer Res.*, **1986**, 46, 1980–1989.

[24] Benbow, U.; Schoenermark, MP.; Orndorff, KA.; Givan, AL.; Brinckerhoff, CE. Human breast cancer cells activate procollagenase-1 and invade type I collagen: invasion is inhibited by all-trans retinoic acid. *Clin. Exp. Metastasis*, **1999**, 17, 231–238.

[25] Soares-Maia, R.; Faustino-Rocha, AI.; Teixeira-Guedes, CI.; Pinho-Oliveira, J.; Talhada, D.; Rema, A.; Faria, F.; Ginja, M.; Ferreira, R.; Gil da Costa, RM.; Oliveira, PA.; Lopes, C. MNU-induced rat mammary carcinomas: immunohistology and estrogen receptor expression. *J. Environ. Pathol. Toxicol. Oncol.*, **2013**, 32, 157–163.

[26] Blank, U. The mechanism of exocytosis in mast cells. In *Mast cell biology*:

contemporary and emerging topics (Gilfillan, A. M. and Metcalfe, D. D., eds), **2011**, pp. 107–122, Springer.

[27] Ribatti, D.; Crivellato, E. Mast cells and tumors. In *Mast cells and tumors: from biology to clinic* (Ribatti, D. and Crivellato, E, eds), **2011**, pp. 83–88, Springer.

CHAPTER 7

EFFECTS OF LIFELONG EXERCISE TRAINING ON MAMMARY TUMORIGENESIS INDUCED BY MNU IN FEMALE SPRAGUE- DAWLEY RATS

THE CONTENT OF THIS CHAPTER WAS PUBLISHED IN:

Faustino-Rocha AI, Gama A, Oliveira PA, Alvarado A, Neuparth MJ, Ferreira R, Ginja M. 2016. Effects of lifelong exercise training on mammary tumorigenesis induced by MNU in female Sprague-Dawley rats. *Clinical and Experimental Medicine* 17 (2): 151-160. DOI: 10.1007/s10238-016-0419-0. (Full paper)

Faustino-Rocha AI, Gama A, Oliveira PA, Alvarado A, Ferreira R, Ginja M. 2015. Effects of lifelong exercise training on the expression of estrogen receptors α and β in rat mammary tumors. *Laboratory Animals* 49 (Suppl 3): 40. DOI: 10.1177/0023677215601807. (Abstract)

Faustino-Rocha AI, Gama A, Oliveira PA, Ferreira R, Ginja M. 2015. Inflammation in healthy animals and animals with mammary tumors: effects of lifelong exercise training. *Laboratory Animals* 49 (Suppl 3): 59. DOI: 10.1177/0023677215601807. (Abstract)

Faustino-Rocha AI, Gama A, Oliveira PA, Alvarado A, Vala H, Ferreira R, Ginja M. 2015. Expression of estrogen receptors-alpha and beta in chemically-induced mammary tumors. *Virchows Archiv* 467 (Suppl 1): S51. DOI: 10.1007/s00428-015-1805-9. (Abstract)

Faustino-Rocha AI, Gama A, Oliveira PA, Alvarado A, Ferreira R, Ginja M. 2015. Effects of lifelong exercise training on the expression of estrogen receptors α and β in rat mammary tumors. I Congresso Ibérico de Ciências de Animais de Laboratório - XIII Congresso SECAL - III Congresso SPCAL, 18th to 20th November, Cáceres, Spain. (Oral presentation)

Faustino-Rocha AI. 2015. Exercício físico e cancro: potencial efeito benéfico. Seminário de Saúde Pública - Investigação Biomédica em Saúde Pública, 13th April, Vila Real, Portugal. (Oral presentation)

Faustino-Rocha AI, Gama A, Talhada D, Teixeira-Guedes CI, Duarte JA, Ferreira R, Oliveira PA 2013. Avaliação do potencial efeito benéfico do exercício físico no cancro

da mama. III Jornadas de Saúde Pública, 2nd November, Vila Real, Portugal. (Oral presentation)

Faustino-Rocha AI, Gama A, Oliveira PA, Ferreira R, Ginja M. 2015. Inflammation in healthy animals and animals with mammary tumors: effects of lifelong exercise training. I Congresso Ibérico de Ciências de Animais de Laboratório - XIII Congresso SECAL - III Congresso SPCAL, 18th to 20th November, Cáceres, Spain. (Poster presentation)

Faustino-Rocha AI, Gama A, Oliveira PA, Vala H, Ferreira R, Ginja M. 2015. Expression of estrogen receptors-alpha and beta in chemically-induced mammary tumors. 27th European Congress of Pathology (ECP), 5th to 9th September, Belgrade, Serbia. (Poster presentation)

Faustino-Rocha AI, Gama A, Oliveira PA, Moutinho M, Ferreira R, Ginja M. 2015. Biochemical profile of female Sprague-Dawley rats with chemically-induced mammary cancer. VIII Jornadas de Bioquímica UTAD. 15th to 16th April, University of Trás-os-Montes and Alto Douro, Vila Real, Portugal. (Poster presentation)

Faustino-Rocha AI, Ferreira R, Duarte JA, Oliveira PA. 2014. Effects of long-term physical exercise on breast cancer development. Congresso de Ciências do Desporto, Exercício e Saúde. 1st to 3rd May, University of Trás-os-Montes and Alto Douro, Vila Real, Portugal. (Poster presentation)

7. Effects of lifelong exercise training on mammary tumorigenesis induced by MNU in female Sprague-Dawley rats

Abstract

Breast cancer is the most common malignancy in women worldwide. Several studies have suggested that exercise training may decrease the risk of breast cancer development. This study aimed to evaluate the effects of long-term exercise training on mammary tumorigenesis in an animal model of mammary cancer. Fifty female Sprague-Dawley rats were randomly divided into four groups: MNU sedentary, MNU exercised, control sedentary and control exercised. Animals from MNU groups received an intraperitoneal administration of *N*-methyl-*N*-nitrosourea (MNU). Animals were exercised on a treadmill during 35 weeks. When animals were killed, blood samples were collected to determine the hematocrit and to perform the biochemical analysis. Mammary tumors were collected and histologically evaluated; the expression of estrogen receptors (ERs) α and β was evaluated in tumor sections by immunohistochemistry. All survived animals from both MNU groups developed mammary tumors. The number of mammary tumors ($p>0.05$) and lesions ($p=0.056$) was lower in MNU exercised animals when compared with MNU sedentary animals. MNU exercised animals showed lower number of malignant lesions when compared with MNU sedentary animals ($p=0.020$). C-reactive protein (CRP) serum concentration was lower in exercised animals; however, the levels of 17- β estradiol were higher in exercised animals. Tumors from exercised animals exhibited higher expression of ER α when compared with tumors from sedentary animals ($p<0.05$). This study analyzes the impact of the longest exercise training protocol on mammary tumorigenesis ever performed. We concluded that the lifelong endurance training has beneficial effects on mammary tumorigenesis in female rats (reduced the inflammation, the number of mammary tumors and lesions, and malignancy). Additionally, the mammary tumors from MNU exercised group exhibited higher immunoexpression of ER α that is an indicator of well-differentiated tumors and better response to hormone therapy.

Keywords: estradiol, estrogen receptors, exercise, mammary tumors, MNU

7.1. Introduction

Breast cancer is so far the most commonly diagnosed cancer among women worldwide, with an estimated 1.67 million new cases diagnosed worldwide in 2012 (25% of all cancers) [1,2]. Breast cancer development is associated with several risk factors, namely estrogen exposure (early menarche, late menopause, hormone replacement therapy), nulliparity, obesity, family history and mutation in the Breast Cancer gene (*BRCA*) 1 and *BRCA*2 [3–6].

According to several authors, the longer the estrogen exposure, the higher is the breast cancer risk [3,6]. Estrogens are steroid hormones mainly produced from the precursor cholesterol in the male and female gonads (testis and ovaries), but they may also be produced in brain, adrenal gland and in adipose tissue [7,8]. There are nine estrogens in humans, being the 17- β estradiol the predominantly circulating estrogen and the most biologically active [9].

Nowadays, it is known that estrogens act by binding to two specific nuclear receptors: estrogen receptors (ERs) α and β . ER α is highly expressed in the pituitary, ovary, uterus, testis, prostate, epididymis, kidney and adrenal gland, while ER β is highly expressed in ovary, prostate and lung, and moderately expressed in testis and uterus [10,11]. These receptors are also expressed in normal mammary gland, being ER β the most expressed [12]. In clinical practice, the ER α is a well-established marker in mammary cancer; it reflects the biology of the tumor and the prognosis, and it is used as a predictive factor of responsiveness to endocrine therapy [13,14]. Despite several years of research on this field, the specific role played by ER β in mammary cancer is not fully understood. However, it seems that when it is simultaneously expressed with ER α , they have opposite functions: the ER α acts as a proliferation promoter, while ER β has pro-apoptotic and pro-differentiating functions [15].

The concept that breast cancer may be preventable by lifestyle, namely physical activity, is supported by epidemiologic data worldwide [16]. Among the potential anticancer effects of physical activity are the decrease in endogenous sex hormone concentrations and exposure (later age of menarche, decreased estrogen concentrations, decreased number of ovulatory cycles), favorable changes in body weight, insulin resistance, up-regulation in immune system and chronic low-grade inflammation [1,17–21]. However, there is a need for consistent molecular evidences of the putative

preventive effect of exercise training programs to allow the public to better understand the benefits of an active lifestyle. In order to give new insights on the impact of lifelong exercise training on mammary tumorigenesis, we used a recognized animal model of breast cancer that was submitted to treadmill exercise during 35 weeks. The *N*-methyl-*N*-nitrosourea (MNU)-induced mammary cancer in rats is the most used model to study mammary carcinogenesis [22,23]. To our knowledge, this is the first study to evaluate the effects of the long-term exercise training on rat mammary tumorigenesis.

7.2. Material and Methods

7.2.1. Animals

Fifty female Sprague-Dawley rats with 4-5 weeks of age were purchased from Harlan Laboratories Inc. (Barcelona, Spain). Animals were maintained in the facilities of the University of Trás-os-Montes and Alto Douro, under controlled conditions of temperature ($23\pm 2^{\circ}\text{C}$), humidity ($50\pm 10\%$), air system filtration (10-20 ventilations/hour) and on a 12h:12h light:dark cycle. A standard diet (4RF21[®], Mucedola, Settimo Milanese, Milan, Italy) and tap water were provided *ad libitum*. All procedures were made in accordance with the European Directive 2010/63/EU and approved by the Portuguese Ethics Committee for Animal Experimentation (approval no. 008961).

7.2.2. Experimental design

After one week of quarantine and two weeks of acclimatization to the environmental conditions, animals were randomly assigned to four experimental groups: MNU sedentary (n = 15), MNU exercised (n = 15), control sedentary (n = 10) and control exercised (n = 10) groups. At seven weeks of age, animals from MNU groups received an intraperitoneal injection of MNU (ISOPAC[®], Sigma Aldrich S.A., Madrid, Spain) at a dose of 50 mg/kg of body weight; animals from control groups received a single administration of the vehicle (saline solution 0.9%). After MNU and vehicle administration, animals from exercised groups (MNU and control) were acclimated to treadmill running (Treadmill Control[®] LE 8710, Panlab, Harvard Apparatus, Holliston, MA, USA) for a five-day period at a speed of 20 m/min increasing progressively from 20 to 60 min/day. After this acclimatization period, animals were exercised at a speed of 20

m/min, 60 min/day, five times a week, during 35 weeks. The exercise protocol was conducted during the 12h dark period of the light:dark cycle. Rats from sedentary groups (MNU and control) remained in their cages, and they were daily handled in order to be exposed to similar conditions to the exercised animals. Animals' body weight was measured on a weekly basis with a top-loading scale (Mettler PM4000, LabWrench, Midland, ON, Canada). Animals were monitored twice a day to assess their health status and the appearance of the first mammary tumor. At the end of the experimental protocol, mortality index (MI) was calculated according to the formula:

$$MI = \frac{\text{Number of animals that died during the study}}{\text{Number of animals at the beginning of the study}} \times 100.$$

7.2.3. Animals' killing

Thirty-five weeks after MNU administration (female rats with 42 week of age) all survived animals were killed by intraperitoneal administration of ketamine (75 mg/kg of body weight, Imalgene[®] 1000, Merial S.A.S., Lyon, France) and xylazine (10 mg/kg of body weight, Rompun[®] 2%, Bayer Healthcare S.A., Kiel, Germany), followed by exsanguination by cardiac puncture as indicated by the Federation of European Laboratory Animal Science Associations [24]. Blood samples were collected from the inferior vena cava directly into capillary tubes and tubes with separator gel. The tubes were centrifuged for 5 min at 5000×g, and the serum was obtained and stored at -80°C for biochemical determinations.

Animals were skinned and the skin was evaluated under a light; the number and weight of mammary tumors were recorded. Tumor volume (V) was calculated based on their weight as previously described by Faustino-Rocha *et al.* [25]. Animal accurate body weight was obtained by the subtraction of tumor weight to the total body weight. The organs were also collected and weighed. Mammary tumors and all organs were immersed in phosphate-buffered formaldehyde during 12 hours.

7.2.4. Blood samples analysis

Hematocrit was determined immediately after centrifugation of the capillary tubes. The serum concentrations of interleukin (IL)-6 and C-reactive protein (CRP) were determined by immunoblotting. In brief, serum samples were diluted (1:20) in Tris-buffered saline (TBS; 100 mM Tris, 1.5 mM NaCl, pH8.0) and 100 μ L was slot-blotted into a nitrocellulose membrane (Whatman, Protan). Then, nonspecific binding was blocked with 5% (w/v) dry nonfat milk in TBS-T (TBS and 0.5% Tween 20). Membranes were incubated with primary antibodies diluted 1:1000 in 5% (w/v) nonfat free milk in TBS-T (rabbit monoclonal anti-CRP antibody (ab32412, Abcam, Cambridge, UK) and rabbit polyclonal anti-IL6 (ab6672 Abcam, Cambridge, UK)) for 2 hours at room temperature, washed and incubated with secondary horseradish peroxidase-conjugated anti-rabbit or anti-mouse (1:1000, General Electric Healthcare, Milwaukee, WI, USA). Immunoreactive bands were detected by enhanced chemiluminescence (ECL) (Amersham Pharmacia Biotech) according to the manufacturer's procedure, and images were recorded using X-ray films (Kodak Biomax Light Film, Sigma, St. Louis, MO, USA). The films were scanned in Molecular Imager[®] Gel Doc XR System (Bio-Rad, Hercules, CA, USA) and analyzed with Quantity One software (version 4.6.3 Bio-Rad, Hercules, CA, USA).

Serum levels of 17- β estradiol were determined using a commercial enzyme-linked immunosorbent assay (ELISA) kit according to manufacturer's instructions (ab108667, Abcam, Cambridge, UK). Serum albumin, total protein, cholesterol, high-density lipoprotein (HDL), low density lipoprotein (LDL), triglycerides, glucose, alanine aminotransferase (ALT), creatinine and creatine kinase were measured in duplicate on an AutoAnalyzer (Prestige 24i, Cormay PZ, Diamond Diagnostics, Holliston, MA, USA).

7.2.5. Histological and immunohistochemical analysis

After fixation, mammary tumors were processed for routine histological evaluation. Paraffin two- μ m-thick sections were stained with hematoxylin and eosin (H&E), and mammary tumor lesions were histologically evaluated under a light microscopy by a pathologist and classified according to Russo and Russo [26].

Immunohistochemical detection of ERs α and β was performed using the standard protocol of NovoLink Polymer Detection System (Leica Biosystems, Newcastle, UK). Sections were incubated during one and half hour at room temperature with primary antibodies for ER α (clone 6F11, Novocastra, Newcastle, UK) and for ER β (clone MCA1974S, AbD Serotec, Oxford, UK) at a dilution of 1:50. To quantify the immunoexpression of both ERs α and β , at least 1000 neoplastic cells were evaluated *per* lesion [27] and the percentage of immunopositive cells was calculated. Additionally, the staining was assigned at four levels: level 0 (unstained), level 1 (weak staining), level 2 (moderate staining) and level 3 (intense staining). Normal mammary gland with and without the primary antibody was used as positive and negative control, respectively.

7.2.6. Statistical analysis

Data were statistically analyzed with Statistical Package for the Social Sciences (SPSS[®], version 23 for Windows, SPSS Inc., Chicago, IL, USA) using independent sample *t*-test and analysis of variance (ANOVA) with the Bonferroni correction for multiple comparisons. Histological results were analyzed using Chi-square tests. All data were expressed as mean \pm standard deviation (S.D.); *p* values lower than 0.05 were considered statistically significant.

7.3. Results

7.3.1. Animals

Animals from exercised groups (MNU and control) were successfully adapted to the exercise protocol with the exception of one rat that from MNU exercised group that was excluded from the study (MNU exercised group consisted of 14 animals). Nine animals died along the experimental protocol: four animals from MNU sedentary group (MI=27%), four animals from MNU exercised group (MI=29%) and one animal from control sedentary group (MI=10%); data from these animals were excluded from the study. At the end of the experiment, animal accurate body weight was lower in MNU groups when compared with control ones; however, these differences did not reach the level of statistical significance ($p>0.05$) (Table 7.1). The spleen weight was higher in animals from MNU groups when compared with animals from control groups; the

differences reached the level of statistical significance between MNU sedentary and control sedentary groups ($p < 0.05$) (Table 7.2). These data are suggestive of an inflammatory response due to the process of carcinogenesis [28,29].

Table 7.1. Final body weight, tumor weight and accurate body weight (mean \pm S.D.).

Group		Final body weight (g)	Tumor weight (g)	Accurate body weight (g)
MNU groups	Sedentary	290.30 \pm 17.45	13.35 \pm 17.70	278.16 \pm 22.19
	Exercised	296.73 \pm 24.73	19.10 \pm 24.28	279.54 \pm 25.05
Control groups	Sedentary	294.64 \pm 18.05	-	294.64 \pm 18.05
	Exercised	296.87 \pm 24.70	-	296.87 \pm 24.70

Statistically significant differences were not found ($p > 0.05$).

Table 7.2. Organs' weight in all groups at the end of the experiment (mean \pm S.D.).

Organ weight (g)	MNU groups		Control groups	
	Sedentary	Exercised	Sedentary	Exercised
Heart	1.26 \pm 0.17	1.25 \pm 0.15	1.15 \pm 0.09	1.13 \pm 0.08
Lung	1.70 \pm 0.11	1.62 \pm 0.13	1.66 \pm 0.16	1.65 \pm 0.18
Liver	10.04 \pm 1.89	10.85 \pm 1.70	8.52 \pm 1.03	9.25 \pm 0.96
Spleen	1.77 \pm 1.29 ^a	1.53 \pm 0.62	0.72 \pm 0.13	0.70 \pm 0.09
Left kidney	1.31 \pm 0.58	1.12 \pm 0.15	1.09 \pm 0.14	1.08 \pm 0.12
Right kidney	1.24 \pm 0.24	1.17 \pm 0.17	1.21 \pm 0.14	1.14 \pm 0.14

^a $p < 0.05$ versus control sedentary.

7.3.2. Blood samples analysis

The results obtained from blood samples analysis are listed in Table 7.3. The serum levels of total protein and HDL were lower in MNU groups when compared with control groups ($p < 0.05$). Similarly, the animals from MNU groups exhibited lower hematocrit, albumin, ALT, cholesterol, LDL, triglycerides and glucose when compared with respective control groups, though not statistically significant ($p > 0.05$). Inversely, the creatine kinase levels were higher in MNU sedentary and exercised groups when compared with respective control groups; however, the difference was not of sufficient magnitude to reach the level of statistical significance ($p > 0.05$).

The IL-6 and CRP serum concentrations were higher in MNU groups when compared with control ones, more notorious for CRP levels ($p < 0.05$). Nevertheless, in general the serum levels of IL-6 and CRP were lower in exercised animals than in sedentary animals in both MNU and control groups, which supports the anti-inflammatory effects of lifelong exercise training [29]. Curiously, the serum levels of 17- β estradiol were higher in exercised groups (MNU and control) when compared with respective sedentary groups; however, a statistically significant difference was only observed between MNU sedentary and MNU exercised groups ($p < 0.05$).

Table 7.3. Characterization of animals' response to MNU-induced mammary tumors and physical exercise: biochemical profile (mean \pm S.D.).

Parameter	MNU groups		Control groups	
	Sedentary	Exercised	Sedentary	Exercised
Hematocrit (%)	39.68 \pm 11.48	40.00 \pm 9.54	43.28 \pm 2.79	44.35 \pm 1.94
Total protein (mg/dL)	55.37 \pm 4.03 ^a	54.37 \pm 8.11 ^b	64.80 \pm 3.80	61.24 \pm 3.94
Albumin (mg/dL)	39.56 \pm 3.01	37.46 \pm 5.62	40.73 \pm 1.36	39.56 \pm 3.02
ALT (U/L)	53.20 \pm 24.24	49.34 \pm 13.78	53.38 \pm 13.78	54.94 \pm 11.72
Creatinine (mg/dL)	0.45 \pm 0.06	0.45 \pm 0.09	0.44 \pm 0.05	0.46 \pm 0.06
Creatine kinase (U/L)	487.19 \pm 327.30	476.26 \pm 256.84	415.54 \pm 189.14	420.31 \pm 121.97
Cholesterol (mg/dL)	87.51 \pm 17.99	88.35 \pm 40.51	107.56 \pm 6.78	106.19 \pm 18.44
HDL (mg/dL)	21.77 \pm 5.57 ^a	27.08 \pm 7.58	33.39 \pm 2.43	33.91 \pm 9.43
LDL (mg/dL)	384.46 \pm 139.56	370.24 \pm 150.78	466.67 \pm 275.26	459.27 \pm 101.95
Triglycerides (mg/dL)	56.22 \pm 21.43	57.19 \pm 11.80	59.03 \pm 17.55	58.65 \pm 17.25
Glucose (mg/dL)	300.88 \pm 56.89	287.43 \pm 86.62	322.27 \pm 76.10	306.57 \pm 59.31
IL-6 (AU)	1170.75 \pm 89.36	1042.00 \pm 137.88	939.80 \pm 345.25	856.00 \pm 142.84
CRP (AU)	1293.67 \pm 152.03 ^a	1138.83 \pm 171.06	1082.40 \pm 146.76	1086.33 \pm 113.49
17- β estradiol (pg/mL)	17.43 \pm 3.21 ^c	22.74 \pm 6.19	18.39 \pm 4.61	20.54 \pm 7.60

^a $p < 0.05$ versus control sedentary; ^b $p < 0.05$ versus control exercised; ^c $p < 0.05$ versus MNU exercised.

7.3.3. Mammary tumors

Animals from control groups (sedentary and exercised) did not develop any mammary tumor, and except one animal that died during the experiment, they maintained healthy along all the experiment. All animals from both MNU sedentary and MNU exercised groups developed mammary tumors (incidence of 100%). The first mammary tumor was recorded in MNU sedentary group ten weeks after MNU administration; in the MNU exercised group, the first mammary tumor was identified two weeks later, at the 12th week after MNU administration (Figure 7.1). At the end of the study, the number of mammary

tumors was higher in MNU sedentary group (28 mammary tumors; 2.55 ± 1.44 tumors *per* animal) when compared with MNU exercised group (23 mammary tumors; 2.30 ± 1.42 tumors *per* animal); however, none of these differences was of sufficient magnitude to reach the level of statistical significance ($p > 0.05$).

Tumor weight was higher in MNU exercised animals when compared with MNU sedentary ones ($p > 0.05$) (Table 7.1). Although numerical difference exists, tumor volume was also not statistically different between MNU exercised and sedentary animals ($7.87 \text{ cm}^3 \pm 12.24$ *versus* $4.88 \text{ cm}^3 \pm 9.86$ for MNU exercised and MNU sedentary groups, respectively) ($p > 0.05$).

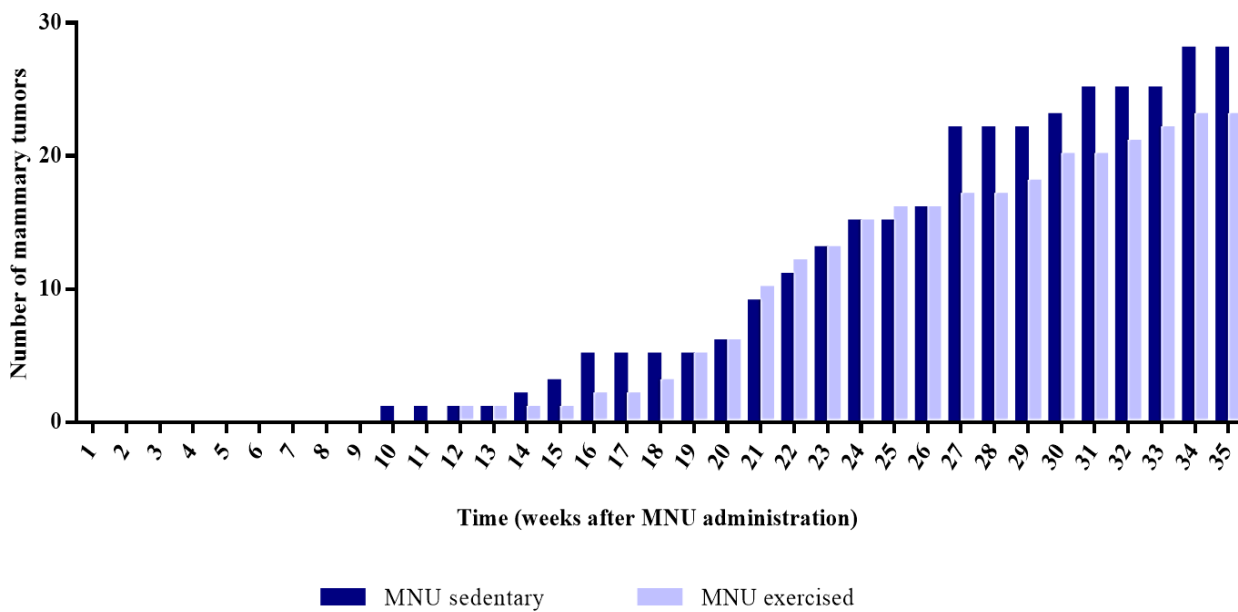


Figure 7.1. Effects of exercise training on carcinogenic response of the mammary gland: cumulative number of mammary tumors in MNU sedentary and MNU exercised groups during the experimental protocol. Statistically significant differences between groups were not found ($p > 0.05$).

7.3.4. Histological and immunohistochemical analysis

The histological classification of the mammary tumors is summarized in Table 7.4. Histological evaluation revealed that each macroscopic mammary tumor exhibited distinct histological lesions. The total number of mammary lesions was lower in MNU exercised group when compared with MNU sedentary group; however, this difference did not reach the level of statistical significance ($p=0.056$). The number of benign and preneoplastic lesions was similar between both MNU sedentary and MNU exercised groups ($p=0.593$ and $p=0.655$, respectively). Nevertheless, the number of malignant mammary lesions was lower in MNU exercised animals when compared with MNU sedentary animals ($p=0.020$). It was also observed that the animals from group MNU exercised developed lower number of invasive carcinomas and did not develop any invasive comedocarcinoma, which was the most aggressive mammary lesion identified in this study (Table 7.4).

All mammary lesions from both MNU sedentary and MNU exercised groups exhibited positive immunostaining for ERs α and β . The immunostaining for ER α was observed in the nuclei of luminal epithelial cells, while the immunostaining for ER β was observed in the nuclei for both epithelial and stromal components (Figure 7.2). In both MNU sedentary and MNU exercised groups, the percentage of immunopositive cells for ER β was higher when compared with the percentage for ER α ($p<0.05$). The immunoexpression for ER α was higher in MNU exercised group when compared with MNU sedentary group ($p<0.05$); however, the immunoexpression for ER β was similar between groups ($p>0.05$) (Table 7.5). The intensity of the staining for ER α (2.56 ± 0.67 and 2.64 ± 0.72 for MNU sedentary and MNU exercised groups, respectively) and for ER β (2.32 ± 0.73 and 2.44 ± 0.67 for MNU sedentary and MNU exercised groups, respectively) was not different between groups ($p>0.05$).

Table 7.4. Histological classification of mammary tumors developed by animals from MNU sedentary and exercised groups.

	Lesions	Number of lesions	
		MNU sedentary	MNU exercised
Benign lesions	Intraductal papilloma	19	8
	Papillary cystadenoma	0	5
	Tubular adenoma	4	6
	Lactating adenoma	0	1
	Fibroma	0	1
	Fibroadenoma	7	5
	Total:	30^a	26
Preneoplastic lesions	Intraductal proliferation	2^b	3
	Papillary non-invasive carcinoma	16	8
Malignant lesions	Cribriform non-invasive carcinoma	11	8
	Papillary invasive carcinoma	5	4
	Cribriform invasive carcinoma	5	1
	Comedo invasive carcinoma	2	0
	Total:	39^c	21
Total number of lesions:		71^d	50

Bold italic values indicate the number of lesions according to their malignancy (benign lesions, preneoplastic lesions and malignant lesions). Bold values indicate the total number of lesions. ^a $p=0.593$; ^b $p=0.655$; ^c $p=0.020$; ^d $p=0.056$.

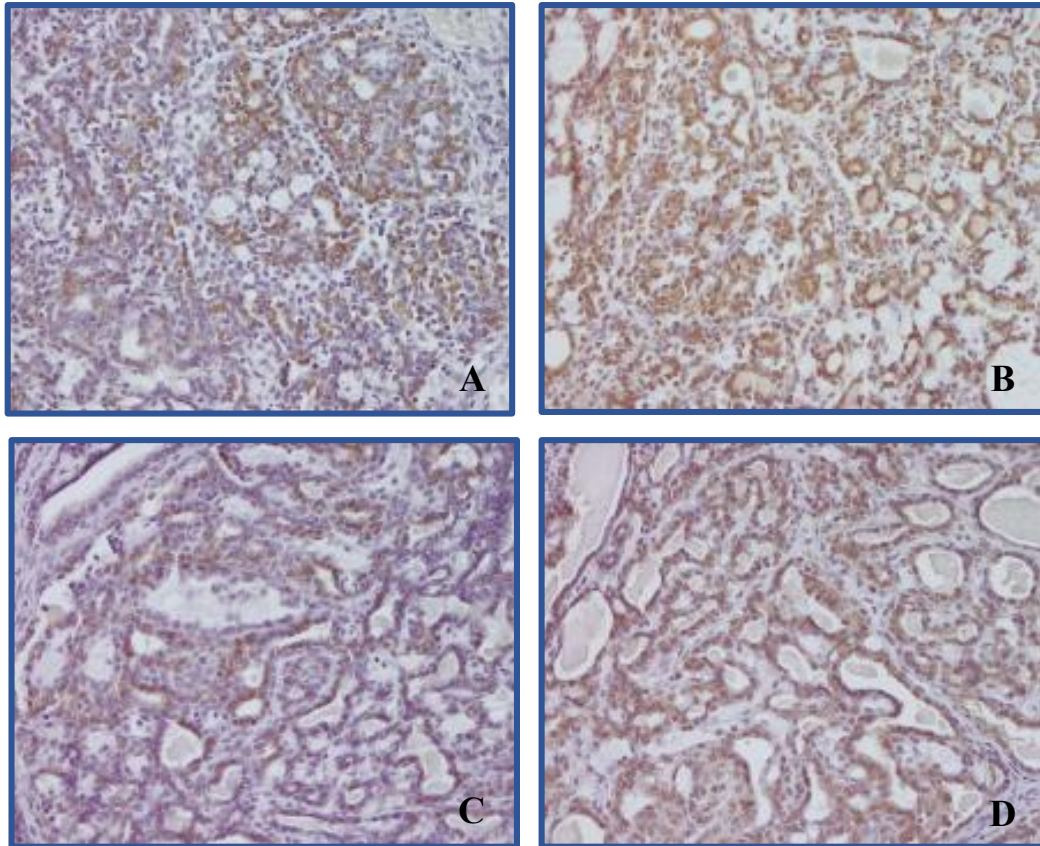


Figure 7.2. Immunohistochemical staining for ERs α (A and C) and β (B and D) in mammary tumors from sedentary (A and B) and exercised (C and D) animals. ER α staining was observed in the nuclei of epithelial cells, while the ER β staining was seen in the nuclei of epithelial and some stromal cells. Statistically significant differences were found in the immunoexpression of ER α between groups ($p < 0.05$). Statistically significant differences were also observed between the immunoexpression of ER α and ER β in both groups ($p < 0.05$). Magnification of 200 \times in all images.

Table 7.5. Immunohistochemical expression of estrogen receptors α and β in MNU groups (% of immunopositive cells) (mean \pm S.D.).

Estrogen receptor (ER)	MNU sedentary (n=71)	MNU exercised (n=50)
ER α (%)	55.14 \pm 13.26 ^{a,b}	61.57 \pm 13.49 ^b
ER β (%)	70.06 \pm 18.5	70.70 \pm 15.08

^a Statistically different from ER α immunoexpression in MNU exercised group ($p < 0.05$); ^b Statistically different from ER β immunoexpression ($p < 0.05$).

7.4. Discussion

The association between exercise and mammary cancer is not consensual in the literature, which may be justified, at least in part, by the fact that the majority of the studies are epidemiological; in addition to this, the existing animal model based studies are characterized by distinct protocols of exercise training. To give new insights on this association, we analyzed the histological changes, and ER α and ER β expression in the mammary tumors of rats submitted to treadmill exercise since infancy. The rat model of MNU-induced mammary tumors reflects important aspects of women breast tumorigenesis, namely the estrogen-dependence and ductal-lobular organization [30,31].

No statistically significant differences in body weight between exercised (MNU and control) and sedentary animals (MNU and control) were observed in the present study, similarly to that previously reported for MNU-induced mammary tumorigenesis [21,32]. The IL-6 and CRP serum concentrations and the spleen weight were higher in MNU groups (sedentary and exercised) when compared with control groups (sedentary and exercised), suggesting the occurrence of an interplay between the tumor and the immune system. Exercise training prevented tumor-induced increase in CRP and spleen weight ($p > 0.05$), which suggest that treadmill exercise reduced mammary tumor-related inflammation [33–35]. Our research team had recently verified that the exercise training prevented the increase in serum and cardiac levels of the pro-inflammatory cytokine TWEAK promoted by cancer [36].

Lifelong exercise training also impacted mammary tumorigenesis. Indeed, MNU-exposed animals that performed 35 weeks of exercise training showed a lower number of mammary tumors (23 *versus* 28 mammary tumors in MNU exercised and MNU sedentary animals, respectively; Figure 7.1). A similar effect was previously reported in MNU rats submitted to four weeks of exercise training. In fact, Whittal-Strange *et al.* [32] identified 33 mammary tumors in MNU exercised animals and 58 in MNU sedentary ones. Moreover, in exercised animals, the tumors appeared later (week 12 after MNU administration in MNU exercised group *versus* week 10 after MNU administration in MNU sedentary group), similarly to that observed by Westerlind and collaborators [22]. However, the tumor weight and volume were higher in MNU exercised animals, which is not in accordance with the results previously described by Whittal-Strange *et al.* [32]. As the animals of this experiment were exercised during a longer period, these different results may be associated with the improvement of blood perfusion of mammary tumors induced by exercise training [18]. We also observed that the expression of vascular endothelial growth factor (VEGF)-A and the mean number of microvessels were higher in exercised animals [37]. Although there was a numerical difference in the carcinogenic response (number, volume and weight of mammary tumors) between MNU sedentary and exercised groups, it did not reach the level of statistical significance.

Histological analysis revealed that the total number of mammary lesions was lower in MNU exercised group (50 mammary lesions) when compared with MNU sedentary group (71 mammary lesions) ($p=0.056$). The number of malignant mammary lesions was also lower in MNU exercised animals (21 malignant lesions in MNU exercised group *versus* 39 malignant lesions in MNU sedentary animals) ($p=0.020$). Interestingly, we verified that MNU exercised animals developed five invasive carcinomas (papillary or cribriform), while animals from group MNU sedentary developed 12 invasive carcinomas (papillary, cribriform or comedo). It is also important to note that the animals from MNU exercised group did not develop any invasive comedocarcinoma, which was the most aggressive mammary lesion identified in this experiment. These data are also suggestive of beneficial effects of physical exercise on the malignancy of mammary tumors.

Immunohistochemistry has been used by several researchers to evaluate the expression of ERs in mammary glands [38–40]. Although human mammary tumors are classified as positive or negative for ER only based on the evaluation of ER α , it is important to note

that approximately 59% of human mammary tumors simultaneously express ER α and ER β , and 17% of them only express ER β [40,41]. So, it seems also important to clarify the role of ER β in mammary carcinogenesis.

As previously reported by other investigators, in the present work, ERs α and β were co-expressed in the cell nuclei; the ER α was only expressed in the luminal epithelial cells, while the ER β was also expressed in the surrounding stroma [42,43]. All mammary lesions from both MNU groups simultaneously expressed ERs α and β , but the expression of ER β was higher when compared with the expression of ER α ($p < 0.05$). In a previous study performed by Allred *et al.* [30] using the same animal model, it was observed that the majority of mammary tumors evaluated by immunohistochemistry expressed ER α . It was also previously observed that there are more cells in the rodent mammary gland expressing ER β than ER α ; the ER β is always present and the percentage of immunopositive cells for this receptor is around 30-47%, while the ER α is rarely expressed [12]. Taking this into account, it seems that the expression of ERs α and β was increased in MNU-induced mammary tumors. This is in accordance with previous reports that observed an increase in the ratio of ER α /ER β during human breast carcinogenesis [33,34]. Moreover, the enhancement of ER α expression was higher in tumors from exercised animals than in sedentary ones ($p < 0.05$). This highest enhancement of ER α in mammary tumors from MNU exercised group may be beneficial, since the low levels of this receptor are associated with poorly differentiated breast tumors (less differentiated tumors are more aggressive) and with a unfavorable response to different therapeutic approaches, namely endocrine therapy and surgery [35].

The high expression of ER β observed in all induced mammary tumors has probably stimulated their differentiation and inhibited their proliferation. Several studies described that knockout ER α mice did not develop a functional mammary gland (mammary ducts and the ductal tree were very rudimentary), while knockout ER β mice developed normal mammary glands, although with a decreased differentiation and increased proliferation in the alveoli of lactating mammary glands [44–47]. In an *in vitro* study using MCF7 breast cancer cell line and HC11 mouse mammary cells that simultaneously express ER α and ER β , it was demonstrated that two different pathways are activated by 17- β estradiol, leading to proliferation by the stimulation of only ER α and to apoptosis by the stimulation of only ER β . The simultaneous activation of both pathways is responsible for the

inhibition of proliferation and enhancement in apoptosis [42,48]. When compared with tumors that only express ER α , human mammary tumors that co-express both receptors have a more favorable prognosis and low aggressiveness [49,50].

According to some studies, the serum concentrations of estradiol have been found to be higher in human patients with malignant breast tumors compared to patients with nonmalignant breast tumors [51]. Inversely to that was expected, the serum levels of 17- β estradiol were higher in animals from MNU exercised group, which developed lower number of malignant mammary tumors. Similarly, Hao *et al.* [52] and Rauf *et al.* [53] verified that the serum levels of 17- β estradiol were higher in Sprague-Dawley rats exercised for 12 weeks ($p>0.05$). Data seem to suggest that serum levels of 17- β estradiol are associated with ER α /ER β expression in mammary tumors but not with their aggressiveness.

7.5. Conclusion

To our knowledge, this is the first study that has evaluated the effects of the lifelong moderate exercise training on mammary tumorigenesis after carcinogen exposure. Exercise training reduced the inflammation and inhibited the carcinogenic response, reducing cancer incidence, multiplicity and burden, and increasing the cancer latency. Additionally, all mammary tumors simultaneously expressed ERs α and β , suggesting that the proliferation was inhibited and the apoptosis was induced. The mammary tumors from MNU exercised group exhibited higher immunoexpression of ER α , which is an indicator of tumor differentiation and better response to hormone therapy. More studies are needed to clarify the relation of 17- β estradiol serum levels with the aggressiveness of mammary tumors and the practice of physical exercise.

7.6. References

- [1] Harvie, M.; Howell, A.; Evans, DG. Can diet and lifestyle prevent breast cancer: what is the evidence? *Am. Soc. Clin. Oncol.*, **2015**, 35, 66–73.
- [2] Siegel, R.; Naishadham, D.; Jemal, A. Cancer statistics, 2012. *CA Cancer J. Clin.*, **2012**, 62, 10–29.
- [3] Brekelmans, CTM. Risk factors and risk reduction of breast and ovarian cancer.

- Curr. Opin. Obstet. Gynecol.*, **2003**, 15, 63–68.
- [4] Hunter, DJ.; Kelsey, KT. Pesticide residues and breast cancer: the harvest of a silent spring. *J. Natl. Cancer Inst.*, **1993**, 85, 598–599.
- [5] Kelsey, JL.; Gammon, MD. Epidemiology of breast cancer. *Epidemiol. Rev.*, **1990**, 12, 228–240.
- [6] MacMahon, B. Epidemiology and the causes of breast cancer. *Int. J. Cancer*, **2006**, 118, 2373–2378.
- [7] Payne, AH.; Hales, DB. Overview of steroidogenic enzymes in the pathway from cholesterol to active steroid hormones. *Endocr. Rev.*, **2004**, 25, 947–970.
- [8] Ghayee, HK.; Auchus, RJ. Basic concepts and recent developments in human steroid hormone biosynthesis. *Rev. Endocr. Metab. Disord.*, **2007**, 8, 289–300.
- [9] Simpson, ER. Sources of estrogen and their importance. *J. Steroid Biochem. Mol. Biol.*, **2003**, 86, 225–230.
- [10] Kuiper, GGJM.; Carlsson, B.; Grandien, K.; Enmark, E.; Haggblad, J.; Nilsson, S.; Gustafsson, JA. Comparison of the ligand binding specificity and transcript tissue distribution of estrogen receptors alpha and beta. *Endocrinology*, **1997**, 138, 863–870.
- [11] Miyakoshi, T.; Miyajima, K.; Takekoshi, S.; Osamura, RY. The influence of endocrine disrupting chemicals on the proliferation of ER alpha knockdown-human breast cancer cell line MCF-7; new attempts by RNAi technology. *Acta Histochem. Cytochem.*, **2009**, 42, 23–28.
- [12] Saji, S.; Jensen, E V.; Nilsson, S.; Rylander, T.; Warner, M.; Gustafsson, JA. Estrogen receptors alpha and beta in the rodent mammary gland. *Proc. Natl. Acad. Sci. U.S.A.*, **2000**, 97, 337–342.
- [13] Rastelli, F.; Crispino, S. Factors predictive of response to hormone therapy in breast cancer. *Tumori*, **2008**, 94, 370–383.
- [14] Ma, CX.; Sanchez, CG.; Ellis, MJ. Predicting endocrine therapy responsiveness in breast cancer. *Oncol. York*, **2009**, 23, 133–142.
- [15] Morani, A.; Warner, M.; Gustafsson, JA. Biological functions and clinical implications of oestrogen receptors alfa and beta in epithelial tissues. *J. Intern. Med.*, **2008**, 264, 128–142.
- [16] Coyle, YM. Physical activity as a negative modulator of estrogen-induced breast

- cancer. *Cancer Causes Control*, **2008**, 19, 1021–1029.
- [17] Adams, SA.; Matthews, CE.; Hebert, JR.; Moore, CG.; Cunningham, JE.; Shu, XO.; Fulton, J.; Gao, YT.; Zheng, W. Association of physical activity with hormone receptor status: the Shanghai breast cancer study. *Cancer Epidemiol. Biomarkers Prev.*, **2006**, 15, 1170–1178.
- [18] Jones, LW.; Eves, ND.; Courneya, KS.; Chiu, BK.; Baracos, VE.; Hanson, J.; Johnson, L.; Mackey, JR. Effects of exercise training on antitumor efficacy of doxorubicin in MDA-MB-231 breast cancer xenografts. *Clin. Cancer Res.*, **2005**, 11, 6695–6698.
- [19] McTiernan, A.; Ulrich, C.; Slate, S.; Potter, J. Physical activity and cancer etiology: associations and mechanisms. *Cancer Causes Control*, **1998**, 9, 487–509.
- [20] Tehard, B.; Friedenreich, CM.; Oppert, JM.; Clavel-Chapelon, F. Effect of physical activity on women at increased risk of breast cancer: results from the E3N cohort study. *Cancer Epidemiol. Biomarkers Prev.*, **2006**, 15, 57–64.
- [21] Westerlind, KC.; McCarty, HL.; Gibson, KJ.; Strange, R. Effect of exercise on the rat mammary gland: implications for carcinogenesis. *Acta Physiol. Scand.*, **2002**, 175, 147–156.
- [22] Westerlind, KC.; McCarty, HL.; Schultheiss, PC.; Story, R.; Reed, AH.; Baier, ML.; Strange, R. Moderate exercise training slows mammary tumour growth in adolescent rats. *Eur. J. Cancer Prev.*, **2003**, 12, 281–287.
- [23] Oberbach, A.; Lehmann, S.; Kirsch, K.; Krist, J.; Sonnabend, M.; Linke, A.; Tonjes, A.; Stumvoll, M.; Bluher, M.; Kovacs, P. Long-term exercise training decreases interleukin-6 (IL-6) serum levels in subjects with impaired glucose tolerance: effect of the-174G/C variant in IL-6 gene. *Eur. J. Endocrinol.*, **2008**, 159, 129–136.
- [24] Forbes, D.; Blom, H.; Kostomitsopulos, N.; Moore, G.; Perretta, G. Euroguide: on the accommodation and care of animals used for experimental and other scientific purposes. *Federation of European Laboratory Animal Science Associations*, **2007**.
- [25] Faustino-Rocha, AI.; Silva, A.; Gabriel, J.; Teixeira-Guedes, CI.; Lopes, C.; Gil da Costa, R.; Gama, A.; Ferreira, R.; Oliveira, PA.; Ginja, M. Ultrasonographic, thermographic and histologic evaluation of MNU-induced mammary tumors in female Sprague-Dawley rats. *Biomed. Pharmacother.*, **2013**, 67, 771–776.

- [26] Russo, J.; Russo, IH. Atlas and histologic classification of tumors of the rat mammary gland. *J. Mammary Gland Biol. Neoplasia*, **2000**, *5*, 187–200.
- [27] Ting, AY.; Kimler, BF.; Fabian, CJ.; Petroff, BK. Characterization of a preclinical model of simultaneous breast and ovarian cancer progression. *Carcinogenesis*, **2007**, *28*, 130–135.
- [28] Ueno, T.; Toi, M.; Saji, H.; Muta, M.; Bando, H.; Kuroi, K.; Koike, M.; Inadera, H.; Matsushima, K. Significance of macrophage chemoattractant protein-1 in macrophage recruitment, angiogenesis, and survival in human breast cancer. *Clin. Cancer Res.*, **2000**, *6*, 3282–3289.
- [29] Murphy, EA.; Davis, JM.; Barrilleaux, TL.; McClellan, JL.; Steiner, JL.; Carmichael, MD.; Pena, MM.; Hebert, JR.; Green, JE. Benefits of exercise training on breast cancer progression and inflammation in C3(1)SV40Tag mice. *Cytokine*, **2011**, *55*, 274–279.
- [30] Allred, CD.; Allred, KF.; Ju, YH.; Clausen, LM.; Doerge, DR.; Schantz, SL.; Korol, DL.; Wallig, MA.; Helferich, WG. Dietary genistein results in larger MNU-induced, estrogen-dependent mammary tumors following ovariectomy of Sprague-Dawley rats. *Carcinogenesis*, **2004**, *25*, 211–218.
- [31] Russo, J.; Russo, IH. Experimentally induced mammary tumors in rats. *Breast Cancer Res. Treat.*, **1996**, *39*, 7–20.
- [32] Whittal-Strange, KS.; Chadau, S.; Parkhouse, WS. Exercise during puberty and NMU induced mammary tumorigenesis in rats. *Breast Cancer Res. Treat.*, **1998**, *47*, 1–8.
- [33] Leygue, E.; Dotzlaw, H.; Watson, PH.; Murphy, LC. Altered estrogen receptor alpha and beta messenger RNA expression during human breast tumorigenesis. *Cancer Res.*, **1998**, *58*, 3197–3201.
- [34] Roger, P.; Sahla, ME.; Makela, S.; Gustafsson, JA.; Baldet, P.; Rochefort, H. Decreased expression of estrogen receptor beta protein in proliferative preinvasive mammary tumors. *Cancer Res.*, **2001**, *61*, 2537–2541.
- [35] Zeleniuch-Jacquotte, A.; Toniolo, P.; Levitz, M.; Shore, RE.; Koenig, KL.; Banarjee, S.; Strax, P.; Pasternack, BS. Endogenous estrogens and risk of breast cancer by estrogen receptor status: a prospective study in postmenopausal women. *Cancer Epidemiol. Biomarkers Prev.*, **1995**, *4*, 857–860.

- [36] Padrao, AI.; Moreira-Goncalves, D.; Oliveira, PA.; Teixeira, C.; Faustino-Rocha, AI.; Helguero, L.; Vitorino, R.; Santos, LL.; Arnado, F.; Duarte, JA.; Ferreira, R. Endurance training prevents TWEAK but not myostatin-mediated cardiac remodelling in cancer cachexia. *Arch. Biochem. Biophys.*, **2015**, 567, 13–21.
- [37] Faustino-Rocha, AI.; Silva, A.; Gabriel, J.; Gil da Costa, R.; Moutinho, M.; Oliveira, P.; Gama, A.; Ferreira, R.; Ginja, M. Long-term exercise training as a modulator of mammary cancer vascularization. *Biomed. Pharmacother.*, **2016**, 81, 273–280.
- [38] Leung, YK.; Lee, MT.; Lam, HM.; Tarapore, P.; Ho, SM. Estrogen receptor-beta and breast cancer: translating biology into clinical practice. *Steroids*, **2012**, 77, 727–737.
- [39] Fox, EM.; Davis, RJ.; Shupnik, MA. ER beta in breast cancer - onlooker, passive player, or active protector? *Steroids*, **2008**, 73, 1039–1051.
- [40] Murphy, L.; Cherlet, T.; Lewis, A.; Banu, Y.; Watson, P. New insights into estrogen receptor function in human breast cancer. *Ann. Med.*, **2003**, 35, 614–631.
- [41] Hammond, MEH.; Hayes, DF.; Dowsett, M.; Allred, DC.; Hagerty, KL.; Badve, S.; Fitzgibbons, PL.; Francis, G.; Goldstein, NS.; Hayes, M.; Hicks, DG.; Lester, S.; Love, R.; Mangu, PB.; McShane, L.; Miller, K.; Osborne, CK.; Paik, S.; Perlmutter, J.; Rhodes, A.; Sasano, H.; Schwartz, JN.; Sweep, FCG.; Taube, S.; Torlakovic, EE.; Valenstein, P.; Viale, G.; Visscher, D.; Wheeler, T.; Williams, RB.; Wittliff, JL.; Wolff, AC. American Society of Clinical Oncology/College of American Pathologists guideline recommendations for immunohistochemical testing of estrogen and progesterone receptors in breast cancer. *J. Clin. Oncol.*, **2010**, 28, 2784–2795.
- [42] Helguero, LA.; Faulds, MH.; Gustafsson, JA.; Haldosen, LA. Estrogen receptors alfa (ER alpha) and beta (ER beta) differentially regulate proliferation and apoptosis of the normal murine mammary epithelial cell line HC11. *Oncogene*, **2005**, 24, 6605–6616.
- [43] Speirs, V.; Skliris, GP.; Burdall, SE.; Carder, PJ. Distinct expression patterns of ER alpha and ER beta in normal human mammary gland. *J. Clin. Pathol.*, **2002**, 55, 371–374.
- [44] Palmieri, C.; Cheng, GJ.; Saji, S.; Zelada-Hedman, M.; Warri, A.; Weihua, Z.; Van

- Noorden, S.; Wahlstrom, T.; Coombes, RC.; Warner, M.; Gustafsson, JA. Estrogen receptor beta in breast cancer. *Endocr. Relat. Cancer*, **2002**, 9, 1–13.
- [45] Forster, C.; Makela, S.; Warri, A.; Kietz, S.; Becker, D.; Hultenby, K.; Warner, M.; Gustafsson, JA. Involvement of estrogen receptor beta in terminal differentiation of mammary gland epithelium. *Proc. Natl. Acad. Sci. U.S.A.*, **2002**, 99, 15578–15583.
- [46] Feng, Y.; Manka, D.; Wagnert, KU.; Khan, SA. Estrogen receptor-alpha expression in the mammary epithelium is required for ductal and alveolar morphogenesis in mice. *Proc. Natl. Acad. Sci. U.S.A.*, **2007**, 104, 14718–14723.
- [47] Bocchinfuso, WP.; Korach, KS. Mammary gland development and tumorigenesis in estrogen receptor knockout mice. *J. Mammary Gland Biol. Neoplasia*, **1997**, 2, 323–334.
- [48] Hartman, J.; Muller, P.; Foster, JS.; Wimalasena, J.; Gustafsson, JA.; Strom, A. HES-1 inhibits 17 beta-estradiol and heregulin-beta-1-mediated upregulation of E2F-1. *Oncogene*, **2004**, 23, 8826–8833.
- [49] Warner, M.; Gustafsson, JA. The role of estrogen receptor beta (ER beta) in malignant diseases - a new potential target for antiproliferative drugs in prevention and treatment of cancer. *Biochem. Biophys. Res. Commun.*, **2010**, 396, 63–66.
- [50] Williams, C.; Edvardsson, K.; Lewandowski, SA.; Strom, A.; Gustafsson, JA. A genome-wide study of the repressive effects of estrogen receptor beta on estrogen receptor alpha signaling in breast cancer cells. *Oncogene*, **2008**, 27, 1019–1032.
- [51] Yager, JD.; Davidson, NE. Mechanisms of disease: estrogen carcinogenesis in breast cancer. *N. Engl. J. Med.*, **2006**, 354, 270–282.
- [52] Hao, LK.; Wang, YJ.; Duan, YS.; Bu, SM. Effects of treadmill exercise training on liver fat accumulation and estrogen receptor alpha expression in intact and ovariectomized rats with or without estrogen replacement treatment. *Eur. J. Appl. Physiol.*, **2010**, 109, 879–886.
- [53] Rauf, S.; Soejono, SK.; Partadiredja, G. Effects of treadmill exercise training on cerebellar estrogen and estrogen receptors, serum estrogen, and motor coordination performance of ovariectomized rats. *Iran. J. Basic Med. Sci.*, **2015**, 18, 587–592.

CHAPTER 8

LONG-TERM EXERCISE TRAINING AS A MODULATOR OF MAMMARY CANCER VASCULARIZATION

THE CONTENT OF THIS CHAPTER WAS PUBLISHED IN:

Faustino-Rocha AI, Silva A, Gabriel J, Gil da Costa RM, Moutinho M, Oliveira PA, Gama A, Ferreira R, Ginja M. 2016. Long-term exercise training as a modulator of mammary cancer vascularization. *Biomedicine & Pharmacotherapy* 81 (2016): 273-280. DOI: 10.1016/j.biopha.2016.04.030. (Full paper)

Moutinho M, Gama A, Ferreira R, Ginja M, Oliveira PA, **Faustino-Rocha AI**. 2016. Immunoexpression of VEGF-A in chemically-induced mammary tumors. *Experimental Pathology and Health Sciences* 8 (1): 31-32. (Short communication)

Faustino-Rocha AI, Silva A, Gabriel J, Gil da Costa RM, Oliveira PA, Gama A, Ferreira A, Ginja M. 2017. Long-term exercise training and mammary tumors' vascularization: thermography, ultrasonography and immunohistochemistry. *Journal of Comparative Pathology* 156 (1): 119. (Abstract)

Moutinho M, Gama A, Ferreira R, Ginja M, Oliveira PA, **Faustino-Rocha AI***. 2015. Immunoexpression of VEGF-A in chemically-induced mammary tumors. V Congresso Luso-Brasileiro de Patologia Experimental - XV International Symposium of Experimental Techniques, 3rd to 5th December, Coimbra, Portugal. (Oral presentation)

* The presentation was performed by this author.

Faustino-Rocha AI, Silva A, Gabriel J, Gil da Costa RM, Moutinho M, Oliveira PA, Gama A, Ferreira R, Ginja M. 2015. Mammary tumors' vascularization: ultrasonographic and thermographic evaluation. New Advances in Animal Mammary tumors' vascularization Models and Preclinical Imaging for Translational Research in Cancerology, 30th September to 3rd October, La Pointe de Pen Bron, France. (Oral presentation)

Faustino-Rocha AI, Silva A, Gabriel J, Gil da Costa RM, Oliveira PA, Gama A, Ferreira R, Ginja M. 2016. Long-term exercise training and mammary tumors' vascularization: thermography, ultrasonography and immunohistochemistry. 34th Annual Meeting of the ESVP and 27th Annual Meeting of the ECVP, 7th to 10th September, Bologna, Italy. (Poster presentation)

8. Long-term exercise training as a modulator of mammary cancer vascularization

Abstract

Breast cancer remains a leading cause of death by cancer worldwide. It is commonly accepted that angiogenesis and the expression of angiogenic factors such as vascular endothelial growth factor (VEGF)-A are associated with the increased risk of metastasis and poor patient outcome. This work aimed to evaluate the effects of long-term exercise training on the growth and vascularization of mammary tumors in a rat model. Fifty female Sprague-Dawley rats were divided into four groups: two *N*-methyl-*N*-nitrosourea (MNU)-exposed groups (exercised and sedentary) and two control groups (exercised and sedentary). MNU was administered once, intraperitoneally at seven weeks-old. Animals were then exercised on a treadmill for 35 weeks. Mammary tumors were evaluated using thermography, ultrasonography [Power Doppler (PDI), B Flow and contrast-enhanced ultrasound (CEUS)], and immunohistochemistry (VEGF-A immunoeexpression). Both, MNU sedentary and exercised groups showed 100% of tumor incidence, but exercised animals showed less tumors with an increased latency period. Exercise training also enhanced VEGF-A immunoeexpression and vascularization (microvessel density, MVD) ($p < 0.05$), and reduced histological aggressiveness. Ultrasound and thermal imaging analysis confirmed the enhanced vascularization of tumors from exercised animals. Long-term exercise training increased VEGF-A expression, leading to enhanced tumor vascularization and reduced tumor burden, multiplicity and histological aggressiveness.

Keywords: histopathology, mammary tumors, MNU, rat, thermography, ultrasonography, vascularization

8.1. Introduction

Despite recent advances in diagnostic and therapeutic approaches, breast cancer remains one of the leading causes of death by cancer worldwide [1,2]. Angiogenesis, the formation of new blood vessels from pre-existing vessels and vascular endothelial cells, is essential for tumor growth, by supplying nutrients and oxygen [3,4]. Angiogenesis is regulated by a balance between proangiogenic and antiangiogenic factors, produced by both tumor and host cells, namely endothelial cells, pericytes and leukocytes [5]. Vascular endothelial growth factor (VEGF) is the most potent and widely distributed angiogenic

factor [6]. The VEGF family is composed of several members - VEGF-A, -B, -C, -D and -E - of which VEGF-A is the most potent [7]. VEGF-A stimulates endothelial cell proliferation and migration, prevents the regression of newly formed vessels and increases microvascular permeability [5,6]. VEGF-A expression has been associated with cancer progression, increased risk of metastasis and poor outcome of lung, esophagus, colorectal and breast cancer [8,9]. Tumor vascularization may be non-invasively assessed by imaging tools such as ultrasonography and thermography [10]. Ultrasonography is very useful in women with dense breasts and in the characterization of breast lesions identified in mammographic examination [11], being frequently used as an adjuvant tool for clinical breast examination. Thermography measures the infrared radiation emitted from the body, revealing superficial temperature patterns which are directly related to local vascularization, and may therefore be used to study physiological and pathological vascular changes [12–14]. This technique was first introduced for breast cancer screening in 1956 and later recognized by the Food and Drug Administration as a tool for breast cancer risk assessment [15].

It is largely accepted that exercise training exerts a beneficial effect in some lymphomas and in colon, lung, endometrial, prostate and breast cancer [16–23]. Systematic reviews have concluded that the practice of physical activity improves important clinical (quality of life and fatigue) and physiological outcomes (muscle strength) in cancer patients [24]. Furthermore, several investigators have studied the effects of exercise training on the biopathology of mammary tumors themselves. However, these studies have focused their attention on the effects of shorter exercise training protocols using xenograft models [25–27]. Despite their usefulness and widespread application, xenograft models show important limitations, related to the lack of a functional immune system and of the complex tumor cell population which, in spontaneous tumors, evolves through a lengthy multi-step process of carcinogenesis. In particular, xenograft models are considered too artificial for studying tumor angiogenesis, and more realistic models are being called for [28]. This work intends to address these concerns, by choosing a mammary cancer model induced in immune-competent rats by *N*-methyl-*N*-nitrosourea (MNU). We hypothesized that exercise training may modulate the microenvironment of mammary tumors, and thus it was studied the effects of long-term exercise training on tumor growth and vascularization, employing thermography, ultrasonography and immunohistochemical techniques.

8.2. Material and Methods

8.2.1. Animals

Fifty female Sprague-Dawley rats, with 4-5 weeks of age were obtained from Harlan Laboratories Inc. (Barcelona, Spain). Animals were housed at the facilities of the University of Trás-os-Montes and Alto Douro in filter capped polycarbonate cages (1500U Eurostandard Type IV S, Tecniplast, Buguggiate, Italy) with corncob for bedding (Mucedola, Settimo Milanese, Milan, Italy) under controlled conditions of temperature ($23\pm 2^{\circ}\text{C}$), humidity ($50\pm 10\%$), air system filtration (10–20 ventilations/hour) and on a 12h:12h light:dark cycle. Tap water and a basic standard laboratory diet (4RF21[®], Mucedola, Settimo Milanese, Milan, Italy) were supplied *ad libitum* during the study. Cages were cleaned and water was changed once per week. All procedures were done in accordance with European legislation (European Directive 2010/63/EU). The Portuguese Ethics Committee for Animal Experimentation approved all the experiments and procedures carried out on the animals (approval no. 008961).

8.2.2. Animal experiments

After one week of quarantine, animals were allowed to acclimate to laboratory conditions for two weeks. Then, they were randomly divided into four experimental groups: MNU sedentary (n=15), MNU exercised (n=15), control sedentary (n=10) and control exercised (n=10). The development of mammary tumors was induced in animals from both MNU sedentary and MNU exercised groups by a single intraperitoneal administration of the carcinogen agent MNU (ISOPAC[®], Sigma Aldrich S.A., Madrid, Spain) at a dose of 50 mg/kg of body weight, at seven weeks of age. MNU was used within one hour after its preparation. Animals from control groups received a single administration of the vehicle (saline solution 0.9%). After this, animals from exercised groups were acclimated to the treadmill running (Treadmill Control[®] LE 8710, Panlab, Harvard Apparatus, Holliston, MA, USA) for a five-day period at a speed of 20 m/min increasing progressively from 20 to 60 min/day. Then, the duration of the exercise was maintained as 60 min/day, five times/week during 35 weeks. Animals were observed twice a day to monitor their general health status. They were weekly palpated for the detection of mammary tumor development. The animal body weight was measured weekly using a top-loading scale (Mettler PM4000, LabWrench, Midland, ON, Canada).

The day of the MNU administration was considered the first day of the study and the animals' sacrifice 35 weeks later was considered the end of the study. At the end of the study, the accurate body weight was calculated by subtracting the tumor weight to the total body weight, and the mortality index (MI) was calculated using the following equation:

$$MI = \frac{\text{Number of animals that died during the study}}{\text{Number of animals at the beginning of the study}} \times 100.$$

8.2.3. Mammary tumors evaluation

Twenty-four hours before the examination, the skin overlying the mammary tumors was shaved using a machine clipper (Aesculap GT420 Isis, Aesculap Inc., Center Valley, PA, USA). At the end of the experimental protocol, immediately before the animals' sacrifice, the mammary tumors were evaluated by thermography and ultrasonography. For these examinations, all survived animals were anesthetized by intraperitoneal administration of ketamine (75 mg/kg of body weight, Imalgene® 1000, Merial S.A.S., Lyon, France) and xylazine (10 mg/kg of body weight, Rompun® 2%, Bayer Healthcare S.A., Kiel, Germany).

8.2.4. Thermographic evaluation

The thermographic evaluation was performed using a far infrared camera from FLIR® model A325 (FLIR® Systems Inc., Wilsonville, OR, USA), with a sensitivity of 68 mK and a spatial resolution of 320 × 240 pixels. The images were recorded at one frame *per* second for future analyses but the integration time for the micro bolometer was approximately 16.6 ms. The animals were manually held and filmed at a constant distance (0.35 m). The animal emissivity was set to 0.98 and the tumor borders were marked to overlap with a visible image [29]. Representative frames were selected and analyzed using the ThermoCam Researcher Pro 2.10 (FLIR® Systems Inc., Wilsonville, OR, USA) software. In this analysis, the maximum, minimum and average temperatures of each region of interest were obtained. These measurements reflect the vascularization and the extension of necrotic areas of mammary tumors. Higher vascularized tumors are expected to exhibit less extensive necrotic areas and consequently to present higher maximum,

minimum and mean temperature, and lower thermal amplitude. The opposite is expected to poor vascularized tumors.

8.2.5. Ultrasonographic evaluation

For ultrasonographic analysis it was used a real-time scanner (Logiq P6[®], General Electric Healthcare, Milwaukee, WI, USA) and a 10 MHz linear transducer with a standoff pad (Sonokit, MIUS Ltd., Gloucestershire, UK). Animals were placed in supine position and it was applied acoustic gel (Aquasonic, Parker Laboratories Inc., Fairfield, NJ, USA), the ultrasonographic images using Power Doppler (PDI) and B Flow modes were obtained in sagittal planes using light pressure to avoid the distortion of tumor shape. The images were recorded and the color pixel density (CPD) in PDI and B Flow images was determined according to the formula previously published by Denis *et al.* [30], using Adobe Photoshop[®] version 7.0 (Adobe Systems Inc., San Jose, CA, USA).

8.2.6. Necropsy

Following ultrasonographic examination, all survived animals were humanely sacrificed by exsanguination by cardiac puncture as indicated by the Federation of European Laboratory Animal Science Associations [31]. All animals were skinned and the skin was carefully observed under a light for the detection of small mammary tumors. All tumors were removed and weighed. Mammary tumor volume was calculated based on tumors' weight applying a previously published formula [32]. All mammary tumors and organs were fixated in buffered formalin during 12 hours.

8.2.7. Histology and immunohistochemistry

After fixation, mammary tumors were routinely processed for histological analysis; two μm -thick sections were stained with hematoxylin and eosin (H&E) and histologically classified by a pathologist according to the classification previously established by Russo and Russo [33]. Each mammary tumor was classified according to the histological pattern with higher proportion in each tumor section. The mean area of necrosis was quantified in each histological section. For this purpose, three different fields were randomly selected and analyzed using ImageJ software (National Institutes of Health, Bethesda, MD, USA).

The immunohistochemical detection of VEGF-A was performed using the standard NovoLink Polymer Detection System protocol (Leica Biosystems, Newcastle, UK). Sections were incubated overnight at 4°C with a primary antibody for VEGF-A (clone JH121, Merck Millipore, Darmstadt, Germany) at a dilution of 1:100. The VEGF-A immunoexpression was semi-quantitatively and quantitatively assessed. For the semi-quantitative way, a minimum of 1000 neoplastic cells were evaluated in each mammary tumor and the VEGF-A immunoexpression was assessed according to five levels: grade 0 (no staining detected in tumor cells), grade 1 (1–24% of tumor area showed positive staining), grade 2 (25–49% of tumor stained), grade 3 (50–75% of tumor stained) and grade 4 (>75% of tumor stained). The staining intensity was also evaluated as: level 0 (unstained), + (weak staining), ++ (moderate staining) and +++ (intense staining) [34]. For the quantitative way, a representative image from each tumor was taken with a 40× objective and the VEGF immunoexpression was quantified using an Image Manipulation Program 2.8 (GNU Image Manipulation Program 2.8, CNE, Free Software Foundation, Boston, USA) [35]. The microvessels were counted in the three most vascularized hot spots, in 200× magnification fields (corresponding to approximately 0.76 mm²) from which the mean was obtained in order to determine the microvessel density (MVD). Areas of fibrosis, necrosis and inflammation, and vessels with muscular walls were not counted.

8.2.8. Statistical analysis

Continuous data were statistically analyzed with Statistical Package for the Social Sciences (SPSS[®] version 23 for Windows, SPSS Inc., Chicago, IL, USA) using independent sample *t*-test and analysis of variance (ANOVA) with the Bonferroni correction for multiple comparisons. Histological and immunohistochemical results were analyzed using Chi-square tests. Pearson correlation was used to assess the correlation between tumor volume, temperature (maximum, minimum, mean and thermal amplitude), CPD (for PDI and B Flow) and MVD. All data were expressed as mean ± standard error (S.E.); *p* values lower than 0.05 were considered statistically significant.

8.3. Results

8.3.1. General findings

One animal from MNU exercised group did not adapt to the exercise training and was excluded from the study. During the experiment nine animals died: four animals from the MNU sedentary group (MI=27%), four animals from the MNU exercised group (MI=29%) and one animal from the control sedentary group (MI=10%). Data from these animals were not included in the study. The final accurate body weight was not statistically different among groups; however, it was slightly lower in MNU groups when compared with control ones ($p>0.05$) (data not shown).

8.3.2. Mammary tumors

Animals from control groups did not develop any mammary tumor. All animals from both MNU groups developed mammary tumors (incidence of 100%). The first mammary tumor was palpated ten weeks after MNU administration in MNU sedentary group, while animals from MNU exercised group developed the first mammary tumor two weeks later, at 12th week after MNU administration. At the end of the experiment, the MNU sedentary group developed a total of 28 mammary tumors (2.55 ± 1.44 tumors *per* animal), while the MNU exercised group developed 23 mammary tumors (2.30 ± 1.42 tumors *per* animal); the difference did not reach the level of statistical significance ($p=0.484$) (Table 8.1). Although the differences were not statistical significant, the tumor weight and volume were higher in MNU exercised animals compared with MNU sedentary ones ($p>0.05$). Similarly, the mean area of necrosis was higher in tumors from exercised animals compared with tumors from sedentary ones ($p>0.05$) (Table 8.1). All mammary tumors from both groups were histologically evaluated according to the predominant histological pattern (Table 8.1). Different histological patterns of benign and malignant mammary lesions were identified. Animals from the MNU exercised group developed a higher number of benign lesions and less malignant lesions ($p=0.123$) compared with animals from the MNU sedentary group. In both groups MNU sedentary and MNU exercised, the number of malignant lesions was higher than the number of benign ones, being the papillary non-invasive carcinoma the most frequent histological pattern. It was also important to note that animals from the MNU exercised group did not develop any invasive comedocarcinoma, which was the most aggressive lesion identified in this

experimental protocol, while animals from MNU sedentary group developed two invasive comedocarcinomas.

Table 8.1. Histological classification, weight, volume and area of necrosis of mammary tumors identified in both MNU sedentary and exercised groups taking into account the predominant histological pattern.

Histological classification		Number of tumors	
		MNU sedentary	MNU exercised
Benign lesions	Intraductal papilloma	0	1
	Papillary cystadenoma	0	2
	Tubular adenoma	2	2
	Lactating adenoma	0	1
	Fibroadenoma	0	1
	Total:	2	7
Malignant lesions	Papillary non-invasive carcinoma	13	7
	Cribriform non-invasive carcinoma	5	4
	Papillary invasive carcinoma	4	4
	Cribriform invasive carcinoma	2	1
	Comedo invasive carcinoma	2	0
	Total:	26^a	16
	Total	28^b	23
	Tumor weight (g)	5.15 ± 2.04	8.31 ± 2.82
	Tumor volume (cm³)	4.88 ± 1.93	7.87 ± 2.67
	Area of necrosis (mm²)	0.34 ± 0.05	0.61 ± 0.17

^a*p*=0.123 from MNU exercised group; ^b*p*=0.484 from MNU exercised group.

8.3.3. Thermographic and ultrasonographic analysis

At thermographic analysis of MNU-induced mammary tumors, it was observed that the maximum temperature was very similar between groups ($p>0.05$). Although the differences did not reach the level of statistical significance, the minimum and mean temperatures were slightly higher in MNU sedentary group compared with MNU exercised one; inversely, the thermal amplitude was higher in MNU exercised group ($p>0.05$). Although the maximum temperature was very similar between groups, the lower minimum temperature in MNU exercised group when compared with MNU sedentary one led to a lower mean temperature and higher thermal amplitude in exercised group. This lower minimum temperature in MNU exercised group was probably due to the higher volume of these mammary tumors and the consequent occurrence of more extensive necrotic areas that are characterized by low temperature. The minimum temperature was statistically different from the maximum temperature in both groups MNU sedentary and MNU exercised ($p<0.05$) (Table 8.2, Figure 8.1), suggesting that the tumors from both experimental groups were not uniform and there were very distinct areas in each one. Some of these areas were highly vascularized with high temperature, and other ones were necrotic with low temperature.

In both groups the CPD detected by B Flow was higher than CPD detected by PDI, however the difference was only statistically significant in MNU exercised group ($p<0.05$). The CPD detected in MNU exercised group was higher than that detected in MNU sedentary group ($p>0.05$). Similarly, the MVD determined in MNU exercised animals was higher when compared with that detected in MNU sedentary animals ($p<0.05$) (Table 8.2, Figure 8.2). These data together suggest that B Flow mode is more sensitive than PDI in the detection of small blood vessels and that exercise training increased the mammary tumors vascularization (tumors from MNU exercised group were more vascularized than those from animals from MNU sedentary group).

Table 8.2. Thermographic, ultrasonographic and immunohistochemical evaluation of mammary tumors in both groups MNU sedentary and exercised (mean \pm S.E.).

Parameter		Groups	
		MNU sedentary	MNU exercised
Temperature (°C)	Maximum	37.46 \pm 0.21 ^a	37.43 \pm 0.38 ^a
	Minimum	34.12 \pm 0.42	32.78 \pm 1.20
	Thermal amplitude	3.35 \pm 0.54	4.66 \pm 1.02
	Mean	36.28 \pm 0.16	35.96 \pm 0.55
CPD (%)	Power Doppler (PDI)	1.30 \pm 0.29	1.47 \pm 0.27 ^b
	B Flow	2.40 \pm 0.52	3.68 \pm 0.88
VEGF-A immunoeexpression by GIMP (%)		59.91 \pm 3.11	66.04 \pm 4.65
MVD (microvessel density)		11.82 \pm 1.09 ^c	18.35 \pm 2.93

^a Statistically different from minimum temperature ($p < 0.05$); ^b Statistically different from B Flow ($p < 0.05$); ^c Statistically different from MNU exercised group ($p < 0.05$). CPD: color pixel density.

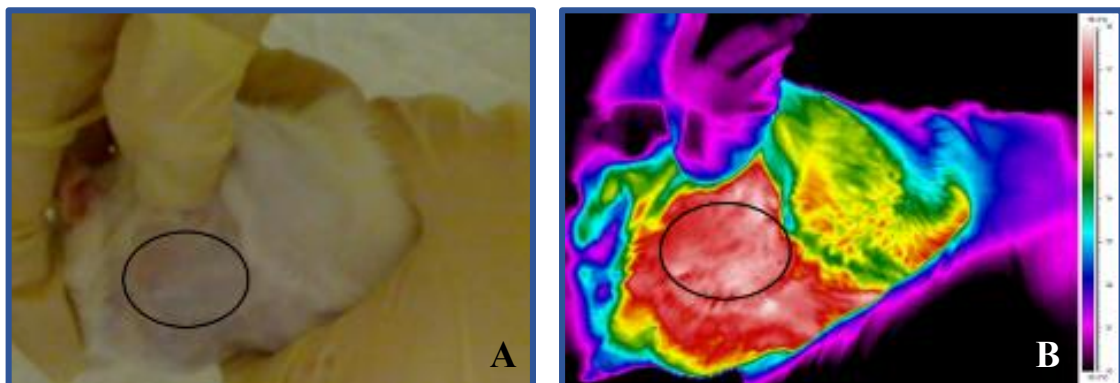


Figure 8.1. Visible image (A) and thermographic analysis (B) of a MNU-induced mammary tumor (temperature range 30-38°C). Mammary tumor is delimited in both images by the black circle.

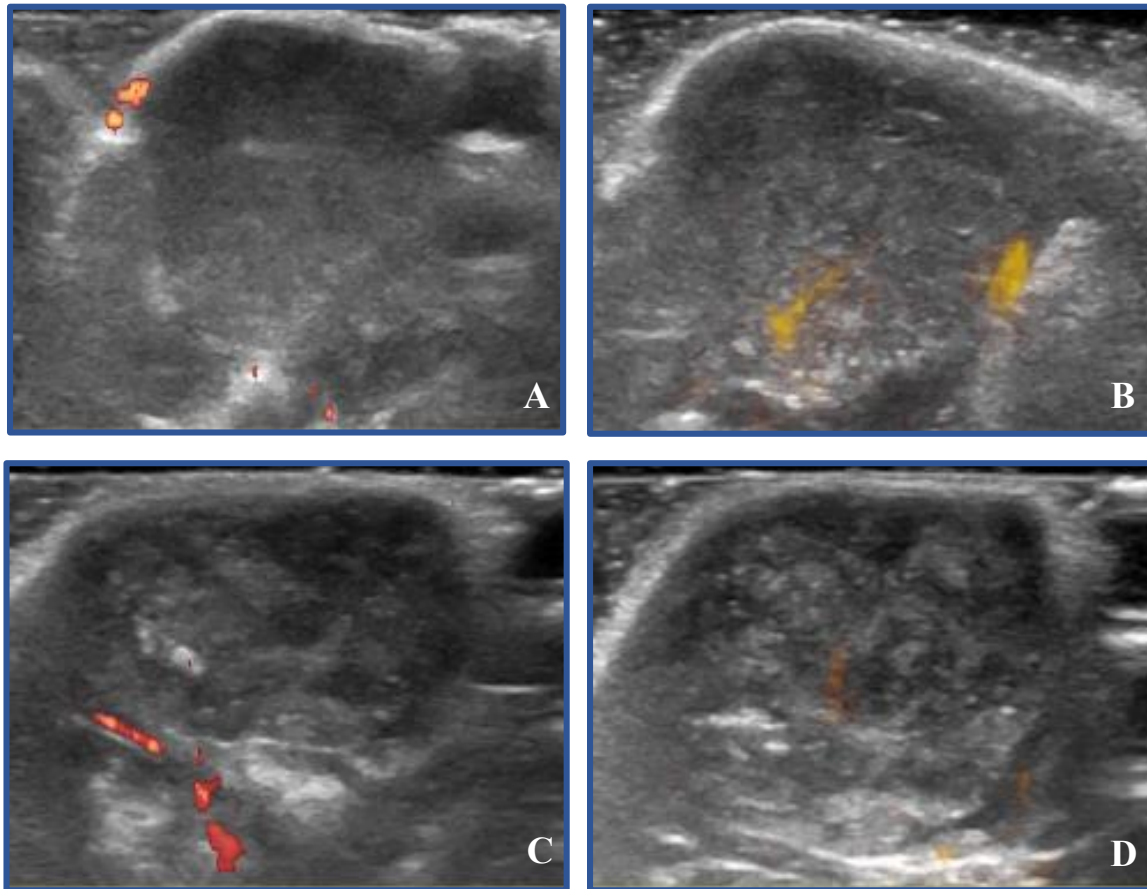


Figure 8.2. Evaluation of mammary tumors from MNU sedentary (**A** and **B**) and MNU exercised (**C** and **D**) groups by Power Doppler (**A** and **C**) and B Flow (**B** and **D**).

8.3.4. Mammary tumors histology

VEGF-A showed a cytoplasmic and homogenous immunolabelling in neoplastic cells (Figure 8.3), while endothelial cells exhibited variably intense cytoplasmic VEGF-A immunoexpression. All mammary lesions from both groups exhibited immunolabelling for VEGF-A (no lesions were classified with score 0) (Table 8.3).

The majority of mammary lesions from MNU sedentary group were classified with score 3 (46.4% of the lesions) ($p < 0.05$ from scores 1 and 2). The score 4 was the most frequently identified in MNU exercised group (47.8% of the lesions were classified with this score) ($p < 0.05$ from score 1) (Table 8.3). In the same way, the VEGF-A immunoexpression evaluated by GIMP revealed a higher immunoexpression of this

marker in tumors from MNU exercised groups compared with tumors from sedentary one ($p>0.05$) (Table 8.2).

The staining intensity in the lesions from MNU sedentary group was mainly classified as moderate (++) (71.4% of the lesions). This score was statistically different from the remaining scores ($p<0.05$ from weak (+) and intense (+++) intensity). Additionally, the number of mammary tumors classified with moderate (++) intensity in MNU sedentary group was higher when compared with those classified with this score in MNU exercised group ($p<0.05$). In the MNU exercised group, the intensity of immunostaining was mainly classified as weak (+) (this score was attributed to 47.8% of the lesions) ($p>0.05$, not statistically different from the remaining scores of intensity) (Table 8.3).

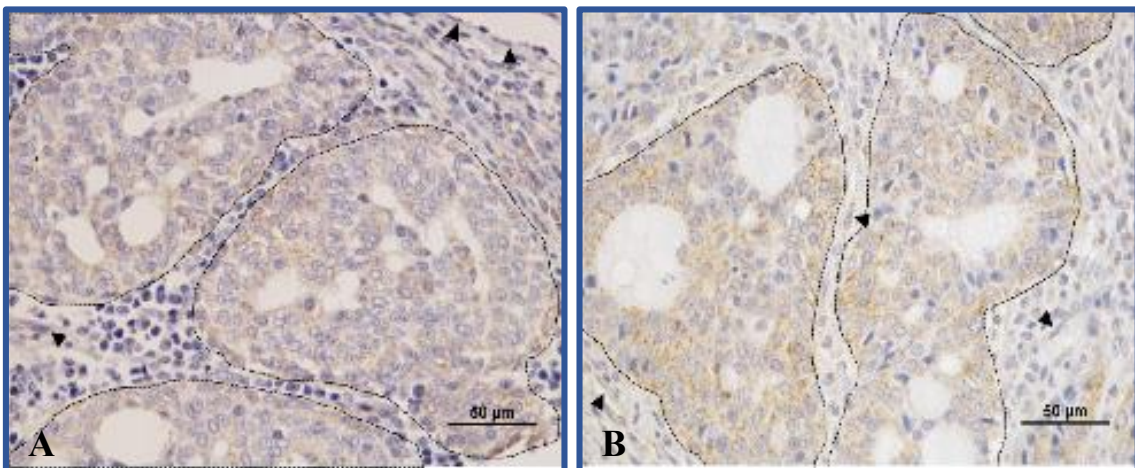


Figure 8.3. Immunoeexpression of VEGF-A in mammary tumors from MNU sedentary (**A**) and MNU exercised (**B**) animals. (**A**) 50.35% of immunopositive cells for VEGF-A (grade 3), moderate staining (++) . (**B**) 64.30% of immunopositive cells for VEGF-A (grade 3), intense staining (+++). Some endothelial cells were immunopositive for VEGF-A (arrowheads).

Table 8.3. Semi-quantitative evaluation of VEGF-A immunoexpression in neoplastic cells of MNU-induced mammary tumors from sedentary and exercised animals (only the data from malignant tumors were compared between groups).

Score/ Group			MNU sedentary (n=28)	MNU exercised (n=23)	
Neoplastic cells	Immunopositive cells	0	0 (0%)	0 (0%)	
		1	3 (10.7%) ^a	2 (8.7%)	
		2	3 (10.7%) ^a	4 (17.4%)	
		3	13 (46.4%)	6 (26.1%)	
		4	9 (32.1%)	11 (47.8%) ^b	
	Intensity of immunostaining	0	Unstained	0 (0%)	0 (0%)
		+	Weak	6 (2.4%)	11 (47.8%)
		++	Moderate	20 (71.4%) ^{c, d}	5 (21.7%)
		+++	Intense	2 (7.1%)	7 (30.4%)

^a Statistically different from Score 3 ($p < 0.05$); ^b Statistically different from Score 1 ($p < 0.05$); ^c Statistically different from weak (+) and intense staining (+++) ($p < 0.05$); ^d Statistically different from moderate staining (++) in MNU exercised group ($p < 0.05$).

8.3.5. Correlations between data

A significant negative correlation was observed between tumor volume and minimum temperature, and between thermal amplitude and minimum and mean temperature ($p < 0.05$). A positive significant correlation was observed between tumor volume and thermal amplitude, and between maximum, minimum and mean temperature ($p < 0.05$) (Table 8.4). Correlation between MVD and tumor vascularization as detected with ultrasound and thermography images was weak and statistically non-significant ($p > 0.05$).

Table 8.4. Correlation between data from thermography, ultrasonography and immunohistochemistry.

Parameter	Tumors' volume	Maximum T°	Minimum T°	Mean T°	Thermal amplitude	CPD PDI	CPD B Flow	MVD
Tumors' volume	-	0.113 (<i>p</i> =0.626)	-0.491* (<i>p</i> =0.024)	-0.197 (<i>p</i> =0.393)	0.568* (<i>p</i> =0.007)	0.098 (<i>p</i> =0.599)	0.007 (<i>p</i> =0.969)	-0.160 (<i>p</i> =0.281)
Maximum T°	-	-	0.362 (<i>p</i> =0.107)	0.870* (<i>p</i> =0.000)	-0.028 (<i>p</i> =0.904)	-0.250 (<i>p</i> =0.275)	0.001 (<i>p</i> =0.996)	-0.023 (<i>p</i> =0.922)
Minimum T°	-	-	-	0.731* (<i>p</i> =0.000)	-0.942* (<i>p</i> =0.000)	0.251 (<i>p</i> =0.273)	0.137 (<i>p</i> =0.553)	-0.184 (<i>p</i> =0.425)
Mean T°	-	-	-	-	-0.472* (<i>p</i> =0.031)	0.028 (<i>p</i> =0.905)	0.108 (<i>p</i> =0.641)	-0.195 (<i>p</i> =0.398)
Thermal amplitude	-	-	-	-	-	-0.270 (<i>p</i> =0.237)	-0.369 (<i>p</i> =0.099)	0.195 (<i>p</i> =0.396)
CPD PDI	-	-	-	-	-	-	0.012 (<i>p</i> =0.945)	0.073 (<i>p</i> =0.740)
CPD B Flow	-	-	-	-	-	-	-	0.359 (<i>p</i> =0.101)
MVD	-	-	-	-	-	-	-	-

* These correlations were considered statistically significant ($p < 0.05$).

8.4. Discussion

Breast cancer is the most frequently diagnosed cancer in women worldwide [1]. Angiogenesis is essential for breast cancer growth and invasion [3] but hypoxic tumors often show poor prognosis, developing an aggressive phenotype and resistance to systemic (chemotherapy) and regional (radiotherapy) therapy [24,36]. This resistance occurs due to the lack of oxygen, which is necessary to fixate deoxyribonucleic acid (DNA) damage caused by chemotherapy or radiotherapy, and also due to the non-proliferative status of many neoplastic cells in hypoxic microenvironments [37]. Tumor

vascularization thus appears as a double-edged sword that requires a deeper understanding before rational modulation approaches may be applied.

In the present study, mortality was associated with the development of mammary tumors in the MNU-exposed groups, and was lower than previously reported in a similar work [38]. MNU-exposed animals also showed a lower accurate body weight compared with control animals, revealing a loss of body condition, which had not been reported in a comparable study [39]. Exercise training increased the latency period and reduced the number of tumors, which may be due to the up-regulation of immunity induced by exercise training [40]. These effects are in line with previous findings from related models [39,41]. However, exercise training increased the tumor weight and volume, which may be due to the enhancement of blood perfusion, as previously reported [42]. A similar observation was made in prostate tumors in exercised mice [36]. Histologically, exercised animals developed more benign and less malignant lesions compared with sedentary animals. However, in both groups, the number of malignant lesions was higher than the number of benign ones. Papillary carcinoma was the most frequently identified histological pattern, in accordance with previous findings [38,43]. It worth to note that exercised animals did not develop any invasive comedocarcinoma, the most aggressive lesion diagnosed in sedentary animals, further suggesting that exercise training played a protective effect.

Mammography and ultrasonography are well-established techniques for breast cancer screening [44], especially when used in combination [44]. It is worth noting that B Flow consistently detected higher CPD than PDI and seems to be a more sensitive technique for assessing tumor vascularization, as previously observed [32]. Concerning to thermography, the Society of Breast Imaging reported that no studies show clear benefits when using this technique alone or as an adjunct to mammography [45]. In fact, breast infrared thermography has rarely been used to monitor tumor growth in experimental animals [46,47]. The use of thermography for studying cancer is based on the detection of heat generated by the metabolic activity of the proliferating tumor cells and of heat generated by new blood vessels supporting the growth of tumor [44,48]. Thus, the process of neoangiogenesis associated with carcinogenesis induces an increase of the skin temperature above the developing tumor [49–51]. In this study, larger tumors were correlated with lower minimum temperature ($p<0.05$) and increased thermal amplitude ($p<0.05$), most likely because they had wider central necrotic areas. Previous studies also

reported a thermographic association between tumor necrosis and reduced surface skin temperature [52–54].

Elevated VEGF-A levels have been correlated with higher proliferation rate, infiltrative growth and poor prognosis in many solid tumors including those of the breast [55], lung [56], colon [57], liver [58] and bladder [59]. In the present study, higher VEGF-A expression was found among exercised animals, and this correlated with higher tumor vascularization, as assessed by MVD and CPD. This is in line with previous studies using lung [60] and breast cancer [24] xenografts, but in contrast with other reports [20,61–65]. Importantly, tumors from the exercised group showed higher VEGF-A expression and vascularization, and they were histologically less aggressive and exhibited a longer latency period. This agrees with findings from canine models [66] and supports the hypothesis that enhanced tumor vascularization may have a beneficial effect and help countering tumor progression.

8.5. Conclusion

Although, we hypothesized that long-term exercise training could inhibit mammary tumor growth and aggressiveness by the inhibition of tumor vascularization, surprisingly we verified that the exercise training promoted tumor vascularization (increased VEGF-A immunoexpression, MVD, and CPD detected by PDI and B Flow) and growth (tumors with higher volume), but reduced the number of mammary tumors and their aggressiveness, and increased latency period.

This study is the first to evaluate the effects of long-term exercise training in an immunocompetent model of mammary tumorigenesis, and comparisons with data from xenograft models should be made cautiously. The present results pave the way for further studies on modulation approaches for tumor vascularization using relevant immunocompetent models, particularly those addressing the relationship between exercise training, angiogenesis and tumor progression.

8.6. References

- [1] Jemal, A.; Siegel, R.; Ward, E.; Murray, T.; Xu, JQ.; Thun, MJ. Cancer statistics, 2007. *CA Cancer J. Clin.*, **2007**, *57*, 43–66.
- [2] Siegel, R.; Naishadham, D.; Jemal, A. Cancer statistics, 2012. *CA Cancer J. Clin.*,

- 2012, 62, 10–29.
- [3] Culy, C. Antiangiogenic cancer therapy. *Drugs of Today*, **2005**, 41, 23–36.
- [4] McDonald; Baluk, P. Significance of blood vessel leakiness in cancer. *Cancer Res.*, **2002**, 62, 5381-5385.
- [5] Rosen, LS. VEGF-targeted therapy: therapeutic potential and recent advances. *Oncologist*, **2005**, 10, 382–391.
- [6] Gasparini, G. Prognostic value of vascular endothelial growth factor in breast cancer. *Oncologist*, **2000**, 5, 37–44.
- [7] Mohammed, RAA.; Green, A.; El-Shikh, S.; Paish, EC.; Ellis, IO.; Martin, SG. Prognostic significance of vascular endothelial cell growth factors-A, -C and -D in breast cancer and their relationship with angio- and lymphangiogenesis. *Br. J. Cancer*, **2007**, 96, 1092–1100.
- [8] Hu, ZY.; Fan, C.; Livasy, C.; He, XP.; Oh, DS.; Ewend, MG.; Carey, LA.; Subramanian, S.; West, R.; Ikpatt, F.; Olopade, OL.; van de Rijn, M.; Perou, CM. A compact VEGF signature associated with distant metastases and poor outcomes. *BMC Med.*, **2009**, 7, 9.
- [9] Qiu, CW.; Lin, DG.; Wang, JQ.; Li, CY.; Deng, GZ. Expression and significance of PTEN and VEGF in canine mammary gland tumours. *Vet. Res. Commun.*, **2008**, 32, 463–472.
- [10] Ko, EY.; Lee, SH.; Kim, HH.; Kim, SM.; Shin, MJ.; Kim, N.; Gong, G. Evaluation of tumor angiogenesis with a second-generation US contrast medium in a rat breast tumor model. *Korean J. Radiol.*, **2008**, 9, 243–249.
- [11] Crystal, P.; Strano, SD.; Shcharynski, S.; Koretz, MJ. Using sonography to screen women with mammographically dense breasts. *Am. J. Roentgenol.*, **2003**, 181, 177–182.
- [12] Bhowmik, A.; Repaka, R.; Mishra, SC. Thermographic evaluation of early melanoma within the vascularized skin using combined non-Newtonian blood flow and bioheat models. *Comput. Biol. Med.*, **2014**, 53, 206–219.
- [13] Diakides, NA.; Bronzino, JD. *Medical infrared imaging*. **2008**, CRC Press.
- [14] Just, M.; Chalopin, C.; Unger, M.; Halama, D.; Neumuth, T.; Dietz, A.; Fischer, M. Monitoring of microvascular free flaps following oropharyngeal reconstruction using infrared thermography: first clinical experiences. *Eur. Arch. Otorhinolaryngol.*, **2016**, 273, 2659-2667.

- [15] Moore, G. Breast cancer: early detection needed. *Bus Heal.*, **2001**, 19, 39.
- [16] Yamashita, AS.; Lira, FS.; Rosa, JC.; Paulino, EC.; Brum, PC.; Negrao, CE.; dos Santos, R V.; Batista, ML.; do Nascimento, CO.; Oyama, LM.; Seelaender, M. Depot-specific modulation of adipokine levels in rat adipose tissue by diet-induced obesity: the effect of aerobic training and energy restriction. *Cytokine*, **2010**, 52, 168–174.
- [17] Murphy, EA.; Davis, JM.; Brown, AS.; Carmichael, MD.; Mayer, EP.; Ghaffar, A. Effects of moderate exercise and oat beta-glucan on lung tumor metastases and macrophage antitumor cytotoxicity. *J. Appl. Physiol.*, **2004**, 97, 955–959.
- [18] Giannini, C.; de Giorgis, T.; Mohn, A.; Chiarelli, F. Role of physical exercise in children and adolescents with diabetes mellitus. *J. Pediatr. Endocrinol. Metab.*, **2007**, 20, 173–184.
- [19] Esser, KA.; Harpole, CE.; Prins, GS.; Diamond, AM. Physical activity reduces prostate carcinogenesis in a transgenic model. *Prostate*, **2009**, 69, 1372–1377.
- [20] Al-Jarrah, M.; Matalka, I.; Al Aseri, H.; Mohtaseb, A.; Smirnova, I V.; Novikova, L.; Stehno-Bittel, L.; AlKhateeb, A. Exercise training prevents endometrial hyperplasia and biomarkers for endometrial cancer in rat model of type 1 diabetes. *J. Clin. Med. Res.*, **2010**, 2, 207–214.
- [21] Wang, RY.; Yang, YR.; Yu, SM. Protective effects of treadmill training on infarction in rats. *Brain Res.*, **2001**, 922, 140–143.
- [22] Hoveida, R.; Alaei, H.; Oryan, S.; Parivar, K.; Reisi, P. Treadmill running improves spatial memory in an animal model of Alzheimer’s disease. *Behav. Brain Res.*, **2011**, 216, 270–274.
- [23] Marcuzzo, S.; Dutra, MF.; Stigger, F.; do Nascimento, PS.; Ilha, J.; Kalil-Gaspar, PI.; Achaval, M. Beneficial effects of treadmill training in a cerebral palsy-like rodent model: walking pattern and soleus quantitative histology. *Brain Res.*, **2008**, 1222, 129–140.
- [24] Jones, LW.; Viglianti, BL.; Tashjian, JA.; Kothadia, SM.; Keir, ST.; Freedland, SJ.; Potter, MQ.; Moon, EJ.; Schroeder, T.; Herndon, JE.; Dewhirst, MW. Effect of aerobic exercise on tumor physiology in an animal model of human breast cancer. *J. Appl. Physiol.*, **2010**, 108, 343–348.
- [25] Holick, CN.; Newcomb, PA.; Trentham-Dietz, A.; Titus-Ernstoff, L.; Bersch, AJ.; Stampfer, MJ.; Baron, JA.; Egan, KM.; Willett, WC. Physical activity and survival

- after diagnosis of invasive breast cancer. *Cancer Epidemiol. Biomarkers Prev.*, **2008**, 17, 379–386.
- [26] Irwin, ML.; Smith, AW.; McTiernan, A.; Ballard-Barbash, R.; Cronin, K.; Gilliland, FD.; Baumgartner, RN.; Baumgartner, KB.; Bernstein, L. Influence of pre- and postdiagnosis physical activity on mortality in breast cancer survivors: The health, eating, activity, and lifestyle study. *J. Clin. Oncol.*, **2008**, 26, 3958–3964.
- [27] Tehard, B.; Friedenreich, CM.; Oppert, JM.; Clavel-Chapelon, F. Effect of physical activity on women at increased risk of breast cancer: results from the E3N cohort study. *Cancer Epidemiol. Biomarkers Prev.*, **2006**, 15, 57–64.
- [28] Eklund, L.; Bry, M.; Alitalo, K. Mouse models for studying angiogenesis and lymphangiogenesis in cancer. *Mol. Oncol.*, **2013**, 7, 259–282.
- [29] Soerensen, DD.; Clausen, S.; Mercer, JB.; Pedersen, LJ. Determining the emissivity of pig skin for accurate infrared thermography. *Comput. Electron. Agric.*, **2014**, 109, 52–58.
- [30] Denis, F.; Bougnoux, P.; de Poncheville, W.; Prat, M.; Catroux, R.; Tranquart, FO. *In vivo* quantitation of tumour vascularisation assessed by Doppler sonography in rat mammary tumours. *Ultrasound Med. Biol.*, **2002**, 28, 431–437.
- [31] Forbes, D.; Blom, H.; Kostomitsopulos, N.; Moore, G.; Perretta, G. Euroguide: on the accommodation and care of animals used for experimental and other scientific purposes. *Federation of European Laboratory Animal Science Associations*, **2007**.
- [32] Faustino-Rocha, AI.; Silva, A.; Gabriel, J.; Teixeira-Guedes, CI.; Lopes, C.; Gil da Costa, R.; Gama, A.; Ferreira, R.; Oliveira, PA.; Ginja, M. Ultrasonographic, thermographic and histologic evaluation of MNU-induced mammary tumors in female Sprague-Dawley rats. *Biomed. Pharmacother.*, **2013**, 67, 771–776.
- [33] Russo, J.; Russo, IH. Atlas and histologic classification of tumors of the rat mammary gland. *J. Mammary Gland Biol. Neoplasia*, **2000**, 5, 187–200.
- [34] Chan, CML.; Ma, BBY.; Hui, EP.; Wong, SCC.; Mo, FKF.; Leung, SF.; Kam, MKM.; Chan, ATC. Cyclooxygenase-2 expression in advanced nasopharyngeal carcinoma - a prognostic evaluation and correlation with hypoxia inducible factor 1 alpha and vascular endothelial growth factor. *Oral Oncol.*, **2007**, 43, 373–378.
- [35] Mendonça, MCP.; Soares, ES.; Stávale, LM.; Rapôso, C.; Coope, A.; Kalapothakis, E.; Cruz-Höfling, MA. Expression of VEGF and Flk-1 and Flt-1

- receptors during blood-brain barrier (BBB) impairment following *Phoneutria nigriventer* spider venom exposure. *Toxins (Basel)*, **2013**, 5, 2572–2588.
- [36] McCullough, DJ.; Nguyen, LMD.; Siemann, DW.; Behnke, BJ. Effects of exercise training on tumor hypoxia and vascular function in the rodent preclinical orthotopic prostate cancer model. *J. Appl. Physiol.*, **2013**, 115, 1846–1854.
- [37] Vordermark, D.; Brown, JM. Endogenous markers of tumor hypoxia - predictors of clinical radiation resistance? *Strahlentherapie und Onkol.*, **2003**, 179, 801–811.
- [38] McCormick, DL.; Adamowski, CB.; Fiks, A.; Moon, RC. Lifetime dose-response relationships for mammary tumor induction by a single administration of *N*-methyl-*N*-nitrosourea. *Cancer Res.*, **1981**, 41, 1690–1694.
- [39] Whittal-Strange, KS.; Chadau, S.; Parkhouse, WS. Exercise during puberty and NMU induced mammary tumorigenesis in rats. *Breast Cancer Res. Treat.*, **1998**, 47, 1–8.
- [40] Teicher, BA. Tumor models for efficacy determination. *Mol. Cancer Ther.*, **2006**, 5, 2435–2443.
- [41] Westerlind, KC.; McCarty, HL.; Schultheiss, PC.; Story, R.; Reed, AH.; Baier, ML.; Strange, R. Moderate exercise training slows mammary tumour growth in adolescent rats. *Eur. J. Cancer Prev.*, **2003**, 12, 281–287.
- [42] Jones, LW.; Eves, ND.; Courneya, KS.; Chiu, BK.; Baracos, VE.; Hanson, J.; Johnson, L.; Mackey, JR. Effects of exercise training on antitumor efficacy of doxorubicin in MDA-MB-231 breast cancer xenografts. *Clin. Cancer Res.*, **2005**, 11, 6695–6698.
- [43] Faustino-Rocha, A.; Gama, A.; Oliveira, PA.; Alvarado, A.; Neuparth, MJ.; Ferreira, R.; Ginja, M. Effects of lifelong exercise training on mammary tumorigenesis induced by MNU in female Sprague-Dawley rats. *Clin. Exp. Med.*, **2016**, Epub ahead of print.
- [44] Kennedy, DA.; Lee, T.; Seely, D. A comparative review of thermography as a breast cancer screening technique. *Integr. Cancer Ther.*, **2009**, 8, 9–16.
- [45] Brkljacic, B.; Miletic, D.; Sardanelli, F. Thermography is not a feasible method for breast cancer screening. *Coll. Antropol.*, **2013**, 2, 589–593.
- [46] Poljak-Blazi, M.; Kolaric, D.; Jaganjac, M.; Zarkovic, K.; Skala, K.; Zarkovic, N. Specific thermographic changes during Walker 256 carcinoma development: differential infrared imaging of tumour, inflammation and haematoma. *Cancer*

- Detect. Prev.*, **2009**, 32, 431–436.
- [47] Song, C.; Appleyard, V.; Murray, K.; Frank, T.; Sibbett, W.; Cuschieri, A.; Thompson, A. Thermographic assessment of tumor growth in mouse xenografts. *Int. J. Cancer*, **2007**, 121, 1055–1058.
- [48] Head, JF.; Wang, F.; Lipari, CA.; Elliott, RL. The important role of infrared imaging in breast cancer - new technology improves applications in risk assessment, detection, diagnosis, and prognosis. *IEEE Eng. Med. Biol. Mag.*, **2000**, 19, 52–57.
- [49] Anbar, M. Clinical thermal imaging today. *IEEE Eng. Med. Biol. Mag.*, **1998**, 17, 25–33.
- [50] Eddie, Y-K.; Fork, S-C. A framework for early discovery of breast tumor using thermography with artificial neural network. *Breast J.*, **2003**, 9, 341–343.
- [51] Xie, W.; McCahon, P.; Jakobsen, K.; Parish, C. Evaluation of the ability of digital infrared imaging to detect vascular changes in experimental animal tumours. *Int. J. Cancer*, **2004**, 108, 790–794.
- [52] Hanahan, D.; Folkman, J. Patterns and emerging mechanism of the angiogenic switch during tumorigenesis. *Cell*, **1996**, 86, 353–364.
- [53] Fox, SB.; Gatter, KC.; Harris, AL. Tumour angiogenesis. *J. Pathol.*, **1996**, 179, 232–237.
- [54] Folkman, J. What is the evidence that tumors are angiogenesis dependent. *J. Natl. Cancer Inst.*, **1990**, 82, 4–6.
- [55] Schneider, BP.; Miller, KD. Angiogenesis of breast cancer. *J. Clin. Oncol.*, **2005**, 23, 1782–1790.
- [56] Herbst, RS.; Onn, A.; Sandler, A. Angiogenesis and lung cancer: prognostic and therapeutic implications. *J. Clin. Oncol.*, **2005**, 23, 3243–3256.
- [57] Ferroni, P.; Spila, A.; Martini, F.; D’Alessandro, R.; Mariotti, S.; Del Monte, G.; Graziano, P.; Buonomo, O.; Guadagni, F.; Roselli, M. Prognostic value of vascular endothelial growth factor tumor tissue content of colorectal cancer. *Oncology*, **2005**, 69, 145–153.
- [58] Cui, J.; Dong, BW.; Liang, P.; Yu, XL.; Yu, DJ. Effect of c-myc, Ki-67, MMP-2 and VEGF expression on prognosis of hepatocellular carcinoma patients undergoing tumor resection. *World J. Gastroenterol.*, **2004**, 10, 1533–1536.
- [59] Bartoletti, R.; Cai, T.; Nesi, G.; Sardi, I.; Rizzo, M. Qualitative and quantitative

- analysis of angiogenetic factors in transitional cell bladder carcinoma: relationship with clinical course at 10 years follow-up. *Oncol. Rep.*, **2005**, 14, 251–255.
- [60] Meng-Shu, T.; Min-Liang, K.; Cheng-Chi, C.; Ying-Tai, W. The effects of exercise training on levels of vascular endothelial growth factor in tumor-bearing mice. *Cancer Biomark.*, **2015**, 13, 307-313.
- [61] Isanejad, A.; Alizadeh, AM.; Shalamzari, SA.; Khodayari, H.; Khodayari, S.; Khori, V.; Khojastehnjad, N. MicroRNA-206, let-7a and microRNA-21 pathways involved in the anti-angiogenesis effects of the interval exercise training and hormone therapy in breast cancer. *Life Sci.*, **2016**, 151, 30–40.
- [62] Macneil, B.; Hoffmangoetz, L. Exercise training and tumor-metastasis in mice - influence of time of exercise onset. *Anticancer Res.*, **1993**, 13, 2085–2088.
- [63] Macneil, B.; Hoffmangoetz, L. Effect of exercise on natural cytotoxicity and pulmonary tumor-metastases in mice. *Med. Sci. Sports Exerc.*, **1993**, 25, 922–928.
- [64] Shalamzari, SA.; Agha-Alinejad, H.; Alizadeh, S.; Shahbazi, S.; Khatib, ZK.; Kazemi, AR.; Saei, MA.; Minayi, N. The effect of exercise training on the level of tissue IL-6 and vascular endothelial growth factor in breast cancer bearing mice. *Iran. J. Basic Med. Sci.*, **2014**, 17, 231–236.
- [65] Zielinski, MR.; Muenchow, M.; Wallig, MA.; Horn, PL.; Woods, JA. Exercise delays allogeneic tumor growth and reduces intratumoral inflammation and vascularization. *J. Appl. Physiol.*, **2004**, 96, 2249–2256.
- [66] Restucci, B.; Papparella, S.; Maiolino, P.; De Vico, G. Expression of vascular endothelial growth factor in canine mammary tumors. *Vet. Pathol.*, **2002**, 39, 488–493.

CHAPTER 9

**A CONTRAST-ENHANCED ULTRASONOGRAPHIC STUDY
ABOUT THE IMPACT OF LONG-TERM EXERCISE TRAINING
ON MAMMARY TUMORS VASCULARIZATION**

THE CONTENT OF THIS CHAPTER WAS PUBLISHED IN:

Faustino-Rocha AI, Gama A, Oliveira PA, Vanderperren K, Saunders JH, Pires MJ, Ferreira R, Ginja M. 2017. A contrast-enhanced ultrasonographic study about the impact of long-term exercise training on mammary tumors vascularization. *Journal of Ultrasound in Medicine*. (Accepted for publication) (Full paper)

Faustino-Rocha AI, Talhada D, Andrade A, Teixeira-Guedes CI, Ferreira R, Gama A, Oliveira PA, Ginja M. 2014. Evaluation of MNU-induced mammary tumours in female Sprague-Dawley rats by histology and contrast enhanced ultrasound. *Journal of Comparative Pathology* 150 (1): 110. DOI: 10.1016/j.jcpa.2013.11.141. (Abstract)

Faustino-Rocha AI, Talhada D, Andrade A, Teixeira-Guedes CI, Gil da Costa RM, Ferreira R, Gama A, Oliveira PA, Ginja M. 2013. Evaluation of MNU-induced mammary tumours in female Sprague-Dawley rats by histology and contrast enhanced ultrasound. 31st Meeting of the ESVP and Annual Meeting of the ECVP, 4th to 7th September, London, United Kingdom. (Poster presentation)

9. A contrast-enhanced ultrasonographic study about the impact of long-term exercise training on mammary tumors vascularization

Abstract

This study aimed to evaluate the impact of long-term exercise training on the vascularization of rat mammary tumors. Female rats were divided into four groups: *N*-methyl-*N*-nitrosourea (MNU)-sedentary, MNU-exercised, control sedentary and control exercised. Tumor development was induced in MNU groups by the MNU administration. Exercised groups were trained for 35 weeks. Tumor vascularization was evaluated by Pulsed Doppler and contrast-enhanced ultrasound (CEUS). The pulsatility and resistive indexes were slightly higher in MNU sedentary group ($p>0.05$). Mammary tumors mainly exhibited a centripetal and heterogeneous enhancement of the contrast, clear margins and presence of penetrating vessels. MNU exercised group exhibited lower arrival time (AT) and time to peak (TTP), and higher peak intensity (PI), wash-in and wash-out ($p>0.05$). Area under the curve (AUC) was similar between groups ($p>0.05$). The CEUS study did not detect the differences in the mammary tumor vascularization between MNU-sedentary and MNU-exercised groups previously detected by Power Doppler (PDI), B Flow and immunohistochemistry.

Keywords: contrast-enhanced ultrasound, exercise training, mammary cancer, Pulsed Doppler, rat

9.1. Introduction

Breast cancer is one of the most common cancers in both developed and developing countries. According to the World Health Organization, it was responsible by approximately 521 000 deaths worldwide in 2012 [1]. Tumor angiogenesis is recognized as a crucial factor for cancer growth and progression [2,3]. Immunohistochemistry has been widely used in experimental studies to quantify tumor vascularization [4,5]. However, it may be performed only after tumor excision and it is significantly affected by variations in the methodology [4–7]. So, the imaging methods that allow a non-invasive evaluation of tumor vascularization, such as ultrasonography, computed

tomography and magnetic resonance imaging have been extensively used in experimental studies aiming to develop new antiangiogenic strategies [8,9]. Although computed tomography and magnetic resonance imaging have a good spatial resolution and higher accuracy compared to ultrasonography, these advanced imaging techniques are non-movable and much more expensive what constitutes a limitation for several research teams [10]. Due to its characteristics, namely it does not impose radiation [11], it allows a dynamic and real-time study, it is more adequate for patients with claustrophobia, it can be used in patients with pacemaker or other metal implants, it is portable and less expensive when compared with other imaging modalities, ultrasonography has been frequently used in clinical practice [2,3]. Different ultrasonographic methods, such as Doppler (Color Doppler, Power Doppler (PDI) and Pulsed Doppler), B Flow and more recently contrast-enhanced ultrasound (CEUS) may be used to visualize and characterize tissues angiogenesis. From these, the CEUS is considered the most accurate method for visualizing tumor angiogenesis [12,13].

The impact of lifestyle (diet, smoking, alcohol consumption, sedentarism) on cancer risk has been extensively studied [14]. The practice of exercise training has been associated with the decreased risk of development of several types of cancer, namely breast, endometrial, prostate, colon and lung cancer [15–17]. It was previously observed by our research team that the long-term exercise training reduced the number and malignancy of tumors and increased the estrogen receptors expression in mammary tumors chemically-induced in female rats [18].

The present work intended to evaluate the impact of long-term exercise training on the vascularization of mammary tumors chemically-induced in a rat model by ultrasonography using a second-generation contrast agent.

9.2. Material and Methods

9.2.1. Animals

Fifty female Sprague-Dawley rats (*Rattus norvegicus*) with 4-5 weeks of age were acquired from Harlan Laboratories Inc. (Barcelona, Spain). Animals were placed at the facilities of University of Trás-os-Montes and Alto Douro, under controlled conditions of temperature ($23\pm 2^{\circ}\text{C}$), humidity ($50\pm 10\%$), air system filtration (10-20 ventilations/hour)

and on a 12h:12h light:dark cycle. They were provided with tap water and a basic standard diet (4RF21[®], Mucedola, Settimo Milanese, Milan, Italy) *ad libitum*. Cages were cleaned and water was changed weekly. All procedures were done in accordance with European legislation (European Directive 2010/63/EU). The Portuguese Ethics Committee for Animal Experimentation approved all the experiments and procedures carried out on the animals (approval no. 008961).

9.2.2. Experimental protocol

After one week of quarantine and two weeks of acclimatization to the laboratory conditions, animals were randomly divided into four experimental groups: *N*-methyl-*N*-nitrosourea (MNU) sedentary (n=15), MNU exercised (n=15), control sedentary (n=10) and control exercised (n=10). Mammary tumors development was induced in animals from both MNU groups (sedentary and exercised) by the intraperitoneal administration of the carcinogen agent MNU (50 mg/kg of body weight) (ISOPAC[®], Sigma Aldrich S.A., Madrid, Spain) at seven weeks of age. At same age, control animals (sedentary and exercised) received an intraperitoneal injection of saline 0.9%. On the day after the MNU or saline injection, the animals from exercised groups (MNU and control) were acclimated to the treadmill running (Treadmill Control[®] LE 8710, Panlab, Harvard Apparatus, Holliston, MA, USA) for five days at a speed of 20 m/min. They started with a training of 20 min/day that was progressively increased until 60 min/day. The exercise protocol (20 m/min, 60 min/day, five days/week) was maintained for 35 weeks. The animals were trained during the 12h dark period of the light:dark cycle. Sedentary animals (MNU and control) were daily handled in order to be exposed to similar stress conditions. Animals were observed twice a day to check their health status. They were weekly palpated for the detection of mammary tumor development.

9.2.3. Animal experiments

At the end of the protocol, all survived animals (animals with 42 weeks of age) were anesthetized with ketamine (75 mg/kg of body weight, Imalgene[®] 1000, Merial S.A.S., Lyon, France) and xylazine (10 mg/kg of body weight, Rompun[®] 2%, Bayer Healthcare S.A., Kiel, Germany) and the mammary tumor vascularization was evaluated by

ultrasonography (Power Doppler (PDI), B Flow, Pulsed Doppler and CEUS). PDI and B Flow analysis were performed as previously described by our research team using a real-time scanner Logiq P6® (General Electric Healthcare, Milwaukee, WI, USA) and a 10 MHz linear probe [19,20]. The pulsatility index and resistive index were determined in Pulsed Doppler images by means of the equipment's software autotrace function using the following formulas [21].

$$\text{Pulsatility index} = \frac{\text{Peak systolic velocity} - \text{End diastolic velocity}}{\text{Mean velocity}}$$

$$\text{Resistive index} = \frac{\text{Peak systolic velocity} - \text{End diastolic velocity}}{\text{Peak systolic velocity}}$$

9.2.4. CEUS

System settings were optimized for the contrast study with a mechanical index of 0.09, the gain compensation was adjusted for each mammary tumor. The position of the probe was maintained during the examination. The contrast agent SonoVue® (Bracco, Milan, Italy) was reconstituted by adding 5 mL of 0.9% saline solution. The SonoVue® was injected as a bolus (0.1 mL) through a tail vein catheter followed by a 1 mL saline flush. The injection technique was carefully performed by the same researcher to avoid personal variations, and produce acceptable and reproducible results. The real-time perfusion process and the dynamic enhancement of each mammary tumor were observed in real time and continuously recorded in the ultrasonography apparatus immediately after the intravenous injection of the contrast agent. Posteriorly, the qualitative and quantitative analysis of CEUS videos was performed. Qualitative analysis included the following parameters: enhancement order (centripetal or centrifugal), margin (blurred or clear), enhancement homogeneity (homogenous or heterogeneous) and penetrating vessels (absent or present) [22]. The quantitative analysis was performed using the time intensity curve (TIC) analysis of the ultrasonography apparatus. An ovoid region of interest (ROI)

was drawn in the most enhanced area of each mammary tumor and the signal was immediately plotted and fitted using the following gamma variate function:

$$I(t) = At^c \times \exp(-kt) + B,$$

where t is the time, k is a constant scale factor, and A and B are parameters that define the shape of the curve. The following parameters were determined: contrast agent arrival time (AT), time to peak (TTP, defined as the time from the initiation of the injection to the point of maximum contrast intensity of the lesions from the baseline), peak intensity (PI, maximum intensity), wash-in (upslope), wash-out (downslope) and area under the curve (AUC).

9.2.5. Statistical analysis

Data were statistically analyzed using Statistical Package for the Social Sciences (SPSS[®], version 23 for Windows, SPSS Inc., Chicago, IL, USA). Continuous data were compared between MNU exercised and sedentary groups using unpaired t -test. Data from qualitative analysis of CEUS were analyzed using Chi-square test. Continuous data are expressed as mean \pm standard error (S.E.) and p values lower than 0.05 were considered statistically significant.

9.3. Results

9.3.1. General findings

Nine animals died during the experimental protocol: four animals from MNU sedentary group, four animals from MNU exercised group and one animal from control sedentary group. The high mortality index observed in MNU-exposed groups was probably related with the carcinogenesis (each animal developed more than one mammary tumor); the animal from control group died suddenly and the cause of death could not be determined. Additionally, one animal from MNU exercised group did not adapt to the exercise training and was excluded from the experiment. In this way, the size of these experimental groups was reduced as follows: MNU sedentary (n=11), MNU

exercised (n=10), control sedentary (n=9). The size of the control exercised group remained as previously defined (n=10).

9.3.2. Mammary tumors' development

The first mammary tumor was detected by palpation in MNU sedentary and MNU exercised groups ten and 12 weeks after the MNU administration, respectively. At the end of the study, all animals from both MNU groups developed mammary tumors (incidence of 100%). A total of 51 mammary tumors were counted: 28 mammary tumors in MNU sedentary group and 23 mammary tumors in MNU exercised one. As expected, animals from control groups (sedentary and exercised) did not develop any mammary tumor.

9.3.3. Mammary tumors' vascularization

Due to their small size, only 15/28 (54%) mammary tumors from MNU sedentary group and 11/23 (48%) mammary tumors from MNU exercised one were evaluated by CEUS. All of them were histologically classified as malignant (mammary carcinomas) [19;20]. The resistive and pulsatility indexes determined in Pulsed Doppler analysis of the mammary tumors were slightly higher in MNU sedentary group when compared with MNU exercised one ($p>0.05$) (Table 9.1, Figure 9.1).

Concerning to the qualitative evaluation of CEUS, in an overall view, the majority of mammary tumors exhibited a centripetal enhancement order ($p<0.05$), clear margins, a heterogeneous enhancement ($p=0.05$) and presence of penetrating vessels. Looking for each group independently, the enhancement order of the contrast agent was mainly centripetal in MNU sedentary group ($p<0.05$), while the number of mammary tumors with centripetal and centrifugal enhancement order in MNU exercised group was similar ($p>0.05$). Although the difference did not reach the level of statistical significance ($p>0.05$), it was also observed that the majority of mammary tumors from MNU sedentary group exhibited clear margin, while the number of mammary tumors with clear and blurred margin in MNU exercised group was very similar. Both homogeneous and heterogeneous enhancement of contrast agent were very frequent in MNU sedentary group ($p>0.05$), while the enhancement in the MNU exercised group was mostly

heterogeneous ($p < 0.05$). The majority of mammary tumors from MNU exercised group exhibited penetrating vessels, while the number of mammary tumors from MNU sedentary group with and without penetrating vessels was very similar ($p > 0.05$) (Table 9.2).

Additionally to qualitative analysis, the CEUS study was quantitatively analyzed. Although statistically significant differences were not found between groups ($p > 0.05$), some tendencies were observed; the AT and TTP were slightly lower in MNU exercised group when compared with MNU sedentary one, and the inverse was observed for PI, ascending slope (wash-in) and descending slope (wash-out). Unexpectedly, AUC was very similar between groups ($44.14 \text{ dB} \pm 7.32$ and $44.59 \text{ dB} \pm 6.40$ for MNU sedentary and MNU exercised groups, respectively) (Figure 9.2, Table 9.1).

Table 9.1. Evaluation of mammary tumors vascularization by Pulsed Doppler and CEUS (mean \pm S.E.).

Technique	Parameter/measurement unit	Groups	
		MNU sedentary n=15	MNU exercised n=11
Pulsed Doppler	Resistive index	0.87 ± 0.10	0.79 ± 0.08
	Pulsatility index	3.50 ± 0.73	2.86 ± 0.72
CEUS	Arrival time (AT) (s)	5.93 ± 0.63	4.73 ± 0.27
	Time to peak (TTP) (s)	10.05 ± 0.64	8.79 ± 0.63
	Peak intensity (PI) (dB)	4.81 ± 0.81	5.62 ± 0.82
	Wash-in (dB/s)	1.35 ± 0.27	1.83 ± 0.41
	Wash-out (dB/s)	-0.45 ± 0.09	-0.60 ± 0.13
	Area under the curve (AUC) (dB)	44.14 ± 7.32	44.59 ± 6.40

Statistically significant differences between groups were not found ($p > 0.05$). CEUS: contrast-enhanced ultrasound.

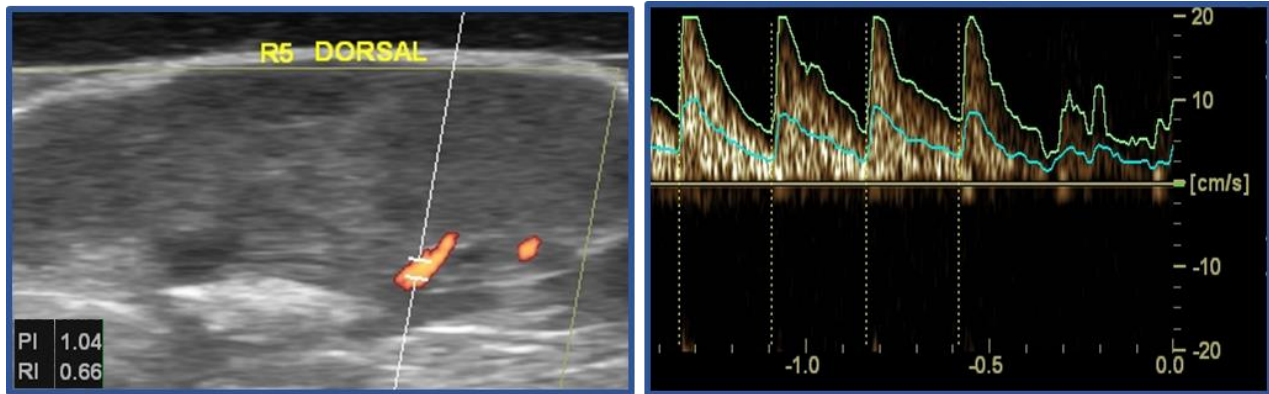


Figure 9.1. Evaluation of a mammary tumor from MNU exercised group by Pulsed Doppler. The pulsatility (1.04) and resistive (0.66) indexes were calculated using the autotrace function of the ultrasound machine.

Table 9.2. Qualitative evaluation of CEUS of mammary tumors in both MNU-exposed experimental groups.

Parameter/Group		MNU sedentary	MNU exercised	n=26
		n=15	n=11	
Enhancement order	Centripetal	14 (93.33%) ^a	7 (63.64%)	21 (80.77%) ^a
	Centrifugal	1 (6.67%)	4 (36.36%)	5 (19.32%)
Margin	Clear	11 (73.33%)	5 (45.45%)	16 (61.54%)
	Blurred	4 (26.67%)	6 (54.55%)	10 (38.46%)
Enhancement homogeneity	Homogeneous	7 (46.67%) ^b	1 (9.09%) ^c	8 (30.77%) ^d
	Heterogeneous	8 (53.33%)	10 (90.91%)	18 (69.23%)
Penetrating vessels	Absent	7 (46.67%)	3 (27.27%)	10 (38.46%)
	Present	8 (53.33%)	8 (72.73%)	16 (61.54%)

^a Statistical different from centrifugal enhancement order; ^b Statistical different from MNU exercised group ($p < 0.05$); ^c Statistically different from heterogeneous enhancement homogeneity ($p < 0.05$); ^d $p = 0.05$ from heterogeneous enhancement homogeneity. The results concerning to MNU sedentary group were previously published, here are presented in order to provide a better comparison with the results of the present work.

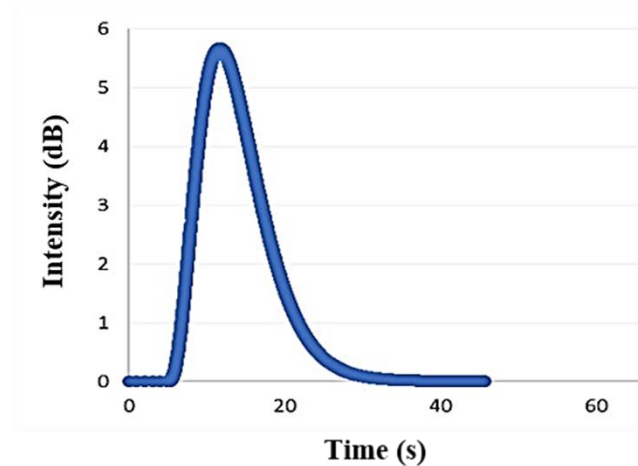


Figure 9.2. Mathematical representation of the evaluation of the vascularization of a mammary tumor from MNU exercised group by CEUS after gamma variate curve fitting. The peak intensity was 5.66 dB and area under the curve was 56.79 dB.

9.4. Discussion

Breast cancer remains as a great concern among female population worldwide. Despite all the research and advances in the field, the existing therapeutic approaches have devastating effects for patients and have sometimes revealed unsuccessful (high rates of cancer metastization, recurrence and mortality) [23]. This has motivated the researchers on the search of new therapeutic (alternative or adjuvant) approaches that may improve the quality of life and increase the lifespan of oncologic patients. As an attempt to contribute to this field and try to find new strategies to inhibit or at least decrease the mammary tumors vascularization, the present work aimed to evaluate the impact of lifestyle on mammary tumor vascularization. For this, a well-recognized rat model of mammary cancer chemically-induced was submitted to treadmill exercise training for a long period of time (35 weeks) and the mammary tumor vascularization was evaluated by CEUS.

The vascularization of the presented mammary tumors was previously evaluated by thermography, ultrasonography (PDI and B Flow modes), and immunohistochemistry using the vascular endothelial growth factor (VEGF)-A immunoexpression and the quantification of microvessel density (MVD). Data from all techniques suggested a higher

vascularization of mammary tumors from MNU-exercised group when compared with mammary tumors from MNU-sedentary one [19,20].

Although the immunohistochemistry and the MVD are considered gold standards for assessment of tumor vascularization, they are invasive techniques that may be performed only after the excision of the tumors and do not allow the evaluation of angiogenesis in different time points throughout an experimental protocol [24]. Additionally, the immunohistochemistry is not reproducible (distinct laboratory conditions, antibodies and antigen retrieval), and its evaluation is relatively subjective, two dimensional and not necessarily representative of vascularity throughout the entire sample [4–7]. Due to this, the evaluation of tumor angiogenesis by using a non-invasive approach like ultrasonography reveals essential.

Despite the quantification of mammary tumor vascularization by PDI and B Flow, we also intended to better characterize it by the calculation of pulsatility and resistive indexes using Pulsed Doppler. According to previous studies, the resistive and pulsatility indexes may be indicators of malignancy [25]. Since all mammary tumors in our sample were malignant, the comparison between malignant and benign tumors was not possible. Although no statistically significant differences were found, the resistive and pulsatility indexes were slightly higher in MNU sedentary group when compared with MNU exercised one. This may be explained by the higher malignancy of mammary tumors from MNU sedentary group when compared with MNU exercised one (animals from MNU exercised group did not develop any mammary comedocarcinoma, which was the most aggressive lesion identified in this experimental protocol) [18].

The mammary tumor vascularization was also quantified by CEUS that is considered more accurate for assessing tumor angiogenesis by increasing the detectable ultrasound signal from the blood pool [26,27]. Microbubble specific techniques allow imaging of vessels down to 50 μm in diameter. In addition, since microbubbles are vascular tracers, their passage through a tissue may be quantified to generate time intensity curves from which several functional indices, such as AT, TTP, PI, wash-in, wash-out and AUC may be derived [28,29]. Similarly to that observed in previous studies [30–32], the mammary tumors from both groups exhibited characteristics of malignant tumors: a centripetal enhancement order of the contrast agent, clear margins, heterogeneous enhancement and presence of penetrating vessels.

According to several researchers, malignant mammary tumors are more vascularized and exhibited lower AT, TTP and higher PI. Although in the present study all tumors were malignant, as mentioned above, the grade of malignancy was lower in MNU exercised group. In this way, a lower vascularization was expected in tumors from MNU exercised group, and consequently a higher AT, TTP and lower PI. Surprisingly, the data from PDI, B Flow and immunohistochemistry suggested a higher vascularization of mammary tumors from MNU exercised group when compared with MNU sedentary one which explains the lower AT and TTP, the higher PI and the faster wash-in and wash-out when compared with tumors from MNU sedentary group. According to previous studies, more vascularized tumors probably have more arteriovenous shunts and higher microvascular density that contribute to a faster arrival of the contrast agent to the tumor (AT) and to the peak (TTP), higher peak (PI) and faster ascending (wash-in) and descending (wash-out) slopes [31,33,34]. Taking all data into account, a higher mean AUC was expected in MNU exercised group; however, it was not observed ($44.14 \text{ dB} \pm 7.32$ in MNU sedentary group *versus* $44.59 \text{ dB} \pm 6.40$ in MNU exercised group).

9.5. Conclusion

The CEUS study did not detect the differences in the mammary tumor vascularization between MNU sedentary and MNU exercised groups that had been previously detected by PDI, B Flow and immunohistochemistry.

9.6. References

- [1] World Health Organization (WHO). Cancer - Fact sheet n° 297. *WHO*, **2015**.
- [2] Folkman, J. Angiogenesis and breast cancer. *J. Clin. Oncol.*, **1994**, 12, 441–443.
- [3] Folkman, J. Role of angiogenesis in tumor growth and metastasis. *Semin. Oncol.*, **2002**, 29, 15–18.
- [4] Savai, R.; Langheinrich, C.; Schermuly, RT.; Pullamsetti, SS.; Dumitrascu, R.; Traupe, H.; Rau, WS.; Seeger, W.; Grimminger, F.; Banat, GA. Evaluation of angiogenesis using micro-computed tomography in a xenograft mouse model of lung cancer. *Neoplasia*, **2009**, 11, 48–56.
- [5] Wang, D.; Stockard, CR.; Karkins, L.; Lott, P.; Salih, C.; Yuan, R.; Buchsbaum,

- D.; Hashim, A.; Zayzafoon, M.; Hardy, R.; Hameed, O.; Grizzle, W.; Siegal, GP. Immunohistochemistry in the evaluation of neovascularization in tumor xenografts. *Biotechnol. Histochem.*, **2008**, 83, 179–189.
- [6] Meert, AP.; Paesmans, M.; Martin, B.; Delmotte, P.; Berghmans, T.; Verdebout, JM.; Lafitte, JJ.; Mascaux, C.; Sculier, JP. The role of microvessel density on the survival of patients with lung cancer: a systematic review of the literature with meta-analysis. *Br. J. Cancer*, **2002**, 87, 694–701.
- [7] Ragel, BT.; Jensen, RL.; Gillespie, DL.; Prescott, SM.; Couldwell, WT. Celecoxib inhibits meningioma tumor growth in a mouse xenograft model. *Cancer*, **2007**, 109, 588–597.
- [8] Tatum, JL.; Hoffman, JM. Role of imaging in clinical trials of antiangiogenesis therapy in oncology. *Acad. Radiol.*, **2000**, 7, 798–799.
- [9] Jeswani, T.; Padhani, AR. Imaging tumour angiogenesis. *Cancer Imaging*, **2005**, 5, 131–138.
- [10] Heijblom, M.; Klaase, JM.; Van den Engh, FM.; van Leeuwen, TG.; Steenbergen, W.; Manohar, S. Imaging Tumor vascularization for detection and diagnosis of breast cancer. *Technol. Cancer Res. Treat.*, **2011**, 10, 607–623.
- [11] Jacobson, JA. Ultrasound in sports medicine. *Radiol. Clin. North Am.*, **2002**, 40, 363–386.
- [12] Cheng, WF.; Lee, CN.; Chu, JS.; Chen, CA.; Chen, TM.; Shau, WY.; Hsieh, CY.; Hsieh, FJ. Vascularity index as a novel parameter for the *in vivo* assessment of angiogenesis in patients with cervical carcinoma. *Cancer*, **1999**, 85, 651–657.
- [13] Ferrara, KW.; Merritt, CRB.; Burns, PN.; Foster, FS.; Mattrey, RF.; Wickline, SA. Evaluation of tumor angiogenesis with US: imaging, Doppler, and contrast agents. *Acad. Radiol.*, **2000**, 7, 824–839.
- [14] Katzke, VA.; Kaaks, R.; Kuhn, T. Lifestyle and cancer risk. *Cancer J.*, **2015**, 21, 104–110.
- [15] Al-Jarrah, M.; Matalka, I.; Al Aseri, H.; Mohtaseb, A.; Smirnova, I V.; Novikova, L.; Stehno-Bittel, L.; AlKhateeb, A. Exercise Training prevents endometrial hyperplasia and biomarkers for endometrial cancer in rat model of type 1 diabetes. *J. Clin. Med. Res.*, **2010**, 2, 207–214.
- [16] Esser, KA.; Harpole, CE.; Prins, GS.; Diamond, AM. Physical activity reduces

- prostate carcinogenesis in a transgenic model. *Prostate*, **2009**, 69, 1372–1377.
- [17] Murphy, EA.; Davis, JM.; Brown, AS.; Carmichael, MD.; Mayer, EP.; Ghaffar, A. Effects of moderate exercise and oat beta-glucan on lung tumor metastases and macrophage antitumor cytotoxicity. *J. Appl. Physiol.*, **2004**, 97, 955–959.
- [18] Faustino-Rocha, A.; Gama, A.; Oliveira, PA.; Alvarado, A.; Neuparth, MJ.; Ferreira, R.; Ginja, M. Effects of lifelong exercise training on mammary tumorigenesis induced by MNU in female Sprague-Dawley rats. *Clin. Exp. Med.*, **2016**, Epub ahead of print.
- [19] Faustino-Rocha, AI.; Silva, A.; Gabriel, J.; Gil da Costa, RM.; Moutinho, M.; Oliveira, PA.; Gama, A.; Ferreira, R.; Ginja, M. Long-term exercise training as a modulator of mammary cancer vascularization. *Biomed. Pharmacother.*, **2016**, 81, 273–280.
- [20] Faustino-Rocha, AI.; Silva, A.; Gabriel, J.; Teixeira-Guedes, CI.; Lopes, C.; Gil da Costa, R.; Gama, A.; Ferreira, R.; Oliveira, PA.; Ginja, M. Ultrasonographic, thermographic and histologic evaluation of MNU-induced mammary tumors in female Sprague-Dawley rats. *Biomed. Pharmacother.*, **2013**, 67, 771–776.
- [21] Ghorbani, A.; Shirazi, AS.; Sametzadeh, M.; Mansoori, P.; Taheri, A. Relation of resistive and pulsatility indices with graft function after renal transplant. *Exp. Clin. Transplant.*, **2012**, 10, 568–572.
- [22] Du, J.; Li, FH.; Fang, H.; Xia, JG.; Zhu, CX. Correlation of real-time gray scale contrast-enhanced ultrasonography with microvessel density and vascular endothelial growth factor expression for assessment of angiogenesis in breast lesions. *J. Ultrasound Med.*, **2008**, 27, 821–831.
- [23] Cao, DF.; Vollmer, RT.; Luly, J.; Jain, S.; Roytman, TM.; Ferris, CW.; Hudson, MA. Comparison of 2004 and 1973 World Health Organization grading systems and their relationship to pathologic staging for predicting long-term prognosis in patients with urothelial carcinoma. *Urology*, **2010**, 76, 593–599.
- [24] Fanelli, M.; Locopo, N.; Gattuso, D.; Gasparini, G. Assessment of tumor vascularization: immunohistochemical and non-invasive methods. *Int. J. Biol. Markers*, **1999**, 14, 218–231.
- [25] Petersen, LJ.; Petersen, JR.; Talleruphuus, U.; Ladefoged, SD.; Mehlsen, J.; Jensen, HA. The pulsatility index and the resistive index in renal arteries.

- Associations with long-term progression in chronic renal failure. *Nephrol. Dial. Transplant.*, **1997**, 12, 1376–1380.
- [26] Eisenbrey, JR.; Forsberg, F. Contrast-enhanced ultrasound for molecular imaging of angiogenesis. *Eur. J. Nucl. Med. Mol. Imaging*, **2010**, 37, S138–146.
- [27] Forsberg, F.; Kuruvilla, B.; Pascua, MB.; Chaudhari, MH.; Merton, DA.; Palazzo, JP.; Goldberg, BB. Comparing contrast-enhanced color flow imaging and pathological measures of breast lesion vascularity. *Ultrasound Med. Biol.*, **2008**, 34, 1365–1372.
- [28] Jakobsen, JA. Ultrasound contrast agents: clinical applications. *Eur. Radiol.*, **2001**, 11, 1329–1337.
- [29] Correas, JM.; Bridal, L.; Lesavre, A.; Mejean, A.; Claudon, M.; Helenon, O. Ultrasound contrast agents: properties, principles of action, tolerance, and artifacts. *Eur. Radiol.*, **2001**, 11, 1316–1328.
- [30] Badea, AF.; Szora, AT.; Clichici, S.; Socaciu, M.; Tabaran, AF.; Baciut, G.; Catoi, C.; Muresan, A.; Buruian, M.; Badea, R. Contrast enhanced ultrasonography (CEUS) in the characterization of tumor microcirculation. Validation of the procedure in the animal experimental model. *Med. Ultrason.*, **2013**, 15, 85–94.
- [31] Balleyguier, C.; Opolon, P.; Mathieu, MC.; Athanasiou, A.; Garbay, JR.; Delaloge, S. New potential and applications of contrast-enhanced ultrasound of the breast: own investigations and review of the literature. *Eur. J. Radiol.*, **2009**, 69, 14–23.
- [32] Du, J.; Wang, L.; Wan, CF.; Hua, J.; Fang, H.; Chen, J.; Li, FH. Differentiating benign from malignant solid breast lesions: combined utility of conventional ultrasound and contrast-enhanced ultrasound in comparison with magnetic resonance imaging. *Eur. J. Radiol.*, **2012**, 81, 3890–3899.
- [33] Buadu, LD.; Murakami, J.; Murayama, S.; Hashiguchi, N.; Sakai, S.; Masuda, K.; Toyoshima, S.; Kuroki, S.; Ohno, S. Breast lesions: correlation of contrast medium enhancement patterns on MR images with histopathologic findings and tumor angiogenesis. *Radiology*, **1996**, 200, 639–649.
- [34] Schneider, BP.; Miller, KD. Angiogenesis of breast cancer. *J. Clin. Oncol.*, **2005**, 23, 1782–1790.

CHAPTER 10

**EFFECTS OF LONG-TERM EXERCISE TRAINING IN
GASTROCNEMIUS MUSCLE IN A RAT MODEL OF *N*-METHYL-
N-NITROSOUREA-INDUCED MAMMARY TUMORS:
ULTRASONOGRAPHIC EVALUATION**

THE CONTENT OF THIS CHAPTER WAS PUBLISHED IN:

Faustino-Rocha AI, Oliveira PA, Duarte JA, Ferreira R, Ginja M. 2013. Ultrasonographic evaluation of *gastrocnemius* muscle in a rat model of *N*-methyl-*N*-nitrosourea-induced mammary tumor. *In vivo* 27 (6): 803-807. (Full paper)

Faustino-Rocha AI, Oliveira PA, Pinto C, Gil da Costa RM, Duarte JA, Ferreira R, Ginja M. 2015. Effects of physical exercise on *gastrocnemius* muscle in a rat model of mammary cancer. *Journal of Comparative Pathology* 152 (1): 78. DOI: 10.1016/j.jcpa.2014.10.148. (Abstract)

Faustino-Rocha AI, Oliveira PA, Pinto C, Gil da Costa RM, Duarte JA, Ferreira R, Ginja M. 2014. Effects of physical exercise on *gastrocnemius* muscle in a rat model of mammary cancer. 32nd Meeting of the ESVP and Annual Meeting of the ECVP, 27th to 30th August, Berlin, Germany. (Poster presentation)

Faustino-Rocha AI. 2013. Avaliação ultrassonográfica dos efeitos do exercício físico no músculo gastrocnémio num modelo de cancro da mama quimicamente induzido. IV Fórum de Investigação Farmacológica, 23rd October, Vila Real, Portugal. (Poster presentation)

10. Effects of long-term exercise training in *gastrocnemius* muscle in a rat model of *N*-methyl-*N*-nitrosourea-induced mammary tumors: ultrasonographic evaluation

Abstract

Ultrasonography is frequently used to study body tissues. This study aimed to evaluate by ultrasonography the *gastrocnemius* muscle wasting induced by cancer in a rat model of chemically-induced mammary tumors, and muscular response to exercise. Female Sprague-Dawley rats were divided into four groups. Groups I and II were injected with *N*-methyl-*N*-nitrosourea (MNU). Groups I and III performed endurance training on a treadmill. *Gastrocnemius* muscles were palpated for tonus evaluation. *Gastrocnemius* muscle and fibrous tissue between muscle and tibia were examined by ultrasonography. At necropsy, *gastrocnemius* muscle was collected and weighed. Myostatin was assessed by immunoblotting. The final body weight, *gastrocnemius* weight, length and width were similar among groups. Tone of muscle was higher in exercised animals. Myostatin was higher in MNU-treated groups. Echogenicity of muscle and fibrous tissue was higher in group IV compared with remaining groups ($p < 0.05$). Echogenicity of fibrous tissue was higher than echogenicity of muscle in all groups. Our results showed that muscle ultrasonography is a useful tool to identify alterations in muscle structure. More studies are necessary to understand the influence of fat location in muscle ultrasonographic imaging.

Keywords: exercise, *gastrocnemius* muscle, mammary tumor, MNU, rat, ultrasonography

10.1. Introduction

Since 1950s, when Wild and colleagues discovered the utility of high-frequency ultrasonic waves in observing living tissues, ultrasonography has been extensively used in medical practice [1,2]. Ultrasonography has many advantages compared with other imaging methods: it is an easily accessible and safe method to visualize many different types of body tissue, including the skeletal muscle [3], it does not impose ionizing radiation, and allows dynamic and real-time study [4]; ultrasound equipment is portable and less expensive than magnetic resonance imaging (MRI) and computed tomographic

equipment [4–6]; the ultrasonographic examination is more appropriate for patients with claustrophobia [7,8] and is not contraindicated in patients with cardiac pacemaker or other metal implants [6,8]. Like other imaging methods, ultrasonography has some disadvantages, namely its operator dependency [6]. The echo intensity of ultrasonographic images may be evaluated visually or using a computer assisted grey-scale analysis, the latter being the most accurate method to detect small changes in muscle [9]. Ultrasonography of skeletal muscle may be used as an alternative to or adjuvant non-invasive tool with other imaging methods [2,5,6,10–12].

In ultrasonographic evaluation, skeletal muscle may be easily distinguished from other structures namely, fat, bone, nerves and blood vessels [6,13]. The normal fibers of skeletal muscle appear hypoechogenic (black) and connective tissue is hyperechogenic (white) [10–14]. Fibrous tissue and fat infiltration in muscle cause increased reflections of the ultrasound beam and a consequent white appearance [13,14].

Together with *soleus* muscle, the *gastrocnemius* muscle constitutes the *triceps surae* muscle. The *gastrocnemius* muscle has two parts: the lateral head and medial head, which originate on the lateral and medial condyles of the femur, respectively, and connect to the calcaneus. This muscle is located immediately below the skin, flexes the knee and extends the tarsus [13,15].

Breast cancer is the most frequent malignancy and the principal cause of death in women worldwide [16]. Female rats exposed to *N*-methyl-*N*-nitrosourea (MNU) constitute the most frequently used animal model by researchers aiming to study mammary tumors [17,18]. MNU induces locally aggressive mammary tumors in rats, with the capacity to metastasize, similar to those observed in women [19]. Breast cancer is also associated with cachexia characterized by severe loss of adipose tissue and body weight [20,21]. Animal models are also useful in studying the effects of several exercise modalities, namely treadmill running and swimming [22]. Regular physical exercise has beneficial effects in increasing muscle mass and strength in both animals and humans [23,24].

This study aimed to evaluate by ultrasonography the occurrence of *gastrocnemius* muscle wasting induced by cancer in a rat model of MNU-induced, and the muscular response to exercise.

10.2. Material and Methods

10.2.1. Animals

Fifty outbred female Sprague-Dawley rats (*Rattus norvegicus*), between four and five weeks of age were acquired from Harlan Laboratories Inc. (Barcelona, Spain). Animals were housed in filter capped polycarbonate cages (1500U Eurostandard Type IV S, Tecniplast, Buguggiate, Italy), with corncob for bedding (Mucedola, Settimo Milanese, Milan, Italy). All cages were maintained on a 12h:12h light:dark cycle in a ventilated room under controlled conditions of temperature ($23\pm 2^{\circ}\text{C}$), relative humidity ($50\pm 10\%$), air system filtration (10-20 ventilations/hour) and light:dark cycle (12h:12h). Cages were cleaned once per week and water was changed weekly. Animals had *ad libitum* access to a basic standard diet (4RF21[®], Mucedola, Settimo Milanese, Milan, Italy) and acidified tap water throughout the study. All animal care and experimental procedures were carried out in accordance with the European Directive 2010/63/EU on the protection of animals used for scientific purposes. Animal procedures were approved by the Portuguese Ethics Committee for Animal Experimentation (approval no. 008961).

10.2.2. Animal experiments

After one week of quarantine and two weeks of acclimatization to laboratory conditions, animals were randomly divided into four groups: group I (MNU exercised, n=15), group II (MNU sedentary, n=15), group III (control exercised, n=10) and group IV (control sedentary, n=10). At seven weeks of age, animals from groups I and II were intraperitoneally injected with MNU (ISOPAC[®]; Sigma Aldrich S.A., Madrid, Spain) at a dose of 50 mg/kg of body weight. Animals from groups III and IV were used as negative controls and were not exposed to MNU, they received an intraperitoneal injection of the vehicle (saline solution 0.9%). Animals from groups I and III were exercised on a Treadmill Control[®] LE 8710 (Panlab, Harvard Apparatus, Holliston, MA, USA) at a speed of 20 m/min, 60 min/day, 5 days/week, for 35 weeks. To avoid stress to the animals, they were submitted to a familiarization with the treadmill for a five-day period. During this period, the duration of the exercise training was increased progressively. Animals from sedentary groups (groups II and IV) were daily handled in order to be exposed to similar stress conditions. The first week of the experimental protocol was defined at the

time of MNU administration and the last week was the week when animals were euthanized. The animal body weight was monitored weekly using a top-loading scale (Mettler PM4000, LabWrench, Midland, ON, Canada), starting with the first week of the experiment. The tone of the *gastrocnemius* muscle of both legs of each animal was evaluated at the end of the experiment by palpation by two investigators blinded to group assignment, and considered positive, *i.e.* animals showed an increase in tone of *gastrocnemius* muscle, or negative, *i.e.* the tone of *gastrocnemius* muscle was not increased.

10.2.3. Evaluation of MNU effects

All animals were weekly palpated to detect the presence of mammary tumors. The time of appearance of the first tumor and the total number of tumors were recorded.

10.2.4. Ultrasound examination

At the end of the experimental protocol, the *gastrocnemius* muscle (lateral and medial heads) of the left leg of each animal was examined by B mode ultrasound. Before the examination, the leg was shaved with a machine clipper (Aesculap GT420 Isis, Aesculap Inc., Center Valley, PA, USA). Animals were restrained in prone position and longitudinal ultrasonographic images were obtained under the same conditions in all animals using acoustic gel (Aquasonic, Parker Laboratories Inc., Fairfield, NJ, USA) and a real-time scanner (Logiq P6[®], General Electric Healthcare, Milwaukee, WI, USA) with 10 MHz linear probe. Ultrasonographic apparatus parameters were adjusted as follows: depth of 2 cm and gain of 62 dB. The length and width of *gastrocnemius* muscle were measured by an investigator blinded to the group using electronic cursors integrated into the ultrasound apparatus. Cursors were set at the borders of the muscle (Figure 10.1). The mean echogenicity of each muscle image (lateral and medial heads) and an area of approximately 2 cm² of the fibrous tissue between muscle and tibia was evaluated using the standard histogram function of Adobe Photoshop[®] version 7.0 (Adobe Systems Inc., San Jose, CA, USA) (Figure 10.2).

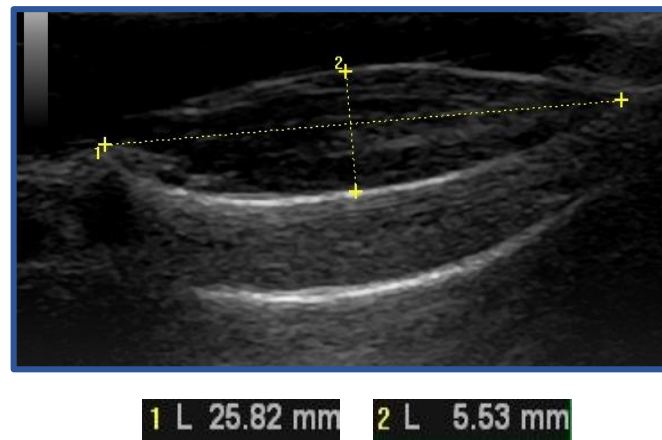


Figure 10.1. Measurement of length (1) and width (2) of *gastrocnemius* muscle.

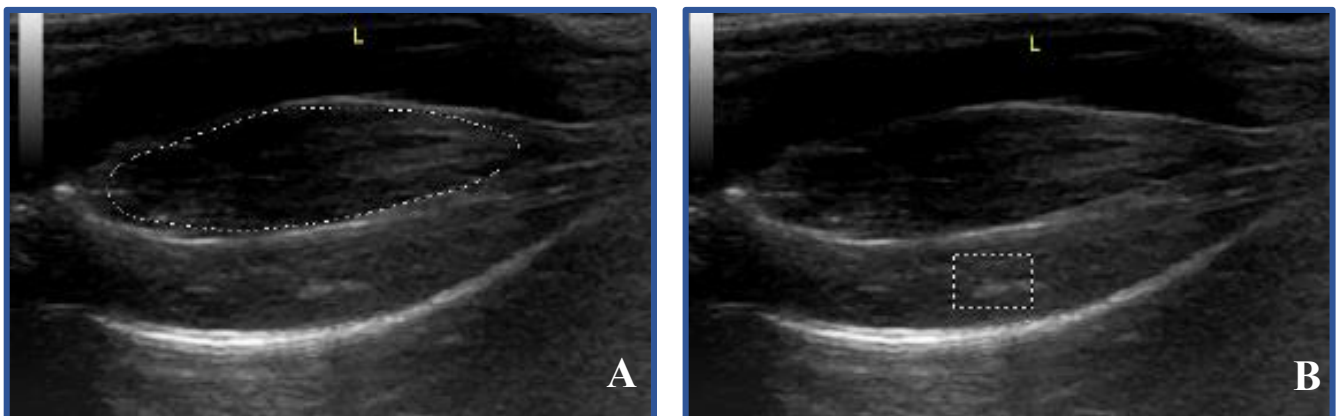


Figure 10.2. Measurement of mean pixels using Adobe Photoshop® in the lateral *gastrocnemius* muscle (A) and in the tissue between muscle and the tibia (B).

10.2.5. Necropsy, sample collection and serum analysis

Thirty-five weeks after the start of the experimental protocol, animals from all groups were sacrificed according to the method described by Faustino-Rocha and collaborators [25]. Blood samples were collected via intracardiac puncture and serum levels of myostatin were posteriorly determined by immunoblotting technique. A complete necropsy was carried out on all animals, and all mammary tumors, organs and the *gastrocnemius* muscle were collected. The mammary tumors and *gastrocnemius* muscle

of each animal were weighed. Accurate body weight of each animal was calculated by the subtraction of the tumor weight from the animal body weight.

10.2.6. Statistics

A descriptive analysis was performed for all variables included in the study. Data were statistically analyzed using Statistical Package for the Social Sciences (SPSS[®], version 23 for Windows, SPSS Inc., Chicago, IL, USA). Final body weight, *gastrocnemius* muscle weight, echogenicity of muscle and fibrous tissue between muscle and tibia, and serum myostatin levels were compared among groups using analysis of variance (ANOVA) with the Bonferroni correction multiple comparison method. Independent *t*-test was also used to compare body weight between MNU (I and II) and control (III and IV) groups, tumor weight and accurate body weight between groups I (MNU exercised) and II (MNU sedentary). Data are presented as mean \pm standard deviation (S.D.). A *p* value of less than 0.05 was considered to be statistically significant.

10.3. Results

10.3.1. General observations

One animal from group I (MNU exercised) did not adapt to the exercised training and was excluded from the experiment. Additionally, nine animals died during the experimental protocol: four animals from each MNU group (MNU sedentary and MNU exercised), and one animal from group IV (control sedentary).

10.3.2. Body weight

Statistically significant differences in body weight and accurate body weight among groups were not detected ($p>0.05$) (Table 10.1). However, the accurate body weight of MNU-treated groups (groups I and II) was slightly lower when compared with body weight of control groups (III and IV) ($p>0.05$).

10.3.3. Mammary tumors

All animals from groups I and II developed mammary tumors (incidence 100%). A total of 51 mammary tumors were palpated: 23 mammary tumors in animals from group I (MNU exercised) and 28 mammary tumors in animals from group II (MNU exercised) (data not shown). Tumor weight was not different between the MNU exercised (group I) and MNU sedentary (group II) animals ($p>0.05$) (Table 10.1).

Table 10.1. Mean \pm S.D. of body weight, tumor weight and accurate body weight.

Group	Body weight (g)	Tumors weight (g)	Accurate body weight (g)
I (MNU exercised)	296.73 \pm 24.73	19.10 \pm 24.28	279.54 \pm 25.05
II (MNU sedentary)	290.30 \pm 17.45	13.35 \pm 17.70	278.16 \pm 22.19
III (control exercised)	296.87 \pm 24.70	-	-
IV (control sedentary)	294.64 \pm 18.05	-	-

Statistically significant differences were not found ($p>0.05$).

10.3.4. Gastrocnemius muscle

All animals from exercised groups (I and III) exhibited an increase in the tone of *gastrocnemius* muscle and were considered positive by both researchers. No statistical significant differences were observed in *gastrocnemius* muscle weight, length and width among groups (Table 10.2).

Table 10.2. Mean \pm S.D. of *gastrocnemius* muscle weight at necropsy, and its length and width as measured by ultrasonography.

Group	<i>Gastrocnemius</i> muscle		
	Weight (g)	Length (mm)	Width (mm)
I (MNU exercised)	1.808 \pm 0.295	25.598 \pm 0.778	5.806 \pm 0.268
II (MNU sedentary)	1.832 \pm 0.134	26.339 \pm 0.971	6.050 \pm 0.239
III (control exercised)	1.998 \pm 0.185	25.872 \pm 0.902	5.770 \pm 0.804
IV (control sedentary)	1.866 \pm 0.241	26.204 \pm 1.175	6.086 \pm 0.236

Statistically significant differences were not found ($p > 0.05$).

10.3.5. Echogenicity of muscle and fibrous tissue between muscle and tibia

No differences in the echogenicity of the *gastrocnemius* muscle were observed among groups I, II and III ($p > 0.05$). The echogenicity of the *gastrocnemius* muscle of the animals from group IV was higher when compared with remaining groups ($p < 0.05$) (Table 10.3).

The echogenicity of the fibrous tissue between muscle and tibia was higher than that of the *gastrocnemius* muscle in all groups ($p < 0.05$). As observed for the echogenicity of *gastrocnemius* muscle, the echogenicity of the tissue between muscle and tibia was similar among groups I, II and III ($p > 0.05$), and different from animals from group IV ($p < 0.05$) (Table 10.4).

Table 10.3. Echogenicity of *gastrocnemius* muscle: mean \pm S.D. of pixels measured using Adobe Photoshop[®] version 7.0.

	Group	Pixels mean \pm S.D.
<i>Gastrocnemius</i> muscle	I (MNU exercised)	18.395 \pm 7.027
	II (MNU sedentary)	18.406 \pm 7.868
	III (control exercised)	20.656 \pm 7.639
	IV (control sedentary)	29.287 \pm 6.313*

* Statistically different from groups I, II and III ($p < 0.05$).

Table 10.4. Echogenicity of fibrous tissue between muscle and tibia: mean \pm S.D. of pixels measured using Adobe Photoshop[®] version 7.0.

	Group	Pixels mean \pm S.D.
Fibrous tissue between muscle and tibia	I (MNU exercised)	40.239 \pm 12.437
	II (MNU sedentary)	41.683 \pm 9.394
	III (control exercised)	44.773 \pm 9.705
	IV (control sedentary)	58.104 \pm 7.918*

* Statistically different from groups I, II and III ($p < 0.05$).

10.3.6. Serum analysis

Serum myostatin levels were higher in MNU groups (groups I and II) when compared with control groups (groups III and IV). However, a statistically significant difference was only observed between MNU groups (groups I and II) and control sedentary group (group IV) (Figure 10.3).

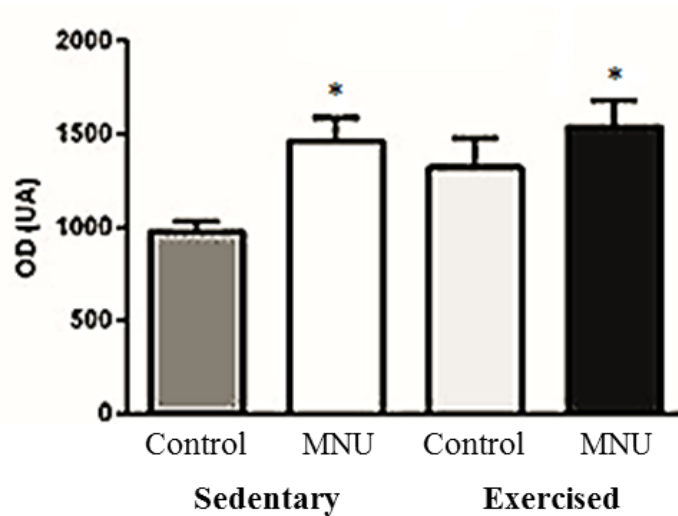


Figure 10.3. Optical density measurements for myostatin. * $p < 0.05$ versus control sedentary group.

10.4. Discussion

Ultrasonography is frequently used to real-time *in vivo* evaluation of different body tissues [2]. In this experimental protocol, the *gastrocnemius* muscle was evaluated by ultrasonography due to its characteristics: it is a superficial muscle being located immediately below the skin, and its ultrasonographic image is easily obtained [13,15].

As previously observed by Yeh and collaborators [22], the animal body weight and *gastrocnemius* muscle weight were not different among groups ($p > 0.05$). All animals from MNU groups developed mammary tumors; however the number of tumors was lower in group I (MNU exercised) when compared with group II (MNU sedentary). The absence of differences of muscle weight agree with the similar ultrasonographic lengths

and widths of the *gastrocnemius* muscle of these animals ($p>0.05$). However, an increase in the tone of the *gastrocnemius* muscle of animals from the exercised groups (I and III) was observed. This may be associated with a greater development of muscle fibers in the exercised animals, not reflected in the increase of the weight or size of the muscle, but associated with a reduction of other constituents, such as muscular fat. This explains the results of our ultrasonographic study, which showed a similar low echogenicity of the *gastrocnemius* muscle between animals from groups exposed to MNU (groups I and II) ($p>0.05$). The tumors developed by animals from groups I and II may have had a catabolic effect on body tissues associated with fat infiltration decrease, as suggested by previous studies [20]. Tumors may also produce molecules, such as lipid mobilizing factor which act on adipose tissue and proteolysis-inducing factor which acts on skeletal muscle [20]. These findings agree with the results for myostatin, as its levels were higher in the MNU-treated groups. Myostatin is a hormone produced in muscle that affects the growth and metabolic state not only of muscle, but also of other body tissues, including fat [26]. High myostatin levels have been described in conditions associated with muscle wasting, including cancer [27,28].

The echogenicity of *gastrocnemius* muscle of animals from group III (control exercised) was similar to the MNU-exposed groups (groups I and II) due to the exercise training and consequent decrease of fat infiltration in muscle. Animals from group IV were healthy and sedentary, and consequently had a higher fat infiltration and muscle echogenicity. In accordance with other researchers, the echogenicity of ultrasonographic images of the *gastrocnemius* muscle is always influenced by fat infiltration [13,14].

In all groups, the echogenicity of the *gastrocnemius* muscle was lower than that of the tissue between the muscle and the tibia ($p<0.05$) due to the intrinsic characteristics of this tissue. This tissue is rich in fibrous tissue and fat, whose are responsible for increased reflections of the ultrasound beam and a consequent whiter appearance of the ultrasonographic images [13,14]. As observed in the *gastrocnemius* muscle, the highest echogenicity was detected in healthy sedentary animals (group IV), possibly also associated with the different fat content at this location. As far as we are aware no previous studies compared the echogenicity of the *gastrocnemius* muscle and the tissue between muscle and the tibia.

10.5. Conclusion

Our results showed that muscle ultrasonography is a useful tool to identify alterations in muscle structure. However, more studies are necessary to understand the influence of fat location in muscle ultrasonographic imaging.

10.6. References

- [1] Wild, JJ.; Neal, D. Use of high-frequency ultrasonic waves for detecting changes of texture in living tissues. *Lancet*, **1951**, 1, 655–657.
- [2] Pillen, S. Skeletal muscle ultrasound. *Eur. J. Transl. Myol.*, **2010**, 1, 145–155.
- [3] Pillen, S.; Verrrips, A.; van Alfen, N.; Arts, IMP.; Sie, LTL.; Zwarts, MJ. Quantitative skeletal muscle ultrasound: diagnostic value in childhood neuromuscular disease. *Neuromuscul. Disord.*, **2007**, 17, 509–516.
- [4] Jacobson, JA. Ultrasound in sports medicine. *Radiol. Clin. North Am.*, **2002**, 40, 363–386.
- [5] Lento, PH.; Primack, S. Advances and utility of diagnostic ultrasound in musculoskeletal medicine. *Curent Rev. Musculoskelet. Med.*, **2008**, 1, 24–31.
- [6] Nazarian, L. The top 10 reasons musculoskeletal sonography in an important complementary or alternative technique to MRI. *Am. J. Roentgenol.*, **2008**, 190, 1621–1626.
- [7] Middleton, WD.; Payne, WT.; Teefey, SA.; Hildbolt, CF.; Rubin, DA.; Yamaguchi, K. Sonography and MRI of the shoulder: comparison of patient satisfaction. *Am. J. Roentgenol.*, **2004**, 183, 1449–1452.
- [8] Bangard, C.; Paszek, J.; Berg, F.; Eyl, G.; Kessler, J.; Lackner, K.; Gossmann, A. MRI imaging of claustrophobic patients in an open 1.0T scanner: motion artifacts and patient acceptability compared with closed bore magnets. *Am. J. Radiol.*, **2007**, 64, 152–157.
- [9] Pillen, S.; Scholten, RR.; Zwarts, MJ.; Verrrips, A. Quantitative skeletal muscle ultrasonography in children with suspected neuromuscular disease. *Muscle Nerve*, **2003**, 27, 699–705.
- [10] Pillen, S.; Tak, RO.; Zwarts, MJ.; Lammens, MM.; Verrijp, KN.; Arts, IM.; Van Der Laak, JA.; Hoogerbrugge, PM.; Van Engelen, BG.; Verrrips, A. Skeletal

- muscle ultrasound: correlation between fibrous tissue and echo intensity. *Ultrasound Med.Biol.*, **2009**, 35, 443–446.
- [11] Pillen, S.; Arts, IMP.; Zwarts, MJ. Muscle ultrasound in neuromuscular disorders. *Muscle Nerve*, **2008**, 37, 679–693.
- [12] Lee, JC.; Healy, J. Sonography of lower limb muscle injury. *Am. J. Roentgenol.*, **2004**, 182, 341–351.
- [13] Peetrons, P. Ultrasound of muscles. *Eur. Radiol.*, **2002**, 12, 35–43.
- [14] Reimers, K.; Reimers, CD.; Wagner, S.; Paetzke, I.; Pongratz, DE. Skeletal muscle sonography: a correlative study of echogenicity and morphology. *J. Ultrasound Med.*, **1993**, 12, 73–77.
- [15] Hashimoto, BE.; Kramer, DJ.; Wiitala, L. Applications of musculoskeletal sonography. *J. Clin. Ultrasound*, **1999**, 27, 293–318.
- [16] Benson, JR.; Jatoi, I. The global breast cancer burden. *Futur. Oncol.*, **2012**, 8, 697–702.
- [17] Huggins, C.; Grand, LC.; Brillantes, FP. Mammary cancer induced by a single feeding of polymucular hydrocarbons, and its suppression. *Nature*, **1961**, 189, 204–207.
- [18] Gullino, PM.; Pettigrew, HM.; Grantham, FH. *N*-nitrosomethylurea as mammary gland carcinogen in rats. *J. Natl. Cancer Inst.*, **1975**, 54, 401–414.
- [19] McCormick, DL.; Adamowski, CB.; Fiks, A.; Moon, RC. Lifetime dose-response relationships for mammary tumor induction by a single administration of *N*-methyl-*N*-nitrosourea. *Cancer Res.*, **1981**, 41, 1690–1694.
- [20] Tisdale, MJ. Pathogenesis of cancer cachexia. *J. Support. Oncol.*, **2003**, 1, 159–168.
- [21] Larkin, M. Thwarting the dwindling progression of cachexia. *Lancet*, **1998**, 351, 1336.
- [22] Yeh, JK.; Niu, Q.; Evans, JF.; Iwamoto, J.; Aloia, JF. Effect of circular motion exercise on bone modeling and bone mass in young rats: an animal model of isometric exercise. *J. Musculoskelet. Neuronal Interact.*, **2001**, 1, 235–240.
- [23] McArdle, A.; Vasilaki, A.; Jackson, M. Exercise and skeletal muscle ageing: cellular and molecular mechanisms. *Ageing Res. Rev.*, **2002**, 1, 79–93.
- [24] Tipton, KD. Muscle protein metabolism in the elderly: influence of exercise and

- nutrition. *Can. J. Appl. Physiol. Can. Physiol. Appl.*, **2001**, 26, 588–606.
- [25] Faustino-Rocha, A.; Oliveira, PA.; Pinho-Oliveira, J.; Teixeira-Guedes, C.; Soares-Maia, R.; Gil da Costa, RM.; Colaço, B.; Pires, MJ.; Colaço, J.; Ferreira, R.; Ginja, M. Estimation of rat mammary tumor volume using caliper and ultrasonography measurements. *Lab. Anim. (NY)*, **2013**, 42, 217–224.
- [26] Roth, SM.; Walsh, S. Myostatin: a therapeutic target for skeletal muscle wasting. *Curr. Opin. Clin. Nutr. Metab. Care*, **2004**, 7, 259–263.
- [27] Kirk, S.; Oldham, J.; Kambadur, R.; Sharma, M.; Dobbie, P.; Bass, J. Myostatin regulation during skeletal muscle regeneration. *J. Cell. Physiol.*, **2000**, 184, 356–363.
- [28] Aversa, Z.; Bonetto, A.; Penna, F.; Costelli, P.; Di Rienzo, G.; Lacitignola, A.; Baccino, FM.; Ziparo, V.; Mercantini, P.; Fanelli, FR.; Muscaritoli, M. Changes in myostatin signaling in non-weight-losing cancer patients. *Ann. Surg. Oncol.*, **2012**, 19, 1350–1356.

CHAPTER 11

MAST CELLS ON MAMMARY CARCINOGENESIS: HOST OR TUMOR SUPPORTERS?

THE CONTENT OF THIS CHAPTER WAS PUBLISHED IN:

Faustino-Rocha AI, Gama A, Neuparth MJ, Oliveira PA, Ferreira R, Ginja M. 2017. Mast cells on mammary carcinogenesis: host or tumor supporters? *Anticancer Research* 37 (3): 1013-1021. (Full paper)

Faustino-Rocha AI, Gama A, Oliveira PA, Ferreira R, Ginja M. 2017. Mast cells as targets on mammary carcinogenesis. *Journal of Comparative Pathology* 156 (1): 63. (Abstract)

Faustino-Rocha AI, Gama A, Oliveira PA, Ferreira R, Ginja M. 2016. Mast cells as therapeutic approach on mammary cancer. *Journal of Cancer Science and Therapy* 8 (5): 53. (Abstract)

Faustino-Rocha AI, Gama A, Oliveira PA, Vala H, Ferreira R, Ginja M. 2015. Effects of histamine on the development of MNU-induced mammary tumors. *Virchows Archiv* 467 (Suppl 1): 51. DOI: 10.1007/s00428-015-1805-9. (Abstract)

Faustino-Rocha AI, Pinto C, Gama A, Oliveira PA. 2014. Effects of ketotifen on mammary tumors volume and weight. *Anticancer Research* 34 (2014): 5902. (Abstract)

Faustino-Rocha AI, Gama A, Oliveira PA, Ferreira R, Ginja M. 2016. Mast cells as targets on mammary carcinogenesis. 34th Annual Meeting of the ESVP and 27th Annual Meeting of the ECVP, 7th to 10th September, Bologna, Italy. (Oral presentation)

Faustino-Rocha AI, Gama A, Oliveira PA, Ferreira R, Ginja M. 2016. Mast cells as therapeutic approach on mammary cancer. Cancer Diagnostics Conference & Expo, 13th to 15th June, Rome, Italy. (Oral presentation)

Pinto C, Gama A, Alvarado A, Oliveira PA, Pires MJ, Ferreira-Cardoso J, **Faustino-Rocha AI**. 2014. Acompanhamento de um protocolo experimental de indução química de cancro da mama em ratos (*Rattus norvegicus*). 8^{as} Jornadas de Biologia. 22nd to 23rd

October, University of Trás-os-Montes and Alto Douro, Vila Real, Portugal. (Oral presentation)

Faustino-Rocha AI, Gama A, Oliveira PA, Ferreira R, Ginja M. 2016. Inhibition of mast cells' degranulation on mammary carcinogenesis. 2nd ASPIC International Congress, 28th to 29th April, IPO-Oporto, Portugal. (Poster presentation)

Faustino-Rocha AI, Gama A, Oliveira PA, Alvarado A, Vala H, Ferreira R, Ginja M. 2015. Effects of histamine on the development of MNU-induced mammary tumors. 27th European Congress of Pathology (ECP), 5th to 9th September, Belgrade, Serbia. (Poster presentation)

Faustino-Rocha AI, Pinto C, Gama A, Oliveira PA. 2014. Effects of ketotifen on mammary tumors volume and weight. 9th International Conference of Anticancer Research, 6th to 10th October, Porto Carras, Sithonia, Greece. (Poster presentation)

11. Mast cells on mammary carcinogenesis: host or tumor supporters?

Abstract

The effects of mast cells on carcinogenesis is not yet fully understood. This work aimed to better disclose the role of mast cells on mammary carcinogenesis in a rat model, through the administration of the antihistamine and mast cell stabilizer drug ketotifen. Mammary tumors were induced by the administration of *N*-methyl-*N*-nitrosourea (MNU) in groups I, II and III. Animals from group II were treated with ketotifen immediately after the MNU administration, and animals from group III only received the ketotifen after the development of the first mammary tumor. Biochemical profile was performed. Mammary tumors were evaluated by histopathology and immunohistochemistry. Animals from ketotifen-treated groups developed less number of mammary tumors, higher number of mammary lesions and exhibited lower histamine levels when compared with non-treated animals. Group II exhibited the lowest proliferation and apoptotic indexes. Ketotifen inhibited mast cell degranulation. The mainly positive effect of this inhibition seems to be the reduction of tumor proliferation when the ketotifen was administered before tumor development.

Keywords: degranulation, ketotifen, mammary tumors, mast cells, MNU, rat

11.1. Introduction

Cancer is a multistage process that involves complex interactions between malignant and non-malignant cells. Lymphatic and vascular endothelial cells, pericytes, adipocytes, mesenchymal stem cells, smooth muscle cells, fibroblasts, myofibroblasts, myeloid cells and inflammatory cells (B and T lymphocytes, neutrophils, dendritic cells, eosinophils, basophils, natural killer cells, macrophages and mast cells) are among the non-malignant cells that constitutes the tumor microenvironment [1].

Mast cells are ovoid or elongated granular cells that arise from the multipotent precursor CD34⁺ in the bone marrow [2]. They are complex, well-engineered and multifunctional cells that play an important role in innate and acquired immunity [3,4]. Although mast cells were first described by Paul Ehrlich as a normal component of connective tissue [5], nowadays it is known that they are physiologically present in

several tissues, especially where the body interacts with the environment (skin, respiratory tree, gastrointestinal tract, mucosal surfaces and connective tissue) [6]. They may also be occasionally seen in the bone marrow and almost never in circulation [7].

Over the years, mast cells have triggered the scientific community and their role has been studied in several conditions, namely dermatitis, bullous pemphigoid, fibrotic lung disease, psoriasis, rheumatoid arthritis, Crohn's disease, ulcerative colitis, interstitial cystitis, asthma, allergic rhinitis, sinusitis and cancer (skin, breast, lung, kidney, and stomach cancer, melanoma and multiple myeloma) [8,9]. Mast cells have several bioactive substances with pro-apoptotic and anti-apoptotic activity in their cytoplasmic granules. In the specific case of cancer, histamine, tryptase and chymase promote tumor angiogenesis, proliferation and metastasis; while heparin, interleukin (IL)-1, IL-21 and tumor necrosis factor (TNF) inhibit tumor growth [10–13]. The association between the presence of mast cells and the conversion of premalignant to malignant lesion in a rat model of chemically-induced skin and mammary tumors [14], as well as, the correlation between the mast cells number in breast cancer and tumor aggressiveness and poor prognosis in both human [15] and canine mammary tumors [16] was previously reported. So arise the idea that mast cells are correlated with tumor progression and the inhibition of their degranulation may suppress the mammary tumor growth.

Ketotifen is a benzocycloheptathiophene compound that, at low concentrations, exerts antihistaminic activity (it is a second-generation histamine 1 receptor (H1) antagonist) [17]. Additionally, ketotifen blocks calcium channels essential for mast cell degranulation, stabilizing their membranes and consequently inhibiting their degranulation [18,19].

As breast cancer remains a leading cancer among women worldwide [20], this study aimed to clarify the role of mast cells on mammary carcinogenesis, through the inhibition of their degranulation by an antihistamine drug in a recognized rat model of *N*-methyl-*N*-nitrosourea (MNU)-induced mammary cancer.

11.2. Material and Methods

11.2.1. Animals

Thirty-four female Sprague-Dawley rats with four weeks of age were used (Harlan Laboratories Inc., Barcelona, Spain). Animals were placed in the facilities of the University of Trás-os-Montes and Alto Douro (UTAD) under controlled conditions of temperature ($23\pm 2^{\circ}\text{C}$), humidity ($50\pm 10\%$), air system filtration (10-20 ventilations/hour) and on a 12h:12h light:dark cycle. Animals were fed with a standard laboratory diet (4RF21[®], Mucedola, Settimo Milanese, Milan, Italy) and tap water *ad libitum*. All procedures followed the European and National legislation on the protection of animals used for scientific purposes (European Directive 2010/63/EU and National Decree-Law 113/2013). The experimental protocol was approved by the Ethics Committee of the UTAD (CE_12-2013) and by the Portuguese Ethics Committee for Animal Experimentation (approval no. 008961).

11.2.2. Experimental protocol

After one week of quarantine and two weeks of acclimatization to the lab conditions, animals were randomly divided into five experimental groups as follows: group I (MNU; n=10), group II (MNU + ketotifen-1; n=10), group III (MNU + ketotifen-2; n=10), group IV (ketotifen; n=2) and group V (control; n=2). At seven weeks of age, all animals from groups I, II and III received an intraperitoneal injection of the carcinogen agent MNU (ISOPAC[®], Sigma Aldrich S.A., Madrid, Spain) at a dose of 50 mg/kg of body weight. Animals from groups IV and V received a single intraperitoneal injection of the vehicle (saline solution 0.9%). These control groups were used in order to ensure that no histological alterations occurred due to the experimental procedures, namely the ketotifen administration. The first day of the experimental protocol was defined as the day of the MNU administration. On the day after the MNU or saline administration, animals from groups II and IV received the mast cell stabilizer ketotifen (Zaditen[®], Defiante Farmacêutica S.A., Portugal) in drinking water, at a concentration of 1 mg/kg of body weight, seven days/week for 18 weeks. Each animal from group III only received the ketotifen after the development of the first mammary tumor. Animals from groups I and V received only water during the protocol (Figure 11.1).

Animals were observed twice a day in order to monitor their health status during the experiment. Mammary chains from all animals were palpated once a week to detect the development of mammary tumors. Food and water consumption and animal body weight were weekly measured using a top-loading scale (Mettler PM4000, LabWrench, Midland, ON, Canada). At the end of the experiment, body weight gain and mortality index were calculated [21,22].

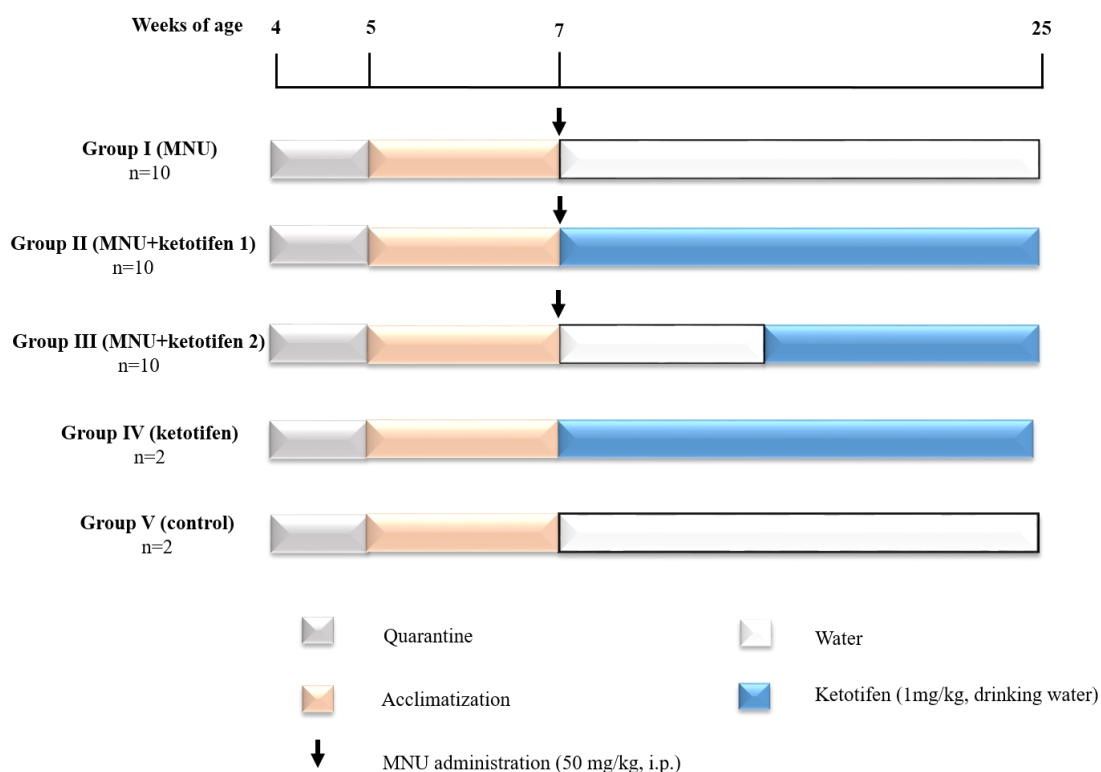


Figure 11.1. Schematic representation of the experimental protocol. MNU: *N*-methyl-*N*-nitrosourea; i.p.: intraperitoneal administration.

11.2.3. Sample collection

At the seventh week after the MNU administration, blood samples were collected from tail vein directly into capillary tubes; the samples were centrifuged and the serum was stored at -80°C to determine the histamine levels. Immediately before the animal sacrifice, urine samples were collected using metabolic cages, the samples were centrifuged and

the urine specific gravity was determined using a refractometer (Atago Co., Tokyo, Japan).

11.2.4. Sacrifice

Eighteen weeks after the MNU administration (animals with 25 weeks of age), all survived animals were humanely sacrificed by intraperitoneal injection of ketamine (75 mg/kg of body weight, Imalgene[®] 1000, Merial S.A.S., Lyon, France) and xylazine (10 mg/kg of body weight, Rompun[®] 2%, Bayer Healthcare S.A., Kiel, Germany), followed by exsanguination by cardiac puncture as indicated by the Federation of European Laboratory Animal Science Associations [23]. At this moment blood samples were collected from the inferior vena cava directly into capillary tubes and tubes with separator gel. The tubes were centrifuged for 5 minutes at 5000×g, the serum was obtained and stored at -80°C for biochemical determinations.

Animals were skinned and the skin was carefully observed under a light in order to detect mammary tumors not previously identified by palpation. Mammary tumors were removed, weighed and the tumor volume determined based on their weight [22]. Animal accurate body weight was obtained by the subtraction of tumor weight to the final body weight. All tumors and organs were collected, weighed and immersed in formalin for 24 hours.

11.2.5. Blood samples analysis

Hematocrit was determined immediately after the centrifugation of the capillary tubes. Serum levels of histamine were determined using a commercial enzyme-linked immunosorbent assay (ELISA) kit (MBS494164, MyBioSource, San Diego, CA, USA) according to manufacturer's instructions. Serum albumin, total protein, cholesterol, glucose, triglycerides, creatinine, alanine aminotransferase (ALT), creatine kinase, lactate dehydrogenase and lactate were measured in duplicate on an AutoAnalyzer (Prestige 24i, Cormay PZ, Diamond Diagnostics, Holliston, MA, USA). C-reactive protein (CRP) was determined by immunoblotting using a rabbit monoclonal anti-CRP antibody (ab32412, Abcam, Cambridge, UK).

11.2.6. Histology and immunohistochemistry

After fixation, mammary tumors were cut, included in paraffin and processed for routine histological evaluation. Two μm -thick sections were stained with hematoxylin and eosin (H&E). Mammary tumors were histologically evaluated under a light microscopy by a pathologist and classified according to Russo and Russo [24]. To determine mast cell density, a section from each mammary tumor was stained with toluidine blue. Mast cells were counted in 15 amplified fields (magnification of 400 \times) in each section and the mean number was determined [25].

The expression of Ki-67, and cleaved caspases-3 and -9 was evaluated by immunohistochemistry in each mammary lesion. For this purpose, the standard protocol of NovoLink Polymer Detection System (Leica Biosystems, Newcastle, UK) was used. Sections were incubated with primary antibodies for Ki-67 (clone MIB-5, Dako, Glostrup, Denmark), caspase 3 (clone Asp 175, Cell Signaling Technology, Danvers, MA, USA) and caspase 9 (clone Asp 353, Cell Signaling Technology, Danvers, MA, USA) at a dilution of 1:50 overnight at 4°C. The immunoexpression of all markers was evaluated as the percentage of stained cells in a total of at least 1000 neoplastic cells.

11.2.7. Statistical analysis

Data were statistically analyzed using Statistical Package for the Social Sciences (SPSS[®], version 23 for Windows, SPSS Inc., Chicago, IL, USA). Continuous data were compared among groups using analysis of variance (ANOVA). Histological results were analyzed using Chi-square tests. Continuous data are expressed as mean \pm standard error (S.E.); p values lower than 0.05 were considered statistically significant.

11.3. Results

11.3.1. General data

One animal from group II died during the experiment (mortality index of 10%). Data from this animal were not included in the study. Statistically significant differences were not found in food and water consumption (data not shown), as well as, animal body weight and ponderal gain ($p > 0.05$). Although the differences did not reach the level of statistical significance, final body weight was slightly lower in animals ketotifen-treated

previously exposed to MNU (groups II and III) when compared with the remaining groups (Table 11.1). Statistically significant differences were not found in organs' weight among groups ($p>0.05$) (Table 11.2).

Table 11.1. Initial and final accurate body weight (g) and ponderal gain (%), and mammary tumor volume and weight in all experimental groups (mean \pm S.E.).

Group	n	Accurate body weight (g)		Ponderal gain (%)	Mammary tumors	
		Initial	Final		Weight (g)	Volume (cm ³)
I (MNU)	6	188.27 \pm 3.78	304.78 \pm 8.54	38.10 \pm 1.27	3.24 \pm 0.66	3.08 \pm 0.63
II (MNU + ketotifen-1)	8	178.40 \pm 3.26	272.78 \pm 11.35	33.75 \pm 3.09	5.40 \pm 1.40	5.11 \pm 1.32
III (MNU + ketotifen-2)	7	187.69 \pm 4.88	286.44 \pm 6.72	34.39 \pm 1.46	2.62 \pm 0.74	2.48 \pm 0.70
IV (ketotifen)	2	198.22 \pm 12.70	304.20 \pm 18.00	34.86 \pm 0.32	-	-
V (control)	2	183.82 \pm 2.84	295.98 \pm 9.78	37.86 \pm 1.10	-	-

Statistically significant differences were not found ($p>0.05$).

Table 11.2. Absolute organs' weight (g) in all groups (mean \pm S.E.).

Group	n	Organ weight (g)					
		Heart	Lung	Spleen	Liver	Left kidney	Right kidney
I (MNU)	6	1.15 \pm 0.08	1.74 \pm 0.09	0.99 \pm 0.10	9.18 \pm 1.01	1.16 \pm 0.03	1.21 \pm 0.03
II (MNU + ketotifen-1)	8	1.17 \pm 0.09	1.62 \pm 0.06	1.20 \pm 0.14	9.37 \pm 0.55	1.16 \pm 0.06	1.21 \pm 0.03
III (MNU + ketotifen-2)	7	1.13 \pm 0.03	1.65 \pm 0.05	2.03 \pm 0.96	9.78 \pm 0.35	1.28 \pm 0.06	1.30 \pm 0.03
IV (ketotifen)	2	1.12 \pm 0.04	1.76 \pm 0.01	0.78 \pm 0.08	8.13 \pm 0.53	1.27 \pm 0.14	1.30 \pm 0.11
V (control)	2	1.13 \pm 0.07	1.95 \pm 0.19	0.89 \pm 0.13	9.04 \pm 0.51	1.20 \pm 0.03	1.20 \pm 0.00

Statistically significant differences were not found ($p>0.05$).

11.3.2. Mammary tumors

As expected, animals from groups IV and V did not develop any mammary tumor. The first mammary tumors were simultaneously identified in all MNU-exposed groups (groups I, II and III) eight weeks after the MNU administration (Figure 11.2).

An incidence of 60% (6/10) in group I, 89% (8/9) in group II and 70% (7/10) in group III was observed at the end of the experimental protocol. As the aim of the study was to evaluate the effects of mast cells on mammary tumorigenesis, we only considered the data from animals that developed mammary tumors. A total of 58 mammary tumors were counted at the end of the experiment: 21 tumors in group I (3.5 tumors *per* animal), 19 tumors in group II (2.4 tumors *per* animal) and 18 tumors in group III (2.6 tumors *per* animal) (Figure 11.2). The number of mammary tumors was not statistically different among groups ($p>0.05$). Although the mammary tumor volume and weight were higher in animals that received the ketotifen immediately after the MNU administration (group II) when compared with non-treated animals (group I) and animals that only received ketotifen after tumors' development (group III), the differences among groups did not reach the level of statistical significance ($p>0.05$) (Table 11.1).

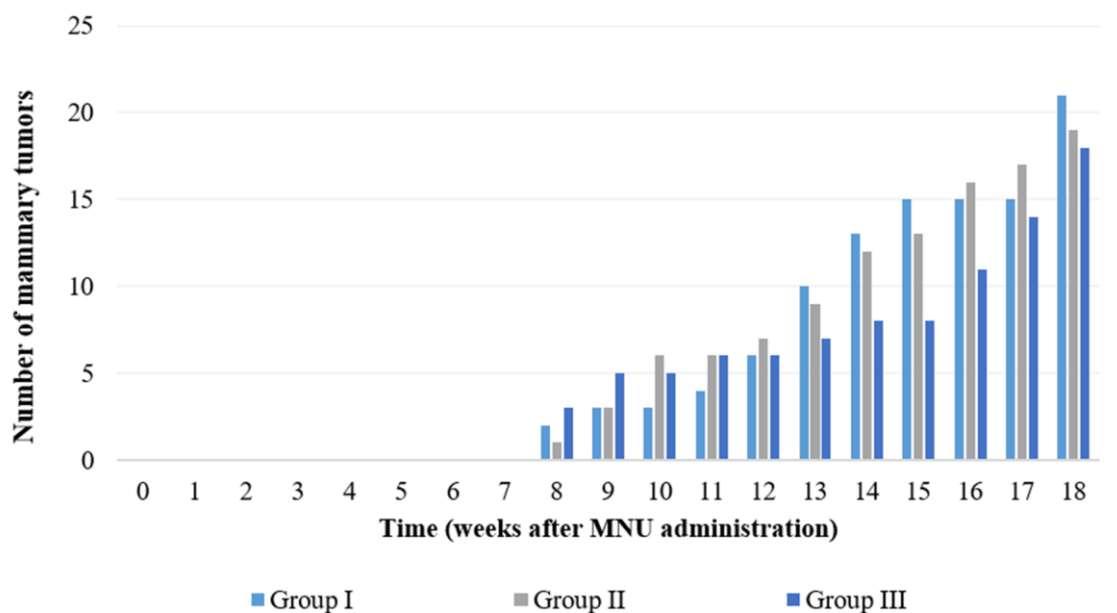


Figure 11.2. Graphic representation of the number of mammary tumors in Groups I, II and III and the respective week of appearance ($p>0.05$).

11.3.3. Blood and urine samples analysis

The serum levels of histamine were measured before (at seventh week of the experiment) and after the development of mammary tumors (at the 18th week of the experiment) in all experimental groups. Histamine serum levels increased between the seventh and the last week of the experimental protocol ($p>0.05$). At the end of the experiment, the animals from group II (MNU + ketotifen-1) exhibited the lowest histamine serum levels followed by animals from group III (MNU + ketotifen-2) (Table 11.3). Concerning to biochemical profile, a statistically significant difference was only observed in the levels of glucose between groups II (MNU + ket-1) and III (MNU + ket-2) ($p<0.05$). The remaining parameters were similar among groups ($p>0.05$) (Table 11.4).

Table 11.3. Histamine serum levels (ng/mL) in all groups before the tumor development and at the end of the experimental protocol (mean \pm S.E.).

Group	n	Histamine serum levels (ng/mL)	
		7 weeks after MNU	18 weeks after MNU
I (MNU)	6	45.46 \pm 5.52	109.55 \pm 31.22
II (MNU + ketotifen-1)	8	46.53 \pm 3.19	91.16 \pm 32.84
III (MNU + ketotifen-2)	7	44.80 \pm 5.42	100.47 \pm 50.24

Statistically significant differences were not found ($p>0.05$).

Table 11.4. Characterization of the animal response to the ketotifen administration: biochemical profile (mean \pm S.E.).

Parameter	I	II	III
	(MNU)	(MNU + ket-1)	(MNU + ket-2)
Hematocrit (%)	48.50 \pm 1.77	48.75 \pm 1.11	44.86 \pm 0.86
Albumin (mg/dL)	29.13 \pm 0.61	27.47 \pm 1.34	29.60 \pm 0.93
Total protein (mg/dL)	58.12 \pm 1.36	57.59 \pm 2.58	61.11 \pm 1.80
Cholesterol (mg/dL)	65.03 \pm 6.96	55.25 \pm 3.89	68.34 \pm 7.37
Glucose (mg/dL)	164.90 \pm 7.24	152.58 \pm 15.80 ^a	226.34 \pm 16.29
Triglycerides (mg/dL)	111.87 \pm 14.63	77.33 \pm 7.23	116.31 \pm 11.30
Creatinine (mg/dL)	0.67 \pm 0.06	0.77 \pm 0.13	0.58 \pm 0.08
ALT (U/L)	18.53 \pm 2.74	15.16 \pm 1.67	17.13 \pm 3.24
Creatine kinase (U/L)	71.67 \pm 11.32	147.69 \pm 31.83	84.76 \pm 11.74
Lactate dehydrogenase (U/L)	1312.93 \pm 254.18	1878.24 \pm 310.48	1164.26 \pm 157.17
Lactate (mg/dL)	31.67 \pm 2.60	43.38 \pm 4.11	31.17 \pm 2.12
CRP (AU)	3632.26 \pm 23.35	36313.53 \pm 54.04	3524.61 \pm 47.34
Urine specific gravity	1.02 \pm 0.00	1.03 \pm 0.00	1.02 \pm 0.00

^a Statistically significant different from group III (MNU + ket-2) ($p < 0.05$)

11.3.4. Histological analysis

Histologically, it was verified that mammary tumors exhibited more than one mammary lesion. In this way, 35 mammary lesions in group I (MNU), 44 mammary lesions in group II (MNU + ketotifen-1) and 48 mammary lesions in group III (MNU + ketotifen-2) were identified. The highest number of benign mammary lesions was identified in group III (MNU + ketotifen-2) (statistically different from group I, $p < 0.05$), while the highest number of malignant lesions was observed in group II (MNU + ketotifen-1). No preneoplastic lesions were identified in groups I and II. The papillary non-invasive carcinoma was the malignant lesion most frequently identified in all groups.

Statistically significant differences were observed in the number of cribriform non-invasive carcinoma among groups ($p < 0.05$) (Table 11.5).

Mast cells appeared as granular mononuclear cells in all mammary tumors. The toluidine blue stained their granules purple in color. The majority of mast cells were observed in the connective tissue around the tumor and in lower number in the tumor core (Figure 11.4A). The mean number of mast cells was higher in mammary tumors when compared with normal mammary gland. Additionally, the mean number of mast cells was higher in group II (MNU + ketotifen-1) when compared with groups I (MNU) and III (MNU + ketotifen-2), reaching the statistically significant difference between groups II and III ($p < 0.05$) (Figure 11.3).

Table 11.5. Histological classification of mammary tumors developed by animals from experimental groups that received the carcinogen agent MNU.

Lesions		Number of lesions		
		I (MNU)	II (MNU + ket-1)	III (MNU + ket-2)
Benign lesions	Intraductal papilloma	1	1	5
	Tubular adenoma	0	2	3
	Fibroadenoma	1	1	1
	Total:	2^a	4	9
Preneoplastic lesion	Intraductal proliferation	0	0	2
Malignant lesions	Papillary non-invasive carcinoma	14	16	13
	Cribriform non-invasive carcinoma	3 ^{b,c}	11	12
	Papillary invasive carcinoma	6	6	7
	Cribriform invasive carcinoma	9	7	4
	Comedo invasive carcinoma	1	0	1
Total:	33	40	37	
Total number of lesions:		35	44	48

Bold italic values indicate the number of lesions according to their malignancy (benign lesions, preneoplastic lesions and malignant lesions). ^a Statistically different from group III ($p=0.035$); ^b Statistically different from group II ($p=0.033$) ^c Statistically different from group III ($p=0.020$).

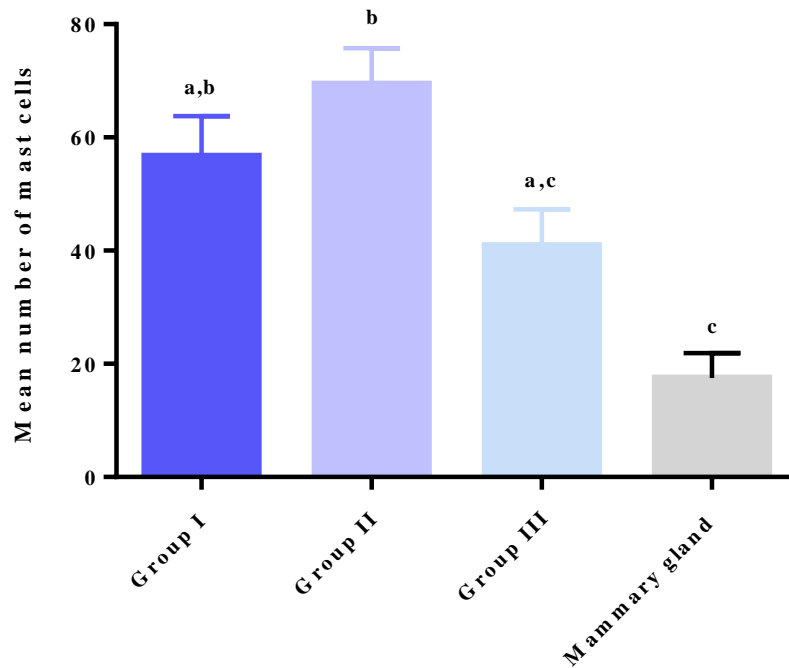


Figure 11.3. Mean number of mast cells in mammary tumors from animals that received the carcinogen agent MNU and in the normal mammary gland. Values with different letters were considered statistically different ($p < 0.05$).

11.3.5. Immunohistochemistry

The proliferation index was higher in groups I (MNU) and III (MNU + ketotifen-2) when compared with group II (MNU + ketotifen-1) ($p < 0.05$). In the same way, the apoptotic index evaluated by the immunoexpression of caspases-3 and -9 was higher in groups I (MNU) and III (MNU + ketotifen-2), when compared with group II (MNU + ketotifen-1) (statistically significant differences were not observed, $p > 0.05$) (Table 11.6, Figure 11.4B, C and D).

Table 11.6. Immunohistochemical evaluation of proliferation and apoptosis of mammary tumors developed by animals from experimental groups that received the carcinogen agent MNU.

Antibody	Parameter	Group		
		I (MNU)	II (MNU + ket-1)	III (MNU + ket-2)
Ki-67	Proliferation index (%)	8.78 ± 1.94 ^a	4.22 ± 0.77	8.08 ± 1.70 ^a
Caspase-3	Apoptotic index (%)	4.16 ± 0.76	3.14 ± 0.50	4.08 ± 0.48
Caspase-9	Apoptotic index (%)	3.24 ± 0.53	2.38 ± 0.37	3.03 ± 0.52

^a Statistically different from group II (MNU + ket-1) ($p < 0.05$).

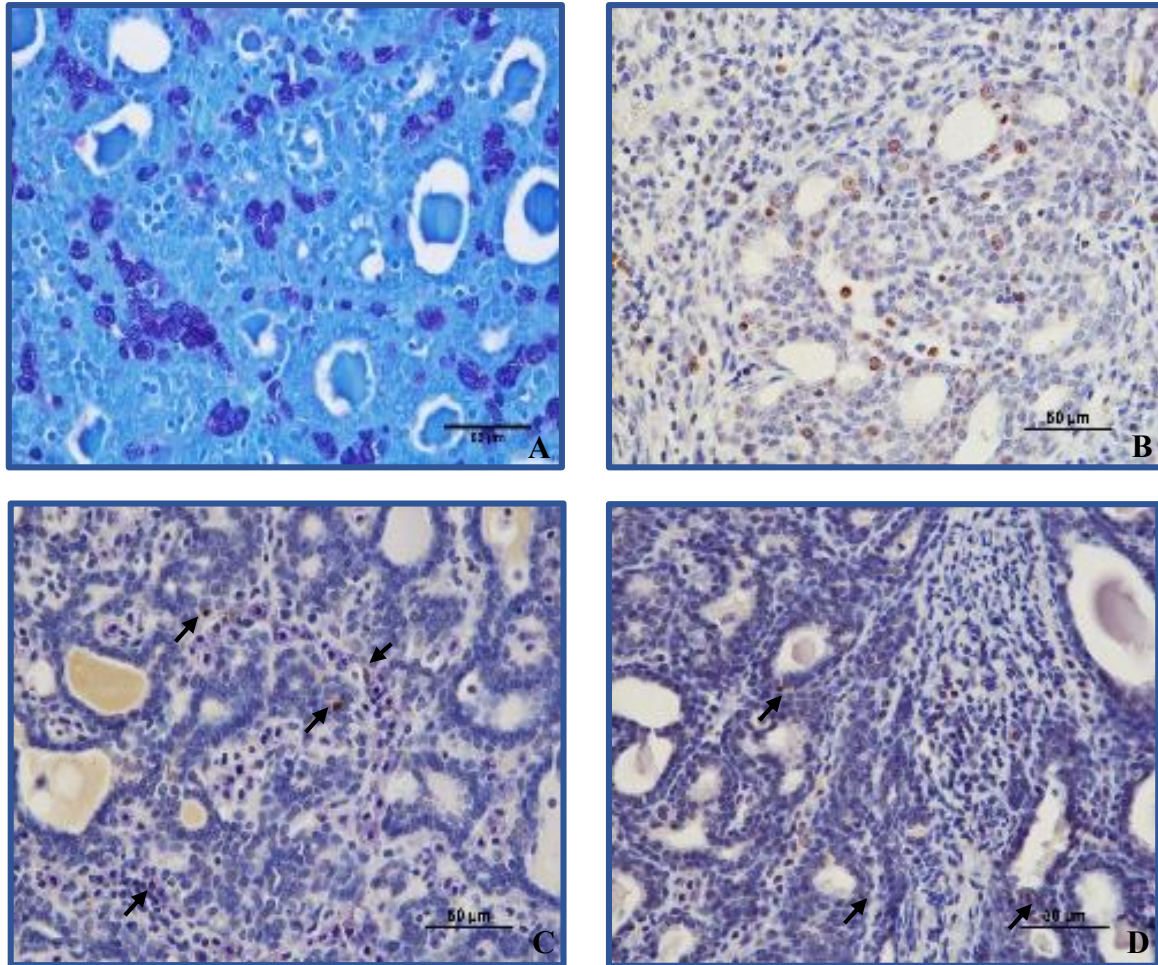


Figure 11.4. Mast cells stained with toluidine blue appearing purple in color in a MNU-induced papillary carcinoma (A). Immunohistochemical staining for Ki-67 (B), caspase-3 (C) and caspase-9 (D) in a mammary cribriform carcinoma induced by MNU in female rats. Immunopositive cells in images stained with caspase-3 and -9 are indicated by arrows. Magnification of 40× in all images.

11.4. Discussion

In the year 2012, cancer was responsible for approximately 8.2 million of deaths around the world [26]. In this way, it is one of the most feared diseases by humans and a disease of a great concern among scientific community. As an attempt to find new preventive and therapeutic strategies, an incessant research, mainly using animal models such as rats and mice, has been performed in this field.

After several years studying carcinogenesis in distinct organs, such as urinary bladder, liver, skin, and more recently mammary gland, our research team observed a marked infiltration of mast cells in these types of cancer. So, arise the doubt: what is the role of

mast cells in cancer? Will they favor tumor progression or will they help the host against the neoplasia? Indeed, the existence of mast cells and their presence near tumors was first described by Paul Ehrlich long time ago [5]. Since then, mast cells have intrigued the scientific community. However, the results about their role have been contradictory and inconclusive, probably due to the different models where they have been studied. In the present work, we intended not only to evaluate the effects of mast cell inhibition before the beginning of the carcinogenesis process (preventive approach), but also after the development of mammary tumors (therapeutic approach). In this way, we decided to administrate the well-known and frequently used antihistamine drug ketotifen. This drug was selected not only due to its inhibitory action of histamine by the blockage of H1 receptors, but also because it stabilizes the mast cell membrane, avoiding the release of other substances contained in their granules that may act as pro- or anti-tumoral agents. In a previous work, promising results such as clotting of blood vessels, hypoxia and tumor cell apoptosis were observed after the treatment of mice model of mammary adenocarcinoma and pancreatic cancer with the mast cell stabilizer drug disodium cromoglycate (cromolyn), even administered after the tumor initiation. However, this mast cell stabilizer drug is a weak inhibitor of human mast cells and consequently is not used in humans [27].

Mammary tumors chemically-induced by the carcinogen agent MNU in female Sprague-Dawley rats have long been used for the study of mammary carcinogenesis [28]. In the present study, mammary tumors were successfully induced eight weeks after MNU administration. However, inversely to the 100% of incidence previously observed in a work performed by our research team using the same model, in the present work a maximum incidence of 89% was reached. This difference is probably related with the duration of the experimental protocol, in the first study the animals were sacrificed 35 weeks after the MNU administration, while in the present one they were sacrificed 18 weeks after the carcinogen administration [28,29]. Although the number of mammary tumors at the end of the experiment was slightly lower in animals from group III (MNU + ketotifen-2) that only received the ketotifen after the development of the first mammary tumor, the mean number of mammary tumors *per* animal was lower in group II (MNU + ketotifen-1) (animals that received the ketotifen immediately after the MNU administration). Tumors from group II (MNU + ketotifen-1) exhibited higher weight and volume when compared with tumors from group III (MNU + ketotifen-2) ($p > 0.05$), what

seems to indicate that the inhibition of mast cells degranulation before tumor development favors tumor growth.

The ketotifen was orally administered at a dose of 1 mg/kg of body weight because it was previously demonstrated as effective in the reversal of anaphylactic reaction in rats [30] and it had been previously observed that ketotifen at low concentration inhibits histamine release but the inverse occurs at higher concentrations in human conjunctival mast cells [31]. In order to evaluate the effectiveness of the inhibition of mast cell degranulation by ketotifen, the serum levels of histamine were evaluated twice during the experiment: before and after the tumor development. At seven weeks after the MNU administration, the serum levels of histamine were very similar among groups. It was also observed an increase in the histamine levels between the seventh and 18th week of the experimental protocol in all groups. The animals that were treated with the ketotifen since the beginning of the study (group II) exhibited the lowest levels of histamine, followed by the animals treated with ketotifen after the development of the first mammary tumor (group III) and non-treated animals (group I), indicating that mast cell degranulation was successfully inhibited by ketotifen. The glucose serum levels were slightly lower in groups I (MNU) and II (MNU + ketotifen-1) when compared with group III (MNU + ketotifen-2). Since the reduction of the glucose levels may be related with the process of carcinogenesis, it will be expected a decrease in all groups MNU-exposed and not only in groups I (MNU) and II (MNU + ketotifen-1). Except for the difference in glucose levels between groups II (MNU + ketotifen-1) and III (MNU + ketotifen-2), the remaining parameters did not present any significant difference among groups. Although changes in lipid profile have long been associated with malignancies, as lipids play a key role in maintenance of cell integrity [32], significant changes were not observed in the present study.

Histologically, a higher number of mammary lesions was observed in groups ketotifen-treated (groups II and III) when compared with non-treated group I (MNU). Uniformly among groups, the majority of lesions were classified as malignant. As previously reported, an intense mast cell infiltrate was observed in all rat mammary tumors chemically-induced, mainly in peri-tumoral fibrous tissue than in tumor core [33]. Similarly to that reported, the mean number of mast cells in all grades of mammary tumors was higher when compared with normal mammary gland [34]. Although it was previously described that as severity of mammary tumors increased the mast cells

counting decreased, in the present work it was observed that the group II (MNU + ketotifen-1) that exhibited the highest number of malignant mammary lesions exhibited the highest mean number of mast cells [35]. Similarly to that had been previously observed in a study in rat intestine and mesenterium (ketotifen injected intravenously), where it was observed that ketotifen did not reduce the number of mast cells in intestine and mesenterium [36,37], in the present work the ketotifen inhibited the mast cell degranulation (lower histamine serum level) but did not reduce the number of mast cells. Although the mast cell number was not reduced, their activity was inhibited.

Ki-67 is involved in the cellular proliferation, being considered an important proliferation marker in mammary cancer [38]. Caspases-3 and -9 act respectively as effector and initiator in both extrinsic and intrinsic pathways of apoptosis that culminate with the degradation of cellular structures and formation of apoptotic bodies [39]. As a higher immunoexpression of Ki-67 (proliferation index) was observed in groups I (MNU) and III (MNU + ketotifen-2) when compared with group II (MNU + ketotifen-1), a lower immunoexpression of caspase-3 and -9 (apoptotic index) was expected in these groups. Surprisingly, both proliferation and apoptotic indexes were lower in group II (MNU + ketotifen-1) where the mast cell degranulation was inhibited before tumor development. These data suggest that the inhibition of mast cell degranulation may inhibit or at least reduce the proliferation of mammary tumors, having a positive effect for host.

11.5. Conclusion

This study was the first to evaluate the effects of ketotifen in the model of chemically-induced mammary cancer in female Sprague-Dawley rats. Ketotifen effectively inhibited mast cell degranulation. The results seem to indicate that this inhibition did not change tumor progression (number of mammary tumors and lesions). The mainly positive effect seemed to be the reduction of tumor proliferation (lower proliferation index) when the ketotifen was administered before tumor development.

11.6. References

- [1] Zudaire, E.; Martinez, A.; Garayoa, M.; Pio, R.; Kaur, G.; Woolhiser, MR.; Metcalfe, DD.; Hook, WA.; Siraganian, RP.; Guise, TA.; Chirgwin, JM.; Cuttitta, F. Adrenomedullin is a cross-talk molecule that regulates tumor and mast cell

- function during human carcinogenesis. *Am. J. Pathol.*, **2006**, 168, 280–291.
- [2] Kamal, R.; Dahiya, P.; Palaskar, S.; Shetty, VP. Comparative analysis of mast cell count in normal oral mucosa and oral pyogenic granuloma. *J. Clin. Exp. Dent.*, **2011**, 3, 1–4.
- [3] Ankle, MR. Mast cells are increased in oral leukoplakia, oral submucous fibrosis, oral lichen planus and oral squamous cell carcinoma. *J. Oral Maxillofac. Pathol.*, **2008**, 11, 18–22.
- [4] Hill, PB.; Martin, RJ. A review of mast cell biology. *Vet. Dermatol.*, **1998**, 9, 145–166.
- [5] Ehrlich, P. Beiträge zur theorie und praxis der histologischen färbung. **1878**.
- [6] Yong, LCJ. The mast cell: origin, morphology, distribution, and function. *Exp. Toxicol. Pathol.*, **1997**, 49, 409–424.
- [7] Blackwood, L.; Murphy, S.; Buracco, P.; De Vos, JP.; De Fornel-Thibaud, P.; Hirschberger, J.; Kessler, M.; Pastor, J.; Ponce, F.; Savary-Bataille, K.; Argyle, DJ. European consensus document on mast cell tumours in dogs and cats. *Vet. Comp. Oncol.*, **2012**, 10, e1–29.
- [8] De Souza, DA.; Toso, VD.; Campos, MRD.; Lara, VS.; Oliver, C.; Jamur, MC. Expression of mast cell proteases correlates with mast cell maturation and angiogenesis during tumor progression. *Plos One*, **2012**, 7, e40790.
- [9] Ganapaty, S.; Chandrashekhar, VM.; Narsu, ML. Evaluation of anti-allergic activity of gossypin and suramin in mast cell-mediated allergy model. *Indian J. Biochem. Biophys.*, **2010**, 47, 90–95.
- [10] Wang, X.; Ruan, Y.; Wu, Z. Studies of mast cells-mediated cytotoxicity to hepatoma cells *in vitro*. *Zhonghua Zo. Zazhi*, **1996**, 18, 276–278.
- [11] Ozdemir, O. Can chymase-positive mast cells play a role in the progression of gastric cancer via angiogenesis? *J. Surg. Oncol.*, **2006**, 94, 260–262.
- [12] Yano, H.; Kinuta, M.; Tateishi, H.; Matsui, S.; Monden, T.; Okamura, J.; Sakai, M.; Okamoto, S. Mast cell infiltration around gastric cancer cells correlates with tumor angiogenesis and metastasis. *Gastric Cancer*, **1999**, 2, 26–32.
- [13] Theoharides, TC.; Conti, P. Mast cells: the jekyll and hyde of tumor growth. *Trends Immunol.*, **2004**, 25, 235–241.
- [14] Flynn, EA.; Schwartz, JL.; Shklar, G. Sequential mast-cell infiltration and degranulation during experimental carcinogenesis. *J. Cancer Res. Clin. Oncol.*,

- 1991**, 117, 115–122.
- [15] Bowrey, PF.; King, J.; Magarey, C.; Schwartz, P.; Marr, P.; Bolton, E.; Morris, DL. Histamine, mast cells and tumour cell proliferation in breast cancer: does preoperative cimetidine administration have an effect? *Br. J. Cancer*, **2000**, *82*, 167–170.
- [16] Elpek, GO.; Gelen, T.; Aksoy, NH.; Erdogan, A.; Dertsiz, L.; Demircan, A.; Keles, N. The prognostic relevance of angiogenesis and mast cells in squamous cell carcinoma of the oesophagus. *J. Clin. Pathol.*, **2001**, *54*, 940–944.
- [17] Ishikawa, T.; Takechi, K.; Rahman, A.; Ago, J.; Matsumoto, N.; Murakami, A.; Kamei, C. Influences of histamine H1 receptor antagonists on maximal electroshock seizure in infant rats. *Biol. Pharm. Bull.*, **2007**, *30*, 477–480.
- [18] Brockman, H.; Graff, G.; Spellman, J.; Yanni, J. A comparison of the effects of olopatadine and ketotifen on model membranes. *Acta Ophthalmol. Scand.*, **2000**, *78*, 10–15.
- [19] Kalesnikoff, J.; Galli, SJ. New developments in mast cell biology. *Nat. Immunol.*, **2008**, *9*, 1215–1223.
- [20] International Agency for Research on Cancer. World cancer report 2014. *WHO*, **2014**.
- [21] Faustino-Rocha, A.; Oliveira, PA.; Pinho-Oliveira, J.; Teixeira-Guedes, C.; Soares-Maia, R.; Gil da Costa, RM.; Colaço, B.; Pires, MJ.; Colaço, J.; Ferreira, R.; Ginja, M. Estimation of rat mammary tumor volume using caliper and ultrasonography measurements. *Lab. Anim. (NY)*, **2013**, *42*, 217–24.
- [22] Faustino-Rocha, AI.; Silva, A.; Gabriel, J.; Reixeira-Guedes, C.; Lopes, C.; Gil da Costa, R.; Gama, A.; Ferreira, R.; Oliveira, P.; Ginja, M. Ultrasonographic, thermographic and histologic evaluation of MNU-induced mammary tumors in female Sprague-Dawley rats. *Biomed. Pharmacother.*, **2013**, *67*, 771–776.
- [23] Forbes, D.; Blom, H.; Kostomitsopulos, N.; Moore, G.; Perretta, G. Euroguide: on the accommodation and care of animals used for experimental and other scientific purposes. *Federation of European Laboratory Animal Science Associations*, **2007**.
- [24] Russo, J.; Russo, IH. Atlas and histologic classification of tumors of the rat mammary gland. *J. Mammary Gland Biol. Neoplasia*, **2000**, *5*, 187–200.
- [25] Lavallo, GE.; Bertagnolli, AC.; Tavares, WLF.; Ferreira, M.; Cassali, GD. Mast cells and angiogenesis in canine mammary tumor. *Arq. Bras. Med. Veterinária e*

- Zootec.*, **2010**, 62, 1348–1351.
- [26] World Health Organization (WHO). Cancer - Fact sheet n° 297. *WHO*, **2015**.
- [27] Ribatti, D.; Crivellato, E. (2011) Mast cells, angiogenesis and cancer. In *Mast cell biology: contemporary and emerging topics* (Gilfillan, A. M. and Metcalfe, D. D., eds), **2011**, pp. 270–288, Springer.
- [28] Faustino-Rocha, AI.; Ferreira, R.; Oliveira, PA.; Gama, A.; Ginja, M. *N*-methyl-*N*-nitrosourea as a mammary carcinogenic agent. *Tumor Biol.*, **2015**, 36, 9095–9117.
- [29] Faustino-Rocha, A.; Gama, A.; Oliveira, PA.; Alvarado, A.; Neuparth, MJ.; Ferreira, R.; Ginja, M. Effects of lifelong exercise training on mammary tumorigenesis induced by MNU in female Sprague-Dawley rats. *Clin. Exp. Med.*, **2016**, Epub ahead of print.
- [30] Craps, LP. Current views on the mechanism of action of ketotifen and their therapeutic implications. *Solunum*, **1983**, 8, 78.
- [31] Yanni, JM.; Stephens, DJ.; Miller, ST.; Weimer, LK.; Graff, G.; Parnell, D.; Lang, LS.; Spellman, JM.; Brady, MT.; Gamache, DA. The *in vitro* and *in vivo* ocular pharmacology of olopatadine (AL-4943A), an effective anti-allergic/antihistaminic agent. *J. Ocul. Pharmacol. Ther.*, **1996**, 12, 389–400.
- [32] Gupta, S.; Gupta, S. Alterations in serum lipid profile patterns in oral cancer and oral precancerous lesions and conditions - a clinical study. *Indian J. Dent. Res.*, **2011**, 2, 2–6.
- [33] Strum, JM.; Lewko, WM.; Kidwell, WR. Structural alterations within *N*-nitrosomethylurea-induced mammary tumors after *in vivo* treatment with cis-hydroxyproline. *Lab. Investig.*, **1981**, 45, 347–354.
- [34] Samoszuk, M.; Kanakubo, E.; Chan, JK. Degranulating mast cells in fibrotic regions of human tumors and evidence that mast cell heparin interferes with the growth of tumor cells through a mechanism involving fibroblasts. *BMC Cancer*, **2005**, 5, 121.
- [35] Rajendran, R.; Radhakrishnan, NS.; Kartha, CC. Light and electron microscopic studies on oral submucous fibrosis. *J. Indian Dent. Assoc.*, **1993**, 64, 157–161.
- [36] Kimura, M.; Mitani, H.; Bandoh, T.; Totsuka, T.; Hayashi, S. Mast cell degranulation in rat mesenteric venule: effects of L-name, methylene blue and ketotifen. *Pharmacol. Res.*, **1999**, 39, 397–402.
- [37] Hei, ZQ.; Gan, XL.; Huang, PJ.; Wei, J.; Shen, N.; Gao, WL. Influence of

- ketotifen, cromolyn sodium, and compound 48/80 on the survival rates after intestinal ischemia reperfusion injury in rats. *BMC Gastroenterol.*, **2008**, 8, 42.
- [38] Mrklic, I.; Capkun, V.; Pogorelic, Z.; Tomic, S. Prognostic value of Ki-67 proliferating index in triple negative breast carcinomas. *Pathol. Res. Pract.*, **2013**, 209, 296–301.
- [39] Ekoff, M.; Nilsson, G. Mast cell apoptosis and survival. *J. Ocul. Pharmacol. Ther.*, **1996**, 12, 389–400.

CHAPTER 12

MODULATION OF MAMMARY TUMORS VASCULARIZATION BY MAST CELLS: ULTRASONOGRAPHIC AND HISTOPATHOLOGICAL APPROACHES

THE CONTENT OF THIS CHAPTER WAS PUBLISHED IN:

Faustino-Rocha AI, Gama A, Oliveira PA, Vanderperren K, Saunders JH, Pires MJ, Ferreira R, Ginja M. 2017. Modulation of mammary tumors vascularization by mast cells: ultrasonographic and histopathological approaches. *Life Sciences* 176 (2017): 35-41. (Full paper)

Faustino-Rocha AI, Gama A, Pires MJ, Oliveira PA, Ginja M. 2014. Effects of a mast cell stabilizer on the vascularization of mammary tumors: ultrasonographic evaluation. *Anticancer Research* 34 (2014): 5901. (Abstract)

Faustino-Rocha AI, Gama A, Pires MJ, Oliveira PA, Ginja M. 2014. Effects of a mast cell stabilizer on the vascularization of mammary tumors: ultrasonographic evaluation. 9th International Conference of Anticancer Research, 6th to 10th October, Porto Carras, Sithonia, Greece. (Oral presentation)

12. Modulation of mammary tumors vascularization by mast cells: ultrasonographic and histopathological approaches

Abstract

Mast cell degranulation has been associated with the promotion of mammary tumors vascularization. In this way, the administration of an antihistamine drug that inhibit mast cell degranulation may be an approach to prevent the formation of new vessels during mammary carcinogenesis. Female Sprague-Dawley rats were randomly divided into five experimental groups. Mammary tumors were induced by the intraperitoneal injection of *N*-methyl-*N*-nitrosourea (MNU). Animals from group II were treated with ketotifen for 18 weeks immediately after MNU administration, while animals from group III only received ketotifen after the development of the first mammary tumor. Mammary tumor vascularization was assessed by ultrasonography (Doppler, B Flow and contrast-enhanced ultrasound (CEUS)) and immunohistochemistry (vascular endothelial growth factor (VEGF)-A). Similar to what occurs with women mammary tumors, the majority of MNU-induced mammary tumors exhibited a centripetal enhancement order of the contrast agent, clear margin and heterogeneous enhancement. Ultrasonographic and immunohistochemical data suggest that the administration of ketotifen and consequent inhibition of mast cell degranulation did not change the mammary tumors vascularization.

Keywords: contrast, Doppler, ketotifen, mast cells, MNU, rat

12.1. Introduction

Breast cancer remains as one of the most frequently diagnosed cancers among female population worldwide [1]. Tumors require the development of new vessels to growth more than 1-2 mm³ and metastasize to distant organs [2,3]. In this way, the assessment of tumor angiogenesis is important in order to predict the prognosis of several tumors, including breast tumors [4].

Ultrasonography is one of the most frequently used imaging modalities in clinical practice. Its use in order to evaluate tumor angiogenesis has gained increasing interest in the cancer research [2,3]. Color and Power Doppler (PDI) have been frequently used to evaluate tumor vascularization. However, these ultrasound methods are not sensitive for

the detection of slow flow and small volume blood flows in capillaries within the tumor parenchyma [5,6]. Pulsed Doppler allows to better characterize the vascularization through the calculation of pulsatility index and resistive index. These indexes are calculated from the blood flow velocities in vessels during cardiac cycle and are indicators of downstream resistance in arteries [7,8]. Increased pulsatility index and resistive index have been associated with malignancy of human mammary tumors [9,10]. B Flow is a non-Doppler technology that improves the visualization of blood vessels. This method uses a morphological approach, similarly to angiography, allowing the real-time visualization of hemodynamic flow in relation to stationary tissues [11]. Beyond these methods, the use of contrast media is a possible approach to improve the detection of tumor vessels by ultrasonography [12,13]. Contrast-enhanced ultrasound (CEUS) constitutes an excellent method to assess the structural and functional features of tumor angiogenesis by measuring tumor flow and vascular volume [12,13]. In the last years, the sensitivity and specificity of CEUS have greatly improved due to the development of more sophisticated ultrasound equipment, the introduction of the second-generation contrast agents, and the development of software able to perform quantitative analysis [14]. The microbubbles of the second-generation contrast agent SonoVue® have high reflectivity, enhancing the detectable ultrasound signal from the blood pool by as much as 40 dB. Its use allows the identification of slow and low-volume blood vessels inside the tumors with 20 to 39 μm in diameter [13,15].

Mast cells have been associated with the tumor angiogenesis by release of several angiogenic factors, such as vascular endothelial growth factor (VEGF), Fibroblast Growth Factor (FGF) 2, Interleukin (IL)-8, tryptase, chymase, heparin, Nerve Growth Factor (NGF), and Transforming Growth Factor (TGF)- β [16–18]. Since the inhibition of angiogenesis may represent a therapeutic approach in cancer, we hypothesized that the inhibition of the mast cell degranulation may be an approach to prevent the formation of new vessels during the carcinogenesis. So, the present study intended to assess the effects of ketotifen on the vascularization of chemically-induced mammary tumors in a rat model.

12.2. Material and Methods

12.2.1. Animals

Thirty-four female Sprague-Dawley rats with four weeks of age were used (Harlan Laboratories Inc., Barcelona, Spain). Animals were placed in the facilities of the University of Trás-os-Montes and Alto Douro (UTAD) under controlled conditions of temperature ($23\pm 2^{\circ}\text{C}$), humidity ($50\pm 10\%$), air system filtration (10-20 ventilations/hour) and on a 12h:12h light:dark cycle. Animals were fed with a standard laboratory diet (4RF21[®], Mucedola, Settimo Milanese, Milan, Italy) and tap water *ad libitum*. All procedures followed the European and National legislation on the protection of animals used for scientific purposes (European Directive 2010/63/EU and National Decree-Law 113/2013), and were approved by the Ethics Committee of UTAD (CE_12-2013) and by the Portuguese Ethics Committee for Animal Experimentation (approval no. 008961).

12.2.2. Experimental protocol

After one week of quarantine and two weeks of acclimatization to the lab conditions, animals were randomly divided into five experimental groups as follows: group I (MNU; n=10), group II (MNU + ketotifen-1; n=10), group III (MNU + ketotifen-2; n=10), group IV (ketotifen; n=2) and group V (control; n=2). At seven weeks of age, all animals from groups I, II and III received an intraperitoneal injection of the carcinogen agent *N*-methyl-*N*-nitrosourea (MNU) (ISOPAC[®], Sigma Aldrich S.A., Madrid, Spain) at a dose of 50 mg/kg of body weight. Animals from groups IV and V received a single intraperitoneal injection of the vehicle (saline solution 0.9%). The first day of the experimental protocol was defined as the day of the MNU administration. On the day after the MNU or saline administration, animals from groups II and IV received the mast cell stabilizer ketotifen (Zaditen[®], Defiante Farmacêutica S.A., Portugal) in drinking water, at a concentration of 1 mg/kg of body weight, seven days/week for 18 weeks. Each animal from group III only received the ketotifen after the detection of the development of the first mammary tumor by palpation. Animals from groups I and V received only water during the protocol. Animals were observed twice a day in order to monitor their health status during the experiment. Mammary chains from all animals were palpated once a week to detect the development of mammary tumors.

12.2.3. Ultrasonographic evaluation

Eighteen weeks after MNU administration, immediately before the sacrifice, all animals were anesthetized by intraperitoneal injection of ketamine (75 mg/kg of body weight, Imalgene[®] 1000, Merial S.A.S., Lyon, France) and xylazine (10 mg/kg of body weight, Rompun[®] 2%, Bayer Healthcare S.A., Kiel, Germany). The vascularization of mammary tumors previously detected by palpation in MNU-exposed animals (groups I, II and III) was evaluated by ultrasonography using the following modes: PDI, Pulsed Doppler, B Flow and CEUS. Mammary tumors were evaluated by two experienced examiners. For this, the animals were placed in supine position. The skin overlying each mammary tumor was shaved using a machine clipper (Aesculap GT420 Isis, Aesculap Inc., Center Valley, PA, USA) and acoustic gel (Aquasonic, Parker Laboratories Inc., Fairfield, NJ, USA) was applied. Ultrasonographic evaluation was performed using the real-time scanner Logiq P6[®] (General Electric Healthcare, Milwaukee, WI, USA) and a 10 MHz linear transducer. A standoff pad (Sonokit, MIUS Ltd., Gloucestershire, UK) made of extremely soft polyvinylchloride especially created for skin-contact sonography was used. A sagittal view of each mammary tumor was obtained. Ultrasonographic exams were recorded in clip format. Then the color pixel density (CPD) was determined in PDI and B Flow images following the methodology previously described [19]. The pulsatility index and resistive index were determined in Pulsed Doppler images by means of the equipment's software using the autotrace function.

12.2.4. CEUS

System settings were optimized for the contrast study with a mechanical index of 0.09, the gain compensation was adjusted for each mammary tumor. The position of the probe was maintained during the examination. The contrast agent SonoVue[®] (Bracco, Milan, Italy) was reconstituted by adding 5 mL of 0.9% saline solution. The SonoVue[®] was injected as a bolus (0.1 mL) through a tail vein catheter followed by a 1 mL saline flush. The injection technique was carefully performed by the same researcher to avoid personal variations, and produce acceptable and reproducible results. The real-time perfusion process and the dynamic enhancement of each mammary tumor were observed in real time and continuously recorded in the ultrasound apparatus immediately after the

intravenous injection of the contrast agent. Posteriorly, the qualitative and quantitative analysis of CEUS videos was performed. Qualitative analysis included the following parameters: enhancement order (centripetal, centrifugal or diffuse), margin (blurred or clear), enhancement homogeneity (homogenous or heterogeneous) and penetrating vessels (absent or present) [20]. The quantitative analysis was performed using the time intensity curve (TIC) analysis of the ultrasound apparatus. An ovoid region of interest (ROI) was drawn in the most enhanced area of each mammary tumor and the signal was immediately plotted and fitted using the following gamma variate function:

$$I(t) = At^c \times \exp(-kt) + B,$$

where t is the time, k is a constant scale factor, and A and B are parameters that define the shape of the curve. The following parameters were determined: contrast agent arrival time (AT), time to peak (TTP, defined as the time the lesions go up to the maximum contrast intensity that is related to the lesions' enhancement speed), peak intensity (PI, maximum intensity), wash-in (upslope), wash-out (downslope) and area under the curve (AUC).

12.2.5. Animals' sacrifice and necropsy

Immediately after ultrasonographic examination, anesthetized animals were sacrificed by exsanguination by cardiac puncture as indicated by the Federation of European Laboratory Animal Science Associations [21]. Animals were skinned and the skin was carefully evaluated under a light in order to detect mammary tumors not previously identified by palpation. All mammary tumors were collected and immersed in formalin for 24 hours.

12.2.6. Histology and immunohistochemistry

After fixation, mammary tumors were cut, included in paraffin and processed for routine histological evaluation. Two μm -thick sections were stained with hematoxylin and eosin (H&E). Mammary tumors were histologically evaluated under a light microscopy by a pathologist and classified according to the predominant histological

pattern (histological pattern with higher proportion in each tumor section), following the classification previously established by Russo and Russo [22].

In order to evaluate the vascularization of each mammary tumor, the immunoexpression of VEGF-A was evaluated using the standard NovoLink Polymer Detection System protocol (Leica Biosystems, Newcastle, UK). Sections of each tumor were incubated overnight at 4°C with a primary antibody for VEGF-A at a dilution of 1:100 (clone JH121, Merck Millipore, Darmstadt, Germany). A representative image of each tumor was taken with a 40× objective and the quantification of the VEGF immunoexpression was assessed using the Image Manipulation Program 2.8 (GNU Image Manipulation Program, CNE, Free Software Foundation, Boston, MA, USA) as previously described [23].

12.2.7. Statistical analysis

Data were statistically analyzed using Statistical Package for the Social Sciences (SPSS®, version 23 for Windows, SPSS Inc., Chicago, IL, USA). Continuous data were compared among groups using analysis of variance (ANOVA) with the Bonferroni correction. Histological results and data from qualitative analysis of CEUS were analyzed using Chi-square test. Continuous data are expressed as mean ± standard error (S.E.) and *p*-values lower than 0.05 were considered statistically significant.

12.3. Results

12.3.1. General findings and mammary tumor development

One animal from group II (MNU + ketotifen-1) died unexpectedly during the experiment, the size of this group was reduced to nine animals. The first mammary tumors were simultaneously identified in groups I, II and III eight weeks after the carcinogen agent administration. At the end of the study (18 weeks after MNU administration), not all animals developed mammary tumors (an incidence of 100% was not observed). In this way, six animals from group I (MNU) developed 21 mammary tumors (incidence of 60%), eight animals from group II developed 19 mammary tumors (incidence of 89%) and seven animals from group III developed 18 mammary tumors (incidence of 70%). As the number of tumors was very similar among groups, no statistically significant

differences were found ($p>0.05$). As expected, no mammary tumors were observed in groups IV (ketotifen) and V (control).

12.3.2. Histological classification of mammary tumors

At histopathological analysis, it was observed that each mammary tumor exhibited more than one histological pattern. Each tumor was classified taking into account the predominant histological pattern. The number of malignant mammary tumors was higher when compared with the number of benign mammary tumors in all experimental groups [20 *versus* 1 in group I (MNU), 19 *versus* 0 in group II (MNU + ketotifen-1) and 17 *versus* 1 in group III (MNU + ketotifen-2)] ($p<0.05$). No tumors were classified as benign in group II (MNU + ketotifen-1) (Table 12.1). It was also observed that the number of non-invasive mammary tumors was higher when compared with the number of invasive ones (13 *versus* 7 in group I, 12 *versus* 7 in group II, and 9 *versus* 8 in group III). It worth to note that no comedo invasive carcinoma was identified in group II (MNU + ketotifen-1) that was the most aggressive lesion identified in this experimental protocol (Table 12.1).

Table 12.1. Histological classification of each mammary tumor according to the predominant histological pattern.

Histological classification		Number of tumors		
		I (MNU)	II (MNU + ket-1)	III (MNU + ket-2)
Benign lesion	Fibroadenoma	1	0	1
Non-invasive	Papillary carcinoma	12	5	3
	Cribriform carcinoma	1	1	2
	Papillary-cribriform carcinoma	0	6	4
	Total:	13	12	9
Malignant lesions				
Invasive	Papillary carcinoma	3	2	3
	Cribriform carcinoma	3	2	2
	Papillary-cribriform carcinoma	0	3	2
	Comedo carcinoma	1	0	1
	Total:	7	7	8
	Malignant lesions:	20 ^a	19	17 ^a
Total number of tumors:		21	19	18

^a Statistically different from the number of benign tumors ($p < 0.05$).

12.3.3. Mammary tumor vascularization

Due to their small size, some mammary tumors could not be detected by palpation and consequently they were not evaluated by ultrasonography. A total of 40 mammary tumors were evaluated by ultrasonography: 14 tumors from group I (MNU), 13 tumors from group II (MNU + ketotifen-1) and 13 mammary tumors from group III (MNU + ketotifen-2). In both modes PDI and B Flow, the vascularization of mammary tumors was slightly higher in ketotifen treated groups (groups II and III) when compared with non-treated one (group I), this difference was more evident between group I (MNU) and group II (MNU + ketotifen I) in PDI analysis ($p > 0.05$), and statistically different among groups I (MNU), II (MNU + ketotifen-1) and III (MNU + ketotifen-2) in B Flow ($p < 0.05$). Although

statistically significant differences were not found ($p>0.05$), the vascularization detected by PDI was higher when compared with that detected by B Flow in groups I and II. The opposite was observed in group III (MNU + ketotifen-2) (Table 12.2, Figures 12.1A and B). No statistical significant differences were found in the pulsatility and resistive indexes among groups ($p>0.05$) (Table 12.2, Figure 12.1C).

In a general view, independently of the experimental group, mammary tumors mainly exhibited a centripetal enhancement order ($p<0.05$), a clear margin ($p<0.05$), a heterogeneous enhancement and presence of penetrating vessels in CEUS ($p>0.05$) (Table 12.3). Evaluating by group, it was observed that the majority of mammary tumors from all groups exhibited a centripetal enhancement order, the majority of tumors from group I (MNU) exhibited blurred margin while the tumors from groups II (MNU + ketotifen-1) and III (MNU + ketotifen-2) exhibited mainly clear margin. The number of mammary tumors with homogeneous and heterogeneous enhancement was very similar among group ($p>0.05$). The number of mammary tumors without penetrating vessels was higher than the number of mammary tumors with penetrating vessels in groups I (MNU) and III (MNU + ketotifen-2), and lower in group II (MNU + ketotifen-1) ($p>0.05$) (Table 12.3).

Regarding to the quantitative analysis (Figure 12.1D), although no statistical significant differences were found among groups, it was observed that the AT and TTP were slightly higher in group III (MNU + ketotifen-2). Inversely, the PI, wash-in and AUC were higher in group I (MNU) than in ketotifen treated groups (II and III). Accordingly, the VEGF-A immunoexpression was very similar among groups ($p>0.05$) (Table 12.2, Figure 12.2).

Table 12.2. Evaluation of mammary tumor vascularization by ultrasonography (Doppler, B Flow and CEUS) and immunohistochemistry (mean \pm S.E.).

Technique	Parameter/measurement unit	Groups		
		I (MNU) (n=14)	II (MNU + ket-1) (n=13)	III (MNU + ket-2) (n=13)
Power Doppler B Flow	CPD (%)	2.59 \pm 0.78	4.33 \pm 0.86	3.04 \pm 0.44
		2.45 \pm 0.57 ^{a, b}	4.03 \pm 0.54	5.04 \pm 0.98
Pulsed Doppler	Resistive index	6.88 \pm 1.67	6.30 \pm 0.89	4.24 \pm 0.86
	Pulsatility index	14.09 \pm 2.68	16.00 \pm 1.70	14.19 \pm 1.81
CEUS	Arrival time (AT) (s)	5.36 \pm 0.49	5.38 \pm 0.43	6.77 \pm 0.65
	Time to peak (TTP) (s)	9.38 \pm 0.91	8.67 \pm 0.97	11.07 \pm 1.28
	Peak intensity (PI) (dB)	3.57 \pm 0.47	3.10 \pm 0.32	2.51 \pm 0.34
	Wash-in (dB/s)	1.18 \pm 0.20	1.22 \pm 0.22	0.87 \pm 0.18
	Wash-out (dB/s)	-0.40 \pm 0.08	-0.45 \pm 0.07	-0.32 \pm 0.06
	Area under the curve (AUC) (dB)	29.04 \pm 6.49	21.35 \pm 4.16	25.37 \pm 6.86
VEGF-A immunoexpression (%)		33.97 \pm 1.05	33.66 \pm 1.50	35.39 \pm 1.10

^a $p=0.055$ from group II (MNU + ketotifen-1); ^bStatistically different from group III (MNU + ketotifen-2) ($p<0.05$).
CPD: color pixel density; CEUS: contrast-enhanced ultrasound.

Table 12.3. Qualitative evaluation of CEUS of mammary tumors in all experimental groups.

Parameter/Group		I (MNU)	II (MNU + ket-1)	III (MNU + ket-2)	n=40
		n=14	n=13	n=13	
Enhancement order	Centripetal	11 (78.6%) ^a	10 (76.9%) ^{a, b}	9 (69.2%) ^b	30 (75%) ^{a, b}
	Centrifugal	0 (0%)	1 (7.7%)	1 (7.7%)	2 (5%)
	Diffuse	3 (21.4%)	2 (15.4%)	3 (23.1%)	8 (20%)
Margin	Clear	5 (35.7%) ^d	12 (92.3%) ^c	11 (84.6%) ^c	28 (70%) ^c
	Blurred	9 (64.3%) ^{d, e}	1 (7.7%)	2 (15.4%)	12 (30%)
Enhancement homogeneity	Homogeneous	7 (50.0%)	5 (38.5%)	6 (46.2%)	18 (45%)
	Heterogeneous	7 (50.0%)	8 (61.5%)	7 (53.8%)	22 (55%)
Penetrating vessels	Absent	8 (57.1%)	3 (23.1%)	8 (61.5%)	19 (47.5%)
	Present	6 (42.9%)	10 (76.9%)	5 (38.5%)	21 (52.5%)

^a Statistically different from diffuse enhancement order ($p < 0.05$); ^b Statistically different from centrifugal enhancement order ($p < 0.05$); ^c Statistically different from blurred margin ($p < 0.05$); ^d Statistically different from group II ($p < 0.05$); ^e Statistically different from group III ($p < 0.05$).

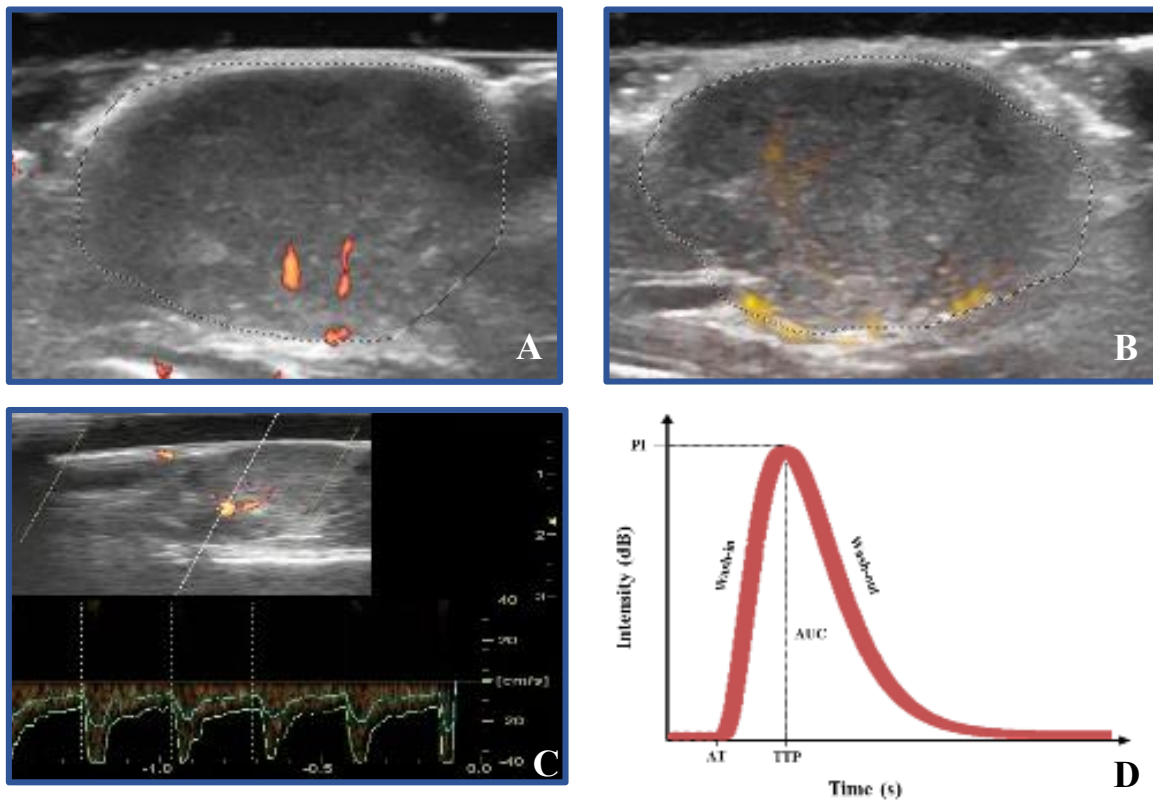


Figure 12.1. Evaluation of mammary tumors by PDI (A), B Flow (B) and Pulsed Doppler (C). Graphic representation of contrast intensity in each moment after its administration (TIC analysis): AT: arrival time; TTP: time to peak; PI: peak intensity; AUC: area under the curve, wash-in (upslope) and wash-out (downslope) (D).

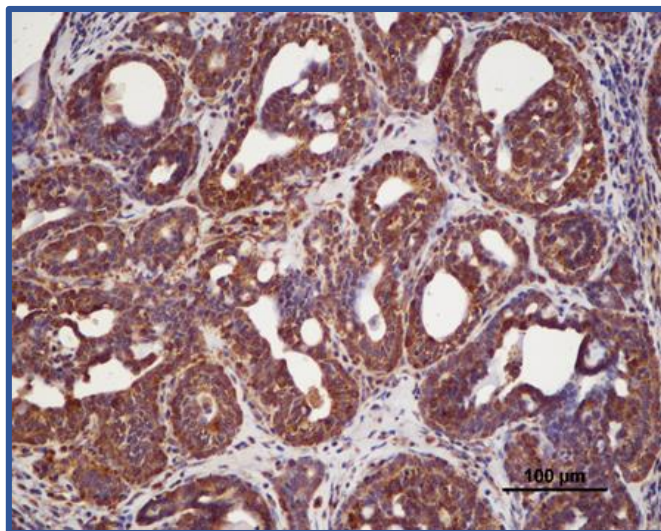


Figure 12.2. Immunorexpression of VEGF-A in a cribriform carcinoma (magnification of 40×).

12.4. Discussion

Vascularization is essential for cancer growth and metastization. Since mast cells were associated with aggressiveness and poor prognosis in women and female dog mammary tumors, the hypothesis arises that the inhibition of mast cell degranulation could inhibit mammary tumors vascularization. So, this work intended to verify the hypothesis of modulation of mammary tumors vascularization by the inhibition of mast cell degranulation through the administration of a mast cells stabilizer drug. In this way, a model of mammary cancer chemically-induced by the carcinogen agent MNU in female Sprague-Dawley rats was used. This model of mammary cancer has been used for several years in cancer research and it was already successfully used by our research team [19,23–30].

Due to the low number of benign mammary tumors (n=2) developed by animals, it was not possible to establish comparisons between benign and malignant mammary tumors in the present work. Additionally, not all mammary tumors could be evaluated by ultrasonography due to the small size of some of them (tumor volume ranged from 0.2 cm³ to 17.8 cm³) that did not allow their detection by palpation during the experiment. When compared with Color Doppler, PDI may compensate for slow blood flow, but flow

that is visible with this method differs from the tumor microvessel density assessed by histology [6]. Additionally to PDI, mammary tumors were also evaluated by B Flow, which has some advantages when compared with Doppler. It allows the visualization of blood vessels without the limitations of Doppler mode, namely aliasing, signal dropout at orthogonal detection angles and wall-filter limitations [11,31]. Inversely to that observed in our previous study, where it was observed that B Flow was more sensitive than PDI on the detection of mammary tumors vascularization (the CPD detected by B Flow was higher when compared with CPD detected by PDI) [19,32], surprisingly in the present study, although not statistically different, the CPD detected by PDI in groups I (MNU) and II (MNU + ketotifen I) was higher when compared with that detected by B Flow ($p>0.05$).

Although the resistive and pulsatility indexes were first used to detect peripheral vascular diseases, nowadays they are rarely used with that purpose. They have been used in chronic renal failure in order to detect the severity and progression of the disease [8,33], in the detection of neoplastic lesions in female genital tract through the detection of abnormal flows [34], in the evaluation of hemodynamic characteristics of fetal umbilicus [35], and in breast mammary tumors as an additional tool to differentiate between benign and malignant lesions [36]. Due to the different characteristics from normal vessels, such as lack of muscular layer, atypical branch pattern, irregularity, presence of stenosis and occlusion or arteriovenous fistulas, the vessels from tumor angiogenesis produce alterations in dynamics of blood flow that may be detected by PDI. Although a higher pulsatility and resistive indexes were detected in malignant lesions when compared with benign ones, the values overlap significantly which makes them a not so good tool to differentiate between both types of lesions [5,37]. Despite the fact that pulsatility and resistive indexes themselves did not allow the accurate differentiation of benign and malignant tumors [36,38], they are very useful when analyzed together with the ultrasonographic aspect of mammary tumors, namely posterior acoustic enhancement, less shadowing, lobulated, microlobulated or irregular margins mass, and presence of architectural distortions in the surrounding tissues [39]. Although no benign mammary tumors were analyzed in the present work, the pulsatility index was evaluated in mammary tumors with distinct grades of malignancy (non-invasive *versus* invasive tumors) and no statistical significant differences were found between them.

In order to obtain more information about mammary tumor vascularization, a CEUS study was performed. For this, the contrast agent SonoVue[®] was selected. It is a second generation contrast agent that contains phospholipid-stabilized microbubbles filled with sulfur hexafluoride gas with a mean diameter of 2.5 μm [40]. When compared with other contrast agents, SonoVue[®] has the advantages that its microbubbles are stable against the ultrasound beam, which allows the analysis of the contrast enhancement under real-time conditions [41], they do not extravasate from the vessel lumen, acting as blood pool agents [42], and they are less soluble and much more stable circulating within the blood pool for a long time without being destroyed [40,43]. Although it was previously observed that the SonoVue[®] produces the best images with the combination of a low mechanical index around 0.1 and a low frequency transducer around 4 MHz [44], similarly to that performed by Ko and collaborators [45] a 10 MHz transducer with a low mechanical index of 0.09 was used in the present study, due to the characteristics of rat mammary tumors (small size with superficial location). Although the qualitative evaluation of CEUS may be subjectively influenced, it provides several information about tumor vascularization that may be indicator of malignancy [46]. According with that previously observed in women and rat mammary tumors [46,47], in the present study the enhancement order of the contrast agent was mainly peripheral with a centripetal filling, with a heterogeneous enhancement and the presence of penetrating vessels.

The TIC analysis is the representation of contrast intensity in each moment after its administration. The incorporation of temporal information with parametric imaging may provide a more feasible measure of the tumor microenvironment and it is useful in antiangiogenic studies [12,48]. The estimation of an optimal curve produces a mathematical description of the contrast concentration changes during the first passage of the contrast bolus and allows direct calculation of the AUC and some timing parameters, namely AT and TTP [49]. The curve fitting only uses data during the early part of the first passage of the contrast agent removing the effect of re-circulation of the contrast which is responsible for the elevation of measurements in the later part of the curve [50,51]. Although CEUS has some advantages when compared with Doppler, it is not a perfect method and present some disadvantages, such as the placement of the ROI, and the analysis of only one plane of the mammary tumor and not the entire lesion [52]. According to previous studies, malignant lesions showed higher maximum signal

intensity (PI), fast wash-in, the wash-out is observed immediately after the peak (probably due to the presence of arteriovenous shunts and higher microvascular density) and shorter TTP. The opposite may be observed in benign lesions [47,53–55]. Due to a lack of studies on CEUS in rat models, it is not possible to establish comparisons of the data from this study with other previously obtained by other researchers. The mean TTP observed in this study was different from that observed by Badea *et al.* [46] which may be related with the different animal model (implanted *versus* chemically-induced mammary cancer model).

Considering all data (ultrasonography and immunohistochemical analysis), when compared with a previous work from our research team using the same animal model [19,32], the mammary tumors developed by animals in the present study were less vascularized. This fact is probably related with the duration of the experimental protocol, in the present study the animals were sacrificed 18 weeks after the MNU administration (animals with 25 weeks of age), while in the first one they were sacrificed 35 weeks after MNU administration (animals with 42 weeks of age).

12.5. Conclusion

Ketotifen inhibited mast cell degranulation, as demonstrated by the lower histamine serum levels in ketotifen-treated animals when compared with non-treated ones [56]. Since the mast cell degranulation was inhibited, a lower vascularization of mammary tumors was expected in ketotifen-treated groups. However, the data obtained from ultrasonography (Doppler, B Flow and CEUS) and immunohistochemistry (VEGF-A immunoexpression) suggest that the mammary tumor vascularization was not different among groups, and the administration of ketotifen did not change the mammary tumors vascularization.

12.6. References

- [1] Wan, C.; Du, J.; Fang, H.; Li, F.; Wang, L. Evaluation of breast lesions by contrast enhanced ultrasound: qualitative and quantitative analysis. *Eur. J. Radiol.*, **2012**, 81, 444–450.
- [2] Folkman, J. Angiogenesis and breast cancer. *J. Clin. Oncol.*, **1994**, 12, 441–443.

- [3] Folkman, J. Role of angiogenesis in tumor growth and metastasis. *Semin. Oncol.*, **2002**, 29, 15–18.
- [4] Toi, M.; Bando, H.; Kuroi, K. The predictive value of angiogenesis for adjuvant therapy in breast cancer. *Breast Cancer*, **2013**, 7, 311–314.
- [5] Less, JR.; Skalak, TC.; Sevick, EM.; Jain, RK. Microvascular architecture in a mammary-carcinoma - branching patterns and vessel dimensions. *Cancer Res.*, **1991**, 51, 265–273.
- [6] Peters-Engl, C.; Medl, M.; Mirau, M.; Wanner, C.; Bilgi, S.; Sevelde, P.; Obermair, A. color-coded and spectral Doppler flow in breast carcinomas - relationship with the tumor microvasculature. *Breast Cancer Res. Treat.*, **1998**, 47, 83–89.
- [7] Gosling, RG.; Dunbar, G.; Newman, DL.; Side, CD.; Woodcock, JP.; Fitzgerald, DE.; Keates, JS.; MacMillan, D. The quantitative analysis of occlusive peripheral arterial disease by a non-intrusive ultrasonic technique. *Angiology*, **1971**, 22, 52–55.
- [8] Petersen, LJ.; Petersen, JR.; Talleruphuus, U.; Ladefoged, SD.; Mehlsen, J.; Jensen, HA. The pulsatility index and the resistive index in renal arteries. Associations with long-term progression in chronic renal failure. *Nephrol. Dial. Transplant.*, **1997**, 12, 1376–1380.
- [9] Hollerweger, A.; Rettenbacher, T.; Macheiner, P.; Gritzmann, N. New signs of breast cancer: high resistance flow and variations in resistive indices evaluation by color Doppler sonography. *Ultrasound Med. Biol.*, **1997**, 23, 851–856.
- [10] Schmillevitch, J.; Guimarães, HA.; Nicola, H.; Gorski, AC. Utilization of vascular resistance index in the differentiation between benign and malignant breast nodules. *Radiol. Bras.*, **2009**, 42, 241–244.
- [11] Clevert, DA.; Jung, EM.; Rupp, N.; Reiser, M. Improved diagnosis of vascular neck dissection by ultrasound B-flow imaging. *Am. J. Roentgenol.*, **2005**, 184, 132.
- [12] Eisenbrey, JR.; Forsberg, F. Contrast-enhanced ultrasound for molecular imaging of angiogenesis. *Eur. J. Nucl. Med. Mol. Imaging*, **2010**, 37, S138–146.
- [13] Forsberg, F.; Kuruvilla, B.; Pascua, MB.; Chaudhari, MH.; Merton, DA.; Palazzo, JP.; Goldberg, BB. Comparing contrast-enhanced color flow imaging and pathological measures of breast lesion vascularity. *Ultrasound Med. Biol.*, **2008**,

- 34, 1365–1372.
- [14] Drudi, FM.; Cantisani, V.; Gneccchi, M.; Malpassini, F.; Di Leo, N.; Felice, C. Contrast-enhanced ultrasound examination of the breast: a literature review. *Ultraschall der Medizin*, **2012**, 33, 1–7.
- [15] Ferrara, KW.; Merritt, CRB.; Burns, PN.; Foster, FS.; Mattrey, RF.; Wickline, SA. Evaluation of tumor angiogenesis with US: imaging, Doppler, and contrast agents. *Acad. Radiol.*, **2000**, 7, 824–839.
- [16] Bachelet, I.; Levi-Schaffer, F. Mast cells as effector cells: a co-stimulating question. *Trends Immunol.*, **2007**, 28, 360–365.
- [17] Oldford, SA.; Marshall, JS. Mast cells as targets for immunotherapy of solid tumors. *Mol. Immunol.*, **2014**, 63, 113–124.
- [18] Ribatti, D.; Crivellato, E. The mast cell. In *Mast cells and tumors: from biology to clinic* (Ribatti, D. and Crivellato, E, eds), **2011**, pp. 3–48, Springer.
- [19] Faustino-Rocha, AI.; Silva, A.; Gabriel, J.; Reixeira-Guedes, C.; Lopes, C.; Gil da Costa, R.; Gama, A.; Ferreira, R.; Oliveira, P.; Ginja, M. Ultrasonographic, thermographic and histologic evaluation of MNU-induced mammary tumors in female Sprague-Dawley rats. *Biomed. Pharmacother.*, **2013**, 67, 771–776.
- [20] Du, J.; Li, FH.; Fang, H.; Xia, JG.; Zhu, CX. Correlation of real-time gray scale contrast-enhanced ultrasonography with microvessel density and vascular endothelial growth factor expression for assessment of angiogenesis in breast lesions. *J. Ultrasound Med.*, **2008**, 27, 821–831.
- [21] Forbes, D.; Blom, H.; Kostomitsopulos, N.; Moore, G.; Perretta, G. Euroguide: on the accommodation and care of animals used for experimental and other scientific purposes. *Federation of European Laboratory Animal Science Associations*, **2007**.
- [22] Russo, J.; Russo, IH. Atlas and histologic classification of tumors of the rat mammary gland. *J. Mammary Gland Biol. Neoplasia*, **2000**, 5, 187–200.
- [23] Faustino-Rocha, AI.; Silva, A.; Gabriel, J.; Gil da Costa, R.; Moutinho, M.; Oliveira, P.; Gama, A.; Ferreira, R.; Ginja, M. Long-term exercise training as a modulator of mammary cancer vascularization. *Biomed. Pharmacother.*, **2016**, 81, 273–280.
- [24] Faustino-Rocha, A.; Teixeira-Guedes, C.; Pinho-Oliveira, J.; Soares-Maia, R.; Arantes-Rodrigues, R.; Colaco, B.; Ferreira, R.; Oliveira, P.; Ginja, M. Volume

- measurement of female Sprague-Dawley mammary tumors induced by *N*-methyl-*N*-nitrosourea: comparing ultrasonography and caliper. *Virchows Arch.*, **2012**, 461, S240–240.
- [25] Faustino-Rocha, A.; Oliveira, PA.; Pinho-Oliveira, J.; Teixeira-Guedes, C.; Soares-Maia, R.; Gil da Costa, RM.; Colaço, B.; Pires, MJ.; Colaço, J.; Ferreira, R.; Ginja, M. Estimation of rat mammary tumor volume using caliper and ultrasonography measurements. *Lab. Anim. (NY)*, **2013**, 42, 217–24.
- [26] Faustino-Rocha, A.; Gama, A.; Oliveira, PA.; Alvarado, A.; Neuparth, MJ.; Ferreira, R.; Ginja, M. Effects of lifelong exercise training on mammary tumorigenesis induced by MNU in female Sprague-Dawley rats. *Clin. Exp. Med.*, **2016**, Epub ahead of print.
- [27] Faustino-Rocha, AI.; Gama, A.; Pires, MJ.; Oliveira, PA.; Ginja, M. Effects of a mast cell stabilizer on the vascularization of mammary tumors: ultrasonographic evaluation. *Anticancer Res.*, **2014**, 34, 5901.
- [28] Faustino-Rocha, AI.; Pinto, C.; Gama, A.; Oliveira, PA. Effects of ketotifen on mammary tumors volume and weight. *Anticancer Res.*, **2014**, 34, 5902.
- [29] Faustino-Rocha, AI.; Gama, A.; Oliveira, PA.; Alvarado, A.; Vala, H.; Ferreira, R.; Ginja, M. Expression of estrogen receptors-alpha and beta in chemically-induced mammary tumours. *Virchows Arch.*, **2015**, 467, S51–51.
- [30] Faustino-Rocha, AI.; Gama, A.; Oliveira, PA.; Vala, H.; Ferreira, R.; Ginja, M. Effects of histamine on the development of MNU-induced mammary tumours. *Virchows Arch.*, **2015**, 467, S51–51.
- [31] Umemura, A.; Yamada, K. B-mode flow imaging of the carotid artery. *Stroke*, **2001**, 32, 2055–2057.
- [32] Faustino-Rocha, A.; Silva, A.; Gabriel, J.; Gil da Costa, RM.; Moutinho, M.; Oliveira, P.; Gama, A.; Ferreira, R.; Ginja, M. Long-term exercise training as a modulator of mammary cancer vascularization. *Biomed. Pharmacother.*, **2016**, 81, 273–280.
- [33] McArthur, C.; Geddes, CC.; Baxter, GM. Early measurement of pulsatility and resistive indexes: correlation with long-term renal transplant function. *Radiology*, **2011**, 259, 278–285.
- [34] Tekay, A.; Jouppila, P. Validity of pulsatility and resistance indexes in

- classification of adnexal tumors with transvaginal color Doppler ultrasound. *Ultrasound Obstet. Gynecol.*, **1992**, 2, 338–344.
- [35] Kumar, K.; Chandolia, RK.; Kumar, S.; Jangir, T.; Luthra, RA.; Kumari, S.; Kumar, S. Doppler sonography for evaluation of hemodynamic characteristics of fetal umbilicus in Beetal goats. *Vet. World J.*, **2015**, 8, 412–416.
- [36] Pinero, A.; Reus, M.; Illana, J.; Duran, I.; Martinez-Barba, E.; Canteras, M.; Parrilla, P. Palpable breast lesions: utility of Doppler sonography for diagnosis of malignancy. *Breast*, **2003**, 12, 258–263.
- [37] del Cura, JL.; Elizagaray, E.; Zabala, R.; Legorburu, A.; Grande, D. The use of unenhanced Doppler sonography in the evaluation of solid breast lesions. *Am. J. Roentgenol.*, **2005**, 184, 1788–1794.
- [38] Hsiao, YH.; Kuo, SJ.; Liang, WM.; Huang, YL.; Chen, DR. Intra-tumor flow index can predict the malignant potential of breast tumor: dependent on age and volume. *Ultrasound Med. Biol.*, **2008**, 34, 88–95.
- [39] Wojcinski, S.; Stefanidou, N.; Hillemanns, P.; Degenhardt, F. The biology of malignant breast tumors has an impact on the presentation in ultrasound: an analysis of 315 cases. *BMC Women's Health*, **2013**, 13, 47.
- [40] Schneider, M. SonoVue, a new ultrasound contrast agent. *Eur. Radiol.*, **1999**, 9, 347–348.
- [41] Von Harbay, A.; Vogt, C.; Willer, R.; Häussinger, D. Real-time imaging with the sonographic contrast agent SonoVue. *J. Ultrasound Med.*, **2004**, 23, 1557–1568.
- [42] Caruso, G.; Ienzi, R.; Cirino, A.; Salvaggio, G.; Campione, M.; Lagalla, R.; Cardinale, A. Breast lesion characterization with contrast-enhanced US. Work in progress. *Radiol. Medica*, **2002**, 104, 443–450.
- [43] Schneider, M.; Arditi, M.; Barrau, MB.; Brochot, J.; Broillet, A.; Ventrone, R.; Yan, F. BR1 - a new ultrasonographic contrast agent based on sulfur hexafluoride-filled microbubbles. *Invest. Radiol.*, **1995**, 30, 451–457.
- [44] Cosgrove, D. Future prospects for SonoVue and CPS. *Eur. Radiol.*, **2004**, 14, 116–124.
- [45] Ko, EY.; Lee, SH.; Kim, HH.; Kim, SM.; Shin, MJ.; Kim, N.; Gong, G. Evaluation of tumor angiogenesis with a second-generation US contrast medium in a rat breast tumor model. *Korean J. Radiol.*, **2008**, 9, 243–249.

- [46] Badea, AF.; Szora, AT.; Clichici, S.; Socaciu, M.; Tabaran, AF.; Baciut, G.; Catoi, C.; Muresan, A.; Buruiian, M.; Badea, R. Contrast enhanced ultrasonography (CEUS) in the characterization of tumor microcirculation. Validation of the procedure in the animal experimental model. *Med. Ultrason.*, **2013**, 15, 85–94.
- [47] Balleyguier, C.; Opolon, P.; Mathieu, MC.; Athanasiou, A.; Garbay, JR.; Delalogue, S. New potential and applications of contrast-enhanced ultrasound of the breast: own investigations and review of the literature. *Eur. J. Radiol.*, **2009**, 69, 14–23.
- [48] Streba, CT.; Ionescu, M.; Gheonea, DI.; Sandulescu, L.; Ciurea, T.; Saftoiu, A.; Vere, CC.; Rogoveanu, I. Contrast-enhanced ultrasonography parameters in neural network diagnosis of liver tumors. *World J. Gastroenterol.*, **2012**, 18, 4427–4434.
- [49] Thompson, HK.; Whalen, RE.; Starmer, CF.; McIntosh, HD. Indicator transit time considered as gamma variate. *Circ. Res.*, **1964**, 14, 502–515.
- [50] Barbier, EL.; Lamalle, L.; Decorps, M. Methodology of brain perfusion imaging. *J. Magn. Ressonance Imaging*, **2001**, 13, 496–520.
- [51] Jackson, A. Analysis of dynamic contrast enhanced MRI. *Br. J. Radiol.*, **2004**, 77, 154–166.
- [52] Zhang, HP.; Shi, QS.; Li, F.; Liu, L.; Bai, M.; Gu, JY.; Wu, Y.; Du, LF. Regions of interest and parameters for the quantitative analysis of contrast-enhanced ultrasound to evaluate the anti-angiogenic effects of bevacizumab. *Mol. Med. Rep.*, **2013**, 8, 154–160.
- [53] Buadu, LD.; Murakami, J.; Murayama, S.; Hashiguchi, N.; Sakai, S.; Masuda, K.; Toyoshima, S.; Kuroki, S.; Ohno, S. Breast lesions: correlation of contrast medium enhancement patterns on MR images with histopathologic findings and tumor angiogenesis. *Radiology*, **1996**, 200, 639–649.
- [54] Schneider, BP.; Miller, KD. Angiogenesis of breast cancer. *J. Clin. Oncol.*, **2005**, 23, 1782–1790.
- [55] Zhao, H.; Xu, R.; Ouyang, Q.; Chen, L.; Dong, B.; Huihua, Y. Contrast-enhanced ultrasound is helpful in the differentiation of malignant and benign breast lesions. *Eur. J. Radiol.*, **2010**, 73, 288–293.
- [56] Faustino-Rocha, A.; Gama, A.; Neuparth, M.; Oliveira, P.; Ferreira, R.; Ginja, M. Mast cells on mammary carcinogenesis: host or tumor supporters? (Submitted for publication).

CHAPTER 13

GENERAL DISCUSSION

13. General discussion

Cancer remains as one of the most frightening diseases worldwide. Although a lot of research has been done on cancer prevention, diagnosis and treatment, the statistics are disappointing, indicating that approximately 8.2 million of people were killed by this disease in 2012. These data clearly indicate that cancer is a public health problem that is far from being solved [1]. By the exposed, the researchers have been focused on the search of new prophylactic and therapeutic approaches that may reduce the number of cancers and more effectively treat it, increasing the lifespan and quality of life of oncologic patients. Animal models have been frequently used for the study of cancer, being the intermediate step between *in vitro* cell cultures and clinical assays in humans [2]. In this thesis, we focused on the study of breast cancer. Two *in vivo* experiments using the rat model of mammary cancer induced by a single administration of the chemical carcinogen *N*-methyl-*N*-nitrosourea (MNU) were performed in order to monitor breast cancer growth and vascularization, and to assess the role of long-term exercise training and mast cells on mammary tumor progression and vascularization.

MNU is universally used as a carcinogenic agent that may induce cancer in several organs, namely breast, uterus, prostate, seminal vesicles, kidney, stomach, liver, spleen, lung, colon, small intestine, eye, skin, nervous system and urinary bladder, depending on dose, route of administration and animals' age [3]. MNU-induced mammary tumors in rodents constitute a well-established animal model for breast cancer research. Indeed, mammary tumor development may be easily induced by a single intraperitoneal administration of MNU at a dose of 50 mg/kg of body weight at 50 days of age. Furthermore, MNU-induced mammary tumors resemble those developed by woman in several aspects, namely histology, hormone responsiveness, molecular and genetic characteristics, aggressiveness and ability to metastasize, allowing a better understanding of many aspects of this disease and evaluation of potential therapeutic approaches [3–5].

Since the rat model of MMU-induced mammary cancer is frequently used to evaluate potential therapeutic strategies for mammary cancer, the accurate determination of tumor size and volume is essential to assess tumor response to therapy [6]. Additionally, tumor size is frequently used as a human endpoint in research protocols [7]. Similarly to Pain *et al.* [8] that concluded that physical examination and ultrasound had similar accuracy for predicting tumor size, we observed that tumor length, width and depth were similar

among the methods used for tumor measurement (caliper measurement *in vivo* and after tumor excision during sacrifice, and ultrasound). We also observed that tumor width and length were similar and greater when compared with tumor depth, suggesting that MNU-induced mammary tumors grow as a circular surface with small depth, resembling the shape of an oblate spheroid. Additionally, we also determined tumor volume by distinct ways: water displacement, using the measurements obtained by caliper and ultrasound, and based on tumor weight. We observed that the use of measurements (length and depth) obtained by ultrasonography is the best way to evaluate tumor volume *in vivo*. Beyond the determination of tumor volume by water displacement, the determination of tumor volume based on tumor weight is the best way to determine tumor volume after animal sacrifice or tumor excision. As expected, we also verified that it is not possible to predict if a tumor is invasive or non-invasive based on its dimensions, volume and weight.

Tumor vascularization appears as a double-edged sword that requires a deeper understanding before rational modulation approaches may be applied. Ultrasound is not only important to monitor tumor growth, but also to assess tumor vascularization through the use of distinct modes, namely Power Doppler (PDI), B Flow and contrast-enhanced ultrasound (CEUS) [22]. Beyond ultrasound, thermography is also an imaging modality able to give information concerning tumor angiogenesis based on superficial temperature [23]. We observed that PDI detected vessels mainly at the periphery of mammary tumors, while B Flow mode detected vessels not only at the periphery, but also within the tumor. Consequently, the color pixel density (CPD) detected in images obtained with B Flow was higher when compared with that quantified in images obtained with PDI. These data agree with those previously described [24]. Predictably, thermographic analysis revealed that larger mammary tumors showed higher maximum temperature and thermal amplitude, which may be explained by the richer blood supply of these tumors, simultaneously with the tendency to present more extensive necrotic regions (colder regions). Surprisingly, CPD assessed by PDI was negatively correlated with maximum temperature and thermal amplitude, and a much weaker trend was observed when CPD was detected by B Flow.

Although the model of MNU-induced mammary tumor has been frequently used on mammary cancer research, there is a lack of ultrastructural studies of these tumors. Although several authors consider that ultrastructural features may be useful for the differential diagnosis between benign and malignant mammary tumors, the techniques

that allow an ultrastructural study of these tumors, like transmission electron microscopy (TEM), are time consuming and require advanced skills. The exposed reasons force the TEM use for research purposes only [9,10]. Two histological patterns of mammary lesions most frequently induced by MNU administration in female rats, papillary carcinoma and cribriform carcinoma, were analyzed by TEM. Findings similar to those observed in woman mammary tumors, like nuclei size and shape, and accumulation of heterochromatin in perinuclear region, were observed. Cytoplasmic processes between cancer cells were also observed in an attempt to attach to adjacent cells, and enhance their survival and resistance to apoptosis induced by administration of anticancer drugs [11,12]. Additionally to this, these projections may be also involved in cell migration and invasion [13]. Interestingly, we also observed a loss of cancer cell cytoplasm and formation of vacuoles just near the nuclei. Several mast cells were also identified near tumor cells in fragmentation. The ultrastructural characteristics of the two most common MNU-induced mammary carcinomas in female rats described in the present work may be useful to distinguish them from other histological patterns.

Although several authors consider that lifestyle, namely the practice of physical activity, may be a determinant factor to reduce the risk of cancer development, the association between exercise and mammary cancer development is not consensual. This may be justified, at least in part, by the fact that the majority of the studies on humans are epidemiological and the studies based on the use of animal models are very distinct among them (distinct modality, velocity, duration of the exercise). In order to give new insights on this field, we evaluated the effects of long-term moderate exercise training (35 weeks) on the rat model of MNU-induced mammary cancer. Exercised animals exhibited a lower C-reactive protein (CRP) serum levels and spleen weight when compared with non-exercise animals, suggesting that treadmill exercise reduced tumor related inflammation [14,15]. Furthermore, lifelong exercise training increased the latency period, reduced the number of mammary tumors (palpable masses) and lesions and their aggressiveness (lower number of malignant mammary lesions in exercised animals). As previously described, MNU-induced mammary tumors from both exercised and non-exercised animals were hormone-dependent co-expressing estrogens receptors (ERs) α and β in the cell nuclei [16,17]. However, ER β expression was higher when compared with ER α . This may be explained by the fact that there are more cells in the rodent normal mammary gland expressing ER β than ER α [18]. Moreover, we observed that the

enhancement of the ER α immunoexpression was higher in mammary tumors from exercised animals when compared with mammary tumors from sedentary animals. This highest enhancement of ER α in mammary tumors from MNU exercised group may be beneficial, since the low levels of this receptor are associated with poorly differentiated breast tumors (the less differentiated tumors are more aggressive) and with a unfavorable response to different therapeutic approaches, namely endocrine therapy and surgery [15]. Although the serum concentrations of estradiol have been found to be higher in human patients with malignant breast tumors compared to patients with nonmalignant breast tumors [19], we observed that animals from exercised group that developed lower number of malignant mammary tumors exhibited higher serum levels of 17- β estradiol. This data is in accordance with those described by Hao *et al.* [20] and Rauf *et al.* [21] that observed higher 17- β estradiol serum levels in Sprague-Dawley rats exercised for 12 weeks.

Vascularization of MNU-induced mammary tumors from exercised animals was higher when compared with mammary tumors from non-exercised animals: higher CPD detected by PDI and B Flow, higher vascular endothelial growth factor (VEGF)-A immunoexpression and higher number of microvessels (higher microvessel density (MVD)). Despite this, mammary tumors from exercised animals exhibited higher area of necrosis when compared with tumors from sedentary animals, which is probably related with the higher volume of these tumors. Although, we hypothesized that long-term exercise training could inhibit mammary tumor growth and aggressiveness by the inhibition of tumors vascularization, surprisingly we verified that the exercise training promoted tumor vascularization (increased VEGF-A immunoexpression, MVD, and CPD detected by PDI and B Flow) and growth (tumors with higher volume), but reduced the number of mammary tumors and their aggressiveness, and increased latency period.

From the presented ultrasound modalities to assess tumor vascularization, CEUS is considered the most accurate one, since it is able to detected tumor vessels lower than 50 μm in diameter [35,36]. A second-generation contrast agent (SonoVue[®]) was used to assess the vascularization of MNU-induced mammary tumors. Despite this, the quantitative analysis of CEUS did not detect the differences in the vascularization of mammary tumors between sedentary and exercised animals that were detected by PDI, B Flow and immunohistochemistry. The qualitative analysis of CEUS revealed that MNU-induced mammary tumors exhibited a centripetal enhancement order of contrast agent,

heterogeneous enhancement and clear margins, similarly to that observed in women mammary tumors [37].

Cancer is frequently associated with skeletal muscle wasting. According to several authors, it is a major factor involved in cancer cachexia contributing to physical disability, weakness, reduced tolerance to anticancer therapies and decreased survival [22–24]. Since cancer-induced cachexia has been implicated in up to 20% of cancer-related deaths, it is a major concern in cancer treatment [25]. These changes in skeletal muscle may be non-invasively evaluated by ultrasonography [26]. In the present work, it was observed that cancer and the practice of exercise training promoted some changes in the skeletal muscle. A lower echogenicity of *gastrocnemius* muscle suggestive of lower fat infiltration and higher myostatin serum levels were observed in animals with cancer (MNU-exposed groups) probably due to cancer-associated catabolic effects on body tissues [27]. Myostatin is a hormone produced in muscle that affects the growth and metabolic state not only of the muscle, but also of other body tissues, including fat [28]. High myostatin levels have been described in conditions associated with muscle wasting, including cancer [28,29]. Exercised groups (MNU and control) also exhibited lower echogenicity when compared with respective sedentary groups due to the reduction of fat infiltration in muscle. According with other researchers, the echogenicity of ultrasonographic images of the *gastrocnemius* muscle are always influenced by fat infiltration [30,31].

Tumors are not only masses of malignant cells but complex organs, to which many other cells are recruited and potentially changed by transformed cells [38]. Lymphatic and vascular endothelial cells, pericytes, adipocytes, mesenchymal stem cells, smooth muscle cells, fibroblasts, myofibroblasts, myeloid cells and inflammatory cells (B and T lymphocytes, neutrophils, dendritic cells, eosinophils, basophils, natural killer cells, macrophages and mast cells) are among the non-malignant cells of tumor microenvironment [39,40]. As a significant mast cell infiltrate had been previously observed by our research team in a rat model of MNU-induced mammary cancer [41], we considered that this model was suitable to study the role of these enigmatic cells on mammary carcinogenesis. In this way, we decided to study the role of mast cells on mammary tumor progression and vascularization by their inhibition through the administration of the commonly used antihistamine and mast cell stabilizer drug ketotifen. We verified that mast cell degranulation was effectively inhibited by ketotifen (the levels of histamine were lower in animals ketotifen-treated when compared with non-

treated ones). Inversely to that expected, we observed that the number of palpable masses and mammary lesions, and tumor vascularization as detected by ultrasonography (PDI, B Flow and CEUS) and immunohistochemistry (VEGF-A immunoeexpression) were very similar among groups, suggesting that the inhibition of mast cell degranulation did not affect mammary tumor progression. Indeed, the mainly positive effect of the inhibition of mast cell degranulation on mammary tumorigenesis seemed to be the reduction of tumor proliferation (lower Ki-67 immunoeexpression) when the mast cell degranulation was inhibited before tumor development.

13.1. References

- [1] International Agency for Research on Cancer. Globocan 2012: Estimated cancer incidence, mortality and prevalence worldwide in 2012. *WHO*, **2015**.
- [2] Kamb, A. What's wrong with our cancer models? *Nat. Rev. Drug Discov.*, **2005**, 4, 161–165.
- [3] Faustino-Rocha, AI.; Ferreira, R.; Oliveira, PA.; Gama, A.; Ginja, M. *N*-methyl-*N*-nitrosourea as a mammary carcinogenic agent. *Tumor Biol.*, **2015**, 36, 9095–9117.
- [4] Iannaccone, PM.; Jacob, HJ. Rats! *Dis. Model. Mech.*, **2009**, 2, 206–210.
- [5] Clarke, R. Animal models of breast cancer: their diversity and role in biomedical research. *Breast Cancer Res. Treat.*, **1996**, 39, 1–6.
- [6] Liao, A-H.; LI, C-H.; Cheng, W-F.; Li, P-C. Non-invasive imaging of small-animal tumors: high-frequency ultrasound vs microPET. *Conf. Proc. IEEE Eng. Med. Biol. Soc.*, **2005**, pp. 5695–5698.
- [7] Girit, IC.; Jure-Kunkel, M.; McIntyre, KW. A structured light-based system for scanning subcutaneous tumors in laboratory animals. *Comp. Med.*, **2008**, 58, 264–270.
- [8] Pain, JA.; Ebbs, SR.; Hern, RPA.; Lowe, S.; Bradbeer, JW. Assessment of breast-cancer size - a comparison of methods. *Eur. J. Surg. Oncol.*, **1992**, 18, 44–48.
- [9] Tsuchiya, S.; Li, F. Electron microscopic findings for diagnosis of breast lesions. *Med. Mol. Morphol.*, **2005**, 38, 216–224.
- [10] Winey, M.; Meehl, JB.; O'Toole, ET.; Giddings, TH. Conventional transmission electron microscopy. *Mol. Biol. Cell*, **2014**, 25, 319–323.

-
- [11] Kataoka, S.; Tsuruo, T. Physician Education: apoptosis. *Oncologist*, **1996**, 1, 399–401.
- [12] Luparello, C.; Sheterline, P.; Pucciminfra, I.; Minfra, S. A comparison of spreading and motility behavior of 8701-BC breast-carcinoma cells on type-I, I-trimer and type V collagen substrata - evidence for a permissive effect of type I-trimer collagen on cell locomotion. *J. Cell Sci.*, **1991**, 100, 179–185.
- [13] Kramer, RH.; Bensch, KG.; Wong, J. Invasion of reconstituted basement-membrane matrix by metastatic human-tumor cells. *Cancer Res.*, **1986**, 46, 1980–1989.
- [14] Leygue, E.; Dotzlaw, H.; Watson, PH.; Murphy, LC. Altered estrogen receptor alpha and beta messenger RNA expression during human breast tumorigenesis. *Cancer Res.*, **1998**, 58, 3197–3201.
- [15] Zeleniuch-Jacquotte, A.; Toniolo, P.; Levitz, M.; Shore, RE.; Koenig, KL.; Banarjee, S.; Strax, P.; Pasternack, BS. Endogenous estrogens and risk of breast cancer by estrogen receptor status: a prospective study in postmenopausal women. *Cancer Epidemiol. Biomarkers Prev.*, **1995**, 4, 857–860.
- [16] Helguero, LA.; Faulds, MH.; Gustafsson, JA.; Haldosen, LA. Estrogen receptors alfa (ER alpha) and beta (ER beta) differentially regulate proliferation and apoptosis of the normal murine mammary epithelial cell line HC11. *Oncogene*, **2005**, 24, 6605–6616.
- [17] Speirs, V.; Skliris, GP.; Burdall, SE.; Carder, PJ. Distinct expression patterns of ER alpha and ER beta in normal human mammary gland. *J. Clin. Pathol.*, **2002**, 55, 371–374.
- [18] Saji, S.; Jensen, E V.; Nilsson, S.; Rylander, T.; Warner, M.; Gustafsson, JA. Estrogen receptors alpha and beta in the rodent mammary gland. *Proc. Natl. Acad. Sci. U.S.A.*, **2000**, 97, 337–342.
- [19] Yager, JD.; Davidson, NE. Mechanisms of disease: estrogen carcinogenesis in breast cancer. *N. Engl. J. Med.*, **2006**, 354, 270–282.
- [20] Hao, LK.; Wang, YJ.; Duan, YS.; Bu, SM. Effects of treadmill exercise training on liver fat accumulation and estrogen receptor alpha expression in intact and ovariectomized rats with or without estrogen replacement treatment. *Eur. J. Appl. Physiol.*, **2010**, 109, 879–886.
- [21] Rauf, S.; Soejono, SK.; Partadiredja, G. Effects of treadmill exercise training on

- cerebellar estrogen and estrogen receptors, serum estrogen, and motor coordination performance of ovariectomized rats. *Iran. J. Basic Med. Sci.*, **2015**, 18, 587–592.
- [22] Fearon, K.; Strasser, F.; Anker, SD.; Bosaeus, I.; Bruera, E.; Fainsinger, RL.; Jatoi, A.; Loprinzi, C.; MacDonald, N.; Mantovani, G.; Davis, M.; Muscaritoli, M.; Ottery, F.; Radbruch, L.; Ravasco, P.; Walsh, D.; Wilcock, A.; Kaasa, S.; Baracos, VE. Definition and classification of cancer cachexia: an international consensus. *Lancet Oncol.*, **2011**, 12, 489–495.
- [23] Julienne, CM.; Dumas, J-F.; Goupille, C.; Pinault, M.; Berri, C.; Collin, A.; Tesseraud, S.; Couet, C.; Servais, S. Cancer cachexia is associated with a decrease in skeletal muscle mitochondrial oxidative capacities without alteration of ATP production efficiency. *J. Cachexia. Sarcopenia Muscle*, **2012**, 3, 265–275.
- [24] Argilés, JM.; Busquets, S.; Stemmler, B.; López-Soriano, FJ. Cancer cachexia: understanding the molecular basis. *Nat. Rev. Cancer*, **2014**, 14, 754–762.
- [25] MacDonald, N.; Easson, AM.; Mazurak, VC.; Dunn, GP.; Baracos, VE. Understanding and managing cancer cachexia. *J. Am. Coll. Surg.*, **2003**, 197, 143–161.
- [26] Pillen, S. Skeletal muscle ultrasound. *Eur. J. Transl. Myol.*, **2010**, 20, 145.
- [27] Tisdale, MJ. Pathogenesis of cancer cachexia. *J. Support. Oncol.*, 1, 159–68.
- [28] Roth, S.; Walsh, S. Myostatin: a therapeutic target for skeletal muscle wasting. *Curr. Opin. Clin. Nutr. Metab. Care*, **2004**, 7, 259–263.
- [29] Aversa, Z.; Bonetto, A.; Penna, F.; Costelli, P.; Di Rienzo, G.; Lacitignola, A.; Baccino, FM.; Ziparo, V.; Mercantini, P.; Rossi Fanelli, F.; Muscaritoli, M. Changes in myostatin signaling in non-weight-losing cancer patients. *Ann. Surg. Oncol.*, **2012**, 19, 1350–1356.
- [30] Peetrons, P. Ultrasound of muscles. *Eur. Radiol.*, **2002**, 12, 35–43.
- [31] Reimers, K.; Reimers, CD.; Wagner, S.; Paetzke, I.; Pongratz, DE. Skeletal muscle sonography: a correlative study of echogenicity and morphology. *J. Ultrasound Med.*, **1993**, 12, 73–77.
- [32] Ko, EY.; Lee, SH.; Kim, HH.; Kim, SM.; Shin, MJ.; Kim, N.; Gong, G. Evaluation of tumor angiogenesis with a second-generation US contrast medium in a rat breast tumor model. *Korean J. Radiol.*, **2008**, 9, 243–249.
- [33] Kennedy, DA.; Lee, T.; Seely, D. A comparative review of thermography as a breast cancer screening technique. *Integr. Cancer Ther.*, **2009**, 8, 9–16.

-
- [34] Fleischer, AC.; Wojcicki, WE.; Donnelly, EF.; Pickens, DR.; Thirsk, G.; Thurman, GB.; Hellerqvist, CG. Quantified color Doppler sonography of tumor vascularity in an animal model. *J. Ultrasound Med.*, **1999**, 18, 547–551.
- [35] Cheng, WF.; Lee, CN.; Chu, JS.; Chen, CA.; Chen, TM.; Shau, WY.; Hsieh, CY.; Hsieh, FJ. Vascularity index as a novel parameter for the *in vivo* assessment of angiogenesis in patients with cervical carcinoma. *Cancer*, **1999**, 85, 651–657.
- [36] Ferrara, KW.; Merritt, CRB.; Burns, PN.; Foster, FS.; Mattrey, RF.; Wickline, SA. Evaluation of tumor angiogenesis with US: imaging, Doppler, and contrast agents. *Acad. Radiol.*, **2000**, 7, 824–839.
- [37] Badea, AF.; Szora, AT.; Clichici, S.; Socaciu, M.; Tabaran, AF.; Baciut, G.; Catoi, C.; Muresan, A.; Buruian, M.; Badea, R. Contrast enhanced ultrasonography (CEUS) in the characterization of tumor microcirculation. Validation of the procedure in the animal experimental model. *Med. Ultrason.*, **2013**, 15, 85–94.
- [38] Balkwill, F.; Capasso, M.; Hagemann, T. The tumor microenvironment at a glance. *J. Cell Sci.*, **2012**, 125, 5591–5596.
- [39] Hanahan, D.; Weinberg, RA. The hallmarks of cancer. *Cell*, **2000**, 100, 57–70.
- [40] Coussens, LM.; Werb, Z. Inflammatory cells and cancer: think different! *J. Exp. Med.*, **2001**, 193, F23–26.
- [41] Soares-Maia, R.; Faustino-Rocha, AI.; Teixeira-Guedes, CI.; Pinho-Oliveira, J.; Talhada, D.; Rema, A.; Faria, F.; Ginja, M.; Ferreira, R.; Gil da Costa, RM.; Oliveira, PA.; Lopes, C. MNU-induced rat mammary carcinomas: immunohistology and estrogen receptor expression. *J. Environ. Pathol. Toxicol. Oncol.*, **2013**, 32, 157–163.

CHAPTER 14

FINAL CONCLUSIONS

14. Final conclusions

Cancer is a frightening disease that may affect everybody in any place. Approximately 14 million cases of cancer were estimated to have occurred in 2012 [1]. Disappointing projections are being pointed for the next years, with an increase in the number of new cancer cases *per* year to 22 million over the next two decades [2]. Breast cancer remains as the most frequent cancer among women [1]. In order to reduce the number of cancers and decrease the mortality, future directions are focused on the discovery of new targets, development of new drugs and preventive strategies.

The studies presented in this thesis are based on the use of the model of chemically-induced mammary cancer in female rats by the administration of the carcinogen agent *N*-methyl-*N*-nitrosourea (MNU). The effects of lifelong exercise training and the effects of ketotifen on cancer progression and vascularization were evaluated. The results suggest that:

- MNU-induced mammary tumors in female rats grow as oblate spheroids. Tumor volume may be properly determined *in vivo* by ultrasonography. After tumor excision or animal sacrifice, tumor volume may be determined by water displacement or on the basis of tumor weight. Tumor dimensions, weight or volume do not allow the prediction of tumor invasiveness.
- Similar findings to those described in women mammary tumors, like nucleus size and shape, accumulation of heterochromatin in perinuclear region and interdigitating cytoplasmic processes between cancer cells, were observed at the transmission electron microscopy analysis of MNU-induced mammary tumors. Ultrastructural characteristics of papillary and cribriform carcinomas may be useful to distinguish them from other histological patterns. A marked infiltrate of mast cells was observed, mainly near tumor cells in fragmentation. The loss of neoplastic cell cytoplasm and formation of vacuoles just near the nucleus were also observed.
- Ultrasonographic (Power Doppler, B Flow, contrast enhanced ultrasound) and thermographic techniques are applicable to assess the vascularization of MNU-

induced mammary tumors. Despite this, B Flow is more sensitive when compared with Power Doppler in detecting tumor vessels.

- Long-term moderate exercise training had beneficial effects on mammary tumorigenesis in female rats, by reducing the inflammation, increasing the latency period, and reducing the number of mammary tumors and lesions, as well as their aggressiveness. Additionally, long-term exercise training increased the immunoexpression of estrogen receptor (ER) α , suggesting that mammary tumors from exercised animals were more differentiated and will respond better to hormone therapy when compared with tumors from non-exercised animals. Long-term exercise training also increased vascular endothelial growth factor (VEGF)-A immunoexpression, leading to enhanced tumor vascularization.
- Mammary carcinogenesis induced skeletal muscle wasting and increased myostatin serum levels. These alterations were observed in ultrasonography, by the lower muscle echogenicity due to the decrease of fat infiltration. The muscle echogenicity in exercised animals with and without mammary tumors was lower when compared with the echogenicity of respective sedentary controls due to the decrease of muscular fat induced by the practice of exercise.
- Ketotifen inhibited mast cell degranulation. The reduction of mammary tumor proliferation seemed to be the mainly positive effect of the inhibition of mast cell degranulation. This inhibition did not change tumor vascularization, but reduced tumor proliferation when performed before tumor development.
- Like woman mammary tumors, MNU-induced rat mammary tumors evaluated by contrast-enhanced ultrasound (CEUS) exhibited a centripetal enhancement order of the contrast agent, clear margin and heterogeneous enhancement.

14.1. References

- [1] World Health Organization (WHO). Cancer - Fact sheet n° 297. *WHO*, 2015.
- [2] Stewart, B.; Wild, C. World cancer report. *WHO*, 2014.
- [3] Clarke, R. Animal models of breast cancer: their diversity and role in biomedical

- research. *Breast Cancer Res. Treat.*, **1996**, 39, 1–6.
- [4] Iannaccone, PM.; Jacob, HJ. Rats! *Dis. Model. Mech.*, **2009**, 2, 206–210.